

Characterizing novel ripening related genes linked to
shelf life in tomato

by Michael Thomas, B.Sc.

Thesis submitted to the University of Nottingham for
the degree of Doctor of Philosophy, September 2016

ACKNOWLEDGEMENT

First and foremost, I would like to fully express my gratitude to my parents, Mr Alun Thomas, Mrs Collette Thomas, Mrs Zaffy Lott, and Mr John Lott for their love, guidance, and support. I am grateful to you all for always being with me through every step of my journey in life. This thesis is dedicated to you all.

I would like to express my sincerest gratitude to my supervisors, Professor Graham B. Seymour and Dr Ranjan Swarup for their continued support, advice, and patience throughout this PhD, it would not have been possible without both of you. I would also like to extend my gratitude to Dr Charles Baxter, Dr Charlie Hodgman, Dr Brandon Hurr, and Dr Daniel Rickett of Syngenta for their assistance and expertise in contributing to this project. Many thanks to Dr Rupert Fray, Dr Natalie Chapman, Dr Paul Fraser, and Dr Fereshteh Malekpoor Mansoorkhani for their help and advice which has helped me grow and develop as a researcher and a big thank you to all members of staff within the Plant and crop sciences division and the Doctoral training programme; Professor Jerry Roberts, Dr Rebekah Smith McGloin, Ruth Cornock, GuiPing Sun, Mark Meacham, Linda Sheldrick, Sonoko Mitsui-Angwin, and Andrew Jackson in providing the tools and environment to make this work possible.

I would like to extend my thanks to my close friends and colleagues who shared in this journey with me; James Williamson, Thomas Upton, Raj Gandhi, Jamie Ware and William Hawley for their continual support and companionship in an otherwise isolating endeavour. Thank you to those who have influenced and encouraged me over the years; Dr Tim Ashlin, Dr Wil Chivers, Ad Unitt, Jack Turner, Heather Richardson, and all those I did not have a chance to address here for leading me to this juncture.

Last but not least, I would like to thank Dr Jessica Patel for her unwavering love and understanding over the years. You have provided the foundation on which I can accomplish this work and I am eternally indebted to you.

Abstract

Characterizing novel ripening related genes linked to shelf life in tomato

Fruits play a major role in maintaining a healthy diet and have been shown to reduce instances of heart disease, osteoporosis and cancer. However, the perishable nature of fruits leads to an increased cost and decrease in quality of post-harvest food. A significant crop improvement stratagem is focused toward fruit which retain their health promoting attributes whilst improving quality and reducing post-harvest waste. To provide new insights into the genetic regulation of fruit ripening we have characterised novel ripening related genes linked to shelf life in tomato, the tetraspanins, a zinc-finger protein, and a heat-shock transcription factor.

The tetraspanins are highly conserved integral membrane proteins that act as ligands for extracellular molecules to form tetraspanin-enriched micro-domains which influence cell-cell adhesion, intercellular communication, and plant development. Transgenic tomato lines were generated to determine the role of the tetraspanins in fruit ripening. First and foremost, upregulation of the *SITET-6* gene had no obvious ripening phenotype whilst overexpression or silencing of the *SITET-8* gene appeared to be lethal in tomato, most likely due to the importance of these genes in plant development.

A zinc-finger protein and a heat-shock transcription-like factor were identified as targets of LeMADS-RIN and investigations using constitutive knock-down constructs have shown an increase in fruit firmness in tomato at the Breaker+4 and red-ripe stages of ripening. RNA-seq revealed differential expression of over 4000 ripening related genes associated with silencing which included polygalacturonase, pectinmethylesterase, and pectate lyase. These data emphasise the role of transcriptional regulation in fruit ripening and provide a novel means of regulating fruit development.

TABLE OF CONTENTS

<u>Abstract</u>	<u>ii</u>
<u>LIST OF FIGURES</u>	<u>ix</u>
<u>LIST OF TABLES</u>	<u>xv</u>
<u>ABBREVIATIONS</u>	<u>xvi</u>
<u>Chapter 1</u>	<u>1</u>
<u>Introduction and literature review</u>	<u>1</u>
1.1 FRUITS: HEALTH BENEFITS AND ECONOMIC IMPORTANCE	2
1.2 THE TOMATO, NOMENCLATURE AND EVOLUTION	5
1.3 TOMATO FRUIT DEVELOPMENT AND RIPENING	6
TOMATO WEIGHT AND SHAPE	8
FRUIT RIPENING	10
CLIMACTERIC AND NON-CLIMACTERIC RIPENING	10
ETHYLENE BIOSYNTHESIS AND PERCEPTION	11
ETHYLENE RECEPTORS	11
1.4 TRANSCRIPTIONAL CONTROL OF RIPENING	15
RIPENING-INHIBITOR (RIN)	15
COLOURLESS NON-RIPENING (CNR)	16
NON-RIPENING (NOR)	16
GENE REGULATORY NETWORKS	17
1.5 THE PLANT CELL-WALL AND TEXTURE MODIFICATION DURING FRUIT RIPENING	18
CELL WALL REMODELLING	21
POLYGALACTURONASE (PG)	21
PECTIN METHYL ESTERASE	22
PECTATE LYASE (PL)	22
EXPANSINS, AND CELLULASES XYLOGLUCAN ENDOTRANSGLUCOSEYLASE (XTH)	23

1.6 TETRASPANIN; STRUCTURE, ORIGINS, AND FUNCTION	25
FUNCTION	27
TETRASPANIN TRANSMEMBRANE DOMAINS	27
EXTRACELLULAR LOOPS	28
CYTOPLASMIC DOMAINS	29
TETRASPANIN-ENRICHED MICRO-DOMAINS	29
1.7 HEAT SHOCK TRANSCRIPTION FACTORS	31
STRUCTURE AND FUNCTION	31
REGULATORY NETWORK	34
HEAT-SHOCK PROTEINS	35

AIMS AND OBJECTIVES **36**

Chapter 2 **37**

Materials and Methods **37**

2.1 TOMATO PLANT MATERIAL AND FRUIT SELECTION	38
2.2 ARABIDOPSIS PLANT MATERIAL	38
2.3 SUGAR CONTENT AND COLOUR MEASUREMENTS	38
2.4 FRUIT TEXTURE MEASUREMENTS	40
2.5 PLASMID CONSTRUCTION AND GENERATION OF TRANSGENIC PLANTS	40
POLYMERASE CHAIN REACTION (PCR)	44
GEL EXTRACTION OF DNA FRAGMENTS	45
ADDING A 3' OVERHANG TO A PCR FRAGMENT PRIOR TO CLONING	45
BP AND LR CLONASE REACTIONS	46
TRANSFORMATION OF PLASMIDS INTO CHEMICALLY COMPETENT CELLS	47
TRANSFORMATION INTO <i>AGROBACTERIUM</i> VIA ELECTROPORATION	47
PLASMID PURIFICATION	47
2.6 DNA EXTRACTION	48
2.7 RNA EXTRACTION	49
2.8 QUANTITATIVE – PCR (QPCR)	51
SYNTHESIS OF FIRST STRAND cDNA	51
QPCR PRIMER DESIGN	51
QPCR REACTION AND CONDITIONS	52
2.9 STATISTICAL ANALYSIS	52

2.10 TOMATO PLANT TRANSFORMATION WITH <i>AGROBACTERIUM</i> STRAIN EHA105	53
---	-----------

Chapter 3 **- 54 -**

A novel tetraspanin gene linked to shelf life in melon **- 54 -**

3.1 INTRODUCTION	55
TETRASPANIN	55
3.2 MATERIALS AND METHODS	62
PLANT MATERIALS	62
VECTOR CONSTRUCTION	63
PLANT TRANSFORMATION	67
ANALYSIS OF T ₀ TRANSGENIC LINES AND IDENTIFICATION OF HOMOZYGOUS LINES IN THE T ₀ PROGENY	67
TRANSGENE EXPRESSION IN HOMOZYGOUS SLTET-6 FRUITS	67
3.3 FRUIT PHENOTYPING	68
FRUIT SUGARS AND COLOUR	68
FRUIT TEXTURE MEASUREMENTS	68
3.3 RESULTS AND DISCUSSION	69
GENERATING THE EXPRESSION CLONE FOR THE FULL SOLYC04G049080 GENE FRAGMENT.	69
ASSESSMENT OF FRUIT TEXTURE AND SOLUBLE SOLIDS IN SEGREGATING GENERATION	76
ANALYSIS OF HOMOZYGOUS T ₁ LINES AND AZYGUS CONTROLS	80
PHENOTYPING OF HOMOZYGOUS <i>SLTET-6</i> LINES	83
<i>SLTET-6</i> TRANSGENE EXPRESSION IN IN FRUIT TISSUE	83
ASSESSMENT OF FRUIT WEIGHT AND COLOUR IN THE HOMOZYGOUS T ₁ LINES	84
3.4 CONCLUSION	90

Chapter 4 **91**

***Arabidopsis thaliana* AtTET-5** **91**

4.1 INTRODUCTION	92
4.2 MATERIALS AND METHODS	96
PLANT MATERIALS AND GROWTH CONDITIONS	96
LATERAL ROOT DEVELOPMENT	96

ROOT GRAVITROPISM	96
LATERAL ROOT INDUCTION USING GRAVITROPIC STIMULUS	96
ANALYSIS AND VALIDATION OF T-DNA INSERTIONAL KNOCK OUTS	98
POLYMERASE CHAIN REACTION (PCR)	98
PRIMER DESIGN	98
4.3 RESULTS AND DISCUSSION	100
PROTEIN SEQUENCE ALIGNMENT WITH TOMATO ORTHOLOGUE	100
ENDOGENOUS EXPRESSION OF <i>AtTET-5</i> IN ARABIDOPSIS	102
ANALYSIS AND VALIDATION OF TETRASPANIN 5.1 AND 5.2 T-DNA INSERTIONAL KNOCK OUTS	104
INVESTIGATION OF ROOT RELATED PHENOTYPES IN <i>AtTET-5</i>	107
PRIMARY ROOT GROWTH, LATERAL ROOT EMERGENCE, AND PRIMORDIA DEVELOPMENT	107
ROOT GRAVITROPISM IN TRANSGENIC LINE <i>AtTET-5</i>	113
ROOT GRAVITROPISM IN TOMATO	117

Chapter 5 **120**

Generation of transgenic Tet-8 tomato lines **120**

5.1 INTRODUCTION	121
5.2 MATERIALS AND METHODS	126
POLYMERASE CHAIN REACTION (PCR)	126
ADDING A 3' OVERHANG TO PCR FRAGMENT	127
BP AND LR CLONASE REACTIONS	128
<i>AGROBACTERIUM</i> TRANSFORMATION	133
GENERATION OF TRANSGENIC PLANTS	133
PLANTLET ACCLIMATIZATION	134
5.3 RESULTS AND DISCUSSION	135
GENERATION OF THE <i>SLTET-8</i> PLASMIDS	135
REGENERATION OF TRANSGENIC PLANTS FROM 35S PROMOTER CONSTRUCTS	146
OVEREXPRESSION AND SILENCING OF THE <i>SLTET-8</i> GENE UNDER CONTROL OF A PG PROMOTER.	147
VECTOR CONSTRUCTION AND VALIDATION	147

Chapter 6 **157**

Characterizing the role of a heat shock transcription factor and a zinc finger protein in tomato ripening **157**

6.1 INTRODUCTION	158
6.2 MATERIALS AND METHODS	163
PLANT MATERIALS	163
VECTOR CONSTRUCTION	163
SINGLE COPY ANALYSIS OF T ₁ PROGENY FROM T ₀ TRANSGENIC LINES	163
TRANSGENE EXPRESSION IN HOMOZYGOUS LINES	164
FRUIT PHENOTYPING	164
6.3 RESULTS AND DISCUSSION	165
IDENTIFICATION OF HOMOZYGOUS LINES	165
ASSESSMENT OF FRUIT WEIGHT AND COLOUR IN SELECTED HOMOZYGOUS <i>SLHST-14</i> LINES	168
ASSESSMENT OF FRUIT TEXTURE IN T ₁ LINES AND SUBSEQUENT GENERATIONS	171
THE ROLE OF A ZINC-FINGER PROTEIN ON FRUIT SOFTENING	174

Chapter 7 **176**

The effects of silencing of a heat-shock transcription factor-like gene on the tomato ripening transcriptome **176**

7.1 INTRODUCTION	177
7.2 MATERIALS AND METHODS	178
PLANT MATERIALS AND FRUIT COLLECTION	178
RNA EXTRACTION, STORAGE, AND SEQUENCING	178
EXAMINATION OF RNA INTEGRITY	178
SOFTWARE	178
7.3 RESULTS AND DISCUSSION	179
RNA SEQUENCE QUALITY AND FRAGMENT MAPPING	179
DIFFERENTIAL GENE EXPRESSION IN FRUIT RIPENING	182
RIPENING-RELATED PATHWAYS AFFECTED BY SILENCING <i>SLHST-14</i>	196
CELL WALL GENES AND FRUIT SOFTENING	200

Chapter 8 **203**

General discussion and future work **203****TETRASPANINS** **205****THE TRANSGENIC PLANTS** **207****NOVEL GENES LINKED TO FRUIT SOFTENING AND THE POTENTIAL FOR DISCOVERY OF NEW RIPENING
RELATED GENES** **209****References** **210****Appendices** **210****Conference Poster** **210**

LIST OF FIGURES

Figure 1.1: Global tomato statistics	4
Figure 1.2: Tomato fruit development and ripening	7
Figure 1.3: A comparison of wild-type tomato with Giant Heirloom tomato variety.	9
Figure 1.4: The ethylene signalling pathway	13
Figure 1.5: Structure and Development of the primary cell wall	20
Figure 1.6: The tetraspanin protein	26
Figure 1.7. Structure of tomato Hsfs	33
Figure 2.1. The Hunter L*, a*, and b* colour space	39
Figure 2.2: The four main stages of the cloning procedure for <i>SITET-8</i> using a constitutive 35S promoter	41
Figure 2.3: The four main stages of the cloning procedure for <i>SITET-8</i> using a ripening specific PG promoter	42
Figure 2.4: The main stages of the characterising the effect of <i>SIHST-14</i> suppression on tomato fruit texture and shelf life	43
Figure 3.1: Expression of a Melon tetraspanin-like gene in cultivars Cezanne, Anasta, and Magenta	57
Figure 3.2: Protein sequence alignment of Melon, Tomato, and Arabidopsis tetraspanin	59
Figure 3.3: RNA expression profile of <i>SLTET-6</i>	60
Figure 3.4: Expression of <i>SITET-6</i> in tomato mutants	61
Figure 3.5: Description of the BP reaction to incorporate the <i>SLTET-6</i> gene into the donor vector pDONR221	64

Figure 3.6: Description of the LR reaction to incorporate the <i>SLTET-6</i> gene and PG promoter into the destination vector PK7M24GW3	66
Figure 3.7: The BP reaction identifying the <i>SLTET-6</i> gene fragment inside the pDONR221 entry vector	70
Figure 3.8: The LR reaction identifying the presence, and orientation of the <i>SLTET-6</i> and <i>NPTII</i> gene inside the PK7M24GW3 destination vector	72
Figure 3.9: Comparison of transgenic (right) tomato size compared with Ailsa Craig control (left)	74
Figure 3.10: The comparison of transgenic tomato weight in the <i>SLTET-6</i> lines compared with Ailsa Craig controls	75
Figure 3.11: The comparison of transgenic <i>SLTET-6</i> tomato colour compared with Ailsa Craig controls	76
Figure 3.12: The comparison of fruit texture of transgenic <i>SLTET-6</i> plant lines compared with Ailsa Craig controls.	78
Figure 3.13: The comparison of soluble solids of transgenic <i>SLTET-6</i> fruit compared with Ailsa Craig controls	79
Figure 3.14: Assessment of copy number in tomato plants	81
Figure 3.15: RNA expression of <i>SLTET-6</i> in fruit pericarp tissue	84
Figure 3.16: Assessment of fruit weight in <i>SLTET-6</i> lines vs an azygous control and wild type Ailsa Craig fruits from the Sutton Bonington seed bank	86
Figure 3.17: Assessment of homozygous tomato colour index. The figure shows no colour differences between the <i>SLTET-6</i> and azygous controls	87

Figure 3.18: Assessment of homozygous fruit texture in SlTET-6.1. A)	
Outer pericarp and B) Inner pericarp	88
Figure 3.19: The comparison of the total Soluble solids content of SlTET-6	
transgenic fruit compared with Ailsa Craig fruit	89
Figure 4.1: TET expression patterns in different organs	93
Figure 4.2: Phylogenetic analysis of tetraspanin proteins	95
Figure 4.3: Description of lateral root primordium stages	97
Figure 4.4: T-DNA primer design	99
Figure 4.5: Protein sequence alignment between AtTET-5 and SlTET-6.	101
Figure 4.6: <i>AtTET-5</i> expression values in <i>AtTET-5</i> and <i>SlTET-6</i>	103
Figure 4.7: <i>AtTET-5.1</i> and <i>AtTET-5.2</i> transgenic genotyping	105
Figure 4.8: AtTET-5.1 and AtTET-5.2 double reaction	106
Figure 4.9: Primary root growth in AtTET-5	108
Figure 4.10: Lateral root density in AtTET-5	109
Figure 4.11: Primordia development in AtTET-5.1	111
Figure 4.12: Primordia development in AtTET-5.2.	112
Figure 4.13: Gravitropic time lapse	114
Figure 4.14: Gravitropic time lapse of AtTET-5	115
Figure 4.15: SlTET-6 Gravitropic time lapse	118
Figure 5.1: Visual representation of SlTET-8 RNA expression profile	122
Figure 5.2: RNA expression profile of <i>SlTET-8</i> . Data shows expression	
patterns of <i>SlTET-8</i> in different tissues of tomato	123
Figure 5.3: GUS activity in tomato stably transformed with CaMV 35S, PG,	
and Control	125

Figure 5.4: Description of the BP reaction to incorporate the SISLTET-8 RNAi and over-expression gene fragments into the donor vectors.	129
Figure 5.5: Description of the LR reaction to incorporate the SLTET-8 gene fragment into the pFRN-GW-R1-R2 and PGWB8 destination vectors	131
Figure 5.6: Description of the LR reaction to incorporate the SLTET-8 overexpression gene fragment into the PK8-GW1WG-PG-B4 and PK7M24GWi3 destination vectors.	132
Figure 5.7: Sequence alignment of <i>SITET-8</i> RNAi construct	136
Figure 5.8: Sequence alignment of <i>SITET-8</i> over-expression construct	137
Figure 5.9: The BP reaction identifying the presence of a <i>SITET-8</i> RNAi gene fragment inside the PCR8/GW/TOPO entry vector	138
Figure 5.10: The BP reaction. identifying the presence of a <i>SITET-8</i> overexpression gene fragment inside the PCR8/GW/TOPO entry vector	139
Figure 5.11: The LR reaction identifying the presence of a <i>SITET-8</i> RNAi gene fragment inside the pFRN-GW-R1-R2 destination vector	141
Figure 5.12: The LR reaction identifying the presence of a <i>SITET-8</i> overexpression gene fragment inside the PGWB8 destination vector	142
Figure 5.13: <i>Agrobacterium</i> transformation. Colony PCR analysis identifying the presence of a <i>SITET-8</i> RNAi gene fragment inside <i>Agrobacterium</i> strain EHA105	144

Figure 5.14: <i>Agrobacterium</i> transformation. Colony PCR analysis identifying the presence of a <i>SITET-8</i> overexpression gene fragment inside <i>Agrobacterium</i> strain EHA105	145
Figure 5.15: The BP reaction identifying the presence of <i>SITET-8</i> RNAi and overexpression gene fragments inside the pDONR221 entry vector	148
Figure 5.16: The LR reaction identifying the presence of a <i>SITET-8</i> RNAi gene fragment inside the PK8-GW1WG-PG-B4 destination vector	150
Figure 5.17: The LR reaction identifying the presence of a <i>SITET-8</i> overexpression gene fragment into the PK7M24GWi3 destination vector	151
Figure 5.18: <i>Agrobacterium</i> transformation analysis identifying the presence of a <i>SITET-8</i> RNAi and overexpression gene fragments inside <i>Agrobacterium</i> strain EHA105	153
Figure 6.1: Expression of target genes linked to LeMADS-RIN	159
Figure 6.2: ClustalW analysis of <i>SIHST</i>	160
Figure 6.3: <i>SIZFP</i> protein sequence alignment. The closest characterized protein to	162
Figure 6.4: Assessment of copy number in <i>SIHST-14</i> transformed tomato plants	166
Figure 6.5: RNA expression of <i>SIHST-14</i> in transgenic and azygous lines	167
Figure 6.6: Assessment of fruit weight in homozygous plants from line A and Line B	169
Figure 6.7: Assessment of homozygous tomato colour index	170

Figure 6.8: Effects of silencing <i>SIHST-14</i> on fruit texture	172
Figure 6.9: Assessment of <i>SLZFP</i> homozygous fruit texture at the red-ripe stage	175
Figure 7.1: Gel electrophoresis of RNA sample	180
Figure 7.2: RNA-seq read-count and percentage mapped	181
Figure 7.3: MDS plot showing differentially expressed gene clusters	183
Figure 7.4: Volcano plot of differentially expressed genes	184
Figure 7.5: Heat map of differential gene expression of ripening related genes at B+7	186
Figure 7.6: Heat map of differential gene expression of ripening related genes at B+10	188
Figure 7.7: Cellular localization of differential expression of genes affected by silencing <i>SIHST-14</i> in tomato	195
Figure 7.8: Differential expression of <i>SIHST-14</i> in carotenoid biosynthesis	197
Figure 7.9: Differential expression of <i>SIHST-14</i> in the tomato ethylene response pathway	199
Figure 7.10: Differential expression of ripening related genes at B7 and B10	201

LIST OF TABLES

Table 1.1: Classification of heat shock transcription factors	32
Table 2.2: QPCR reaction and condition	52
Table 3.1: Overview of copy number results.	82
Table 4.1: PCR mix and reaction for confirmation of T-DNA inserts	98
Table 4.2: Hydrophobicity and amphiphilicity of TM regions in AtTET-5.	100
Table 7.1: The 20 most down-regulated genes in B+7 fruit	190
Table 7.2: The 20 most up-regulated genes in B+7 fruit	191
Table 7.3: The 20 most down-regulated genes in B+10 fruit	192

ABBREVIATIONS

A	Anthesis
ABA	Absciscic acid
AC	Ailsa Craig
AMP	Adenosine monophosphate
Au	Arbitrary units
BBSRC	Biotechnology & biological sciences research council
BR	Breaker
Bp	Base pair
Ca ²⁺	Calcium ions
CaMV	Cauliflower mosaic virus
cDNA	Complementary DNA
CmR	Chloramphenicol resistance protein
Cq	Crossing point
DNA	Deoxyribose nucleic acid
dNTPs	Deoxynucleoside triphosphate
DPA	Days post anthesis
EBF	EIN3-binding F-box protein
EDTA	Ethylenediaminetetraacetic acid
EGZ	Exocarp
EF	Elongation factor
END	Endocarp
ER	Endoplasmic reticulum
ERF	Ethylene response factors
GFP	Green fluorescent protein
GMO	Genetically modified organisms
GUS	β-Glucuronidase
HCl	Hydrogen chloride
HSP	Heat-shock protein
JIC	John Innes Centre
LB	Luria-bertani

MDS	Multidimensional scaling plot
MES	Mesocarp
MG	Mature green
mM	Millimolar
MS	Murashige and Skoog medium
MSR3	MS + R3 Vitamins
MSZ	MS + Zeatin
NaCL	Sodium chloride
PCR	Polymerase chain reaction
PDS	Phytoene desaturase
PG	Polygalacturonase
PME	Pectin methylesterase
PP2C	2C protein phosphatases
PYR	Pyrabactin
qPCR	Quantitative PCR
QTL	Quantitative trait loci
RHUL	Royal Holloway, University of London
RNA	Ribonucleic acid
RR	Red ripe
RT-PCR	Reverse transcriptase PCR
SE	Standard error
TAE	Tris-acetate-EDTA
TBE	Tris-borate-EDTA
TCI	Tomato colour index
TET	Tetraspanin
UoN	University of Nottingham
ZFP	Zinc finger protein

Chapter 1

Introduction and literature review

1.1 Fruits: Health benefits and economic importance

Fruits are a major contributor to a balanced diet that help to maintain healthy and active lifestyles as they provide vitamins, minerals, and antioxidants including carotenoids and anthocyanin. Around 10,000 years ago, the diets of hunter-gatherers consisted almost exclusively of fruits and vegetables and very little in fats and starches. The introduction of modern agriculture and animal husbandry saw a dramatic shift away from a varied diet towards a diet rich in cereals and proteins with little variation in the plants consumed. This shift has occurred in a significantly small time-frame on an evolutionary scale and the emergence of modern chronic diseases has been attributed in part to this change (Cordain et al., 2000; Seymour, Ostergaard, Chapman, Knapp, & Martin, 2013).

The health benefits of fruit are well documented, many provide high levels of soluble fibre, fructose, phytonutrients, vitamins, and polyunsaturated fatty acids, all of which have been observed to lower incidences of type-2 diabetes, cardiovascular disease, and obesity (Butelli et al., 2008; Khaw & Barrett-Connor, 1987; Larsson, Bergkvist, & Wolk, 2009; Meyer et al., 2000). Anthocyanin's in particular are a division of flavonoids which exhibit strong antioxidant properties and are of significant importance as they have been shown to inhibit the initiation and progression of tumour growth and neurological disorders including brain ischemia (Shin, Park, & Kim, 2006; Tsuda, Horio, Uchida, Aoki, & Osawa, 2003). In addition to anthocyanins, chlorogenic acids are a biologically active group of phenols which have been shown to reduce the absorption of glucose from the small intestine, helping to reduce instances of increased body mass (Thom, 2007). Many dietary intervention studies have reached a uniform consensus that the regular consumption of fruit helps to sustain a healthy and active lifestyle whilst also minimising the risk of cancers, cardiovascular disease, and obesity (World Cancer Res. Fund (WCRF), 2007).

The tomato is one of the world's leading staple crops and global production has risen substantially since the early nineteen sixties due to increases in yield and value (Fig 1.1: A, U.S. Dept. of Agriculture, National Agricultural Statistics Service 2009). It has also been ranked as one of the ten most important crops in the world when measuring global production value (Fig 1.1: B, Vincent et al. 2013).

This illustrates the growing popularity of the cultivated tomato and the importance of further crop improvement strategies which will introduce high throughput sequencing technologies including marker-assisted selection which allows efficient cloning of genes associated with commercial traits. Pioneering this approach was the publication of the tomato genome by the collaboration of the Tomato Genome Consortium, (Tomato Genome Consortium 2012). The information available thanks to this work will now allow the identification of domestic genes and will provide a reservoir of information to further invest in biodiversity-based breeding.

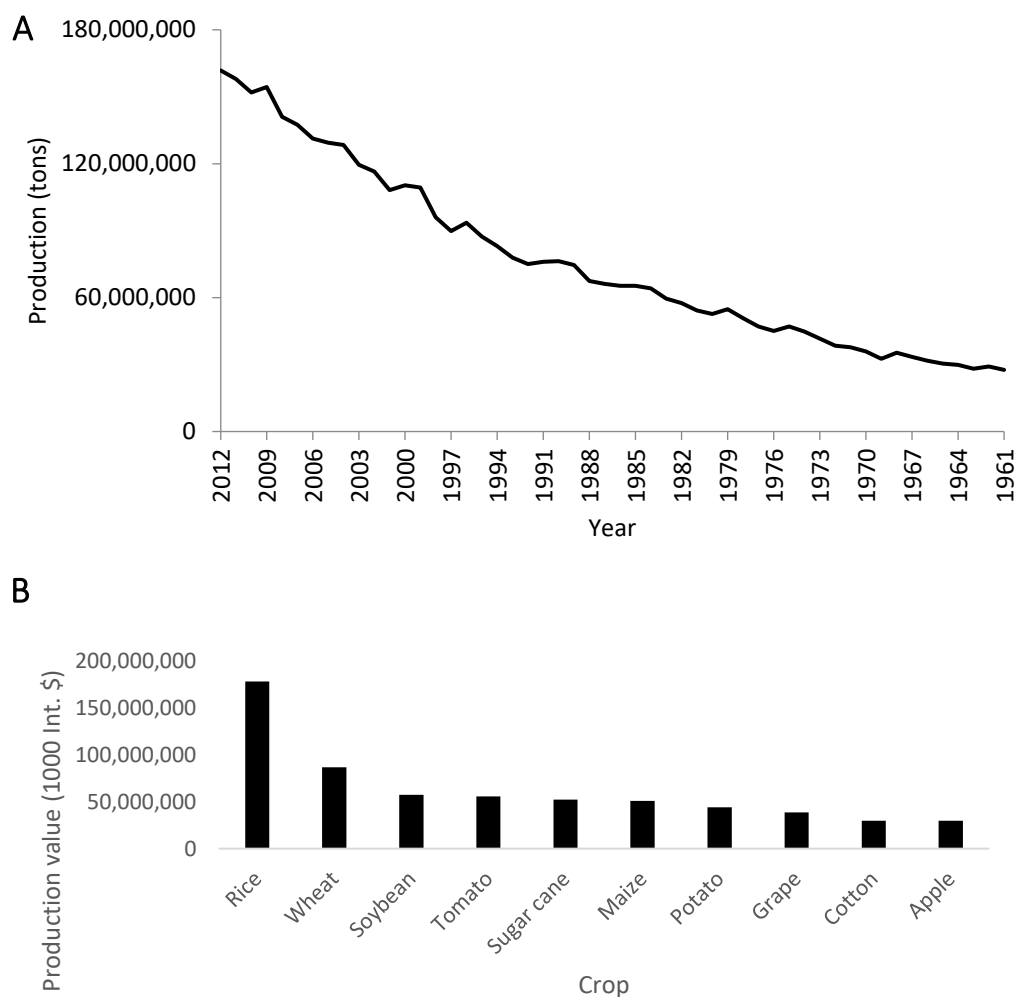


Figure 1.1: Global tomato statistics. **A)** Global Tomato Production from 1961 – 2012. **B)** The ten most important crops in terms of global production value according to FAOSTAT (2012). The production of cultivated tomato has been increasing since the 1960s and is considered one of the most valued crops in the world.

1.2 The Tomato, Nomenclature and Evolution

The tomato originated in South America and was introduced to Europe in the early part of the 16th century. The earliest record of tomato being used for human consumption was in Italy in 1544. However, the tomato wasn't fully accepted in Europe until 1840 as domestication of cultivated *S.lycopersicum* was developed to bear larger fruit of superior quality from a more upright and thick stemmed plant (Paran & Van Der Knaap, 2007).

The development of fleshy fruits is caused by multiple biochemical pathways including hormonal and genetic regulation of thousands of genes associated with the accumulation of sugars, changes in size, colour, and texture. It is these characteristics that contribute to the maturity of the fruit and increases palatability for seed dispersers and consumers. True fruits are derived from the flower gynoecium formed by the conjugation of modified leaves termed carpels (Scutt, 2006). Fertilization, the process by which a male gamete fuses with a female egg, instigates a developmental switch in which fruit develop from the gynoecium. This event is marked by the penetration of the ovule by a pollen tube and the subsequent biosynthesis of phytohormone activities like auxin and gibberellin (GA) (Dorcey, Urbez, Blázquez, Carbonell, & Perez-Amador, 2009; Serrani, Ruiz-Rivero, Fos, & García-Martínez, 2008). Following fertilization, the ovules matures within the ovary which in true fruits then ripen or split to release seeds (Lord & Russell, 2002).

Tomato is the recognised model for the study of fruit ripening due to the genetic and molecular resources available. Recent work by the tomato genome consortium has yielded a high quality genome sequence of the domesticated tomato using a combination of next generation and sanger techniques (see the Sol genomics network <http://solgenomics.net/>).

1.3 Tomato fruit development and ripening

Tomatoes are a multi-locular fruit in which the seeds mature attached to placental tissue which becomes increasingly fluid throughout development of the fruit (Gierson & Kader, 1986). A fully-ripe tomato develops pericarp tissue from the ovary wall which is sub-classified into three tissues; the exocarp (containing the cuticle layer and the skin), the mesocarp (containing high levels of chloroplasts and intracellular vacuoles), and endocarp (providing a layer between the pericarp and the locular region).

Tomato fruit development can be broadly categorized into four stages and is instigated by fertilization of the egg cells by the pollen-tube which leads to rapid cell division and can last for up to two weeks. The next step is an increase in cell expansion whereby the fruit undergoes growth which can last for up to seven weeks and leads to the mature green (MG) stage. After a number of days at the MG stage, the fruit begins to ripen which is marked firstly by the conversion of chloroplasts to chromoplasts producing a change in colour from green to red caused by the accumulation of carotenoids termed the breaker stage (BR). Finally, the end to ripening is marked by the development of an abscission zone in the pedicel which facilitates fruit separation of the fruit from the truss (Fig 1.2) (J. J. Giovannoni, 2004; Szymkowiak & Irish, 1999).



Figure 1.2: Tomato fruit development and ripening. **A)** Tomato fruit development from immature green, mature green, breaker, and red-ripening stages. **B)** Transverse section highlighting development of internal structures during ripening. Scale: 2cm. Image taken and adapted from Pesaresi et al. (2014).

Tomato weight and shape

Tomato fruit size and weight were put under significant selective pressure upon domestication of the tomato cultivar found in South America. Fruit weight is controlled by 28 genetic loci in tomato with varying degrees of influence and seven of these loci were found to have a larger influence on fruit weight (Grandillo, Ku, & Tanksley, 1999; Tanksley, 2009). Moreover, work done by Frary et al., (2000) described the underlying gene *fw2.2* responsible for the control of cell division together with a CKII kinase beta sub-unit which is instrumental in the cell signalling pathway and is a significant contributor to tomato fruit size and weight (Cong & Tanksley, 2006; Frary et al., 2000). Moreover, there is a stark contrast between tomato cultivars with reference to total cell number within the pericarp tissue promoting the importance of cell division and cell size in the total size of the fruit (Cheniclet et al., 2005).

Fruit shape has significant influence over consumer preference towards tomato cultivars. The loci that govern fruit shape in tomato are better understood than those of size and weight, this is due to loci accommodating up to 67% of the variance seen in tomatoes (Brewer, Moyseenko, Monforte, & Van Der Knaap, 2007). There are five major loci that influence fruit shape; these are *ovate*, *sun*, *fruit shape chr-8.1 (fs8.1)*, *fascinated (f)*, and *locule number (lc)* (Tanksley, 2009). *Ovate*, *sun*, and *fs8.1* are responsible for the elongation of tomato fruit with *sun* operating immediately after pollination and fertilization which indicates a role in early fruit formation (van der Knaap & Tanksley, 2001) and *fs8.1* for its phenotype in producing fruit with an uneven surface (van der Knaap & Tanksley, 2003). Moreover, it has been shown that the *f* and *lc* loci are responsible for the number of locules present in the fruit (Lippman & Tanksley, 2001; Paran & Van Der Knaap, 2007). Characterizing the loci that control for these phenotypes allows for commercially important cultivars to be optimized and explains why we have so many varieties available to us today. A commonly found result of this selection is the Giant Heirloom variety which is the combined influence of the *fw1.1*, *fw1.2*, *fw2.2*, *fw3.1*, *lc*, and *f* alleles (Fig. 1.3) (Lippman & Tanksley, 2001).

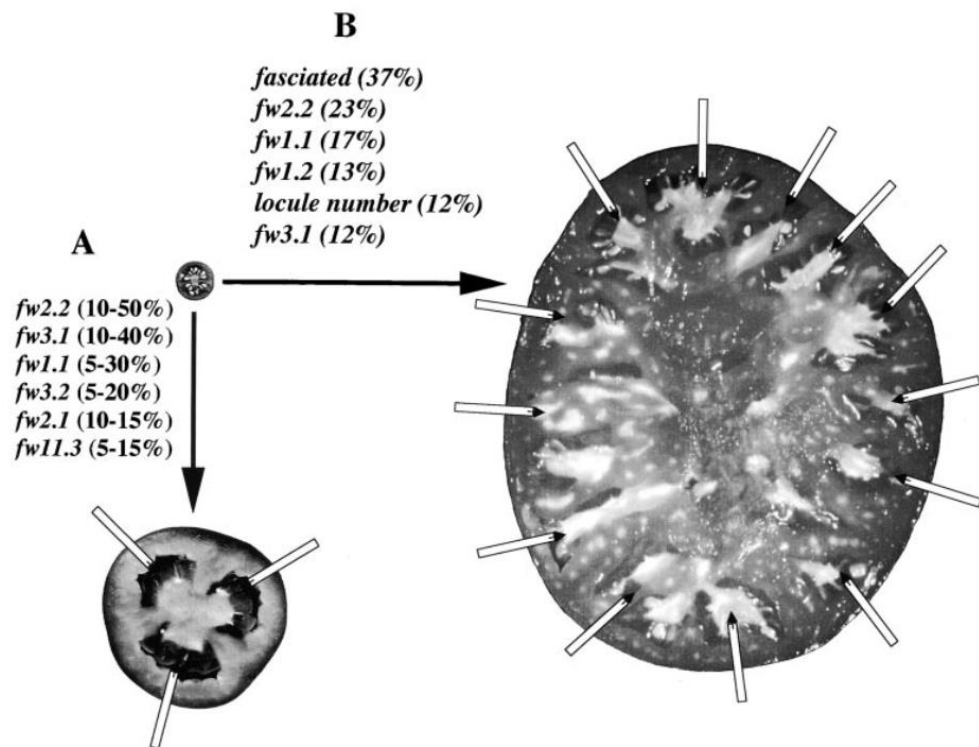


Figure 1.3: A comparison of wild-type tomato with Giant Heirloom tomato variety. **A)** Major QTL influencing fruit from the wild-type cultivar. **B)** Major QTL influencing the development of the Giant Heirloom tomato illustrating the role of *f* and *lc* in locule development. Arrows indicate the presence of locules, scale bar: 2cm. Image taken and adapted from Lippman & Tanksley (2001).

Fruit Ripening

The development of fruits is exclusive to angiosperms which is comprised of up to 400,000 species spread over a number of clades (Bremer, Bremer, & Chase, 2009). Fruits undergo biochemical and physiological changes to attract frugivores that are used as a means of seed dispersal by the plant and fruit ripening is a collection of biochemical and physiological pathways coordinated in such a way as to synchronously produce mature fruit with attractive qualities allowing it to be dispersed efficiently. These pathways range from cell-wall degradation to sugar and carotenoid biosynthesis (Jim Giovannoni, 2001).

Climacteric and non-climacteric ripening

Changes in colour, texture, and volatiles are common among all maturing fruits, however there exists two classifications of fruit. These classifications are climacteric and non-climacteric and are characterized as such based on their respiration and ethylene biosynthesis rates. Climacteric fruits include the tomato, avocado, banana, peach, plum and apples and characteristically exhibit elevated respiration and ethylene biosynthesis at the onset of ripening whereas non-climacteric fruits include strawberries, grapes, and citrus whereby ethylene is not required for a fruit to fully mature and ripen and levels of respiration remain low in the mature fruit (Lelièvre, Latchè, Jones, Bouzayen, & Pech, 1997).

Ethylene biosynthesis and perception

Ethylene (C_2H_4) is a phytohormone that is involved in numerous plant developmental responses including response to abiotic stress and promotion of ripening in certain fleshy fruits. The ethylene biosynthetic pathway was first described by Yang et al., (1984) involving two enzymes (ACC synthase and ACC oxidase) in the conversion of methionine to S-adenosylmethionine and then the formation of 1-aminocyclopropane-1-carboxylic acid and ethylene (Klee & Giovannoni, 2011; S. Yang & Hoffman, 1984).

Ethylene receptors

Plant ethylene receptors are described as “endoplasmic-reticulum associated integral membrane proteins with protein-kinase activities” (Klee & Giovannoni, 2011). Interestingly, the ethylene biosynthetic pathway is negatively regulated by ethylene receptor gene products, in which negative regulation is suppressed when ethylene is bound to the receptor, this naturally leads to an effect whereby decreasing the presence of receptors leads to an increase in ethylene sensitivity (Tieman, Taylor, Ciardi, & Klee, 2000).

In tomato, the family of ethylene receptor genes is comprised of *LeETR1*, *LeETR2*, *NR*, *LeETR4*, and *LeETR5*. These receptors interact with constitutive triple response (CRT) proteins which transmit the ethylene response with a putative MAP-kinase kinase kinase (MPKKK or MAP3K). However, silencing of any single one of these genes in *Arabidopsis* was seen to have no effect on the ethylene response suggesting functional redundancy between receptor genes. Moreover, multiple loss-of-function mutants exhibit significant phenotypes linked to the ethylene response suggesting the ethylene receptors are consistently suppressed in the absence of ethylene (Hua & Meyerowitz, 1998).

However in tomato, of these five genes, silencing of the *NR* and *LeETR1* genes conferred strong phenotypes linked to ethylene response (Wilkinson et al., 1997). Additionally, the *ETHYLENE INSENSITIVE 2 (EIN2)* acts downstream of

CTR1 in which the mutant confers ethylene insensitivity and is thought to influence the role of other hormones including auxin, abscisic acid, and jasmonate which have been shown to be instrumental in plant development and fruit ripening (Zhu, Zhu, & Shao, 2006). *EIN2* promotes downstream expression of *EIN3* and *EIL* which directly interact with ethylene responsive elements (*ERE*) that relate to many senescence and ripening related genes including *ETHYLENE RESPONSE FACTOR 1 (ERF1)* (Chao, Rothenberg, & Solano, 1997; Solano & Stepanova, 1998). The ethylene signalling pathway is illustrated in fig. 1.4 (Klee & Giovannoni, 2011).

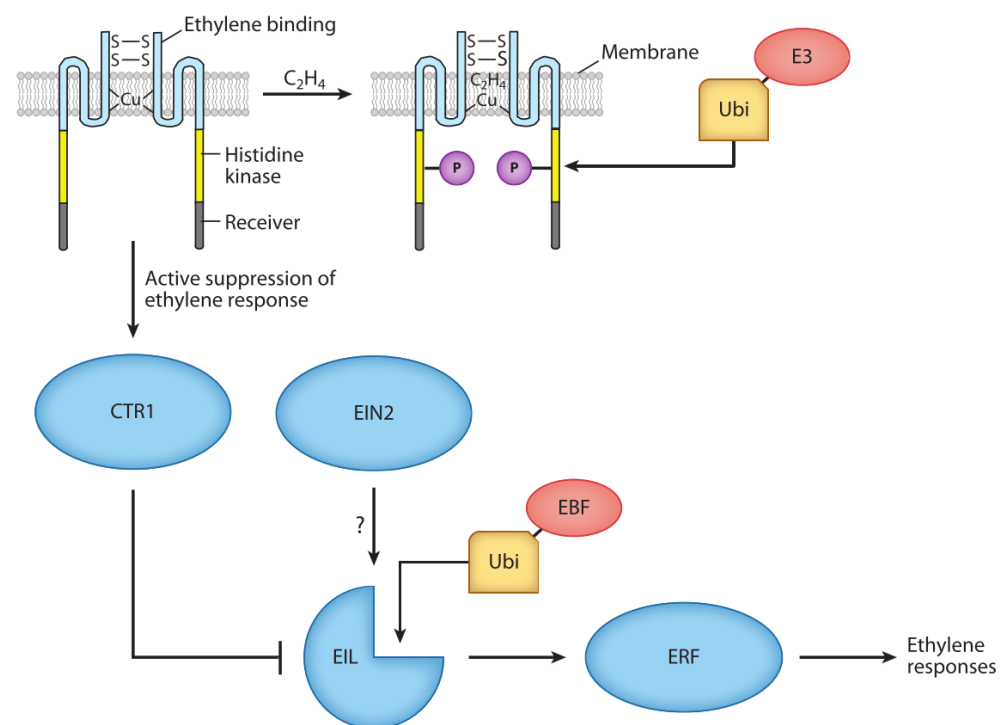


Figure 1.4: The ethylene signalling pathway. Figure illustrates the active suppression of ethylene in the absence of ethylene and the switch to an ethylene response by targeting them for degradation. Taken and adapted from Klee & Giovannoni (2011).

Non-climacteric fruits including strawberries and grapes exhibit the same biochemical and physiological changes that are characteristic in ripening but do not require the presence of ethylene to begin ripening. However, there is evidence that non-climacteric fruits have conserved downstream regulation of *ETHYLENE INSENSITIVE (EIN3)* and *EIN3*-like genes (Cara & Giovannoni, 2008). Moreover, ethylene interacts with the Raf-like kinase protein *CTR1* in tandem with other plant hormones such as *SITPR1* which in turn activate ethylene receptors *LeETR1* and *NEVER RIPE (NR)*, the mutant for which confers ethylene insensitivity and the discontinuation of ripening (Lin et al., 2008).

1.4 Transcriptional control of ripening

The initiation of ripening has been shown to involve transcription factors independent of ethylene-biosynthesis and perception, these factors have been characterised by the mapping of spontaneous ripening single-gene mutants which include the *ripening inhibitor (rin)*, *non-ripening (nor)*, and *Colourless non-ripening (Cnr)* mutants (J. J. Giovannoni, 2007; Manning et al., 2006; Vrebalov, 2002). These mutants all convey strong ripening phenotypes and have been instrumental in the understanding of fruit development and the transcriptional control of ripening.

Ripening-inhibitor (RIN)

RIN is a member of the SEPALLATA4 (*SEP4*) clade of MADs-box genes and is termed *LeMADS-RIN*. The *rin* mutant is dominant and is required in tomato for the biosynthesis of ethylene which has the knock-on effect of instigating cell-wall metabolism, carotenoid formation and the generation of ATP and has such been classified as a master regulator of fruit ripening. *rin* was characterised by sense and anti-sense constructs under a CaMV35 promoter whereby over-expression of the *rin* gene complemented the ripening deficiency found using the antisense construct. Fruits derived from silencing of the *rin* gene are incapable of ripening and remain green with the absence of cell wall enzyme activity and carotenoid pigments (Vrebalov, 2002).

RIN has been observed to interact with a number of promoters of genes also involved in fruit ripening including the *NOR*, *CNR*, and *HB1* transcription factors, ethylene response genes such as EIN4 and EIN8, cell wall modifying genes and carotenoid biosynthesis genes such as PG, EXP1, and PSY1 (Martel, Vrebalov, Tafelmeyer, & Giovannoni, 2011).

Phylogenetic analysis of *RIN* has characterized orthologous genes in *Arabidopsis* and *Antirrhinum*. The APETALA1 (*AP1*) and the *SQUAMOSA (SQUA)* AP1 orthologue are commonly associated with sepal and petal development in

the flowers of *Arabidopsis* and *Antirrhinum* whose expression is absent in *rin* mutants (Gustafson-Brown, Savidge, & Yanofsky, 2016). Silencing of these genes leads to a loss of petal development in most flowers and emphasizes the role and homology of *LeMADS-MC* and *LeMADS-RIN* across species.

Colourless non-ripening (CNR)

The SQUAMOSA promoter binding protein (SBP-box) colourless non-ripening (*Cnr*) mutation is similar to the *rin* mutant in that they both share a significant impact on ethylene dependent & independent fruit ripening. However, *Cnr* is a dominant mutation and acts downstream of *RIN* (Manning et al., 2006). The mutation is induced by the methylation of the *CNR* promoter (Manning et al., 2006), that suppresses further gene expression and therefore prevents interaction of *rin* within the target loci and prevents downstream expression of ripening related genes such as *TDR4* and *PG2A*, a significant polygalacturonase gene (Bemer et al., 2012). The mutation interferes with normal ripening of tomato generating a colourless and mealy texture within fruits and demonstrates a key role in the transcriptional regulation of fruit ripening (Manning et al., 2006).

Like *RIN*, the *Cnr* gene was found to share significant homology with genes associated with reproductive development suggesting that a likely switch has occurred in angiosperm evolution to allow these same genes to act upon fruit ripening (Gustafson-Brown et al., 2016).

Non-ripening (NOR)

NOR is a NAC-domain transcription factor and when mutated also prevents tomato fruits from ripening normally like *rin*. Strong interactions occur between *MADS*-box genes and NAC domain transcription factors which is significant given the extreme phenotypes seen in the mutant lines (Martel et

al., 2011). *NOR* is involved in a positive feedback loop involving *rin*-binding to promote further *NOR* expression among other feedback loops including *AP3*, and *AGL15* (Butelli et al., 2008; j j Giovannoni et al., 1995).

Gene regulatory networks

The MADS-box transcription factor RIN has been chosen as a target for understanding the downstream effects of transcriptional regulators on fruit development in part due to its commercial use and importance in prolonging shelf-life. Using chromatin immunoprecipitation, RIN was found to interact with the promoters of genes linked to cell-wall metabolism, ethylene biosynthesis, carotenoid accumulation, and a number of ripening related transcription factors (Martel et al., 2011).

To fully understand the development of tomato fruit and the transcriptional regulation of fruit ripening, it is important to understand how relevant domains interact with each other and the role of some of the additional 200 transcription factors also involved in fruit maturation. Very little is understood about the downstream effects of key transcriptional regulators and investigations into these processes will produce an overall transcriptional control network to explain the mechanistic basis of fruit development.

1.5 The plant cell-wall and texture modification during fruit ripening

A study in sensory quality of fresh French and Dutch market tomatoes concluded that in addition to size, shape, and colour; fruit texture is instrumental in driving consumer preferences when purchasing fruit. Consumers were found to be less inclined to purchase fruit with softer or mealy textures (Sinesio et al., 2010). This attribute is a major influencing role in the shelf-life of fruit which allow for more efficient shipping and storage where conversely, softening of fruit increases its susceptibility to physical damage and can lead to pathogenicity or postharvest waste (J. K. C. Rose, Labavitch, & Vicente, 2007). For these reasons, understanding the key regulators controlling fruit texture has significant economic benefits, especially if postharvest life can be extended without compromising flavour.

Fruit softening is the result of remodelling within the plant cell wall by cell wall degrading enzymes. Plant cell walls are comprised primarily of polysaccharides, highly glycosylated proteins, and in some instances lignin (Somerville et al., 2004). To give an account of the complexity involved in characterising the plant cell wall, the Arabidopsis and tomato genomes contain in excess of 700 genes associated with glycosyltransferases and hydrolases in addition to several hundred genes affiliated with biosynthesis and function of the plant cell wall of which a very small proportion have been characterised (Henrissat et al. 2001; Tomato Genome Consortium 2012).

Plant cell-wall polysaccharides are the most abundant biopolymers in existence and are the key structural components of cell walls. The plant cell wall is formed by “crystalline cellulose micro-fibrils made up from interlinking unbranched (1, 4)-linked β -D-glucans embedded within complex polysaccharides” (Minic & Jouanin, 2006) subdivided into cellulose, pectins, or hemicelluloses. Hemicelluloses are polysaccharides that help to form a strong interlinking network which provide structure and support to the plant (Cosgrove, 2005).

Similarly, pectins are an equally complex and diverse group of polysaccharides that have a number of functions and are typically responsible for the plants porosity and intracellular adhesive properties (Willats, McCartney, Mackie, & Knox, 2001). Pectins are comprised of homogalacturonam (HG), rhamnogalacturonam I (RG-1), rhamnogalacturonam II (RG-II) and xylogalacturonam (XGA) (Vincken et al., 2003), and cross-link with calcium to form helical chains that further cross-link to form a gel-like structure. This cross-linking with di-hydroxycinnamic acids allows the formation of covalent bonds with other polymers (Minic & Jouanin, 2006). Cellulose biosynthesis is regulated by large membrane based cellulose synthase complexes that produce micro-fibrils directly from the cell surface (Fig. 1.5: Cosgrove 2005).

Matrix polysaccharides differ in that they are synthesised within the Golgi apparatus and are delivered to the cell wall packed into vesicles which are fused by numerous physical interactions, enzymatic ligations, and crosslinking interactions. HG is found in the highest abundance and will therefore have the most significant influence on the integrity, and breakdown of the cell during fruit ripening (Caffall & Mohnen, 2009).

The consistently high turgor pressure of the plant cell has been shown to influence fruit softening (Proseus & Boyer, 2005) and as such, the role of cell wall-associated structural proteins and their corresponding enzymes in fruit development and ripening is under complex control and strongly impacts fruit quality, shelf life and texture (Fry, 2004).

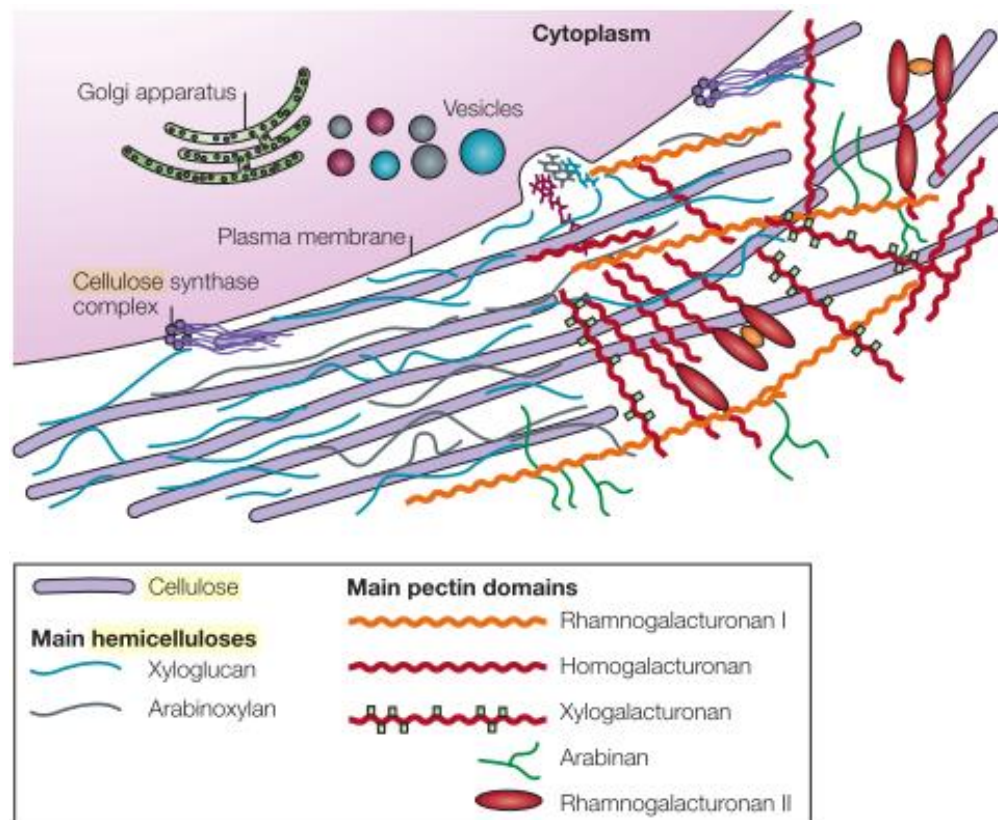


Figure 1.5: Structure and Development of the primary cell wall. The cellulose micro-fibrils are synthesised by the cellulose synthase complex embedded within the plasma membrane. Alternatively, the matrix polysaccharides are synthesised by the Golgi apparatus and transported to the cell wall. Figure taken and adapted from Cosgrove., (2005).

Cell wall remodelling

The degradation of cell wall polysaccharides has been widely observed during fruit development and is dependent on a number of enzymes. These enzymes have previously been characterised by their localised site of activity by Fry (2004), whose sites include exo-polysaccharidases which act on the non-reducing terminus of oligosaccharides, and endo-polysaccharidases which work on the polysaccharide backbone, and other outlying hydrolases whose activity includes O-acetyl, O-methyl, and O-feruloyl (Fry, 2004).

Cell wall remodelling during fruit ripening is a widely adaptable process that varies across species depending on each individual species' rate of maturation. The initial steps of ripening require the solubilisation of pectin and subsequent depolymerisation in the later stages of ripening (Dawson, Melton, & Watkins, 1992).

Polygalacturonase (PG)

PG activity is localized within the middle lamella and appears to be responsible for pectin depolymerisation (Fischer & Bennett, 1991). PG anti-sense constructs where the gene is silenced have shown little effect on overall fruit softening, ethylene bio-synthesis, and colour development suggesting that there are alternative mechanisms that govern pectin depolymerisation in addition to PG (JJ Giovannoni & DellaPenna, 1989; Smith et al., 1988).

Nevertheless, silencing PG has been shown to produce increased viscosity and fruit with lower susceptibility to post-harvest pathogens. This may be due to lower levels of PG preventing depolymerisation of the pectin backbone in the event of post-harvest physical damage; which normally leads to cellular leakage and promotes further deterioration of the cell-wall in the presence of residual polygalacturonases (Goulao & Oliveira, 2008; Kramer et al., 1992).

Pectin methyl esterase

Pectin-methylesterase (PME) is synthesised during ripening and is responsible for the removal of methyl groups from pectic polysaccharides. PME expression is linked closely to PG activity suggesting a key role in fruit ripening. Moreover, the substrates produced from PME include homogalacturonan which then, becomes more susceptible to hydrolysis by PG. Unlike PG though, PME has been shown to promote cell adhesion by facilitating cross-linking between pectin molecules. Conversely, gene silencing of PME produced fruit with an increased rate of ripening (Jolie, Duvetter, Van Loey, & Hendrickx, 2010). Initial experiments into cell wall remodelling suggested that PG and PME activity would need to play significantly larger roles in texture changes to have been negated by silencing experiments. This suggests that other genetic loci may play a greater role in fruit softening during ripening (Seymour, Chapman, Chew, & Rose, 2013).

Pectate lyase (PL)

The PG and PME genes all show elevated expression at the onset of ripening highlighting their roles in tomato fruit ripening, however single-mutant knock-downs were unable to facilitate a significant change in fruit texture (Sheehy, Kramer, & Hiatt, 1988; Smith et al., 1988). PL depolymerizes pectin in the middle lamella and primary cell wall via a β -elimination mechanism that is substantially different to that of hydrolytic cleavage by PG. In 2002, PL was shown to reduce fruit softening in strawberry using an antisense construct (Jiménez-Bermúdez et al., 2002). More recently, PL has been identified under a major QTL and RNAi and CRISPR have been used to silence PL in transgenic tomatoes. These experiments have demonstrated that PL plays a very significant role in tomato fruit softening. These transgenic lines result in fruits with firmer fruit texture in the outer and inner pericarp tissue without detrimental effects on flavour or colour (Uluisik et al., 2016).

Expansins, and cellulases xyloglucan endotransglucosylase (XTH)

The expansins are a class of cell wall localised proteins that are thought to cause cell loosening by disrupting the hydrogen bonds between cellulose micro-fibrils and matrix polysaccharides. In tomato, six expansin genes have been characterised to have overlapping and variable expression patterns leading up to the mature green stage of fruit development followed by the continued expression of 3 expansin genes in ripening fruit (J. K. Rose, Lee, & Bennett, 1997). The precise mode of action of the expansin proteins remains inconclusive, but their importance in maintaining cell wall stability is clear.

Cellulases are a class of enzymes that are upregulated during ripening. Their action may be limited to certain forms of cellulose and promotes cell slippage within the middle lamella causing the fruit to soften as ripening develops (Hobson, 1968). Cellulases are likely to work synergistically with expansins which promote glucan accessibility and therefore increase the rate of enzymatic attack (Cosgrove, 2005).

The XTH enzymes are a group of enzymes that promote the disassembly of xyloglucan from the cell wall for further depolymerisation by other cell-wall degrading enzymes. There are twenty-five XTH protein encoding genes present in tomato, and fifteen are expressed during ripening in an ethylene dependent manner. Overexpression of the *SIXTH* genes produces fruit with decreased xyloglucan depolymerisation and therefore an increase in fruit firmness. This means that the xyloglucan structure is strongly linked to fruit softening and XTH plays a key role in the ripening of climacteric fruits (Muñoz-Bertomeu, Miedes, & Lorences, 2013).

There are a number of other cell wall proteins linked to ripening which show ripening-related changes in gene expression. These include extensins, arabinogalactan proteins and tetraspanins (Tomato Genome Consortium 2012). Work at Syngenta has indicated a relationship between shelf-life, fruit softening and the expression of tetraspanin-like genes in melon along with another class of proteins that have been linked to fruit ripening and have never been fully investigated, the Heat shock proteins (HSPs). Little is known about the role of these gene products in tomato and it is likely that these proteins play a role in fruit softening and may influence shelf-life in tomato.

Tetraspanins have been studied in far more depth in animals due to their prominent role in the pathogenesis of infectious diseases (Annemiek B van Spriel & Figdor 2010). Very little is known about the role of these proteins in plant development and no functional association has been published with regard to fruit development and ripening, although examination of the tomato expression database indicates that there are several tetraspanins expressed in tomato fruit during this part of development.

Additionally, studies at Syngenta (Hurr, unpublished) indicate that a tetraspanin gene was a likely candidate for underlying a melon shelf-life QTL. The melon gene encodes a protein with strong homology to tomato tetraspanin-6 (SolyC04g049080). Previous functional analysis of the tetraspanins has suggested strong links with cell-cell adhesion and anchoring (DeSalle et al. 2010; Charrin et al. 2009), and we hypothesise that it is these properties that play a role in cell adhesion during ripening. We predict that the overexpression of tetraspanins in fruit tissue will enhance the shelf life of tomatoes and other fruits by strengthening cell to cell connections based on the Syngenta melon QTL studies.

1.6 Tetraspanin; Structure, origins, and function

Cell-cell communication is essential for development of multicellular organisms. In plants, the plasmodesmata, plasma membrane, and cell wall are critical interfaces for signal sensing. Many conserved signal recognition proteins are found anchored in the plasma membrane and these proteins typically exhibit ligand binding to extracellular domains that initiate signalling cascades inside the cell (Clark, 2001). Tetraspanins are such a class of integral membrane proteins which include two highly conserved leucine rich extracellular domains and a cytoplasmic carboxy-terminal domain (Charrin et al., 2009) (Fig. 1.6).

The tetraspanins are between 200 and 300 amino acids long and contain four transmembrane domains which include a small extracellular loop (varying in size between 13 and 30 amino acids), an intracellular sequence, and a second larger and more variable extracellular loop thought to be responsible for much of the proteins activity, the larger loop characteristically contains a highly conserved Cys-Cys-Gly (CCG) motif (Todd & Maecker, 1997).

The origins of the tetraspanin superfamily suggests repeated gene duplications and divergence emphasised by gene loss and positive selection as opposed to respective convergence (Garcia-España et al., 2008). Tetraspanins are found in every phylum highlighting their importance in developmental processes, to date 33 tetraspanins have been characterised in humans, 37 in *Drosophila melanogaster*, and 20 in *Caenorhabditis elegans*. Research into the tetraspanins in plants however lag significantly behind their animal counterparts. Seventeen tetraspanins have been characterised in *Arabidopsis thaliana* with the expression data and broad phenotypic analysis of the proteins recently published in 2015 (F. Wang et al., 2015). Moreover, characterisation of tetraspanins in ripening fruits is largely unknown with the recently published tomato genome presenting 12 tetraspanins in *Solanum lycopersicum* (Tomato Genome Consortium 2012).

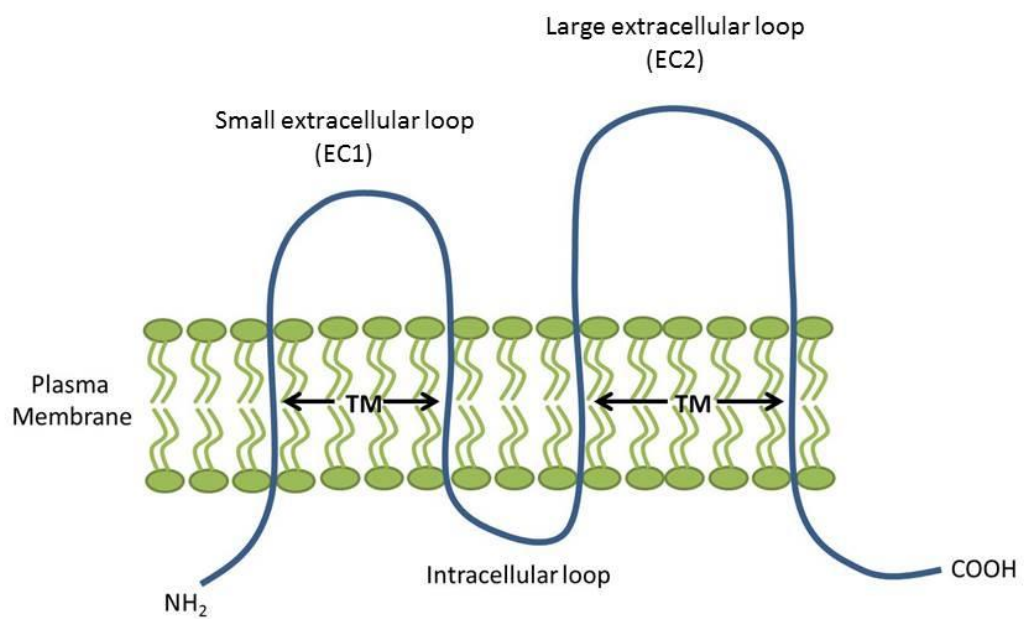


Figure 1.6: The tetraspanin protein. Represented are the five distinct and functional regions. The large extracellular loop (EC2) containing a variable and constant region responsible for inter and intra molecular homo-dimerization. The small extracellular loop (EC1), transmembrane domains (TM), the C-terminal tail (COOH) and the intracellular loop.

Function

It is thought that tetraspanins acts as ligands for extracellular molecules to form tetraspanin-enriched micro-domains. The transmembrane superfamily has been characterised in mammalian systems primarily in the interest of hepatitis-C pathogenesis and reproductive development (Jégou et al., 2011; Seigneuret, 2006). In plants however very little is known about the function of tetraspanins. Seventeen genes (*AtTET1-17*) have been described to date using the model *Arabidopsis thaliana*, and the functions of the majority of these remain unknown (F. Wang et al., 2015). Using “Electronic Fluorescent Pictographs”, Winter et al., have used microarray data to visualize gene expression patterns which has produced the organ type and developmental stage of tetraspanin expression. They found that expression patterns ranged over a variety of organs at all stages in the life of the plant from the shoot apical meristem, primary root, and carpel, to pollen grains (Winter et al., 2007). Interestingly, they have suggested a possible role for the tetraspanin protein in mediating the roles of GENERATIVE CELL SPECIFIC 1 and HAPLESS 2 proteins which are responsible for membrane fusion between gametes (Sprunck & Dresselhaus, 2009). Further proteomic analysis of *TET1* mutant alleles have been shown to disrupt auxin distribution in *Arabidopsis thaliana* leading to reduced primary root growth, smaller leaves, and reduced leaf symmetry suggesting a key role in plant development (Cnops, Neyt, & Raes, 2006).

Tetraspanin transmembrane domains

The transmembrane domains show the highest similarity across species (between 70-90%) and are characteristic of the proteins nomenclature. Six naturally occurring mutations in TM-regions 1, 2, and 4 have been linked with retinol dystrophies in *Drosophila melanogaster* which impart the importance of these regions for effective membrane trafficking (Stipp, Kolesnikova, & Hemler, 2003).

In plants, these domains enable protein trafficking and biosynthesis which include polar residues whose unique chemistry encourage the formation of strong hydrogen bonds which act to stabilize the tetraspanin tertiary structure and drive dimerization (Cnops et al., 2006; Stipp et al., 2003). Phylogenetic study of these regions show an evolutionary divergence in *Arabidopsis* between tetraspanins *AtTET1-10* and *AtTET11-17*. The *AtTET1-10* clade was found to be uniformly expressed in seedlings, roots, leaves, and sepals. Interestingly however, homologues to these tetraspanins showed differential expression (within root hairs, flowers, and leaves) suggestive of functional divergence following gene duplication events. Alternatively, the *AtTET11-17* sub-clade was found to exhibit similar *in-silico* expression patterns as the *AtTET1-10* clade but are spatially contained to pollen highlighting a separate and significant role in plant reproduction (F. Wang, Vandepoele, & Van Lijsebettens, 2012).

Extracellular Loops

The longer extracellular loop in plants is considered one of the primary functional regions of the tetraspanin protein, exhibiting two of the five distinct functional regions (Stipp et al., 2003). These loops show significantly more sequence divergence than the intracellular and trans-membranous regions, for example, conservation of Extracellular loop 1 (EC1), and Extracellular loop 2 (EC2) between human and zebrafish orthologues was shown to vary between “43-58% for extracellular domains and between 72-83% between intracellular regions” (Stipp et al., 2003). The EC2 region was found to contain a variable region which drives interactions with other proteins, and a conserved region responsible for homo-dimerization. The higher number of cysteine residues in plants has been implicated in making the formation of disulphide bridges between molecules and has been strongly linked to offsetting enzymatic action of anti-tetraspanin complexes (F. Wang et al., 2012).

Very little progress has been made with regard to the characterization of the small extracellular loop (EC1), the region has been shown to contain one cysteine residue suggesting a possible role in crosslinking with the large extracellular loop (EC2) (DeSalle, Mares, & Garcia-España, 2010). A study was conducted in which the EC1 region was replaced with a linker sequence, whereby expression of EC2 was found to be significantly decreased. This assessment reinforces the potential role for EC1 in successful development and maturation of EC2 structure and functionality (Masciopinto, Campagnoli, Abrignani, Uematsu, & Pileri, 2001).

Cytoplasmic domains

In addition to the highly variable extracellular regions of the tetraspanin protein, The N- and C- terminal domains are situated within the cytoplasm. These intracellular regions also contain cysteine residues and are termed palmitoylation sites that facilitate ligation between the tetraspanin family and their corresponding interactors (Charrin et al., 2002). These terminal regions are essential for the formation of the tetraspanin-web and have been observed to effect cell adhesion and membrane fusion (Edrington, Yeagle, Gretzula, & Boesze-Battaglia, 2007; H.-X. Wang, Kolesnikova, Denison, Gygi, & Hemler, 2011). Knockout of the C-terminal tail in the plant specific tetraspanin *TET1/TRN2* gene have shown significant phenotypes including defects in plant growth and floral patterning, emphasizing the role of tetraspanins in cell-cell signalling, and stability during plant development (Cnops et al., 2006).

Tetraspanin-enriched micro-domains

The formations of the tetraspanin enriched micro-domain (TEM) are classified into three categories. An interaction between a tetraspanin and a non-tetraspanin ligand is considered a primary interaction. These ligands can include immunoglobulins, ecto-enzymes, intracellular signalling molecules, and

integrins. Of these ligands, the integrins have been seen to affect cell-cell adhesion during reproductive processes and may be a key factor during fruit development (Rubinstein, 2011; F. Wang et al., 2012). Conversely, an interaction involving a tetraspanin and a residue originating from a family member are considered secondary interactions (Rubinstein, 2011). Both primary and secondary interactions are classified as direct interactions, where tertiary interactions differ is in the presence of lipids which act to compete with the primary or secondary complexes forming a tertiary interaction (Charrin et al., 2009).

1.7 Heat shock transcription factors

Abiotic stress is the most significant contributor to loss of crops in the world with yields being affected by up to 50% making the importance of understanding the mechanisms by which plants achieve thermotolerance a high priority (W. Wang, Vinocur, & Altman, 2003). Abiotic stress causes multiple branching responses by either physiological, biochemical, or molecular pathways and thermotolerance requires a number of response mechanisms to work synergistically to prevent cellular damage in order to re-achieve homeostasis (W. Wang et al., 2003). Maintaining the physical and functional properties of proteins is a significant challenge for plants, especially in the face of drought, cold, heat, salinity, and chemical toxicity. As such, all organisms utilise heat shock proteins when exposed to heat stress and plants contain the most abundant and diverse range of these proteins (W. Sun, Bernard, van de Cotte, Van Montagu, & Verbruggen, 2001).

Structure and function

Heat shock proteins (HSPs) are responsible for protein folding, translocation, and degradation in a variety of cellular processes employed by all organisms but especially plants. The expression of genes encoding these proteins is regulated by heat-shock transcription factors (Hsfs) which are characterized into three major families whose classes (A, B, and C) and corresponding Sly codes are described in Table 1.1 (Scharf, Berberich, Ebersberger, & Nover, 2012). These proteins are characterised by their modular structure which includes a DNA binding domain (DBD), a highly conserved intron sequence, an oligomerization domain (OD), a nuclear localisation signal (NLS), Nuclear export signal (NES), and activator motifs (AHA) (Fig. 1.7).

DNA binding domain (DBD)

The DNA binding domain is situated at the N-terminus and contains a highly conserved three-helical bundle and a four-stranded anti-parallel β -sheet (Damberger, Pelton, Harrison, Nelson, & Wemmer, 1994). This structure allows

precise interactions between the Hsfs and heat stress promoter elements (HSE) which promote expression of downstream HSPs.

Oligomerization domain (OD)

The OD is the next significant domain in the Hsf gene family. The length of the flexible linker region between the OD and the DBD is how the Hsfs are characterized into three classes (A, B, and C). For classes A and C, the amino acid linker sequence is less compact than class B with 21 (Class A) and 7 (Class C) insertions.

Nuclear localization and export signal (NLS & NES)

The NLS is situated at the C-terminal region of the OD and works concurrently with the NES to localize Hsf expression between the nucleus and the cytoplasm. A leucine rich, hydrophobic NES promotes nuclear export together with the AHA motifs (Heerklotz, Döring, Bonzelius, Winkelhaus, & Do, 2001).

Table 1.1: Classification of heat shock transcription factors

Name	Tomato Sly (24)			
<i>HsfA1</i>	SI08g005170	SI03g097120	SI08g076590	SI06g072750
<i>HsfA2</i>	SI08g062960			
<i>HsfA3</i>	SI09g009100			
<i>HsfA4</i>	SI03g006000	SI07g055710	SI02g072000	
<i>HsfA5</i>	SI12g098520			
<i>HsfA6</i>	SI09g082670	SI06g053960/50		
<i>HsfA7</i>	SI09g065660			
<i>HsfA8</i>	SI09g059520			
<i>HsfA9</i>	SI07g040680			
<i>HsfB1</i>	SI02g090820			
<i>HsfB2</i>	SI03g026020	SI08g080540		
<i>HsfB3</i>	SI04g016000	SI10g079380		
<i>HsfB4</i>	SI04g078770	SI11g064990		
<i>HsfB5</i>	SI02g078340			
<i>HsfC1</i>	SI12g007070			

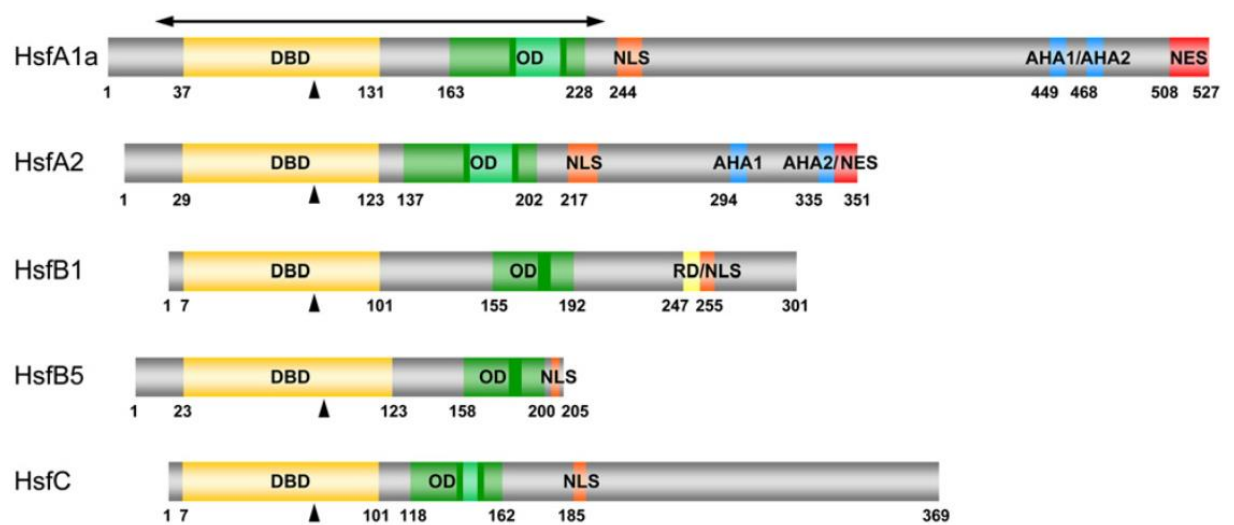


Figure 1.7. Structure of tomato Hsfs. The structure of tomato Hsfs includes the DBD, OD, NLS, NES, and AHA sequences with varying sizes in the linker sequences providing the basis on how they are characterized. The arrow in the DBD signifies the presence of a conserved intron sequence. Figure taken and adapted from Scharf et al., (2012).

Activity of Hsfs is dependent on homo- and hetero- oligomer formation within the OD. Plants are heavily dependent on heat-shock proteins to maintain thermotolerance and as such, the *HsfA1* gene has been characterized as the master regulator of thermotolerance in tomato. Co-suppression of this gene (Sl08g005170) significantly reduces thermotolerance and plant viability and over-expression was shown to increase thermotolerance (Mishra et al. 2002). Whilst the remaining Hsfs are not as essential to plant survival as *HsfA1*, *HsfA2* expression works synergistically with *HsfA1* to form a super-activator complex which promotes higher expression of downstream HSPs than either Hsf is singularly capable of (Chan-Schaminet, Baniwal, Bublak, Nover, & Scharf, 2009). Conversely, *HsfA4* is an antiapoptotic factor that controls the levels of ROS and is inhibited by *HsfA5* DNA binding so modulation of *HsfA4* by *HsfA5* promotes proapoptotic action (Shulaev, Schlauch, & Mittler, 2005).

Regulatory network

Heat-shock regulation comprises a number of molecular networks, of which the Hsfs are considered the master regulators. In the face of changing environmental conditions, plants require a dynamic system to survive the corresponding stress conditions. They achieve this through use of the Hsfs which have been shown to regulate individual HSPs such as Hsp70 and Hsp90 (Hahn, Bublak, Schleiff, & Scharf, 2011). Exposure to heat-stress (HS) initially promotes the release of *HsfA1*, *HsfA2*, and *HsfB1* which immediately initiate the HS response. These three transcription factors work to maintain high levels of HS related gene expression by facilitating activation of the appropriate promoter sites. Upon recovery, inactivation of *HsfA1* is achieved through binding of Hsp70 and Hsp90 with *HspA1* and *HspB1* respectively (Bharti et al., 2004).

Hsf regulation has also been reported at the post-transcriptional and translational level. Under HS, alternative splicing of the intron sequence in the DBD promotes a truncated HsFA2 variant which binds to the TATA box clusters within the AtHSFA2 promoter region, activating its own expression (Sugio,

Dreos, Aparicio, & Maule, 2009). This process is speculated to enhance levels of *Hsf2A* during a heat response but has not been characterized in other splicing events (H. Liu & Charng, 2013).

Heat-shock proteins

In tomato, recent phylogenetic analysis of the genome has characterized twenty-six heat-shock proteins (Fig. 1.7), thirteen of which exhibit fruit and ripening based expression suggesting a significant role in fruit ripening. A further six of these show an increase in expression after HS highlighting their roles in the tomato stress response (The Tomato Genome Consortium, 2012; X. Yang, Zhu, Zhang, Liu, & Tian, 2016). Many of the tomato heat-shock proteins remain uncharacterized. However, Overexpression of the *SlyHSF-02* gene has been linked to the initiation of a stress response leading to increased thermotolerance in tomato (Mishra et al., 2002). Additionally, two heat-shock proteins (*SlyHSF-25* & *SlyHSF-26*) were found to be closely linked to their corresponding *Arabidopsis* genes which exhibit uncharacteristically low expression which has been speculated to be the result of duplication within the *SlyHSF-16* gene (X. Yang et al., 2016).

The role of Hsfs in the stress response of plants is well described, however their role, if any in fruit ripening is still largely unstudied. A number of heat-shock proteins have been linked to fruit-ripening but their transcriptional regulators have not been fully characterized. Phylogenetic analysis of all the heat-shock transcription factors and proteins in tomato will pave the way for future investigations into their effects on plant development and responses to heat-stress. With so many potential targets to influence fruit ripening, a more targeted approach is needed.

AIMS AND OBJECTIVES

The major aim of this project was to investigate the function of novel shelf-life-related genes in fruits using tomato as a model system, specifically tetraspanins and a heat shock transcription factor.

Specific Objectives

1. Characterize the role of tetraspanins during ripening using constitutive knock-down and over-expression constructs in tomato.
2. Examine the effect of silencing a heat shock transcription factor on tomato ripening.
3. Investigate the down-stream effects of silencing the tetraspanin genes and a heat-shock transcription factor on ripening related gene expression.

Chapter 2

Materials and Methods

2.1 Tomato plant Material and Fruit Selection

Tomato (*Solanum lycopersicum*) cv. Ailsa Craig was grown under standard glasshouse conditions at 22°C during the day and 20°C at night. Supplemental lighting was provided when required. To select material at the required developmental stage, the flowers were tagged at anthesis and fruits were then harvested at mature green (40 dpa), breaker (B) when yellow or orange colour first becomes noticeable, and then at selected days' post breaker, typically 4, 7, 10, and 14.

2.2 Arabidopsis plant Material

The mutant lines for *AtTET5.1* (SALK_020009) and *AtTET-5.2* (SALK_148216) were obtained from the European Arabidopsis Stock Centre (<http://www.arabidopsis.org/>). Seeds were surface sterilised in 70% EtOH for 2 minutes, and then washed with sterile water and mixed with 50% bleach for 5-10 minutes. The bleach was discarded and seeds were washed thoroughly with sterile water and dried on sterile blotting paper. Seeds were germinated on Murashige and Skoog medium supplemented with 1% (w/v) Sucrose and 0.8%(w/v) agarose, pH5.7. Seeds were then stratified at 4°C overnight before being moved to a growth chamber. Precise durations of growth and conditions vary and are described in the relevant sections.

2.3 Sugar content and colour measurements

A drop of juice from the pericarp tissue was placed on a hand held refractometer and the percent of soluble sugars was determined.

Fruit colour was determined using a Minolta colorimeter CR400. The three values given are labelled L*, a* and b* (Fig. 2.1). The values are described as the tomato colour index data (TCI) (Richardson & Hobson, 1987).

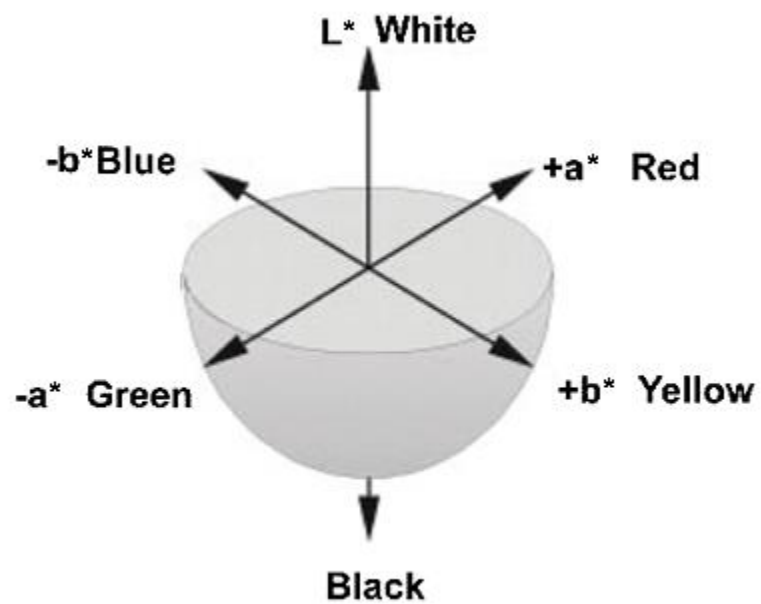


Figure 2.1. The Hunter L^* , a^* , and b^* colour space. The scales depict the three axis on which colour is described using a colorimeter.

2.4 Fruit Texture Measurements

Fruit texture measurements were made from the pericarp tissue of tomato fruits using a NEXYGEN LR machine. A 6-mm transverse section was cut from each fruit, and the maximum load (the force required to penetrate the pericarp tissue at 10 mm min^{-1}) was measured using a Lloyd Instrument LF plus machine equipped with a 10-N load cell and 1.6-mm flat-head cylindrical probe. Measurements were taken separately from the outer and inner pericarp in duplicate. Outer pericarp was defined as the area below the skin but before the vascular boundary. The inner pericarp was defined as the cells between the vascular boundary and the endodermis.

2.5 Plasmid construction and generation of transgenic plants

Plasmids were generated using Gateway cloning technologies, the overview for each cloning step is described below for *SITET-8* (Fig. 2.2 and Fig. 2.3) and *SIHST-14* (Fig. 2.4).

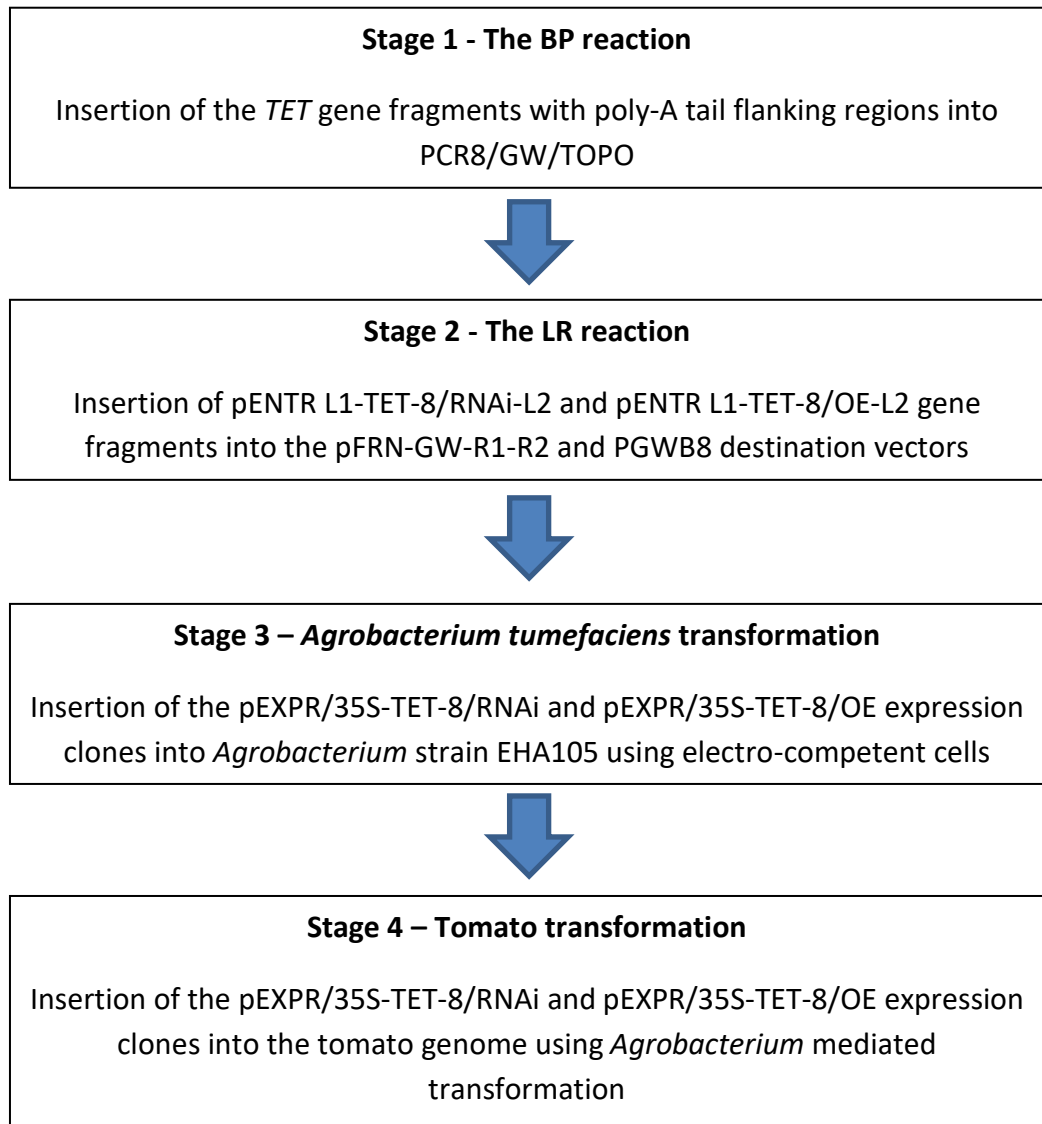


Figure 2.2: The four main stages of the cloning procedure for *SITET-8* using a constitutive 35S promoter.

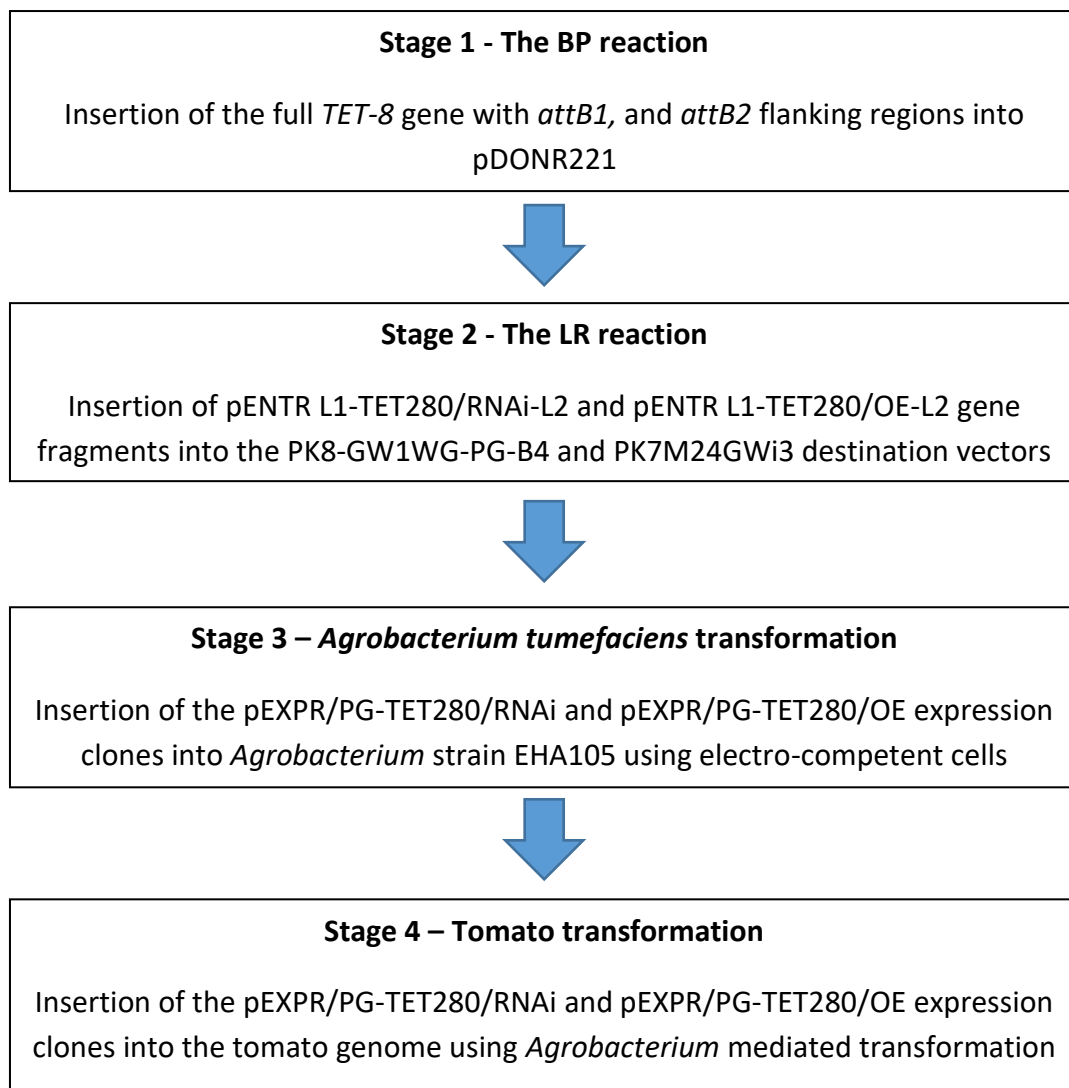


Figure 2.3: The four main stages of the cloning procedure for *SITET-8* using a ripening specific PG promoter.

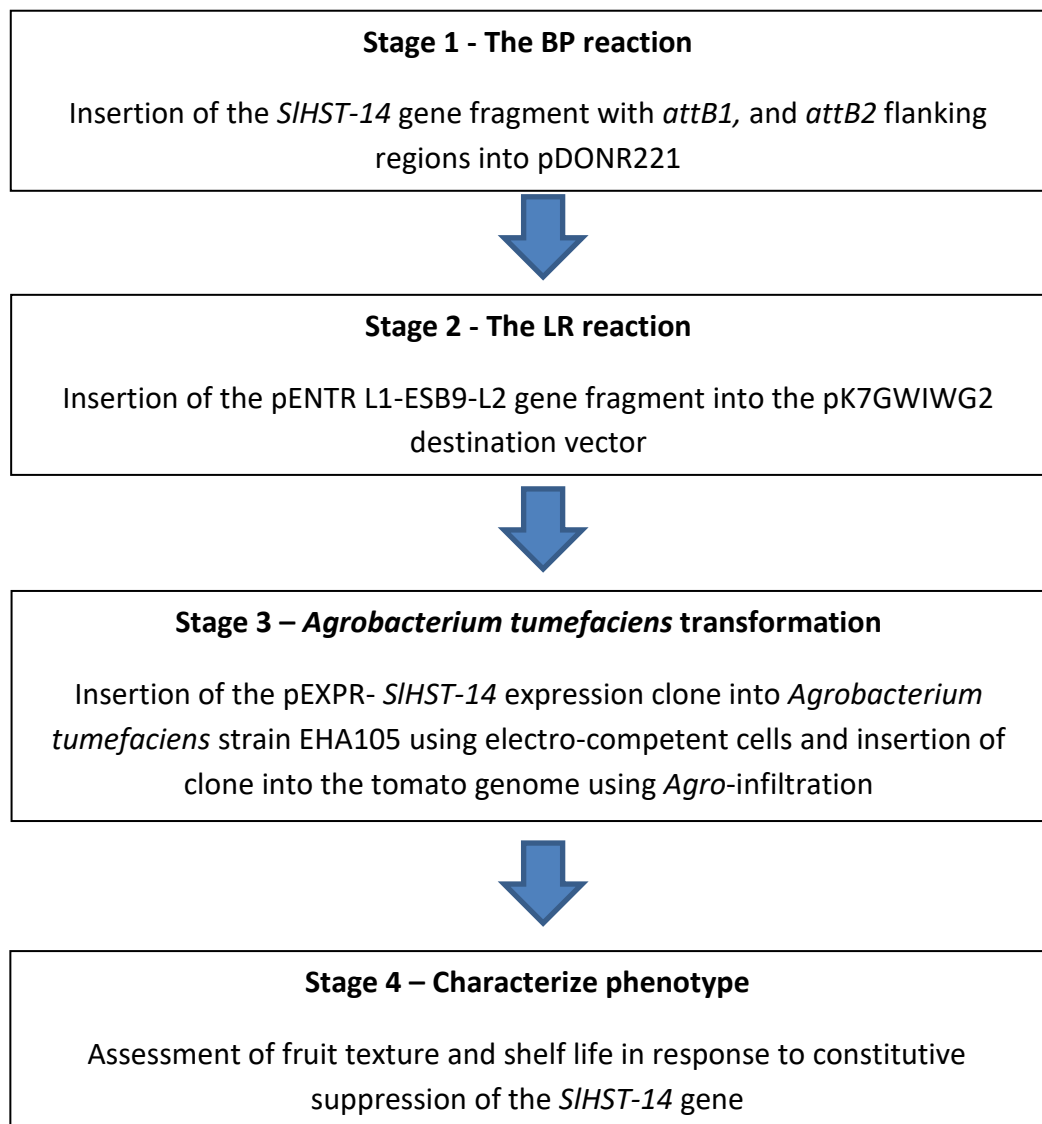


Figure 2.4: The main stages of the characterising the effect of *SIHST-14* suppression on tomato fruit texture and shelf life.

Polymerase Chain Reaction (PCR)

All amplicons for use in vector construction were amplified using Thermo Scientific 10X Taq Buffers for optimised product generation. The PCR reaction was completed in a total volume of 20 μ L in a 0.5mL Eppendorf tube (Table 2.1). Where colony PCR was used, single colonies were selected and dipped into the PCR master mix using a graduated pipette tip before being spread onto an agar plate with presence of selective antibiotic at working concentrations.

Table 2.1: Thermo Scientific PCR mix reaction and conditions

DNA Template	2	μ L
10X PCR Buffer (Fermentas)	2	μ L
dNTPs (10mM)	0.5	μ L
Forward Primer (10pM μ L ⁻¹)	1	μ L
Reverse Primer (10pM μ L ⁻¹)	1	μ L
Taq polymerase	0.5	μ L
Sterilised Water	Up to 20	μ L

Step	Temperature (°C)	Time(min)	Cycles
Init. Denaturation	95	5	1
Denaturation	95	0.5	30
Annealing	56	0.5	30
Elongation	72	1	30
Extension	72	10	1

The PCR product was separated by electrophoresis on a 1% (w/v) agarose gel in 0.5X TAE at 100V for 45 min. Then, if required the band was cut and purified by a QIAquick Gel Extraction Kit (see section 2.4.2, Qiagen, UK). The resulting product was run in a 1% (w/v) agarose gel in 0.5X TAE at 100V for 45 min to confirm product size/orientation.

Gel Extraction of DNA fragments

PCR products were separated by gel electrophoresis in 1% (w/v) agarose gel in 0.5X TAE buffer. Under UV illumination, the portion of the gel contained the specified DNA fragment was excised using a sterile blade and placed into a 1.5mL Eppendorf tube. The sliced gel was weighed and the appropriate volume of buffers was calculated (1g equal to 1mL). Three volumes of QC buffer were added and the tube was incubated at 50°C for 10 min with consistent (2-3 times) mixing to help dissolve the gel. 1 gel volume of isopropanol was added to the sample and mixed. The sample was applied to a QIAquick spin column placed inside a 2mL collection tube provided with the kit. The columns were spun at 13,000 rpm for 1 min and flow-through was discarded. The spin column was placed back into the collection tube and 0.5mL of QG buffer was added and centrifuged for 1 min. The flow-through was discarded and the column was placed back into the collection tube. The sample was then washed with 0.75mL PE buffer and centrifuged for 1 min. The flow-through was discarded and the column was centrifuged once more to remove any residual buffer. The QIAquick column was placed into a clean 1.5mL micro centrifuge tube before adding 50µL of EB buffer to the centre of the QIAquick membrane and incubated at room temperature for 2 min. The column was then centrifuged for 1 min and the purified PCR fragments were kept at -20°C until use.

Adding a 3' overhang to a PCR fragment prior to cloning

3'overhangs were added to PCR products where needed before cloning into pCR8/GW/TOPO vector using the following reaction.

Fresh PCR product (~20 ng µL ⁻¹)	11 µL
10X PCR buffer	1.5 µL
dATP (10 mM)	0.5 µL
<i>Taq</i> DNA polymerase	1 µL
Sterilised water	Up to 15 µL

The PCR product was incubated at 72°C for 1 hour, then placed on ice and used immediately in the TOPO cloning reaction for the pCR8/GW/TOPO vector (pCR8/GW/TOPO TA cloning kit, Invitrogen, UK).

BP and LR Clonase Reactions

The BP Clonase reaction was used to generate entry clones with two *attL* flanking sites. Reactions were set up with 150ng of PCR product (*attB* flanking sites) and 150ng of donor vector (pDONR221) with TE buffer (pH 8.0) to total volume of 8µL. 2µL of BP Clonase II Enzyme mix (Invitrogen) were added to each reaction and incubated overnight at room temperature. The reaction was inactivated by the addition of 2µL of Proteinase K and incubated at 37°C for 10 minutes. 3µL of the inactivated BP reaction was transformed into *E. coli* DH5α and plated on LB agar containing 100mg/ml kanamycin. Colonies obtained the following day were suspended and used for multiplication in liquid LB and for use in plasmid preparations. Entry vectors with the gene of interest were sent for sequencing for confirmation of the correct entry vectors in the correct orientation before use in the LR reaction to generate expression clones.

The LR Clonase reaction was performed using 150ng of entry clones and 150ng destination vector with the addition of TE buffer (pH 8.0) to a final volume of 8µL. To each reaction, 2µL of LR Clonase II Enzyme mix (Invitrogen) was added, mixed and incubated overnight at room temperature. The reaction was inactivated by the addition of Proteinase K and incubated at 37°C for 10 minutes. The LR reaction was then used for transformation into *E. coli* DH5α with the appropriate antibiotic selection in the LB medium. Plasmid preparations were performed on the colonies obtained and confirmation of the insertion of the candidate gene was performed by PCR using primers specific to the gene.

Transformation of plasmids into chemically competent cells

To a vial of 50µL chemically competent *E. coli* DH5α cells, 3µL of each cloning reaction was added and mixed gently. The vial was incubated on ice for 30 min, the cells were then heat shocked for 30 seconds at 42°C without shaking. The vial was then placed immediately on ice and left to stand for 2-3 min and 250 µL of LB medium was added to the vial. The cells were incubated at 37°C for 1 hour with shaking (200rpm). The cells from each transformation were then spread 20, 40 and 100 µL on a pre-warmed LB plate containing selective antibiotic at 37°C for 16-18 hours.

Transformation into *Agrobacterium* via electroporation

Agrobacterium tumefaciens strain EHA105 was thawed on ice from storage at -80°C for five minutes and pipetted into a clean, and chilled electroporation cuvette prior to the addition of 2 µL expression clone. Electroporation was performed at 2.5V, 25 µFD, and 400 OHMS and 300 µL fresh LB medium without antibiotics was added immediately to the cells. The cells were left to incubate at 28°C for 2 hours with agitation (200 rpm) before being plated onto LB agar with the appropriate antibiotics. The transformed *A. tumefaciens* were left to incubate for 2 days at 28°C. Colonies were selected and grown in liquid LB medium with antibiotics and colony PCR was used to confirm the presence of the gene of interest before use in the plant transformations.

Plasmid Purification

Bacterial colonies were picked and cultured in 8-10 mL of LB medium containing selective antibiotic at 37°C for 16-18 hours for *E. coli* or at 28°C for 2 days for *Agrobacterium*. The plasmid DNA was isolated from the transformed cells using the GeneJET Plasmid Miniprep Kit (Fermentas, UK). The transformed cells were centrifuged at 3,000 rpm for 3 min at 25°C. The LB medium was

discarded and the pellet was suspended in 250µL Resuspension Buffer. The cell suspension was then transferred to a fresh 1.5 micro centrifuge tube. Full suspension was achieved by complete mixing of the tube until no clumps remained. 250µL lysis solution was then added and the tube was inverted 4-6 times to ensure thorough mixing, the solution was observed to become viscous and clear. 500µL Neutralisation solution was then added and mixed immediately by inverted the tube 4-6 times. The cell suspension was centrifuged at 13,200 rpm for 5 min and the supernatant was transferred to a GeneJET spin column provided with the kit. The GeneJET column was centrifuged at 13,200 rpm for 1 min and the flow through was discarded before the column was replaced into the collection tube. 500µL wash solution was added to the spin column and was centrifuged at 13,200 rpm for 1 min. The flow-through was discarded and the spin column was replaced into the collection tube and the previous step was repeated. The column was then centrifuged at 13,200 rpm for an additional 1 min to remove any residual buffers and the spin column was then transferred into a fresh 1.5mL micro-centrifuge tube. 50µL elution buffer as added to the centre of the GeneJET membrane and incubated for 2 min at room temperature before centrifuging for 2 min. Samples were stored at -20°C until use.

2.6 DNA Extraction

This method was used for a rapid extraction for DNA from tomato leaf tissue. The technique follows a standard QIAGEN DNeasy Plant Mini Kit protocol. Plant material was collected using immature leaves at the apical tip of growing tomato plants and stored in liquid nitrogen until use. All centrifugation steps were completed at room temperature (15-25°C). 100mg of plant tissue was disrupted using the provided TissueRuptor® under liquid nitrogen conditions. 400µl Buffer AP1 and 4µl RNase A was added. The tubes were mixed and incubated for 10 minutes at 65°C. The tubes were continuously inverted throughout the incubation. 130µl Buffer P3 was added and samples were

mixed and incubated on ice for 5 minutes. Samples were centrifuged for 5 minutes at 20,000g and the lysate was pipetted into a QIAshredder spin column placed in a 2ml collection tube and centrifuged for 2 minutes at 20,000g. The flow through was transferred into a new tube and 1.5 volumes of Buffer AW1 was added and mixed using pipette action. 650µl of the mixture was added to a DNeasy Mini spin column placed in a 2ml collection tube and centrifuged for 1 minute at 6000g. The flow through was discarded and this step was repeated with the remaining sample. The spin column was placed into a new 2ml collection tube and 500µl Buffer AW2 was added and centrifuged for 1 minute at 6000g before discarding the flow through. The spin column was transferred to a new 1.5ml micro centrifuge tube and 51µl Buffer AE was added and incubated for 5 minutes at room temperature for elution before being centrifuged for 1 minute at 6000g. Samples were stored at -20°C until needed.

2.7 RNA Extraction

Total RNA was extracted from pericarp frozen in liquid nitrogen and ground while frozen to a fine powder. A standard operating protocol was implemented with an Ambion® RiboPure™ Kit. 0.1g of ground tissue was added to a 1.5ml Eppendorf tube. 1ml of Trizol solution was added and the solution mixed vigorously before incubation at room temperature for 5 minutes. The solution was centrifuged (10 minutes, 4°C, 12,000g) and the supernatant was added to a fresh 1.5ml Eppendorf tube. 20% total volume of chloroform was added to the sample and mixed. The solution was incubated for 5 minutes at room temperature and centrifuged (12 minutes, 4°C, 12,000g). The supernatant was removed and added to a fresh 1.5ml Eppendorf tube. 50% total volume ethanol (100%) was added and mixed immediately to avoid RNA precipitation. The sample was loaded into a ribopure column and centrifuged (30 seconds, room temperature, 12,000g). The flow-through was discarded and washed twice with 500µl wash solution (centrifuged for 30 seconds, room

temperature, 12,000g). the column was placed inside a new 1.5ml Eppendorf tube and 52µl elution buffer was added. The tube was incubated at room temperature for 5 minutes and centrifuged (30 seconds, room temperature, 12,000g). The column was discarded and samples were run on a 2% agarose gel (100V for 20 minutes) to test the quality of RNA obtained.

2.8 Quantitative – PCR (QPCR)

Synthesis of first strand cDNA

DNA-free RNA samples were used as a template for generating cDNA by reverse transcription. The reactions used followed a standard operating protocol provided with Promega (UK) reverse transcriptase enzyme. The reaction composed of 5 μ L total RNA, 1 μ L of random primers (0.5 μ g μ L) and 9 μ L of nuclease free water. The reaction was incubated at 70°C for 5 minutes. It was transferred directly on to ice. The reverse transcriptase reaction was composed of 5 μ L of 5X MMLV Rev Trans buffer, 1.25 μ L of dNTPs mix (10mM), 0.5 μ L of RNase inhibitor, 1 μ L of MMLV Rev Trans and 2.25 μ L Nuclease free water. The reverse transcriptase reaction was mixed with the RNA mix (final volume 25 μ L), incubated at room temperature for 10 minutes then 42°C for 1 hour. The first strand cDNA volume was adjusted to 52 μ L before keeping at -20°C as a stock solution.

QPCR Primer design

The specific gene primers and Taqman probes for the target and reference genes were designed using the 'Primer3' programme. The primers were designed to be between 18 and 25bp in length and contain an optimal GC content of 40-60% with a melting temperature (T_m) around 59°C. Gene expression can be quantified by Taqman QPCR and calculated from Crossing point value (C_q). The C_q value is defined as the cycle at which there is a significant increase in fluorescent signal from the gene. It is also associated with the exponential increase in the level of the PCR product being detected. The PCR efficiency can be analysed by using a standard curve of a serial dilution (1:10). An ideal PCR reaction will have an efficiency of two ($E=2$) meaning that the target will double with every PCR cycle. The C_q value of the target gene should be in the range of the C_q of the standard curve. Regarding the reference gene, expression should remain stable by treatment and

normalised with the target gene, for use with samples derived from RNA, the elongation factor-1 α (*EF-1 α*) gene was used (see section 7.4). This normalisation provides a relative gene expression value.

QPCR Reaction and Conditions

The qPCR reaction conditions followed that of the Taqman universal PCR Mastermix protocol (Table 2.2).

Table 2.2: QPCR reaction and condition

2X Taqman PCR Mastermix	8	μ L	
Forward Primer	0.5	μ L	
Reverse Primer	0.5	μ L	
Taqman probe	0.3	μ L	
First Strand cDNA	5	μ L	
Sterilised Water	Up to 15	μ L	

Step	Temperature ($^{\circ}$ C)	Time (min)	Cycles
Init. denaturation	95	10	1
Denaturation	95	0.16	45
Annealing	60	0.83	45
Hybridisation	72	0.1	45
Cooling	40	0.16	1

2.9 Statistical Analysis

The mean values for qPCR, texture, colour, and weight were taken from three biological replicates where standard errors of means were also calculated. Data were analysed using Genstat or Microsoft Excel analysis systems by analysis of variance (ANOVA) to assess significant differences between values.

2.10 Tomato plant transformation with *Agrobacterium* strain EHA105

The generation of explant material was generated by surface sterilization of seeds using 50% bleach for 10 minutes. Seeds were then repeatedly washed with sterile water and placed on sterile MSR3 medium using flame sterilized forceps. The petri dishes were kept at 4°C in the refrigerator for 1 day before being transferred to the tissue culture room. Seedlings were then grown at 21°C for 9-10 days under fluorescent light.

After having transformed two expression clones with *Agrobacterium* strain EHA105. A single *Agrobacterium* colony from a freshly sub-cultured plate was grown overnight in LB liquid medium with the appropriate antibiotic (50mg/ L Kanamycin) at 28°C in a rotary shaker. The pre-culture procedure was carried out as following, cotyledons were excised from 9-10 day old seedlings and cotyledon pieces were placed on a sterile tile. The tips of the cotyledons were removed with a scalpel to wound the tissues and the explants were then kept in sterile reverse osmosis water to prevent dehydration. Cotyledon pieces were then placed upside down in petri dishes containing MSZ media and were incubated under low light intensity ($24-48 \mu\text{mol m}^{-2} \text{s}^{-1}$, Daylight fluorescent illumination) for 1 day.

The pre-cultured explants were exposed to the *Agrobacterium* for 10 minutes with OD_{600} between 0.2-0.3. The explants were then transferred to plates containing MSZ media with 50 mg/L Kanamycin. The explants that started forming shoots were places on MS media containing a 50 mg/L kanamycin, 100 mg/L Carbenicillin to overcome *Agrobacterium* contamination in the selection media.

Chapter 3

A novel tetraspanin gene linked to shelf life in melon

3.1 Introduction

The control of cell wall disassembly in tomato and other fruits involves the transcription of more than 50 cell-wall structure related genes (The Tomato Genome Consortium, 2012). Many of them encode cell wall hydrolytic enzymes such as polygalacturonase (PG), pectinmethylesterase (PME), and pectate lyase (PL) which cause β -eliminative cleavage of pectic polysaccharides. Generation of transgenic plants with reduced PL activity indicate that this enzyme plays an important role in fruit softening (Uluisk et al., 2016). Conversely, PG and PME influence levels of pectin solubilisation and degradation in the fruit cell walls (Sheehy et al., 1988; Smith et al., 1988; Tieman et al., 2000). However, the role of proteins that are integral to the extracellular matrix, either as structural proteins or embedded partly in the plasma membrane in fruit texture changes has received little attention.

Tetraspanin

Tetraspanins are found in plants, mammals, insects, and fungi and are a family of highly conserved transmembrane proteins with normally two extra-cellular domains, and one intra-cellular loop (F. Wang et al., 2012). They interact with other proteins as well other tetraspanins facilitating cell-to cell adhesion, ligand binding, and intracellular trafficking through the formation of tetraspanin-enriched micro-domains. The function of these domains is poorly understood but have been associated with development, immune responses, reproduction, and pathogenesis (Cnops et al., 2006; Rubinstein, 2011; F. Wang et al., 2012). Little is known about the role of tetraspanins in plants, although their role in maintaining cell-to-cell adhesion has been linked to reproduction (Sprunck & Dresselhaus, 2009). Moreover, a number of studies have shown that in Arabidopsis, RNAi suppression lines are normally sterile supporting their role in the fusion and

development of gametes. Nothing is known about their role in fruit development and ripening (Cnops et al., 2006).

The industrial partner Syngenta that supported this project at Nottingham has discovered a gene encoding a Tetraspanin-like protein under a quantitative trait locus (QTL) conferring long shelf life in melon. Figure 3.1 illustrates the expression of the *SLTET-6* gene in melon cultivars Magenta, Anasta, and Cezanne from harvest to ripe and overripe stages. The Magenta melons exhibited longer shelf life than the Anasta and Cezanne cultivars and expression of the *SLTET-6* gene is seen to be elevated in this cultivar at harvest, when the fruits are ripe, and overripe. The presence of tetraspanin is hypothesised to be a contributing factor to this phenotype based on the Syngenta QTL mapping experiment.

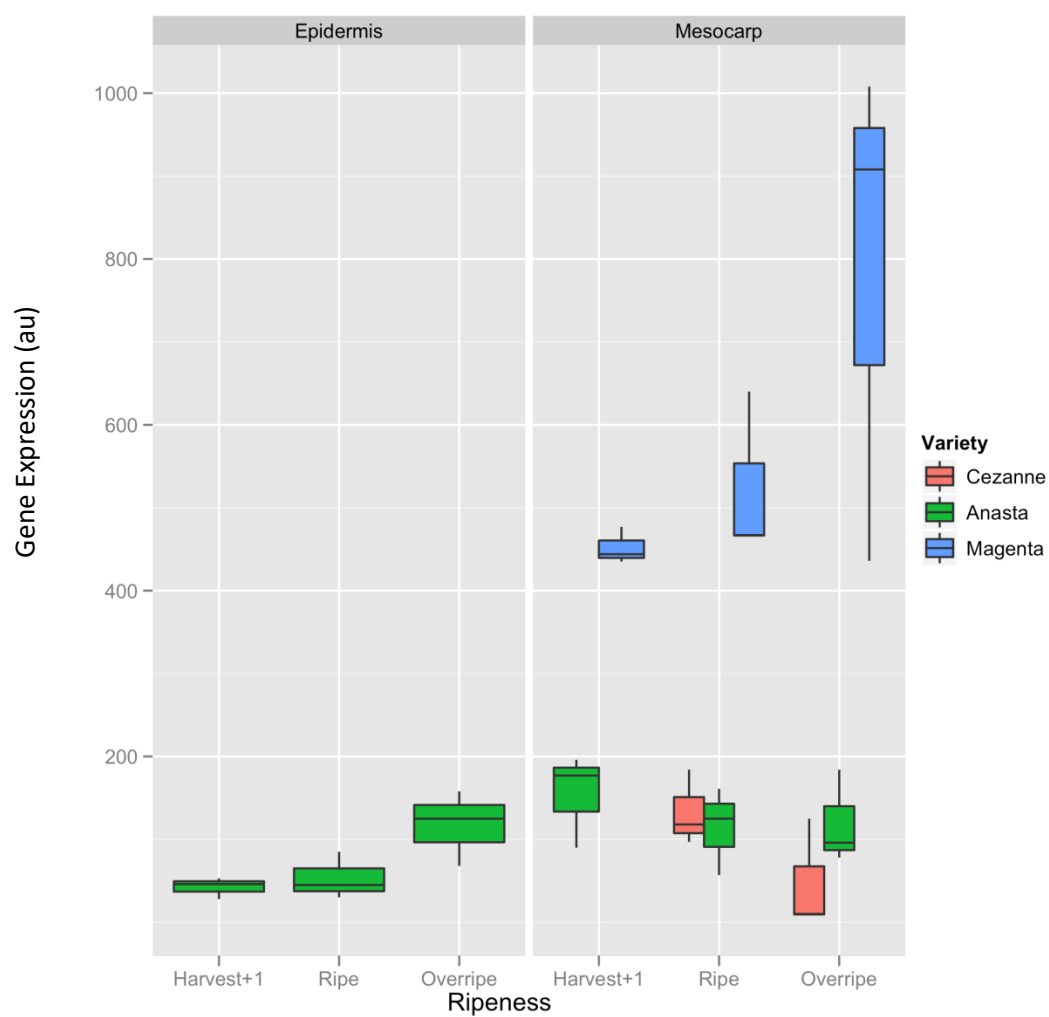


Figure 3.1: Expression of a Melon tetraspanin-like gene in cultivars Cezanne, Anasta, and Magenta. There is an increase in expression of this gene in the Magenta cultivar during ripening. It is also seen during the ripe and overripe stages of the Cezanne cultivar and is constitutively expressed in the Anasta cultivar.

Protein sequence alignment has shown that Solyc04g049080 (*SITET-6*) is a likely tomato orthologue of the melon tetraspanin gene and the Arabidopsis *TET-5* gene (Fig. 3.2). The tomato gene shows the highest expression in roots and has low expression in fruits (Fig. 3.3). However, expression in the *Cnr* ripening mutant was much lower than in wild type fruits (Fig. 3.4). The *Cnr* mutant is known to have reduced cell-to-cell adhesion (Thompson et al, 1999) consistent with a possible relationship between the *SITET-6* gene product and fruit softening. In this chapter we investigated the role of *SITET-6* in tomato by overexpressing the gene in fruit to determine the impact on softening and cell-to-cell adhesion.

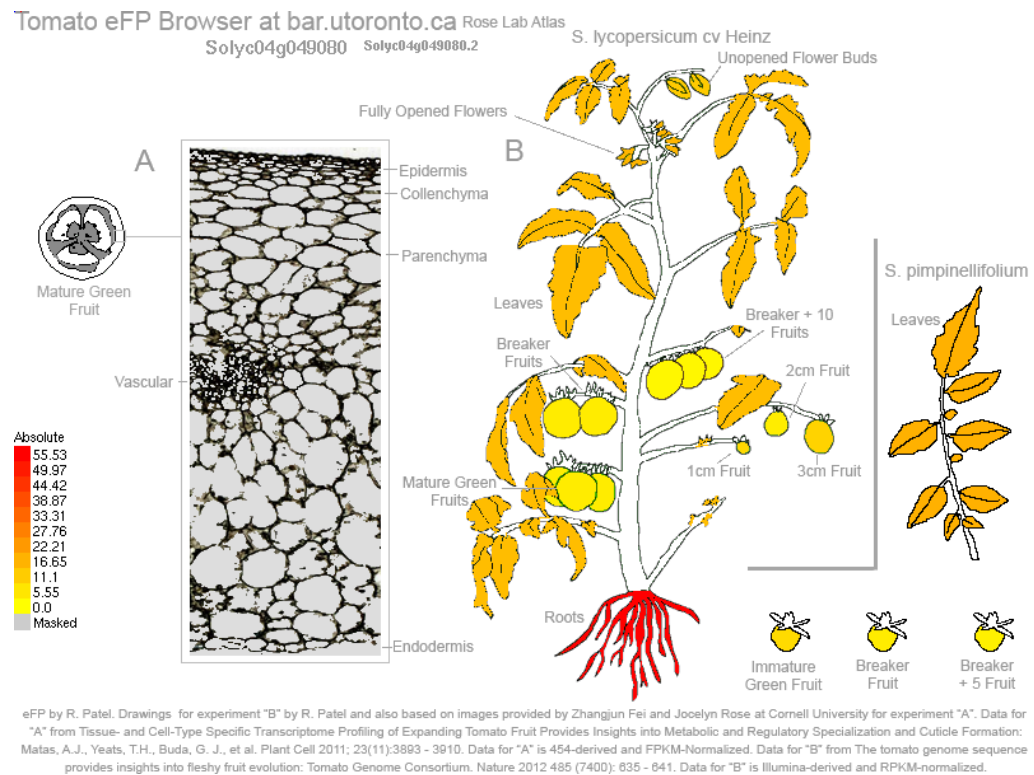


Figure 3.3: RNA expression profile of *SLTET-6*. The *SLTET-6* is shown to be expressed highly in the roots of tomato and at a low level in leaf tissue, no expression is described in developing or ripening fruits. Taken from the Tomato eFP Browser (<http://bar.utoronto.ca>).

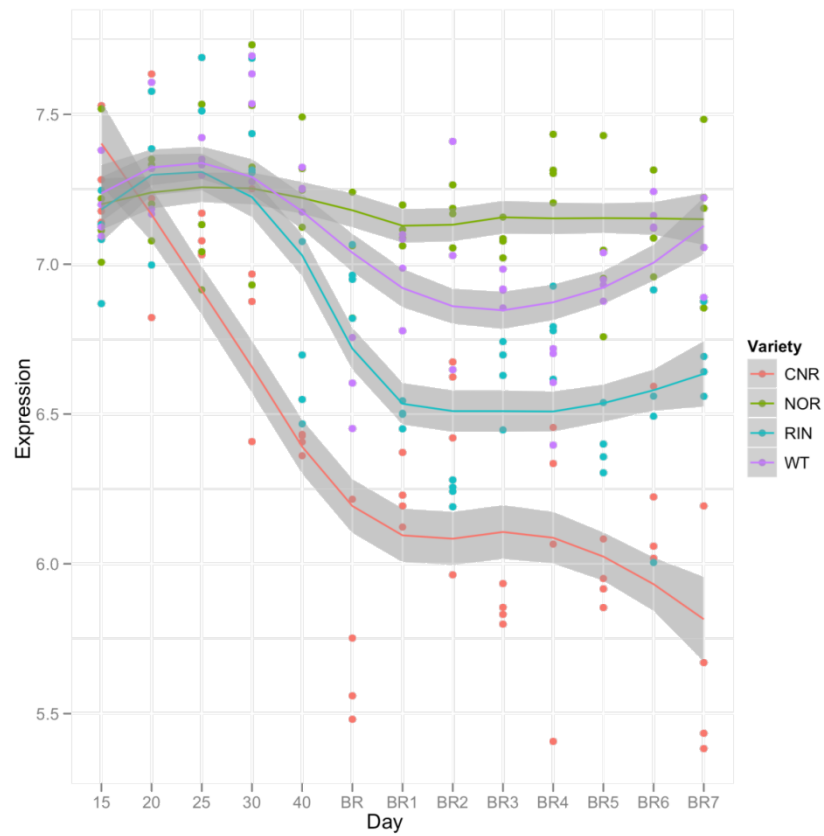


Figure 3.4: Expression of *SITET-6* in tomato mutants. Expression of the *SITET-6* gene can be seen to decrease sharply in the *Cnr* mutant in developing fruit. Expression in the *nor* mutant remains constant throughout ripening and small decreases are seen in the *rin* and WT.

3.2 Materials and Methods

Plant Materials

Tomato (*Solanum lycopersicum*), cv. Ailsa Craig were grown under standard cultural practices with regular supplementary nitrogen, phosphorus and potassium fertilizers. The glasshouse temperature, humidity, and radiation were regulated at different levels during the day and night. Fruits were selected as described in Chapter 2 and harvested at set days after the onset of ripening. After collection, fruits were taken into the lab for weight, colour, texture, and soluble solid measurements to be carried out. Fruit pericarp was cut into quarters before being frozen in liquid nitrogen and stored at -80°C.

Vector construction

The BP Clonase reaction was used to generate entry clones with two *attL* flanking sites. Reactions were set up with 150ng of PCR product and 150ng of donor vector (pDONR221) with TE buffer (pH 8.0) to a total volume of 8μL. 2μL of BP Clonase II Enzyme mix (Invitrogen) were added to each reaction and incubated overnight at room temperature. The reaction was inactivated by 2μL of Proteinase K and incubated at 37°C for 10 minutes. 3μL of the inactivated BP reaction was transformed into *E. coli* DH5α and plated on LB agar containing 100mg/ml kanamycin.

Colonies obtained the following day were suspended in liquid LB for use in plasmid preparations. Entry vectors with the gene of interest were sent for sequencing for confirmation of the correct entry vectors before use in the LR reaction to generate expression clones. Figure 3.5 is a diagram representing the insertion of the *SLTET-6* gene fragment into the donor vector pDONR221 using the BP clonase reaction to produce the pENTR L1-SLTET-6.OE-L2 entry vector.

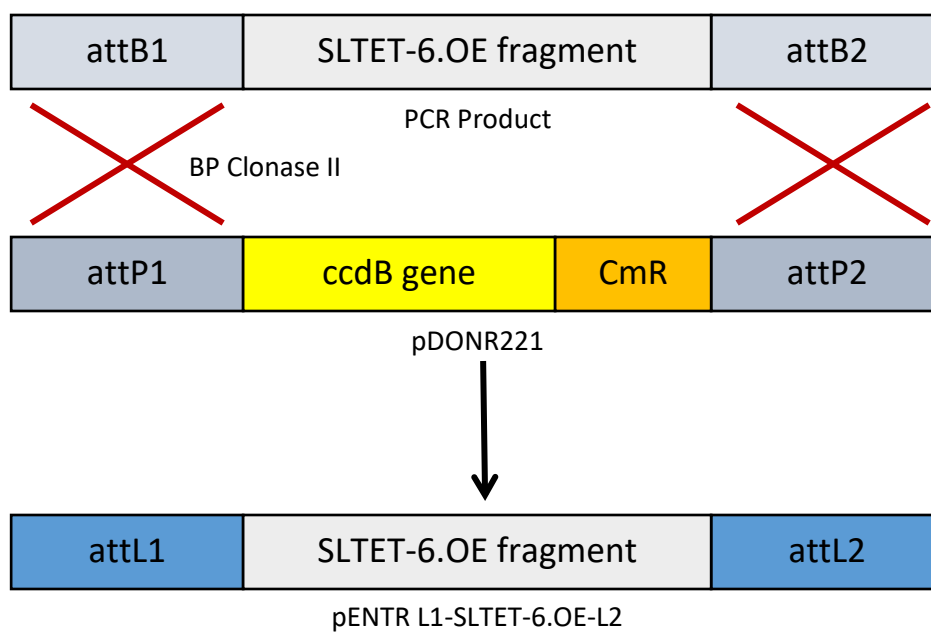


Figure 3.5: Description of the BP reaction to incorporate the SLTET-6 gene into the donor vector pDONR221. The *ccdB* gene is swapped out by the clonase enzyme and replaced with the fragment.

The LR Clonase reaction was performed using 150ng of entry clone, 150ng promoter donor clone and 150ng destination vector with the addition of TE buffer (pH 8.0) to a final volume of 8 μ L. To each reaction, 2 μ L of LR Clonase II Enzyme mix (Invitrogen) was added, mixed and incubated overnight at room temperature. The reaction was inactivated by 2 μ L Proteinase K and incubated at 37°C for 10 minutes. The LR reaction was then used for transformation into *E. coli* DH5 α with the appropriate antibiotic selection in the LB medium.

Plasmid preparations were performed on the colonies obtained and confirmation of the insertion of the candidate gene was performed by PCR using primers specific to the *SLTET-6* and the *NPTII* gene fragments. Figure 3.6 is a diagrammatic representation of the insertion of the *SLTET-6* gene fragment into the donor vector PK7M24GWi3 using the LR clonase reaction. Figure 3.5 is a diagram representing the LR recombination reaction of pENTR L1-SLTET-6.OE-L2, and pEN-L4-PG-R1 into the PK7M24GW3 cassette producing the pEXPR-SLTET-6.OE expression clone.

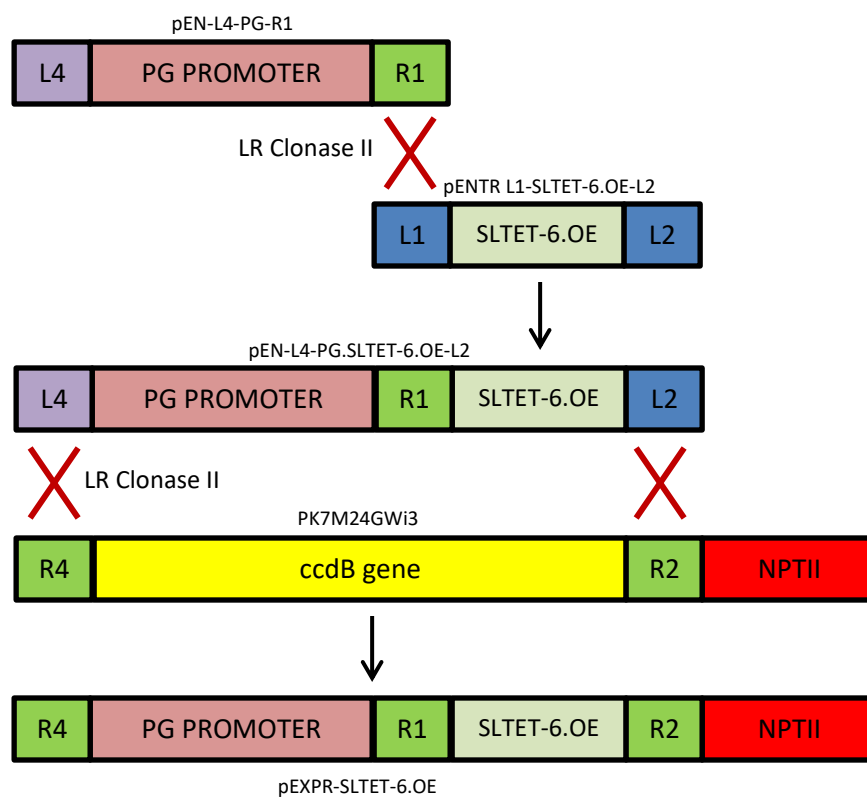


Figure 3.6: Description of the LR reaction to incorporate the SLTET-6 gene and PG promoter into the destination vector PK7M24GW3. This involves a double reaction in which the promoter is attached to the gene fragment and then both are incorporated into the destination vector.

Plant Transformation

The completed expression clone containing the gene of interest was sent to the University of California, Davis for *Agrobacterium* mediated transformation into Ailsa Craig.

Analysis of T₀ transgenic lines and identification of homozygous lines in the T₀ progeny

Twelve seeds from each T₀ line were grown and DNA was extracted from juvenile plants a few weeks after germination from young plant leaves growing close to apical tip and samples were stored at -20°C until use. Gene specific primers and Taqman probes for Solyc04g049080 and phytoene desaturase (PDS) were used and are listed in the appendices. The serial dilutions, qPCR conditions followed the Taqman universal Mastermix protocol (section 2.7.3).

Transgene expression in homozygous SITET-6 fruits

To confirm the expression of the transgene in tomato fruit tissue RNA was obtained from fruits 7 days after the breaker using a column based extraction method. The quality of RNA was assessed by running a 2% agarose gel. The presence of sharp and clear 28s and 18s bands in a 2:1 ratio indicated intact RNA. Samples were taken from each homozygous and azygous line and a cDNA template was constructed, samples were then stored at -20°C until needed. Gene specific primers and Taqman probes for Solyc04g049080 and elongation factor-1 α (*EF-1 α*) were used and are listed in the appendices. The serial dilutions, qPCR reactions and qPCR conditions followed the Taqman universal Mastermix protocol described in section 2.8. Absolute gene expression was calculated from the crossing point (C_q) values of Solyc04g049080 relative to the *EF-1 α* reference gene.

3.3 Fruit phenotyping

Fruit Sugars and Colour

Fruit colour was determined using a Minolta colorimeter CR400 and sugars using a hand held refractometer (Chapter 2).

Fruit Texture Measurements

Fruit texture measurements were made from the pericarp tissue of tomato fruits at different stages of development from the breaker point onwards and based on determination of maximum load (Chapter 2).

3.3 Results and Discussion

Generating the expression clone for the full Solyc04g049080 gene fragment.

The *SLTET-6* gene was isolated by PCR from a cDNA library of leaf tissue from Ailsa Craig plants. In order to insert the gene into the Gateway donor vector pDONR221, the *SLTET-6* gene was amplified using primers with *attB1* and *attB2* sites linked to the 5' end designed only to anneal to a small region of the *SLTET-6* gene at the C-Terminus. The BP reaction serves as a starting point to incorporate the *SLTET-6* gene into an expression clone. Following a successful BP reaction, the resulting entry vector will be flanked by *attL* sites ready for the LR reaction.

Clones obtained after the transformation of the BP reaction were screened for the correct insertion of a *SLTET-6* gene using primers that will amplify a smaller fragment of the gene (250bp) by PCR analysis. Figure 3.7 illustrates the presence the *SLTET-6* gene fragment in pDONR221 by PCR. The correct incorporation of this gene in pDONR221 was assured by the survival of colonies on selective LB agar plates due to the absence of the *ccdB* gene which acts to inhibit the growth of *E. coli* if it is not replaced by a non-lethal gene during the BP recombination step.

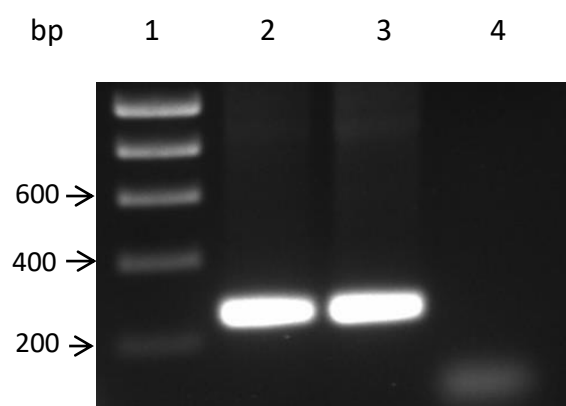


Figure 3.7: The BP reaction identifying the *SITET-6* gene fragment inside the pDONR221 entry vector. Presence of a single band 250bp in size confirms the insertion of the *SITET-6* gene inside the entry vector.

Lane	ID
1	DNA Hyperladder I
2	SLTET-6.OE fragment 1
3	SLTET-6.OE fragment 2
4	Negative Control (Water)

The completed entry construct pENTR L1-SLTET-6.OE-L2 harbouring the *SLTET-6* gene was then used in the LR recombination reaction with the PK7M24GW3 destination vector and the pEN-L4-PG-R1 donor vector containing the PG promoter to produce the pEXPR-SLTET-6.OE expression clone. This gateway binary destination vector contains the appropriate cassettes to facilitate the over expression of the *SLTET-6* gene in fruit tissue using a promoter of our choice.

The successful insertion of the *SLTET-6* gene fragment was confirmed by PCR analysis this time showing a band (1400bp) using a combination of gene and *NPTII* specific primers. The *NPTII* gene confers kanamycin resistance and is present in the PK7M24GW3 gateway cassette. The presence of a band 1400bp in length confirms the presence and correct orientation of the insert after the LR recombination reaction (Fig 3.8). The vector containing the *SLTET-6* transgene driven by the PG promoter were then sent to the University of California, Davis for *Agrobacterium* mediated transformation in tomato cv. Ailsa Craig.

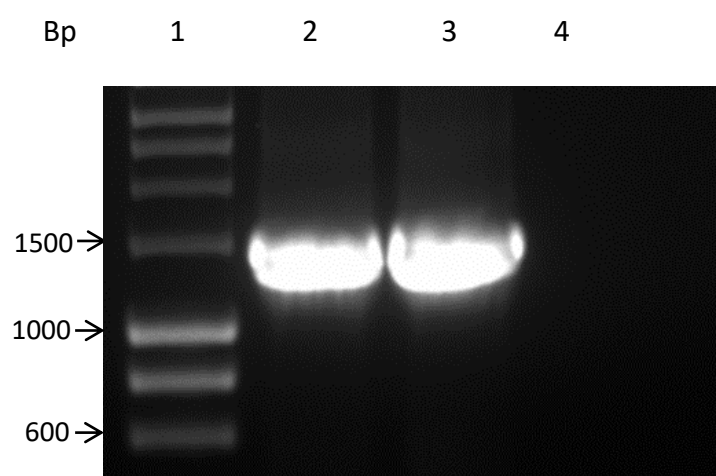


Figure 3.8: The LR reaction identifying the presence, and orientation of the *SLTET-6* and *NPTII* gene inside the PK7M24GWi3 destination vector

Lane	ID
1	DNA Hyperladder I
2	pEXPR-SLTET-6.OE 1
3	pEXPR-SLTET-6.OE 2
4	Negative Control (water)

The phenotype of the T_0 transgenic Ailsa Craig plants obtained from Davis were analysed and then homozygous T_1 lines were generated. Ailsa Craig fruits from our seed batches grown at Sutton Bonington were used as the control as no seeds from the Ailsa Craig material at Davis was provided. It was recognised that the appropriate control would need to be an azygous line arising from the T_1 progeny. This important control would prove to be critical for interpretation of the results of the transgenic experiment as will be described later in this chapter.

Fruit from T_0 transgenic lines containing an over expression construct of the *SITET-6* gene were compared with Sutton Bonington Ailsa Craig tomato as a control to obtain a preliminary phenotype. Four lines representing independent transformation events were obtained from Davis. One of these lines failed to produce fruit and so was omitted from our analysis. All fruits were harvested 7 days' post-breaker at the red ripe stage. The fruits from all the three transgenic lines weighed on average 46% more than the Sutton Bonington Ailsa Craig fruits (Fig 3.9, 3.10, and 3.11). Transgenic lines were also found to have darker (L^*), more red than blue (A^*), and more yellow than green (B^*) skin when compared to control lines at the same developmental stage (Fig 3.12).



Figure 3.9: Comparison of transgenic (right) tomato size compared with Ailsa Craig control (left). The increased size of the mutant line can be easily spotted when placed next to the control line.

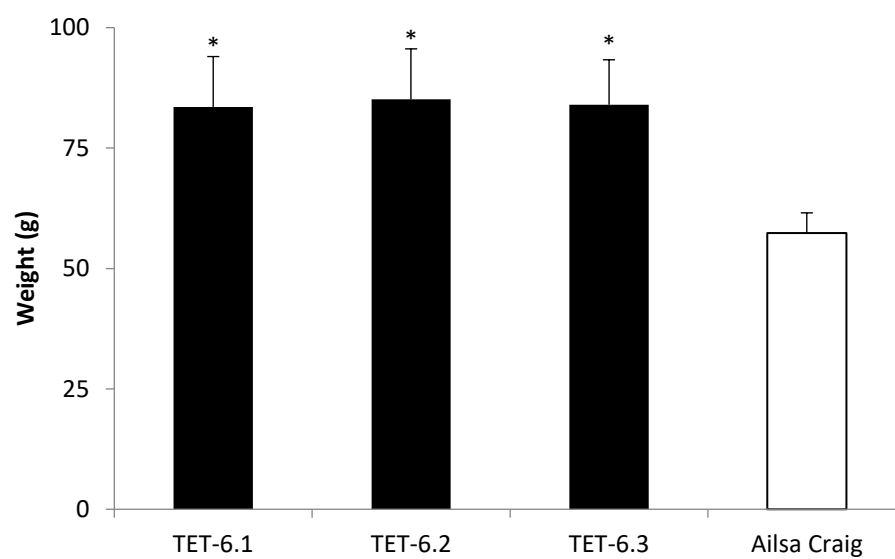


Figure 3.10: The comparison of transgenic tomato weight in the SITET-6 lines compared with Ailsa Craig controls. Values represent the mean \pm SE of three biological replicates. Asterisks in all graphs mark significant differences: P 0.05 = *, P0.01 = **, and P 0.001 = ***.

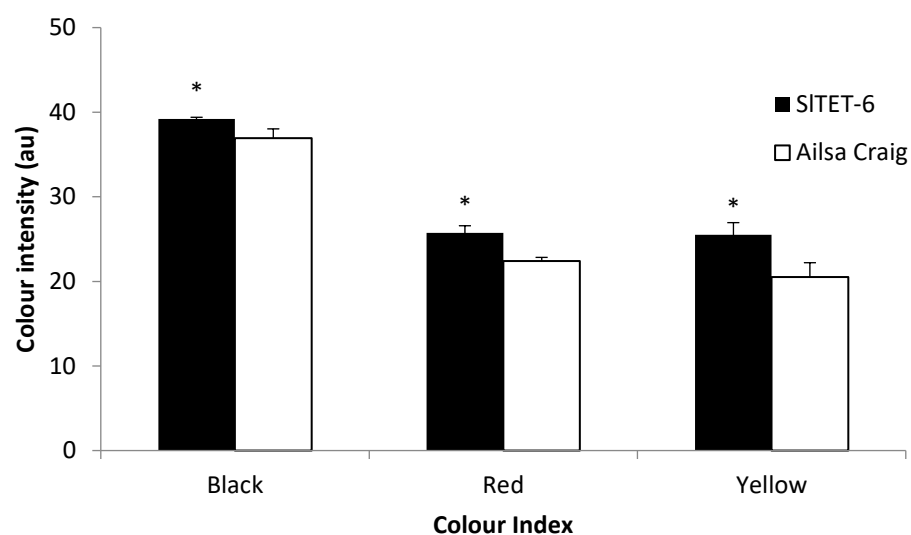


Figure 3.11: The comparison of transgenic *SITET-6* tomato colour compared with Ailsa Craig controls. Values represent the mean \pm SE of three biological and technical replicates. Asterisks in all graphs mark significant differences: P 0.05 = *, P0.01 = **, and P 0.001 = ***.

Assessment of fruit texture and soluble solids in segregating generation

We assessed the firmness of the inner and outer pericarps in fruit tissue by determination of maximum load required to drive a small probe into a transverse section of fruit pericarp. There were no significant differences ($P>0.05$) in the firmness of the outer pericarp tissue. The *SITET-6.2* line was found to have a significant ($P=0.044$) difference in fruit firmness when assessing the inner pericarp and this line was found to be less firm than the control samples (Fig. 3.12).

Soluble solids were assessed using a refractometer (Fig. 3.13). Transgenic fruits had a mean soluble solid concentration of around 5% which was compared with the control which had accumulated 6.25% soluble solids.

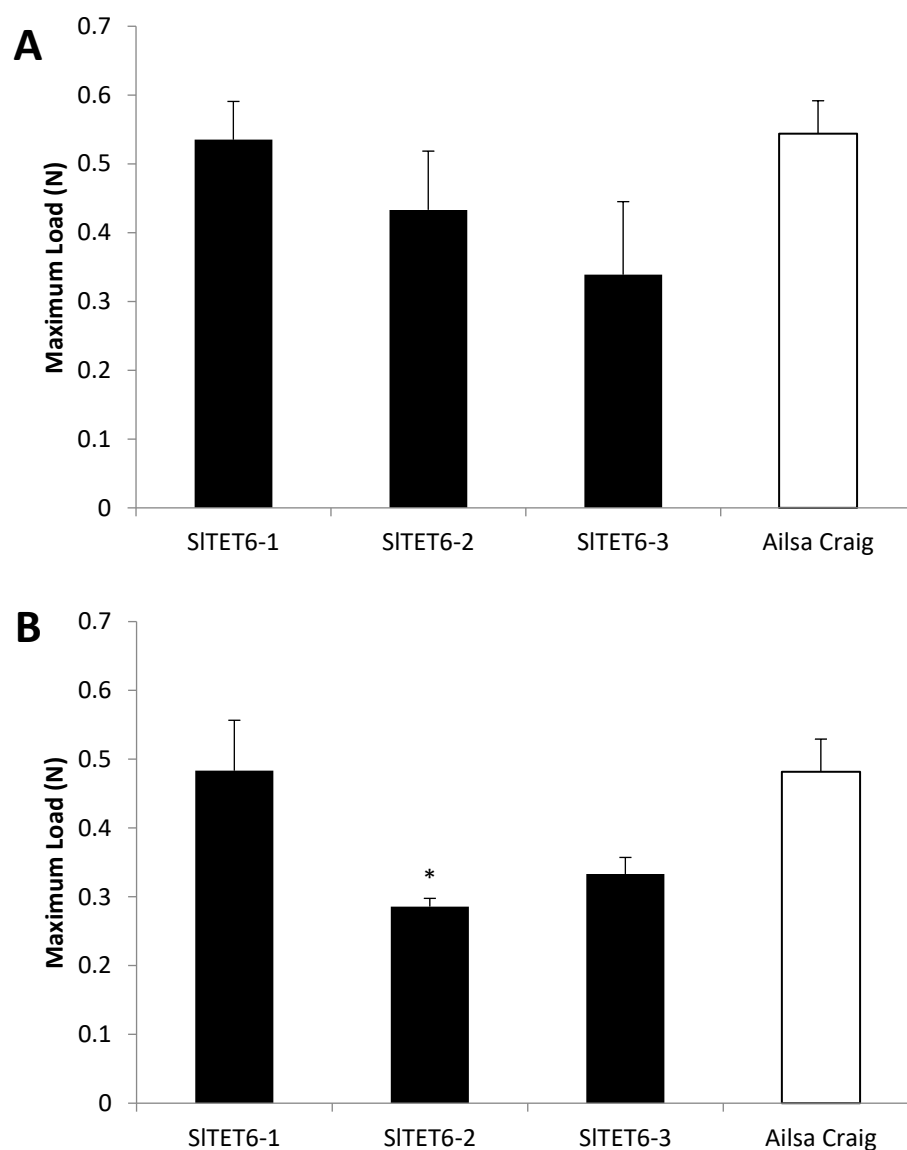


Figure 3.12: The comparison of fruit texture of transgenic SITET-6 plant lines compared with Ailsa Craig controls. **A)** Outer pericarp and **B)** Inner pericarp. Values represent the mean \pm SE of three biological replicates. Asterisks in all graphs mark significant differences: P 0.05 = *, P0.01 = **, and P 0.001 = ***.

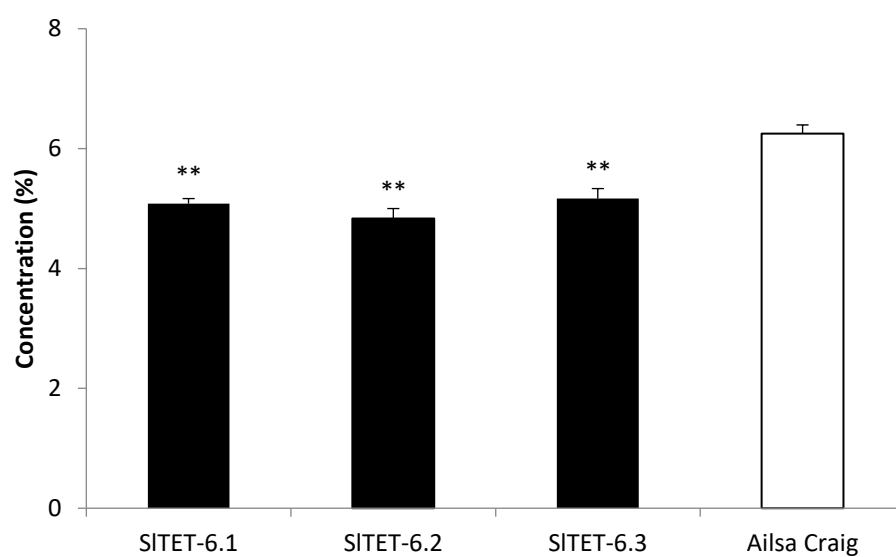


Figure 3.13: The comparison of soluble solids of transgenic SITET-6 fruit compared with Ailsa Craig controls. Values represent the mean \pm SE of three biological replicates (n=12). Asterisks in all graphs mark significant differences: P 0.05 = *, P 0.01 = **, and P 0.001 = ***.

Analysis of homozygous T₁ lines and azygous controls

Between ten and twelve seeds were sown from each of the four T₀ lines to assess the copy number of the plant lines. Quantitative PCR of genomic DNA using fluorescent hybridisation probes was performed to screen for the presence or absence of the transgene and to assess copy number (Fig. 3.14) The assessment of copy number in four lines of tomato each representing a unique transformation event is shown in Figure 3.14.

The first column of each graph labelled T₀ represents the segregating generation's copy number fluorescence value. These samples are known to be heterozygous and will act as a reference for their progeny. Graph A represents plant line A. Of the ten samples tested, 20% were shown to contain two copies of the transgene, lines 1, and 5. These are homozygous and were kept for further study. Five plants were shown to be heterozygous based on their similarity with the T₀ sample and were discarded, these were lines 2,4,7,8, and 9. Finally in lines 3, 6, and 10 no amplification product was detected and these were marked as azygous lines. An Ailsa Craig sample was also assessed (AC) as a negative control, mimicking the value from the wild type azygous lines.

Ten plants were sampled in plant line B, there were no samples that resulted in a fluorescence value representative of a wild type azygous line suggesting the occurrence of a double insert of the candidate gene during transformation. This line was not studied further as the progeny were likely still segregating for the transgene.

Twelve plants were sampled from plant line C. Lines 1 and 12 were homozygous with respect to the transgene and were subsequently kept for further characterisation.

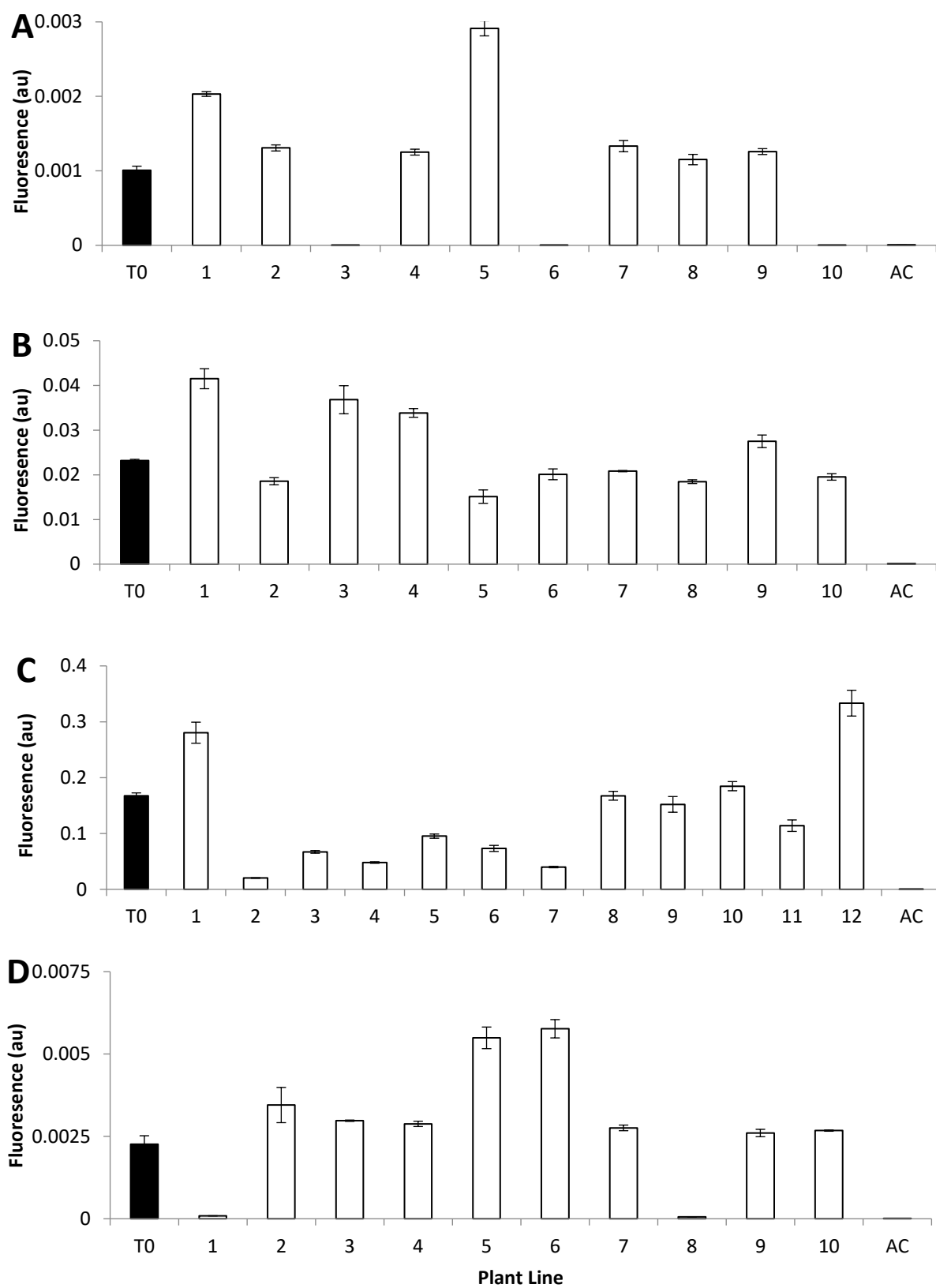


Figure 3.14: Assessment of copy number in tomato plants. **A)** Plant line A. **B)** Plant line B. **C)** Plant line C. **D)** Plant line D. Values represent the mean \pm SE of three technical replicates.

Using qPCR to characterize copy number was a new approach taken in this report and so DNA samples were sent to the John Innes Centre (JIC) to confirm the results from the qPCR analysis seen in Figure 3.13 using southern blot analysis. These results are displayed in Table 3.1. The JIC data substantiate our qPCR analysis.

Table 3.1: Overview of copy number results.

Plant line	qPCR Result	JIC Result
A1	2	2
A3	0	0
A5	2	2
C1	2	2
C12	2	3
D1	0	0
D5	2	2
D6	2	2

Phenotyping of homozygous *SLTET-6* lines

SLTET-6 transgene expression in fruit tissue

The expression clone for the *SLTET-6* gene was constructed using a PK7M24GWi3 destination vector with a PG promoter. PG is a cell wall degrading enzyme whose expression in fruit tissue is a key marker at the onset of ripening and is almost fruit specific (there is a low level of expression in other tomato tissues, Tomato Genome Consortium, 2012). The transgene was highly expressed in transgenic lines A5 and D5 and lower expression was seen in lines A1, C1, C12, and D6. No expression was seen in the Azygous or Ailsa Craig controls (Fig. 3.15).

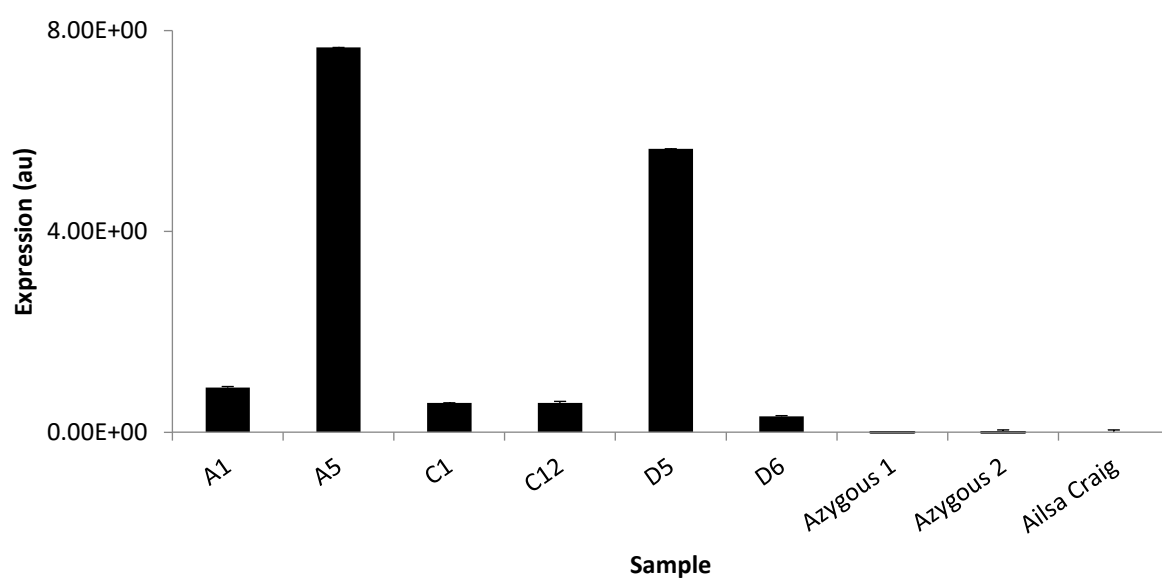


Figure 3.15: RNA expression of SITET-6 in fruit pericarp tissue. Expression of the *SITET-6* gene is confirmed in the mutant lines consolidating the transformation procedure.

Assessment of fruit weight and colour in the homozygous T₁ lines

There was a large size difference between the *S/TET-6* fruits in the T₀ generation compared to the Sutton Bonington Ailsa Craig controls. However, in the T₁ generation comparison of azygous fruit weight with that of the *S/TET-6* fruits indicated no obvious phenotypic differences (Figure 3.16). Similar results were obtained for colour index, texture, and soluble solids (Figures 17, 18, and 19). However, it was apparent that both the azygous fruits and those from the *S/TET-6* transformants were substantially bigger than the Sutton Bonington Ailsa Craig fruits used as a control in the study of the T₀ lines (Figure 3.16).

These findings suggest that the plant line used for transformation in Davis, California was possibly not Ailsa Craig, although this was the cultivar specified for the study. This would explain the differences in size of fruits when the T₀ analysis was undertaken. Azygous control lines were only available in the T₁ generation.

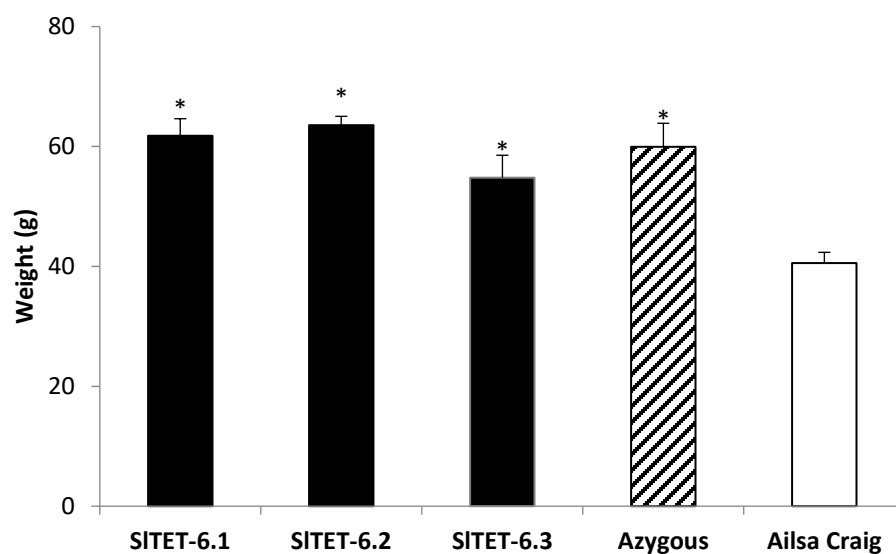


Figure 3.16: Assessment of fruit weight in SITET-6 lines vs an azygous control and wild type Ailsa Craig fruits from the Sutton Bonington seed bank. Values represent the mean \pm SE of three biological replicates. Asterisks in all graphs mark significant differences: P 0.05 = *, P0.01 = **, and P 0.001 = ***.

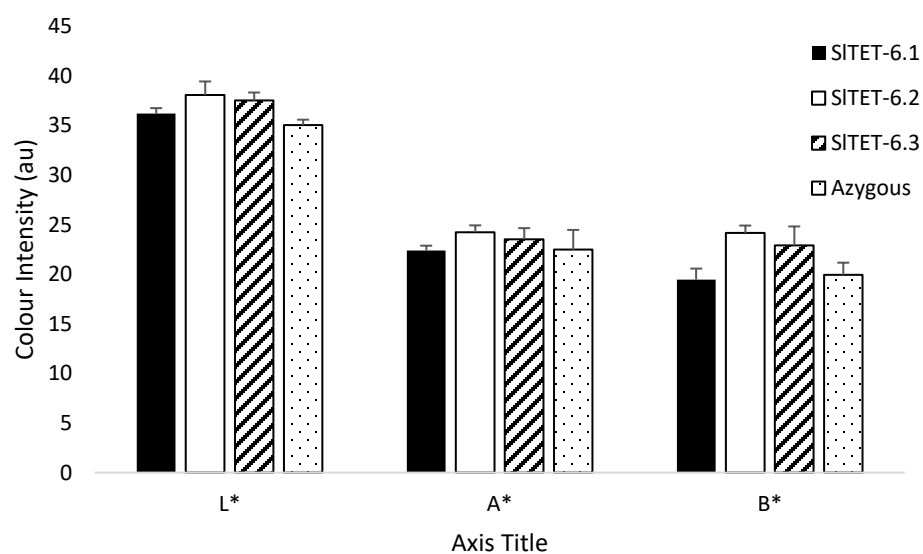


Figure 3.17: Assessment of homozygous tomato colour index. The figure shows no colour differences between the SITET-6 and azygous controls. Values represent the mean \pm SE of three biological and technical replicates. L* = Black / White, A* = Red / Green, B* = Blue / Yellow (Figure 2.1).

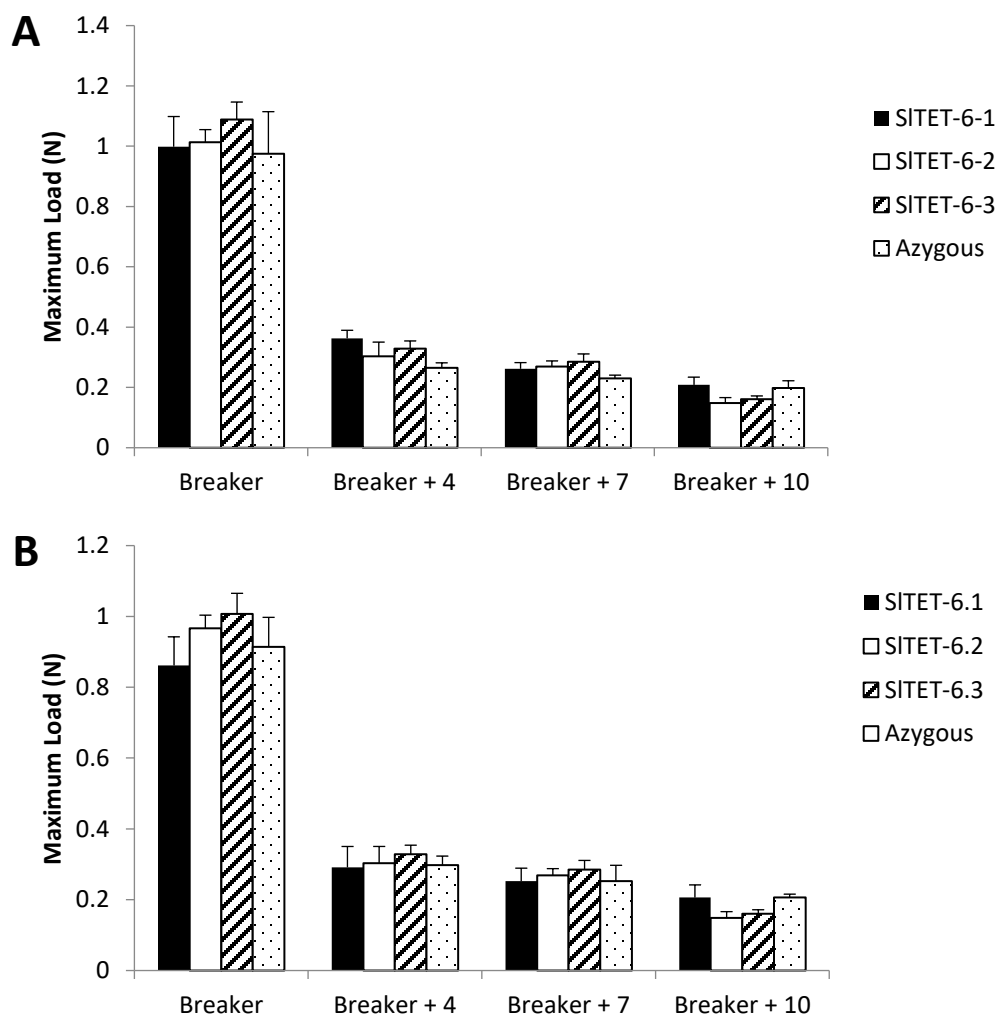


Figure 3.18: Assessment of homozygous fruit texture in SITET-6.1. A) Outer pericarp and B) Inner pericarp. No differences were seen between the transgenic and azygous lines. Values represent the mean \pm SE of three biological replicates.

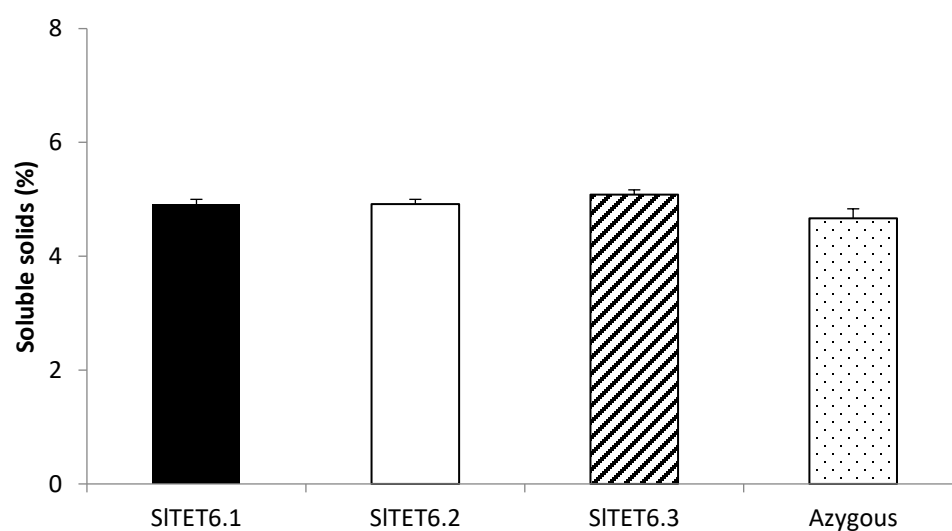


Figure 3.19: The comparison of the total Soluble solids content of SITET-6 transgenic fruit compared with Ailsa Craig fruit. Values represent the mean \pm SE of three biological replicates.

3.4 Conclusion

The generation of transgenic tomato plants over-expressing *SITET-6* using a PG promoter was successful. Preliminary investigation into the transformed plants in comparison with Ailsa Craig material revealed a substantial increase in fruit size in the transformants. However, assessment of the homozygous generation using the azygous control for comparison revealed no obvious ripening or developmental fruit-related phenotypes for the *SITET-6* over expressing lines. The absence of a fruit related phenotype may be a reflection on the endogenous expression pattern of the *SITET-6* gene which is confined to a substantial extent within the root system of the tomato plant. It has been suggested by Wang et al. (2012b) that the protein may have evolved to interact laterally with molecules specific to the root domain. We will therefore focus attention now on a tomato fruit-related tetraspanin, although not a direct orthologue of the melon gene, its fruit related expression is suggestive of a role in ripening. Further work on *SITET-6* and its developmental role in Arabidopsis is described in Chapter 4.

Chapter 4

Arabidopsis thaliana AtTET-5

4.1 Introduction

Work in the previous chapter produced transgenic tomato lines over expressing a tetraspanin gene, but these had no obvious phenotypes. To better understand the mechanism by which tetraspanins operate, it was decided to investigate transgenic RNAi lines in *Arabidopsis*. Information from *Arabidopsis* can be obtained much more quickly than in tomato and it was thought should help to inform the analysis of the function of the tomato tetraspanin.

There are 17 tetraspanins in *Arabidopsis*, many of which remain uncharacterised. The *TORNADO1* and *TORNADO2* genes (*TRN1* and *TRN2*) were among the first to be investigated with functional analysis of double mutants linking their role to leaf development, symmetry, size, and patterning through disruption of auxin distribution in developing plants (Cnops et al., 2006). Moreover, a far more recent review has broadly characterised the expression patterns and distribution of all 17 tetraspanins in *Arabidopsis* which is described in Fig. 4.1 (F. Wang et al., 2015). The tetraspanins are seen to be expressed broadly across all of the plant tissues which are typically but not exclusively responsible for early developmental processes including the early globular and heart stage embryo (F. Wang et al., 2015).

Name	Size (bp)	E	R			C	L	F			
			m	d	lrp			se	pe	st	ca
pAtTET1	3400										
pAtTET2	1217										
pAtTET3	1500										
pAtTET4	1500										
pAtTET5	1938										
pAtTET6	1026										
pAtTET7	396										
pAtTET8	1403										
pAtTET9	1703										
pAtTET10	718										
pAtTET11	960										
pAtTET12	1090										
pAtTET13	1022										
pAtTET14	2000										
pAtTET15	1130										
pAtTET16	410										
pAtTET17	515										

Figure 4.1: TET expression patterns in different organs. Square brackets represent duplicated gene pairs. E: Embryo; R: root; m: primary root meristem and root tip; d: primary root differentiation zone; lrp: lateral root primordia; C: cotyledon; L: rosette leaf; F: flower; se: sepal; pe: petal; st: stamen; ca: carpel.” Figure taken and adapted from Wang et al., (2015).

The *ATTET-5* (At4g23410) gene was selected for investigation based on cluster analysis of the closest orthologue to Solyc04g049080 (*SITET-6*) in tomato (Fig 4.2) studied in Chapter 3 that was found to have no observable phenotypic effect on fruit development and ripening. Characterization of *AtTET-5* in *Arabidopsis* may provide a foundation on which we can better understand the role of tetraspanins in plant development to help identify a more accurate phenotype in the tomato line previously described. It is likely that absence of *ATTET-5* in developing roots will disrupt auxin distribution as seen in the TRN1 and TRN2 mutant and provide a phenotype linked to primary root development, lateral root density, primordia development or in response to a gravistimulus.

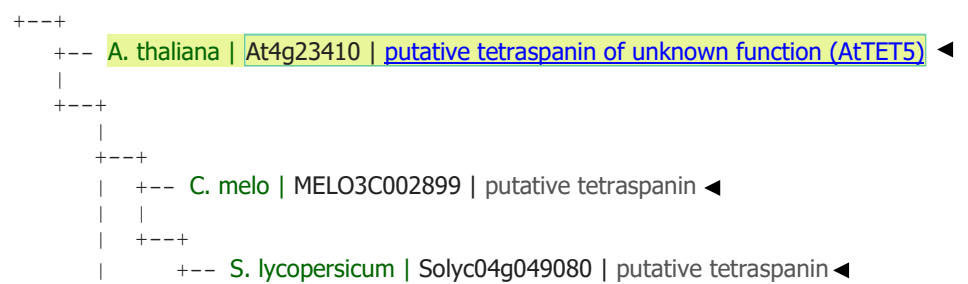


Figure 4.2: Phylogenetic analysis of tetraspanin proteins. A visual representation of the relationship between *AtTET-5* and *SITET-6* characterized in chapter 3. Figure obtained from ARAMEMNON 8.1[®] FlüggeLab, 2002-2016. Arrows represent the *AtTET5*, *SITET-6*, and Melon tetraspanin genes.

4.2 Materials and methods

Plant materials and growth conditions

Plant material was grown according to the criteria described in section 2.2.

Lateral root development

Arabidopsis seedlings were grown vertically on MS agar plates and primary root length and lateral root density were measured at 9, 11, 13, and 15 days after germination.

Root gravitropism

Surface sterilised seeds were grown vertically on MS agar plates for 4-5 days. The plates were then rotated 90° to give a gravitropic stimulus and images were captured using an automated image acquisition system every 20 minutes for 18 hours. Root growth and the angle of the root tip were analysed using the image analysis tool Root-Trace (French et al., 2009).

Lateral root induction using gravitropic stimulus

Lateral root primordia were induced using gravitropic bending as described previously (Voß et al., 2015). In brief, *Arabidopsis* seedlings were grown vertically on MS agar plates for 4-5 days and the plates were then rotated 90° to induce growth of lateral root primordia. Roots were cleared at 24, and 42 hours post bending (Malamy and Benfy 1997) and stages of primordia development were recorded under a light microscope according to predetermined criteria (Fig. 4.3 Péret et al., 2012).

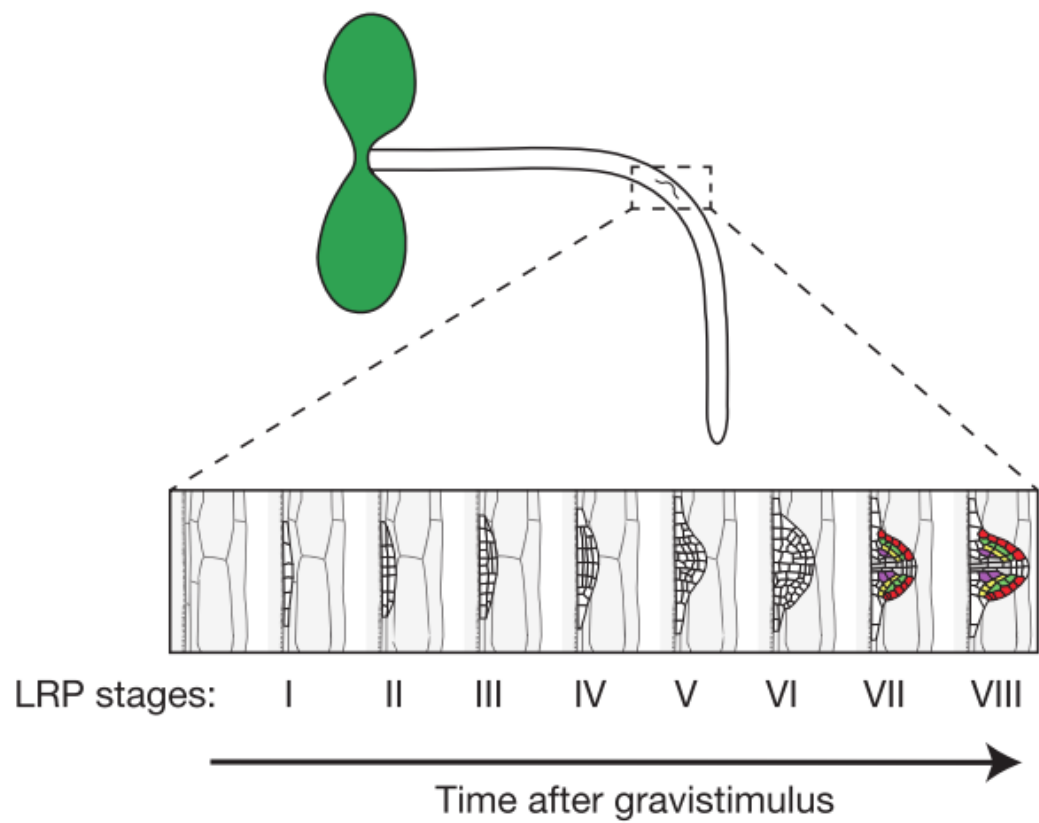


Figure 4.3: Description of lateral root primordium stages. The developmental stages of primordium are described in eight stages after a gravistimulus is applied to a plant. Figure taken and adapted from Péret et al., (2012).

Analysis and validation of T-DNA insertional knock outs

Polymerase chain reaction (PCR)

A typical PCR reaction was set up in a final volume of 20 μ L and the components and cycling conditions are summarised in Table 4.1.

Table 4.1: PCR mix and reaction for confirmation of T-DNA inserts

PCR mix		Volume	
DNA template		2	μ L
10X PCR Buffer		2	μ L
dNTPs (10mM)		0.5	μ L
Forward primer (10pM μ L ⁻¹)		1	μ L
Reverse primer (10pM μ L ⁻¹)		1	μ L
Taq polymerase		0.5	μ L
Sterilised water		Up to 20	μ L

Step	Temperature (°C)	Time	Cycles
Init. denaturation	95	5 min	1
Denaturation	95	30 s	30
Annealing	54-58	30 s	30
Elongation	72	1 min	30
Extension	72	10 min	1

Primer design

Three primers were used to distinguish the genotype of transgenic lines. LP; left border primer, BP; T-DNA border primer, and RP; Right genomic primer (Fig. 4.4). Wild-type (WT) plants will produce a product from the LP primer to the RP, for homozygous (HM) lines the band will be from BP to RP, and heterozygous (HZ) lines will produce both bands (LP to RP, and BP to RP).

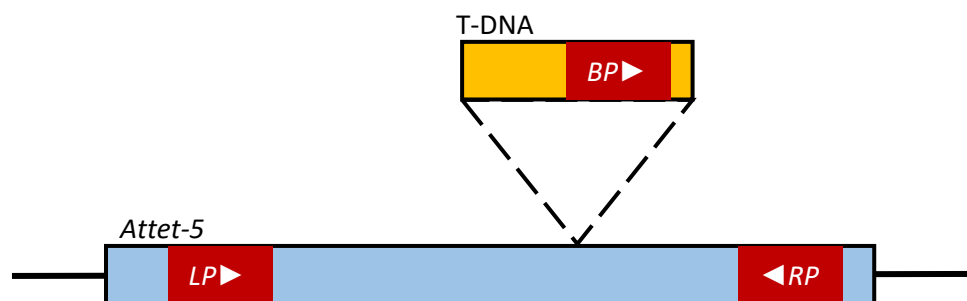


Figure 4.4: T-DNA primer design. Three primers are used to genotype transgenic lines. LP; left upstream primer, BP; T-DNA border primer, and RP; Right downstream primer. WT plants with no T-DNA insert will produce only one band (LP-RP, approx. 900bp), HM plants will get a band from BP-RP only (approx. 180bp), and HZ plants will produce both (LP-RP and BP-RP)

4.3 Results and discussion

Protein sequence alignment with tomato orthologue

A protein sequence alignment was performed on the Arabidopsis gene *AtTET-5* (At4g23410) and the tomato homologue *SlTET-6* (Solyc04g049080) (Fig. 4.5). The *AtTET-5* protein was shown to have an additional three transmembrane (TM) regions. This is peculiar in tetraspanins because the N- and C- terminal domains are cytoplasmic and the presence of a fifth TM region would place the C-terminal domain outside the cell. However, TM 4 was shown to have low hydrophobicity compared to the other TM regions (Table 4.2) and is also localised within the large extracellular loop (EC2) suggesting it has a strong functional role in the protein but not as a TM domain, potentially in the formation of enriched micro-domains between neighbouring tetraspanins (F. Wang et al., 2012).

Table 4.2: Hydrophobicity and amphiphilicity of TM regions in AtTET-5.

TM Region (5'-3')	Start (aa)	End (aa)	HyPhob	AmPhil
1	8	28	0.735	0.402
2	43	63	0.736	0.215
3	72	92	0.899	0.090
4	129	149	0.297	0.211
5	220	240	0.774	0.286

A

Endogenous expression of *AtTET-5* in Arabidopsis

Endogenous expression of *AtTET-5* was investigated using microarray data obtained from the AtGenExpress initiative and the botany array resource (Toufighi, Brady, Austin, Ly, & Provar, 2005) and collated into the Arabidopsis eFP Browser (Fig. 4.6; Winter et al., 2007). Expression of *AtTET-5* was shown to be lowly expressed in all tissues but most highly in the vascular tissue of the developing root. This same pattern was seen in tomato (Matas et al., 2011) suggesting that the two proteins are functionally conserved.

These data allow us to plan our expected phenotypes accordingly with root development. For this reason, primary root growth, lateral root emergence, primordia development and root gravitropism will be investigated.

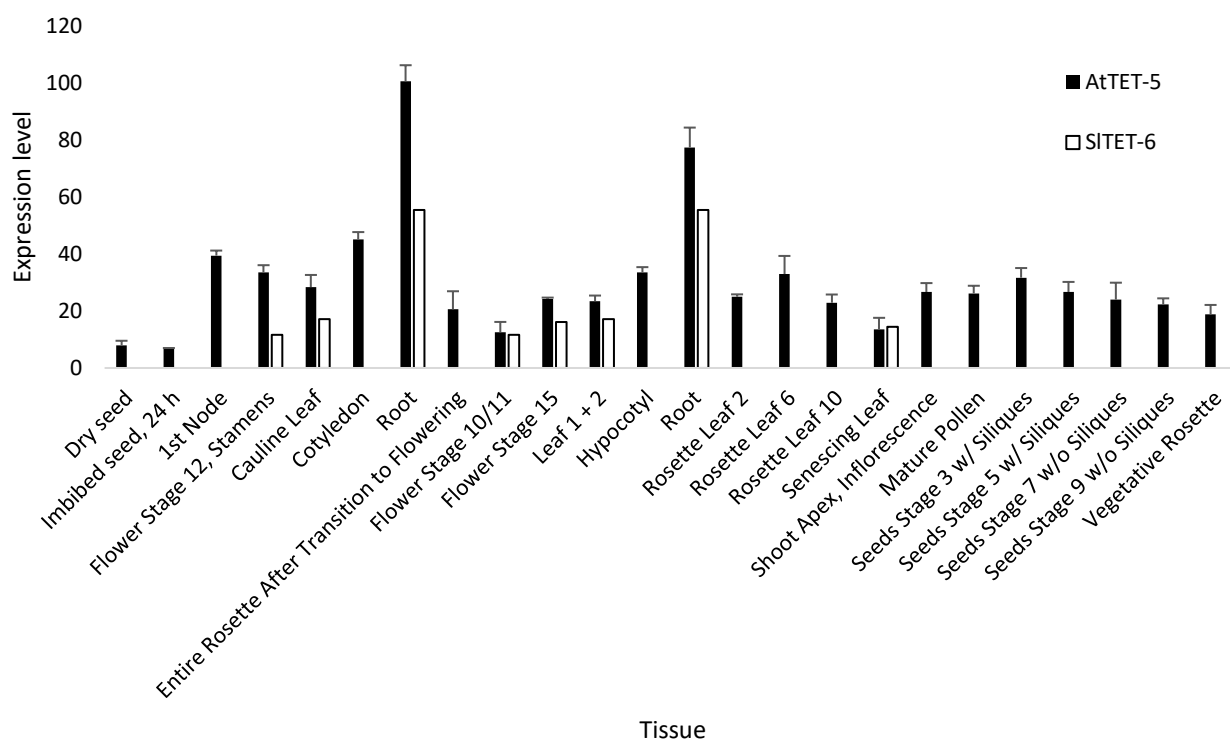


Figure 4.6: *AtTET-5* expression values in *AtTET-5* and *SITET-6*. Expression of *AtTET-5* was seen across all tissues but most highly expressed in the root with a similar pattern being seen in the *SITET-6* line. Data taken and adapted from the Arabidopsis and tomato eFP Browser (Winter et al., 2007).

Analysis and validation of Tetraspanin 5.1 and 5.2 T-DNA insertional knock outs

T-DNA insertions for *AtTET-5.1* (SALK_020009) and *AtTET-5.2* (SALK_148216) were obtained from the European Arabidopsis Stock Centre (<http://www.arabidopsis.org/>). The presence of the insertion was confirmed using PCR with a combination of gene and insert specific primers (Fig 4.7). Three primers are used to distinguish the genotype of the transgenic line depending on the size and number of products seen. This provides a high throughput method that allows the assessment of genotype within the segregating generation.

Nine plants were genotyped for both *AtTET-5.1* and *AtTET-5.2* lines. For the BP-RP reaction, eight plants produced single bands in the *AtTET-5.1* line and seven plants produced single bands in the *AtTET-5.2* line. Presence of these bands confirms the presence of the T-DNA insert. Those reactions that did not produce a band in the BP-RP reaction were removed from further study. In addition, the PCR reaction using the LP-RP primers was unsuccessful making it difficult to distinguish a homozygous line from a heterozygous line. A double reaction was then performed on both SALK lines where single bands approximately 300bp in length indicate a homozygous genotype and single bands approximately 1200bp in length indicate a wild type genotype (Fig 4.8).

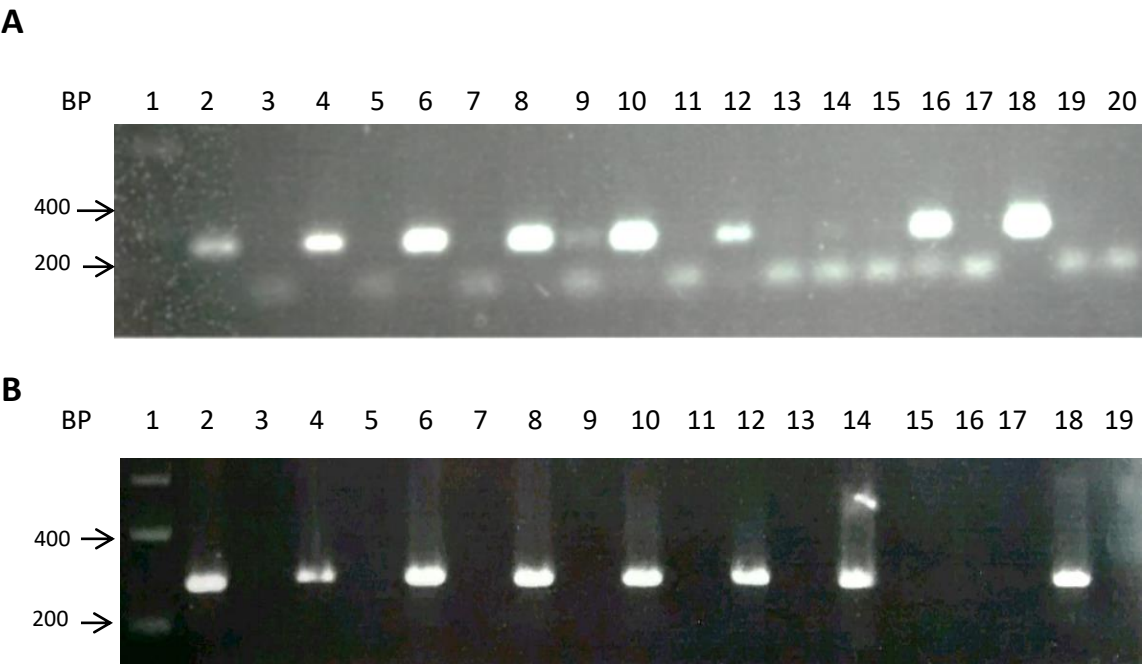


Figure 4.7: *AtTET-5.1* and *AtTET-5.2* transgenic genotyping. **A)** Nine plants were genotyped and eight produced single band products. **B)** Nine plants were genotyped and seven produced single band products.

A			
Lane	ID	Lane	ID
1	DNA Hyperladder I	11	Plant 5 LP-RP
2	Plant 1 BP-RP	12	Plant 6 BP-RP
3	Plant 1 LP-RP	13	Plant 6 LP-RP
4	Plant 2 BP-RP	14	Plant 7 BP-RP
5	Plant 2 LP-RP	15	Plant 7 LP-RP
6	Plant 3 BP-RP	16	Plant 8 BP-RP
7	Plant 3 LP-RP	17	Plant 8 LP-RP
8	Plant 4 BP-RP	18	Plant 9 BP-RP
9	Plant 4 LP-RP	19	Plant 9 LP-RP
10	Plant 5 BP-RP	20	Negative Control

B			
Lane	ID	Lane	ID
1	DNA Hyperladder I	11	Plant 5 LP-RP
2	Plant 1 BP-RP	12	Plant 6 BP-RP
3	Plant 1 LP-RP	13	Plant 6 LP-RP
4	Plant 2 BP-RP	14	Plant 7 BP-RP
5	Plant 2 LP-RP	15	Plant 7 LP-RP
6	Plant 3 BP-RP	16	Plant 8 BP-RP
7	Plant 3 LP-RP	17	Plant 8 LP-RP
8	Plant 4 BP-RP	18	Plant 9 BP-RP
9	Plant 4 LP-RP	19	Plant 9 LP-RP
10	Plant 5 BP-RP		

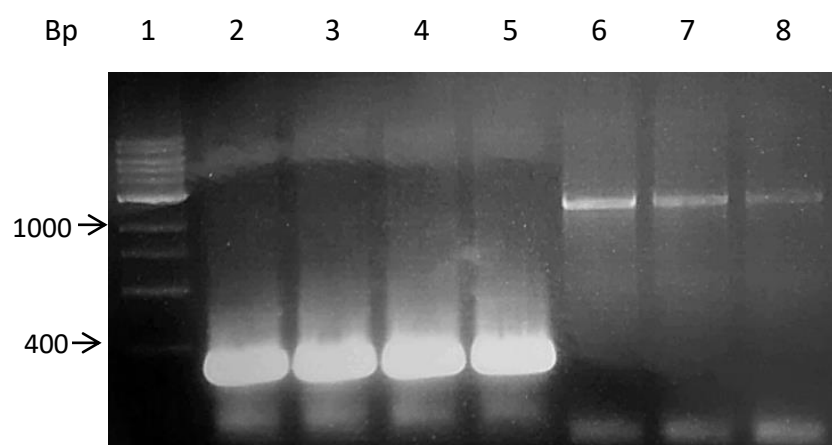


Figure 4.8: *AtTET-5.1* and *AtTET-5.2* double reaction. PCR protocol showing HZ and WT lines using the BP, LP, and RP primers in all reactions

Lane	ID
1	DNA Hyperladder I
2	<i>AtTET-5.1</i> HZ 1
3	<i>AtTET-5.1</i> HZ 2
4	<i>AtTET-5.2</i> HZ 3
5	<i>AtTET-5.2</i> HZ 4
6	<i>AtTET-5.1</i> AZ 1
7	<i>AtTET-5.1</i> AZ 2
8	<i>AtTET-5.2</i> AZ 3

Investigation of root related phenotypes in *AtTET-5*

Primary root growth, lateral root emergence, and primordia development

We have seen that *AtTET-5* is most highly expressed in the root tissue of *Arabidopsis*, this allows us to focus our investigation on root related phenotypes. However, no significant differences ($P > 0.05$) were found between the rate of primary root growth or lateral root density between the *AtTET-5* line when using *Colombia* controls (Fig. 4.9 and Fig. 4.10).

We then moved on to investigate the role of *AtTET-5* in lateral root primordium development.

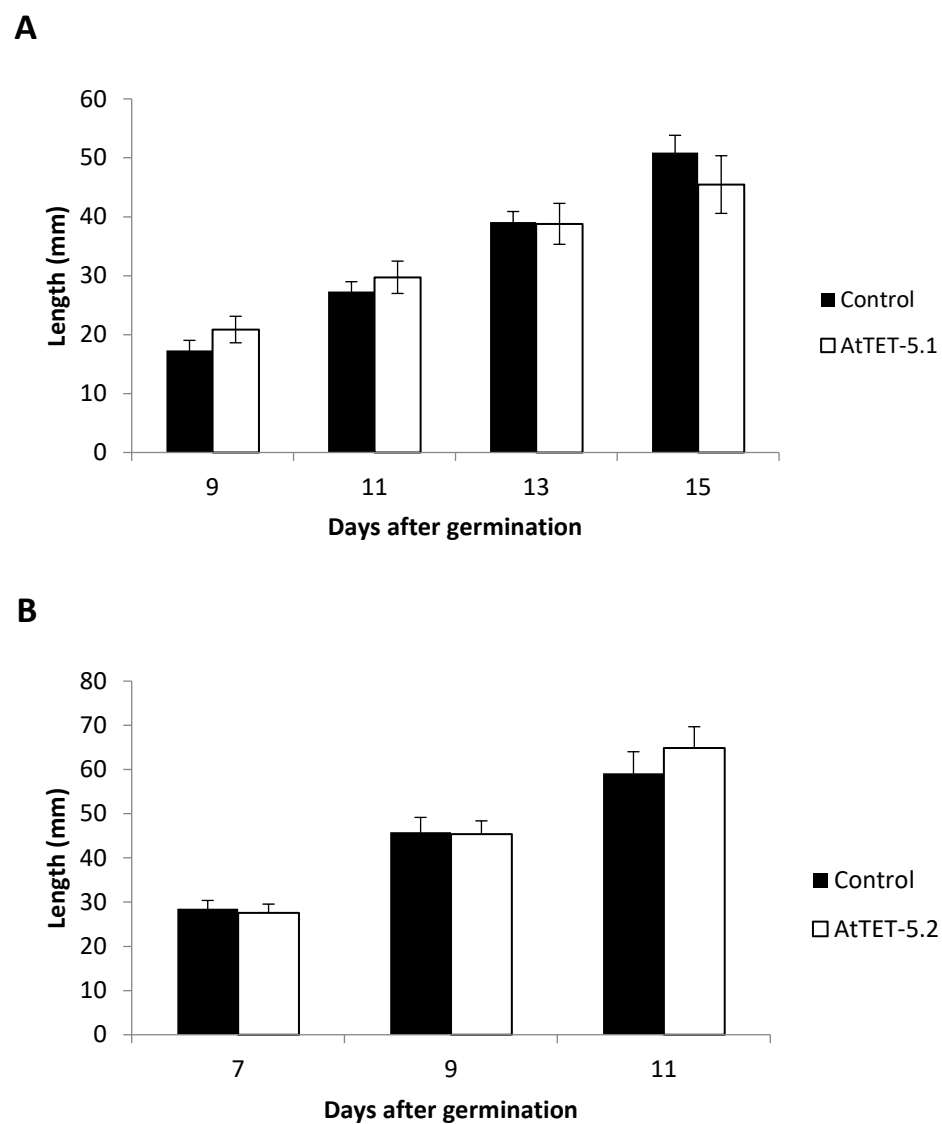


Figure 4.9: Primary root growth in *AtTET-5*. **A)** *AtTET-5.1*. **B)** *AtTET-5.2*.

The rate of growth for both transgenic lines were not significantly different that the control. Values represent the mean + SE of biological replicates.

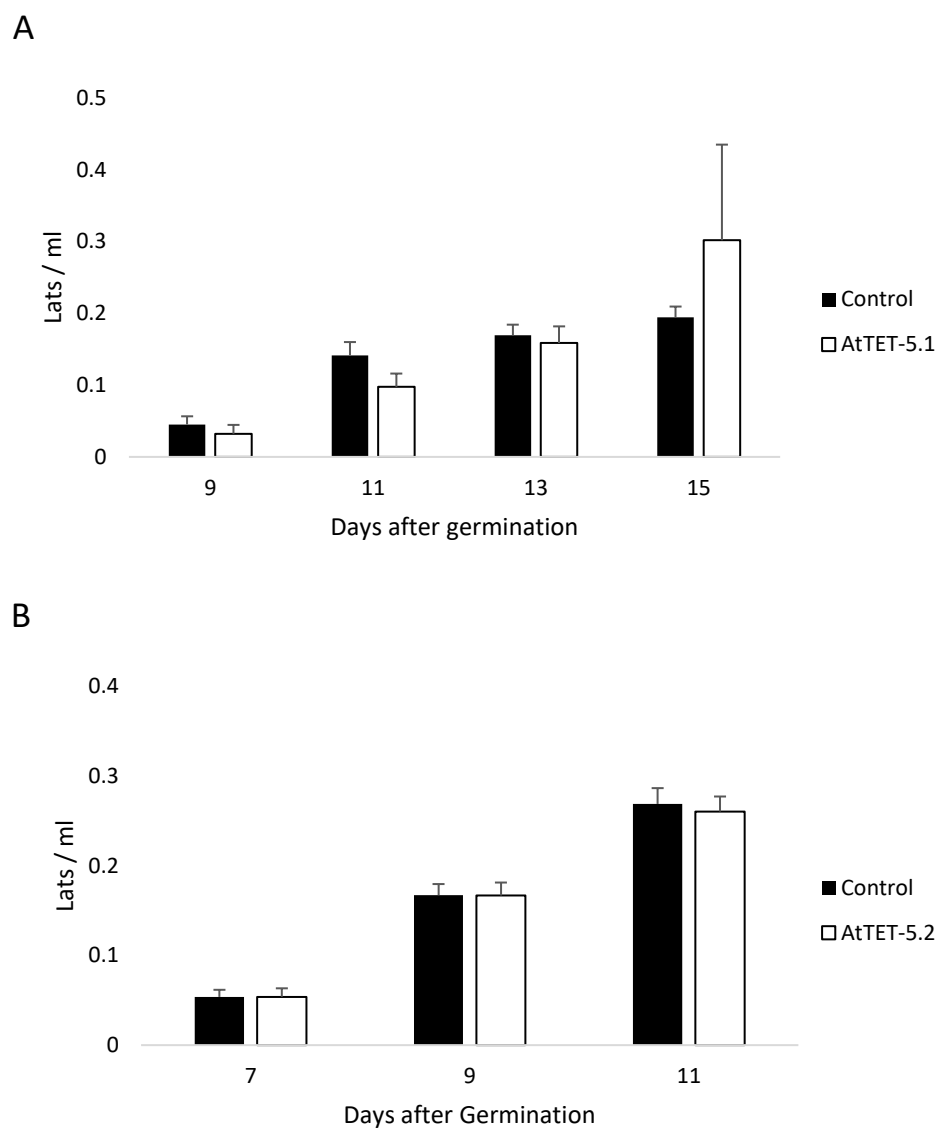


Figure 4.10: Lateral root density in AtTET-5. **A)** *AtTET-5.1*. **B)** *AtTET-5.2*. The number of lateral roots per ml of root is plotted. Values represent the mean + SE of biological replicates.

To assess the effects of *AtTET-5* on lateral root primordia development, a gravitropic response was initiated by tilting growing plants by 90° to initiate lateral root growth and promote the development of primordia. Plants were grown for 4-5 days prior to tilting and left for a period of 24 and 42 hours. Root tissue was then stained and embedded onto glass slides and the development of primordia was investigated. A small difference can be seen during development of primordia 24 hours after the gravistimulus was applied (Fig. 4.11: A). Primordia in the *AtTET-5.1* transgenic lines were seen to be more developed than the Colombia controls. This difference however, had dissipated after 42 hours where there was no longer any difference between the transgenic and control lines (Fig. 4.11: B). For the *AtTET-5.2* line, there was also seen to be no impact on the plant (Fig. 4.12) suggesting that *AtTET-5* doesn't affect the growth and development of primary and lateral root development.

These results suggest that it is possible that removal of the *AtTET-5* gene has no effect of root development, it is also possible that there is redundancy within the root system with another tetraspanin gene which has been observed recently (F. Wang et al., 2015).

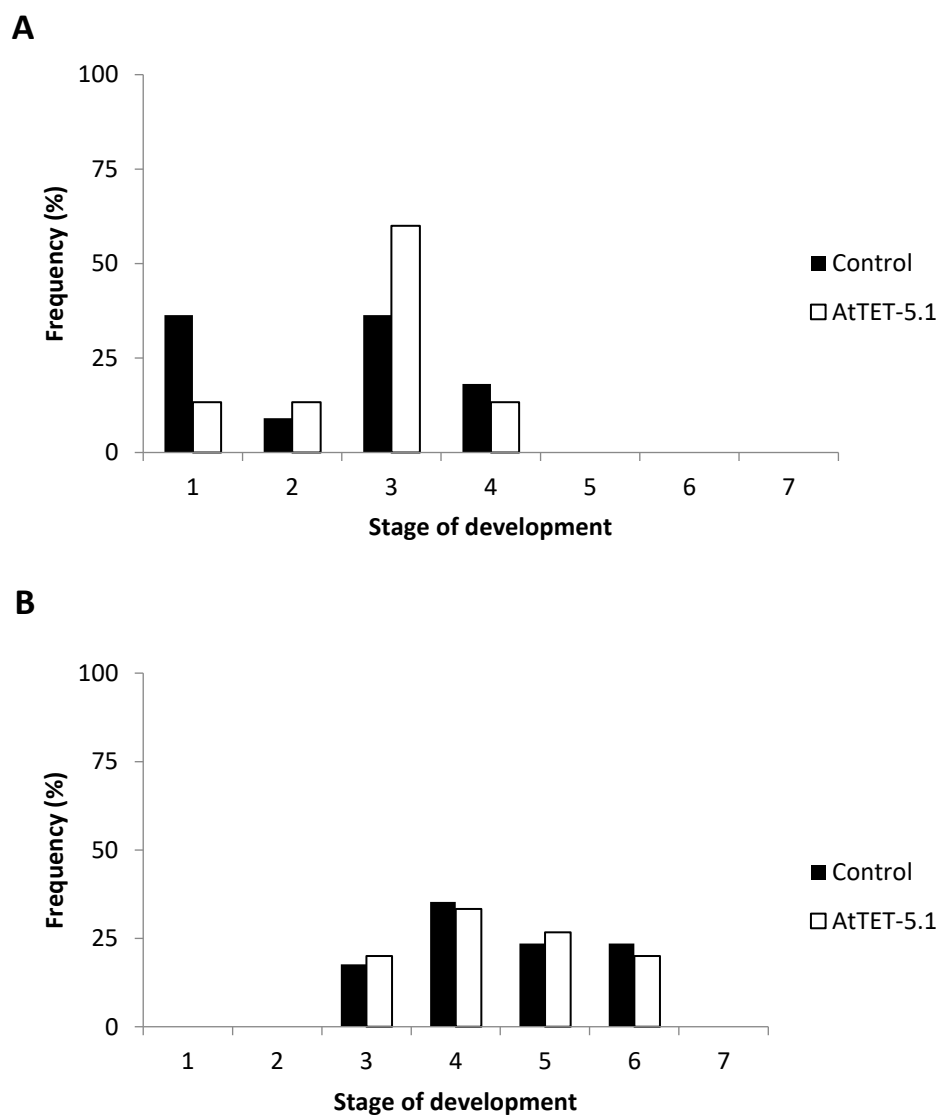


Figure 4.11: Primordia development in AtTET-5.1. **A)** 12 hours. **B)** 24 hours. No difference in primordia development was seen in the *AtTET-5* line. Values represent the percentage of total biological replicates.

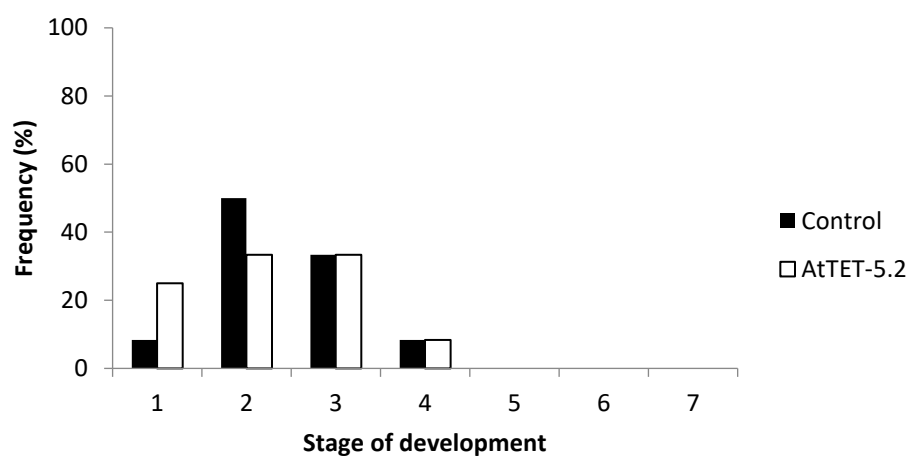
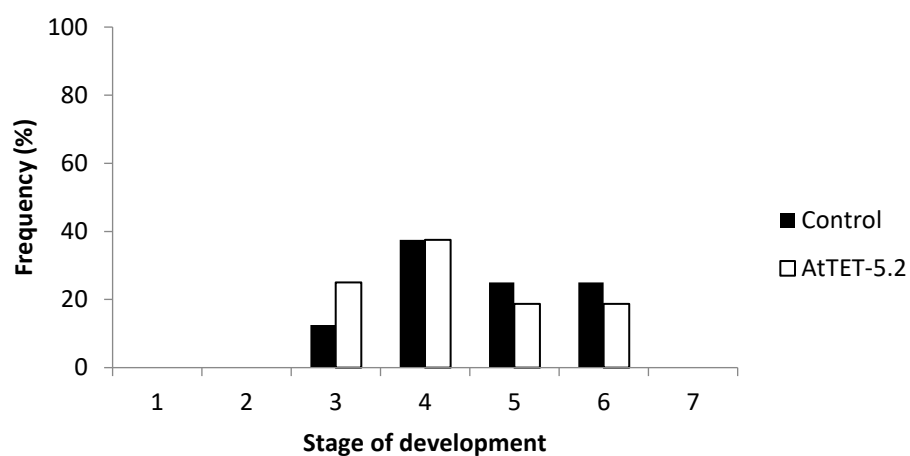
A**B**

Figure 4.12: Primordia development in AtTET-5.2. **A)** 24 hours. **B)** 42 hours. No difference in primordia development was seen in the *AtTET-5* line. Values represent the percentage of total biological replicates.

Root gravitropism in transgenic line *AtTET-5*

Root gravitropism requires the coordination of a number of genes working concurrently to maintain healthy root growth. A gravistimulus is widely used to investigate the role of specific genes in root development. Plants were grown vertically for 4-5 days on ½ MS media. When the roots were approximately 2-3cm in length the plate was rotated 90° to the right and an infrared camera was used to catalogue the curvature of the root at set intervals (Fig 4.13). A slowed response to a gravistimulus was seen in the *AtTET-5* line which becomes more pronounced 5 hours after the gravistimulus was applied.

The gravitropic response was quantified using the image analysis software Root Trace® (French et al., 2009). Root Trace uses an algorithm which allows high throughput measurements of root curvature. Start points are manually selected by the user and the software traces the primary root to the tip and calculates the angle. This allowed us to plot the relative root tip angle of the *AtTET-5* line to assess the plants gravitropic response (Fig. 4.14). The *AtTET-5.1* line was shown to have a significantly ($P<0.05$) slower rate of root curvature five hours after the stimuli was initiated suggesting that silencing the *AtTET-5.1* gene inhibits the roots gravitropic response, possibly by disrupting auxin distribution.

The *AtTET-5.2* line was not seen to show the same rate of curvature in the root as the *AtTET-5.1* line and was not significantly ($P>0.05$) different to the Colombia control (Fig 4.14). This means that the phenotype described in the *AtTET-5.2* line is not due to the *AtTET-5* gene but more likely due to another insertion in the genome.

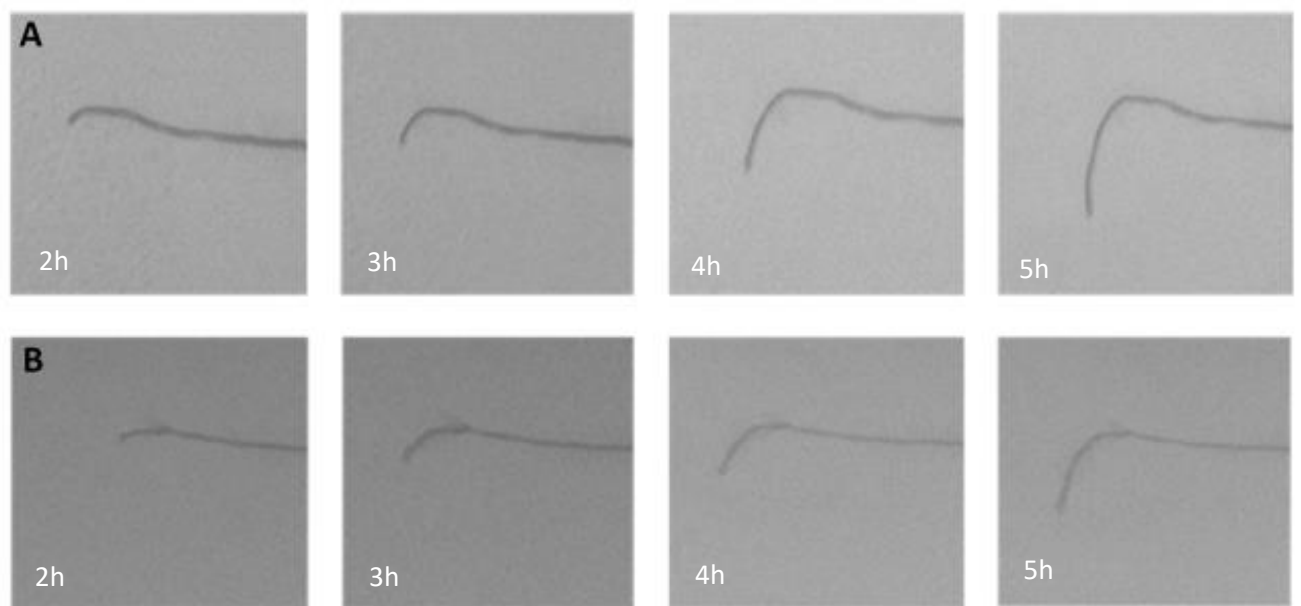


Figure 4.13: Gravitropic time lapse. **A)** Colombia, and **B)** *AtTET-5.1* development 2, 3, 4, and 5 hours after the invocation of the gravitropic response showing a distinct reduction in growth from the *AtTET-5.1* line.

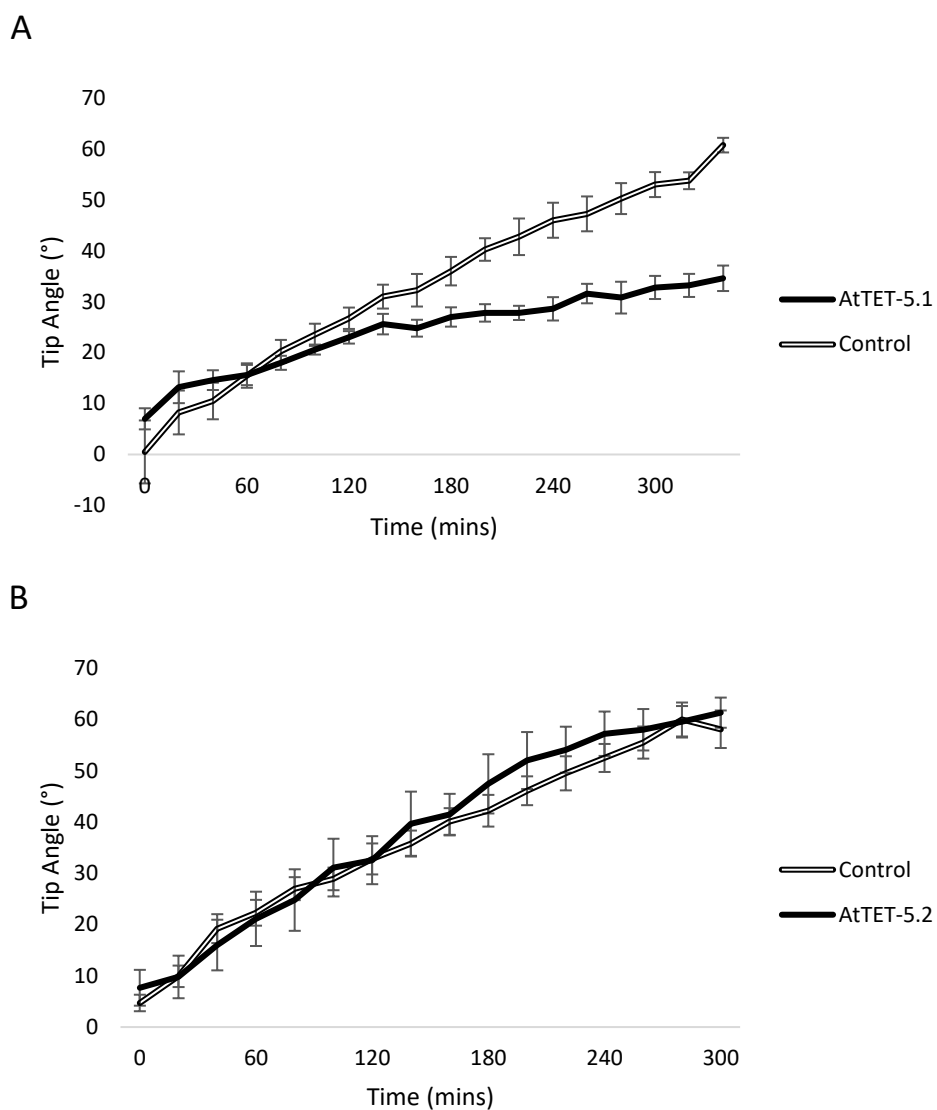


Figure 4.14: Gravitropic time lapse of AtTET-5. **A)** *At-TET5.1*. **B)** *AtTET-5.2*. The *AtTET-5.1* line was found to exhibit a slower response to a gravistimulus than the control line. This effect was not seen in the *AtTET-5.2* line.

The decision to characterise the *AtTET-5* gene in Arabidopsis, the experimental design, and implementation was completed prior to the publication of the functional analysis within tetraspanins completed by Wang et al., (2015). The report localized the expression of all tetraspanin genes in Arabidopsis and characterized initial phenotypes obtained from single and double mutant lines. The single *AtTET-5* mutant (SALK_020009C) was the same T-DNA insertion characterised in this chapter and the results published were consistent with the results described in this report. However, the gravitropic phenotype was not investigated by Wang et al., (2015) highlighting the potential role of *AtTET-5* in root gravitropism remains a novel finding. Additionally, it was found that *AtTET-5* and *AtTET-6* have redundant functions and require a double knock-down mutant to assess their role in Arabidopsis development. These double-mutant lines were found to exhibit synergistic phenotypes including an increase in leaf, rosette, and primary root length and may provide an explanation to the inconsistencies described in this report (F. Wang et al., 2015).

These results reiterate the work described in this chapter, suggesting that functional redundancy between *AtTET-5* and *AtTET-6* is preventing a phenotype from being accurately assessed. It is likely then, that by obtaining a double-mutant line as described by Wang et al., (2015), a more significant curvature phenotype would be apparent in Arabidopsis.

Root gravitropism in tomato

To further characterise the role of the tetraspanins in tomato plants, seeds with fruit specific overexpression of the *S/TET-6* gene were grown on ½ MS media for 7-9 days and a gravistimulus was initiated to assess the relationship between these differentially conserved genes (Fig. 4.15).

Root gravitropism is much slower in tomato roots when compared with *Arabidopsis*. It took around 12 hours for the initial signs of a gravitropic response to be measured compared with up to 5 hours in *Arabidopsis*. There were no significant ($P>0.05$) differences between the root angle of the azygous control and the *S/TET-6* line suggesting that despite the phenotypic differences observed in the *Arabidopsis* mutants, effects on root gravitropism were not observed when the *S/TET-6* gene in tomato was over expressed (Fig. 4.15).

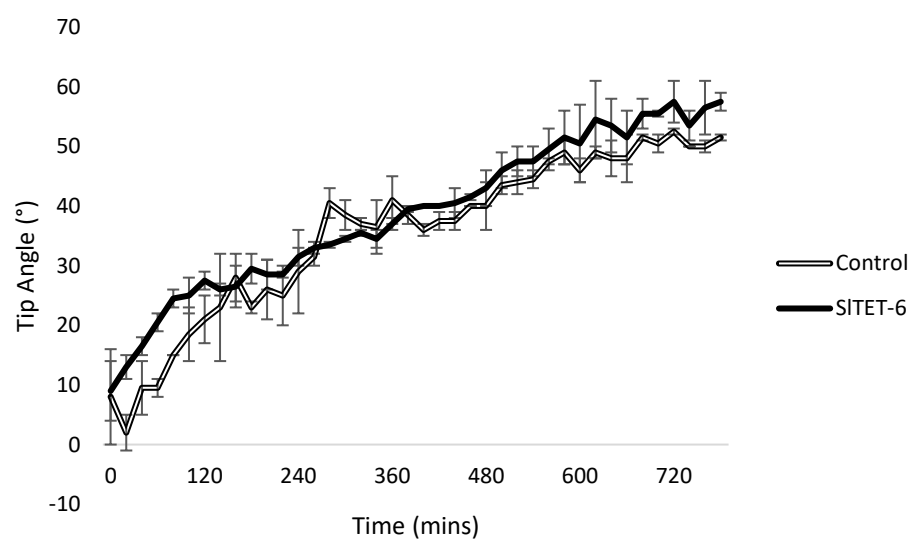


Figure 4.15: SITET-6 Gravitropic time lapse. The *SITET-6* showed no significant different in root curvature when compared to the azygous line.

The most likely explanation for this assessment is the nature of the mutants. Both *Arabidopsis* lines were constitutive single-insert knock-down lines and are in direct contrast to the tomato overexpression line. It is therefore likely, that using a similar knock-down mutant in tomato will provide more comparable data to assess the nature of the tetraspanin and its function in root growth and development. However, the following chapter indicates that silencing tetraspanin genes in tomato may be a substantial challenge. In Chapter 5 we now focus on a tetraspanin in tomato that is highly fruit expressed.

Chapter 5

Generation of transgenic Tet-8 tomato lines

5.1 Introduction

There are twelve genes encoding tetraspanins in tomato (The Tomato Genome Consortium, 2012), six of which show expression patterns confined to the root system (Soly03g059390, Soly08g080730, Soly12g010570, Soly06g075360, Soly08g076850, Soly04g049080). Soly04g049080 was the target of the initial experiments and is the orthologue of a gene in melon linked to longer shelf life. This gene, when over expressed in tomato fruits produced no obvious phenotype (Chapter 3), and previous work in Arabidopsis supports the importance of tetraspanins in root development (Cnops et al., 2006).

The expression of three further tetraspanins in the tomato genome are confined to flower buds (Soly03g114480, Soly12g038410, and Soly06g069320), one to immature fruit development (Soly07g025510), and one to all stages of leaf development (Soly11g072480). However, Soly07g006280 is specifically expressed at the Breaker stage of tomato fruit development with increasing expression as the fruit ripens. This tomato tetraspanin shows sequence homology to the Arabidopsis gene At4g23410, *AtTET-5*. We have named this tomato gene *SITET-8*.

The ripening-related expression of *SITET-8* is based on RNA-seq data from the tomato genome programme (Tomato Genome Consortium 2012) and indicates that it plays a role in this important developmental process (Fig. 5.1). The precise role of these proteins in fruit is however, unknown. It is possible that their primary role is linked to cell adhesion due to their high degree of conservation and significance in other plant developmental processes (Sprunck & Dresselhaus, 2009; van Spriel & Figdor, 2010a). We hypothesise that tetraspanin proteins could play a role in cell-to-cell adhesion and impact on shelf life of the fruit.

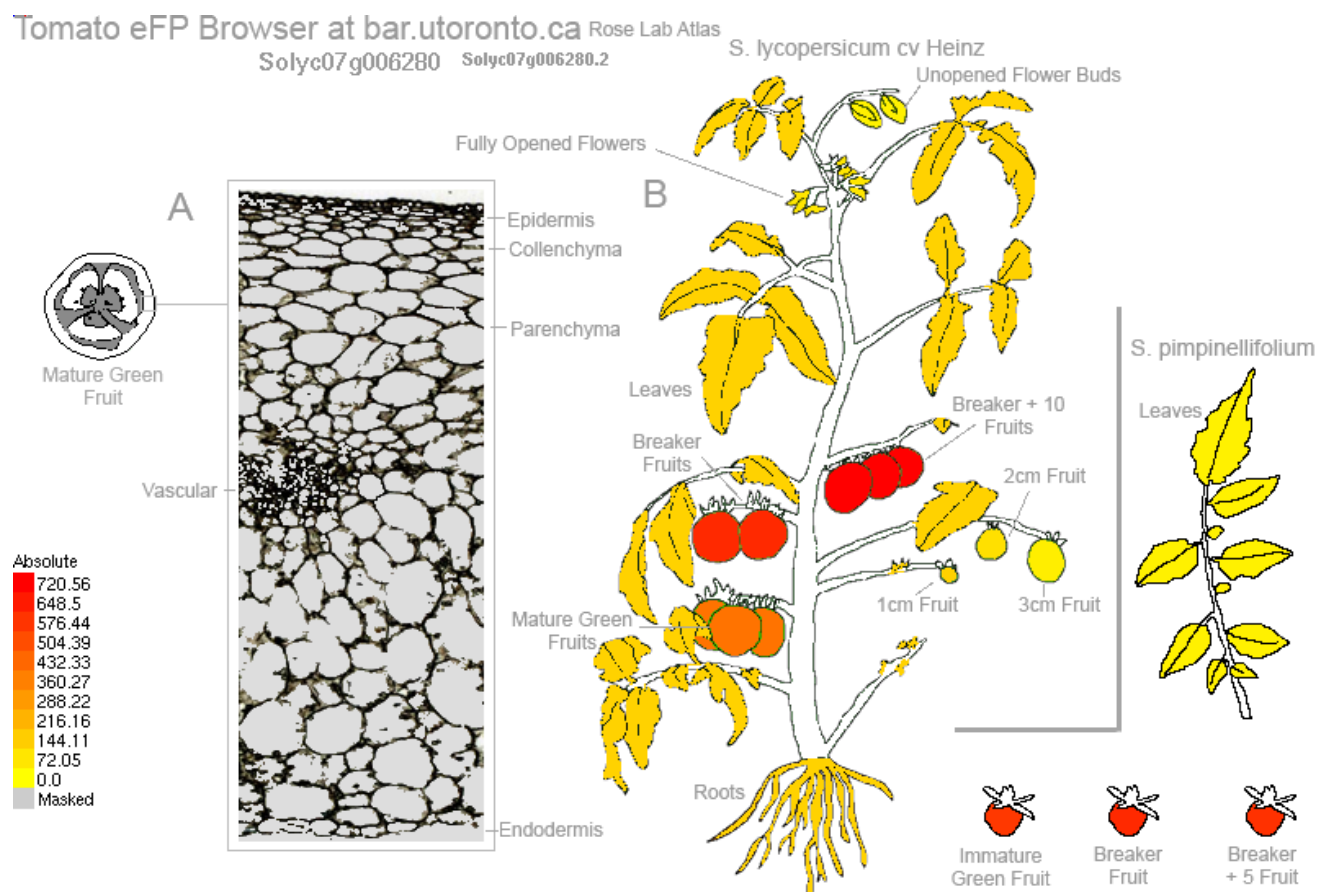


Figure 5.1: Visual representation of SLTET-8 RNA expression profile. The *SITET-8* gene can be seen to be highly expressed in developing and ripening fruits. Taken from the Tomato eFP Browser (http://bar.utoronto.ca/efp_tomato/cgi-bin/efpWeb.cgi)

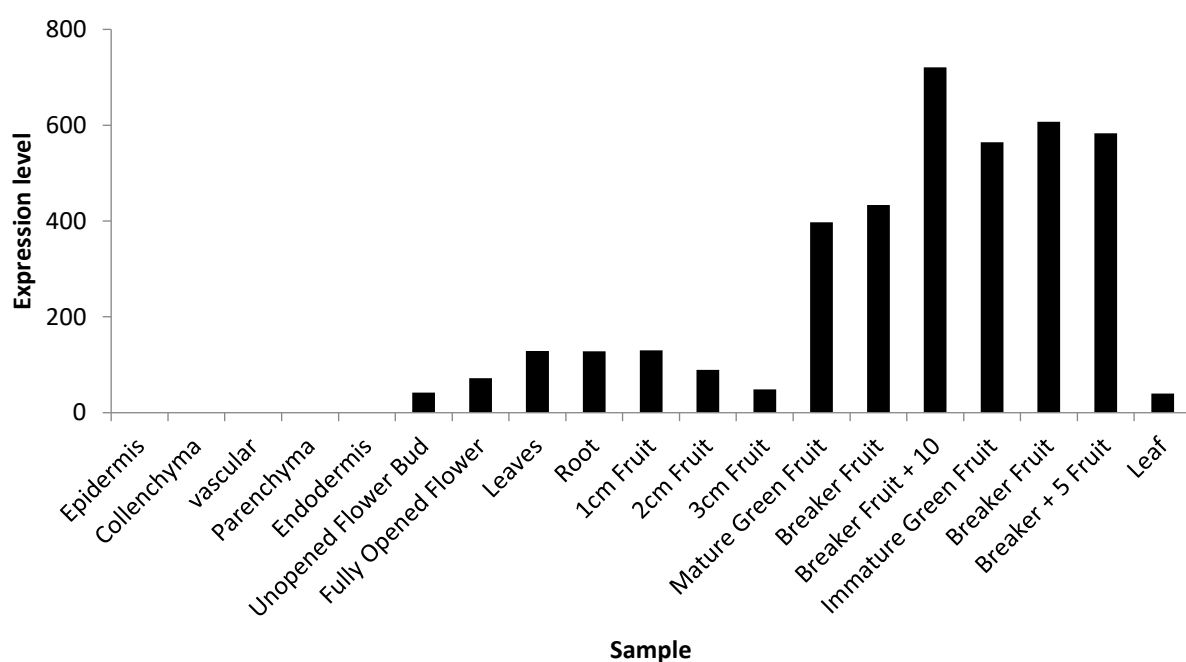


Figure 5.2: RNA expression profile of *SITET-8*. Data shows expression patterns of *SITET-8* in different tissues of tomato. These data highlight the relative expression of the *SITET-8* gene fruit tissues compared with the rest of the plant. Taken from the Tomato eFP Browser (http://bar.utoronto.ca/efp_tomato/cgi-bin/efpWeb.cgi)

Constructs were designed to overexpress and knock down the *SlTET-8* gene in transgenic tomato lines to test the role of this gene in the ripening process. We decided to initially try the strong, but constitutive, 35S promoter and follow this with the PG promoter in reserve if more 'fruit specific' expression was required (Fig. 5.3, from Fernandez et al., 2009).

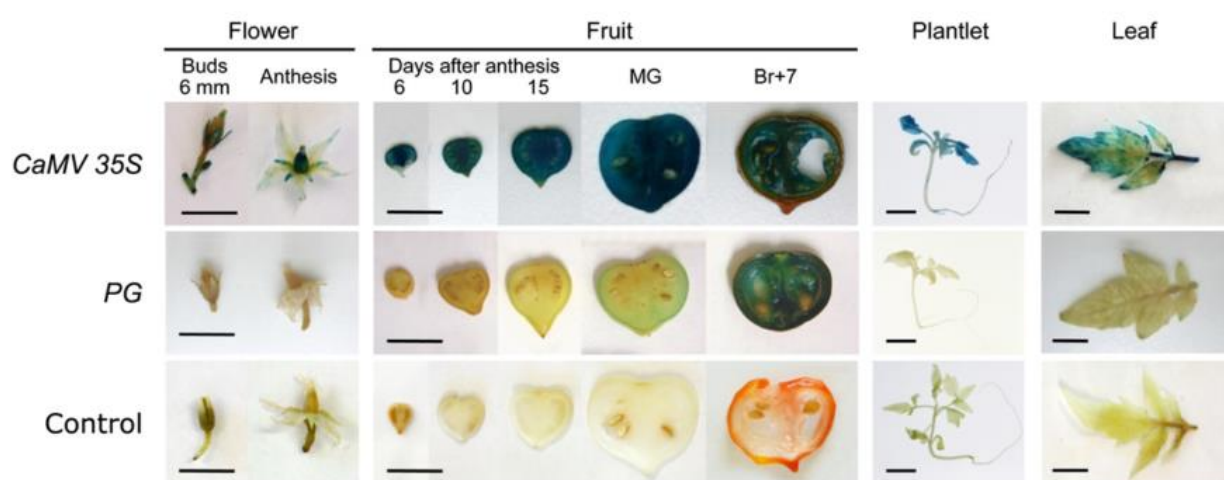


Figure 5.3: GUS activity in tomato stably transformed with CaMV 35S, PG, and Control. Expression of genes using the CaMV 35S promoter exhibit constitutive expression at all developmental stages compared with the PG promoter which exhibits expression only in ripening fruit. Figure taken and adapted from Fernandez et al., (2009).

5.2 Materials and Methods

Polymerase chain reaction (PCR)

For generation of the overexpression construct (801bp) using primers with flanking *attB1* and *attB2* sites, it was necessary to use Touchdown PCR to generate gene fragments with sufficient efficiency for use in the cloning procedure. Touchdown PCR facilitates a higher annealing temperature for the primers in the early cycles followed by a reduction in annealing temperature to allow for more specific and efficient amplification of the target gene in the later cycles. The PCR mix and programme used for this reaction is listed below.

PCR Reaction Mix	Volume (μ L)
2X Phusion master mix	2
dNTPs	0.5
Forward primer	1
Reverse primer	1
Taq polymerase	0.5
Template	2
Sterilised Water	13
Total volume	20

PCR Programme	Temperature ($^{\circ}$ C)	Time	
Initial denaturation	98	3 min	
Denaturation	98	30 sec	} 10 cycles
Annealing	64	30 sec	
Extension	72	60 sec	
Denaturation	98	30 sec	} 25 cycles
Annealing	54	30 sec	
Extension	72	60 sec	
Final extension	72	10 min	
Hold	4		

Adding a 3' overhang to PCR fragment

A 3' adenine overhang was added to PCR products for insertion of the *SLTET-8* gene into the pCR8/GW/TOPO donor vector. The PCR mix and programme used for these reactions is listed below. Samples were kept at -20°C until needed.

PCR Reaction Mix	Volume (μL)
Fresh PCR product	10
10X PCR buffer	1.5
dATP (10mM)	0.5
<i>Taq</i> DNA polymerase	1
Sterilised water	7
Total volume	20

PCR Programme	Temperature(°C)	Time
Annealing	72	60 min
Hold	4	

BP and LR clonase reactions

The BP Clonase reaction was used to generate entry clones with two *attL* flanking sites. The BP reaction makes use of *attB* or 3'-adenine overhang flanking regions on the target sequence to recombine the gene of interest into a donor vector and in the process, disrupt the lethal *ccdB* gene leaving a completed entry clone with *attL* flanking regions ready for use in the LR reaction (Fig 5.4).

Reactions were set up with 150ng of PCR product (*attB* flanking sites) and 150ng of donor vector (pDONR221) with TE buffer (pH 8.0) to total volume of 8μL. 2μL of BP Clonase II Enzyme mix (Invitrogen) were added to each reaction and incubated overnight at room temperature. The reaction was inactivated by the addition of 2μL of Proteinase K and incubated at 37°C for 10 minutes. 3μL of the inactivated BP reaction was transformed into *E. coli* DH5α and plated on LB agar containing 100mg/ml kanamycin. Colonies obtained the following day were suspended and used for multiplication in liquid LB and for use in plasmid preparations. Entry vectors with the gene of interest were sent for sequencing for confirmation of the template sequence in the correct orientation before use in the LR reaction to generate expression clones. Diagrams representing the BP reactions used in this report are illustrated in figure 5.5.

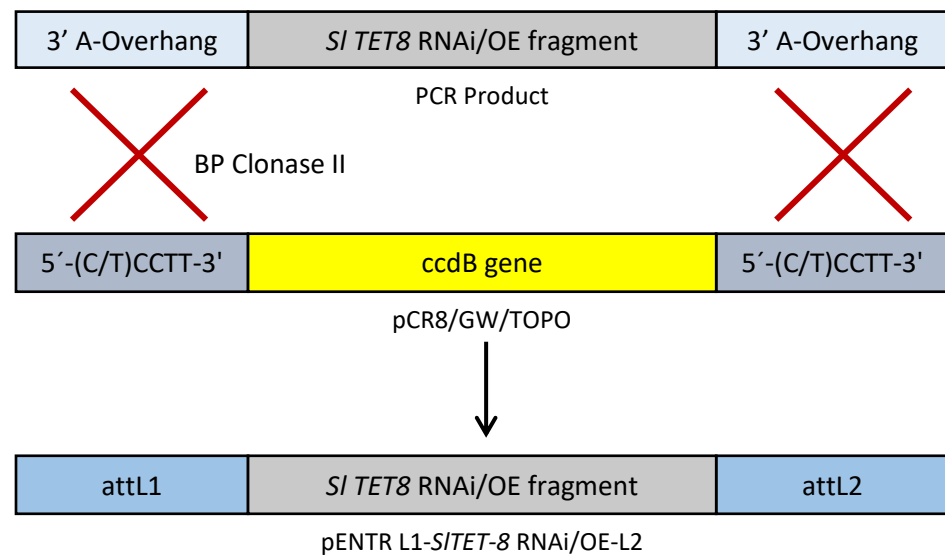
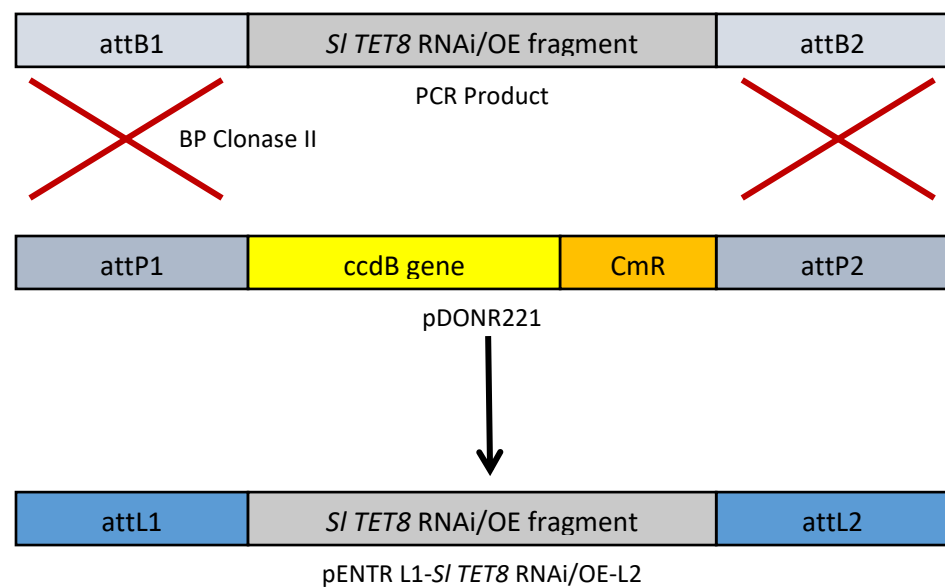
A**B**

Figure 5.4: Description of the BP reaction to incorporate the SISLTET-8 RNAi and over-expression gene fragments into the donor vectors. **A)** PCR8/GW/TOPO and **B)** pDONR221.

The LR Clonase reaction was performed using 150ng of entry clones and 150ng destination vector with the addition of TE buffer (pH 8.0) to a final volume of 8 μ L. To each reaction, 2 μ L of LR Clonase II Enzyme mix (Invitrogen) was added, mixed and incubated overnight at room temperature. The reaction was inactivated by the addition of Proteinase K and incubated at 37°C for 10 minutes. The LR reaction was then used for transformation into *E. coli* DH5 α with the appropriate antibiotic selection in the LB medium. Plasmid preparations were performed on the colonies obtained and confirmation of the insertion of the candidate gene was performed by PCR using primers specific to the gene. (Fig. 5.5 & 5.6).

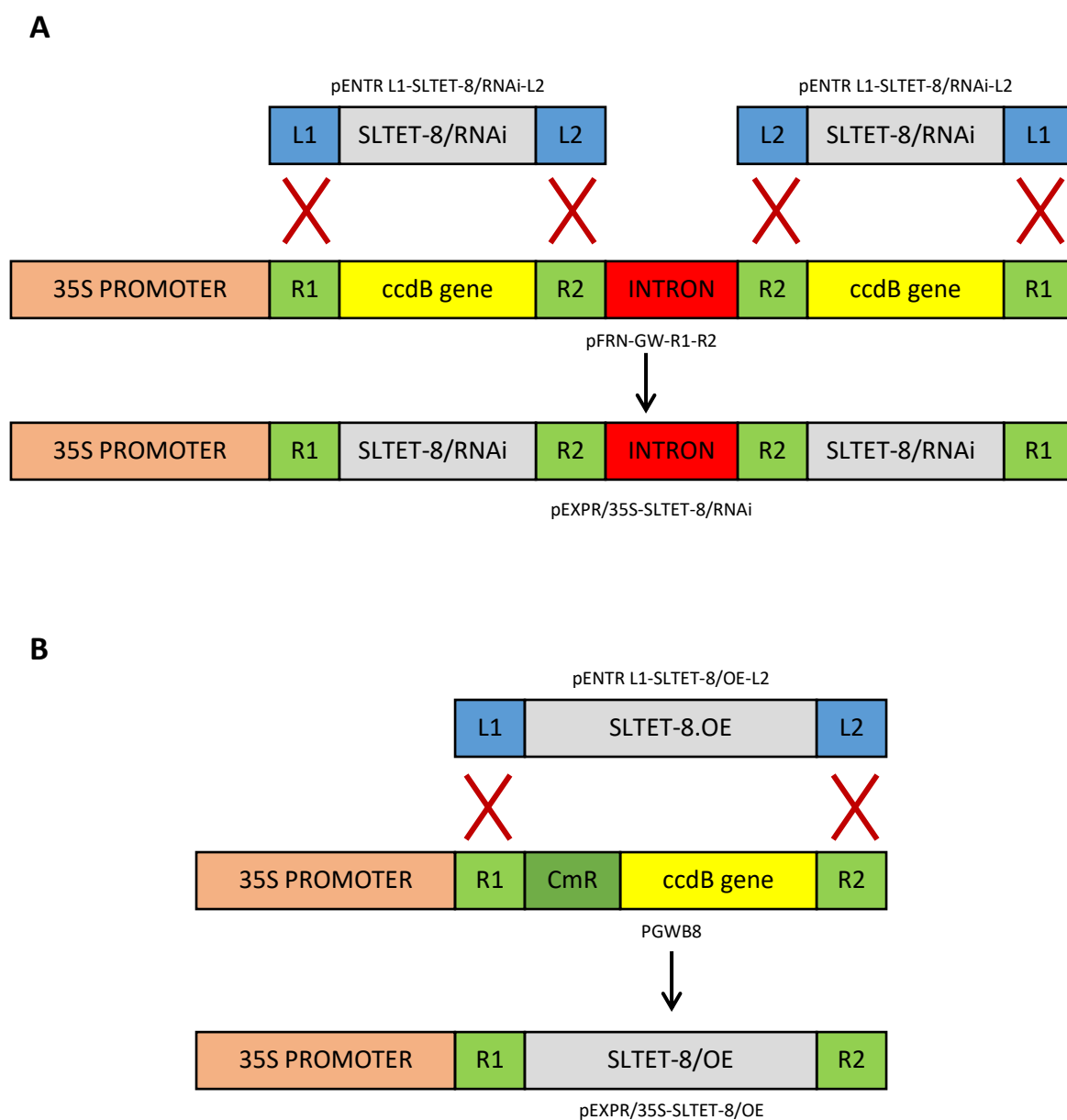


Figure 5.5: Description of the LR reaction to incorporate the SLTET-8 gene fragment into the pFRN-GW-R1-R2 and PGWB8 destination vectors. **A)** pFRN-GW-R1-R2. **B)** PGWB8. For the RNAi constructs, both gateway cassettes are separated by an intron spacer in order to form the hairpin RNA for silencing of the targeted gene.

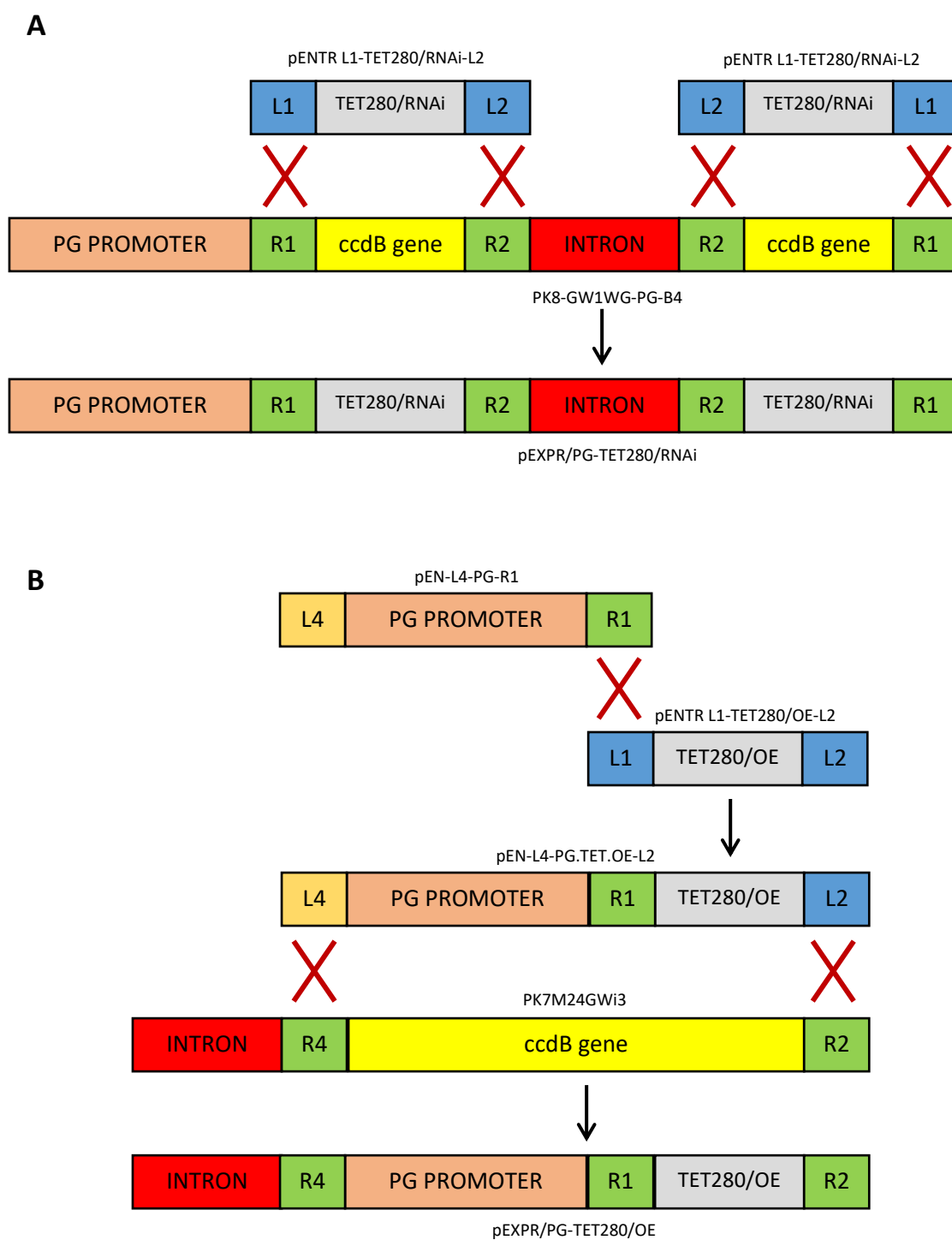


Figure 5.6: Description of the LR reaction to incorporate the SLTET-8 overexpression gene fragment into the PK8-GW1WG-PG-B4 and PK7M24GWi3 destination vectors. **A)** PK8-GW1WG-PG-B4. **B)** PK7M24GWi3. For the RNAi constructs, both gateway cassettes are separated by an intron spacer in order to form the hairpin RNA for silencing of the targeted gene.

***Agrobacterium* transformation**

Agrobacterium tumefaciens strain EHA105 was thawed on ice from storage at -80°C for five minutes and pipetted into a clean, chilled electroporation cuvette. 2µL expression clone was added to the cuvette and electroporation was performed at 2.5V, 25µFD, and 400 OHMS. 300µL fresh LB medium was added immediately to the cells. Cells were left to incubate at 28°C for 2 hours with agitation (200 rpm) before being plated onto LB agar with the appropriate antibiotics. The transformed *Agrobacterium* were left to incubate for 2 days at 28°C. Colonies were selected and grown in liquid LB medium with antibiotics and colony PCR was used to confirm the presence of the candidate gene before use in the plant transformations.

Generation of transgenic plants

Plant transformation followed a standard protocol (McCormick, 1997). Ailsa Craig seeds were surface sterilized using 70% ethanol for 30 seconds and then rinsed with sterile water three times before a further soaking in 50% sodium hypochlorite for 7 minutes. Seeds were repeatedly washed with sterile water to remove all the detergent and placed on sterile filter paper to dry. The seeds were sown on MSR3 medium using flame sterilized forceps. The petri dishes were kept at 4°C in the refrigerator for 1 day before being transferred to the tissue culture room. Seedlings were then grown in sterile magenta pots at 21°C for 9-10 days under fluorescent light.

The pre-culture procedure was carried out as follows, cotyledons were excised from 9-10 day old seedlings and cotyledon pieces were placed on a sterile tile. The tips of the cotyledons were removed with a scalpel to wound the tissues and the explants were kept in sterile reverse osmosis water to prevent dehydration. Cotyledon pieces were then placed upside down in petri dishes containing MSZ media covered in foil and were incubated under low light intensity (24-48µmol m⁻² s⁻¹, Daylight fluorescent illumination) for 1 day. A single *Agrobacterium* colony successfully transformed with the relevant expression clones was grown in LB liquid medium with the appropriate

antibiotic (50mg/L Kanamycin) at 28°C in a rotary shaker for 24-48 hours. The *Agrobacterium* suspension was re-suspended by centrifugation (3000 rpm, 10 minutes) and diluted in liquid MSR3 to a final optical density between 0.1-0.2 (OD₆₀₀). The explants were exposed to the *Agrobacterium* mixture for 10 minutes and transferred to sterile filter paper to dry before being transferred to plates containing MSZ media supplemented with 50mg/L Kanamycin and 100 mg/L Carbenicillin to encourage shoot regeneration. The medium was changed every 10-14 days and when shoots were fully grown they were separated from the callus and placed upwards in rooting medium.

Plantlet acclimatization

Once roots were seen to have fully emerged the plantlets were removed from the agar medium and washed in sterile water. Plantlets were grown in moist F2+S growing compost. After one week, plantlets were potted into 10cm diameter pots in M3 compost and left to produce fruits in the growth room.

5.3 Results and Discussion

Generation of the *SITET-8* plasmids

Plant transformation constructs were designed to over express or silence the *SITET-8* gene initially under the control of the 35S promoter. The coding sequences for the *SITET-8* gene fragments were obtained by amplification from B+4 fruit cDNA and compared with sequence information on the database (Fig 5.7 & 5.8). For the RNAi construct to silence the *SITET-8* gene a smaller fragment crossing the 3' UTR of the gene was selected as a small interfering RNA (Fig. 5.10).

For the initial cloning step the PCR products were ligated into the donor vector (PCR8/GW/TOPO). The BP reaction was used to facilitate the incorporation of the *SITET-8* gene fragments into the donor vector and resulted in the gene fragments being flanked by *attL* sites ready for use in the LR recombination reaction.

PCR to amplify the *SITET-8* fragments (351bp, and 864bp) was performed to confirm the presence of the gene fragments in the donor vector. These are shown in Figures 5.9 and 5.10 for the RNAi and overexpression constructs respectively.

PCR	TACGTGAGCCCAACAACTGGACAAGATCATCGACCTCATCCACTACCAATCCAGACTGT	149
<i>SITET-8</i>	TACGTGAGCCCAACAACTGGACAAGATCATCGACCTCATCCACTACCAATCCAGACTGT	99
PCR	GCTACATGGAGCAACGAGTCAAATTTATTGTGCTATGGCTGCCAATCCTGCAAAGCTGGG	209
<i>SITET-8</i>	GCTACATGGAGCAACGAGTCAAATTTATTGTGCTATGGCTGCCAATCCTGCAAAGCTGGG	159
PCR	CTGCTAGACAACATCAAAAGTGACTGGAAGAGGGTAGCTGTGCTCAACATCATTTTCCTC	269
<i>SITET-8</i>	CTGCTAGACAACATCAAAAGTGACTGGAAGAGGGTAGCTGTGCTCAACATCATTTTCCTC	219
PCR	ATCTTCCTCATCATCGTCTACTCTATCGGATGTTGTGCTTTCAGGAACAACCGAGAGGAC	329
<i>SITET-8</i>	ATCTTCCTCATCATCGTCTACTCTATCGGATGTTGTGCTTTCAGGAACAACCGAGAGGAC	279
PCR	AATGCTTGGAAGCGTTATCCTTAAACACTCTCTGTTGAGTCTCGACTGCTTTATGTTGCG	389
<i>SITET-8</i>	AATGCTTGGAAGCGTTATCCTTAAACACTCTCTGTTGAGTCTCGACTGCTTTATGTTGCG	339
PCR	TA	391
<i>SITET-8</i>	TA	341

Figure 5.7: Sequence alignment of *SITET-8* RNAi construct. The sequence alignment shows the similarity between the sequence isolated from AC⁺ cDNA and the gene fragment of interest.

PCR	ATGGTGCGGTGTAGTAACAATTTAGTGGGGATTCTGAGTATAGTGACACTTTTGCTGTCG	214
<i>SITET-8</i>	ATGGTGCGGTGTAGTAACAATTTAGTGGGGATTCTGAATATAGTGACACTTTTGCTGTCG	60
PCR	ATCCCAATTATAGGAGGAGGGATATGGTTGTCAAACAAGCAAATACAGAGTGTGAGAGG	274
<i>SITET-8</i>	ATCCCAATTATAGGAGGAGGGATATGGTTGTCAAACAAGCAAATACAGAGTGTGAGAGG	120
PCR	TTTCTTGAAAAGCCAGTAATAGCAATAGGTGTTTTATATTGCTTGTTTCATTGGCTGGT	334
<i>SITET-8</i>	TTTCTTGAAAAGCCAGTAATAGCAATAGGTGTTTTATATTGCTTGTTTCATTGGCTGGT	180
PCR	ATAATTGGATCTTGCTGTAGAGTTACTTGGTTACTTTGGgtttatctacttggtatgttt	394
<i>SITET-8</i>	ATAATTGGATCTTGCTGTAGAGTTACTTGGTTACTTTGGGTTTATCTACTTGTTATGTTT	240
PCR	ttgttgattttgttgcttttctgtttcacaaatctttgcttttggTGACTAATAAGGGT	454
<i>SITET-8</i>	TTGTTGATTTTGTGCTTTTCTGTTTCACAATCTTTGCTTTTGGTGACTAATAAGGGT	300
PCR	GCTGGTGAAACAATTTCTGGTAGAGGGTATAAGGAGTATAGATTTGGGGATTACTCTAAT	514
<i>SITET-8</i>	GCTGGTGAAACAATTTCTGGTAGAGGGTATAAGGAGTATAGATTTGGGGATTACTCTAAT	360
PCR	TGGTTGCAGAAAAGAGTTGATAAGCATTGGAATAGAATTCATAGTTGTTTGCAGGATAGT	574
<i>SITET-8</i>	TGGTTGCAGAAAAGAGTTGATAAGCATTGGAATAGAATTCATAGTTGTTTGCAGGATAGT	420
PCR	AAGATTTGTGATACTTTGATTGAGGAATCAAATACTAAAGCTGATGATTTCTTCAAGAAA	634
<i>SITET-8</i>	AAGATTTGTGATACTTTGATTGAGGAATCAAATACTAAAGCTGATGATTTCTTCAAGAAA	480
PCR	CATCTATCTGCTCTTCAGTCTGGTTGCTGCAAGCCATCAAATGACTGTAACCTCCAGTAC	694
<i>SITET-8</i>	CATCTATCTGCTCTTCAGTCTGGTTGCTGCAAGCCATCAAATGACTGTAACCTCCAGTAC	540
PCR	GTGAGCCCAACAACTGGACAAGATCATCGACCTCATCCACTACCAATCCAGACTGTGCT	754
<i>SITET-8</i>	GTGAGCCCAACAACTGGACAAGATCATCGACCTCATCCACTACCAATCCAGACTGTGCT	600
PCR	ACATGGAGCAACGAGTCAAATTTATTGTGCTATGGCTGCCAATCCTGCAAAGCTGGGCTG	814
<i>SITET-8</i>	ACATGGAGCAACGAGTCAAATTTATTGTGCTATGGCTGCCAATCCTGCAAAGCTGGGCTG	660
PCR	CTAGACAACATCAAAAGTGACTGGAAGAGGGTAGCTGTGCTCAACATCATTTTCCTCATC	874
<i>SITET-8</i>	CTAGACAACATCAAAAGTGACTGGAAGAGGGTAGCTGTGCTCAACATCATTTTCCTCATC	720
PCR	TTCCTCATCATCGTCTACTCTATCGGATGTTGTGCTTTAGGTACATCGTATGGATAGGA	934
<i>SITET-8</i>	TTCCTCATCATCGTCTACTCTATCGGATGTTGTGCTTTAGGGAACAACCGA-G---AGGA	776
PCR	CAATGCTTGGAAAGCGTTATCCT	956
<i>SITET-8</i>	CAATGCTTGGAAAGCGTTATCCT	798

Figure 5.8: Sequence alignment of *SITET-8* over-expression construct. The sequence alignment shows the similarity between the sequence isolated from AC⁺ cDNA and the gene fragment of interest.

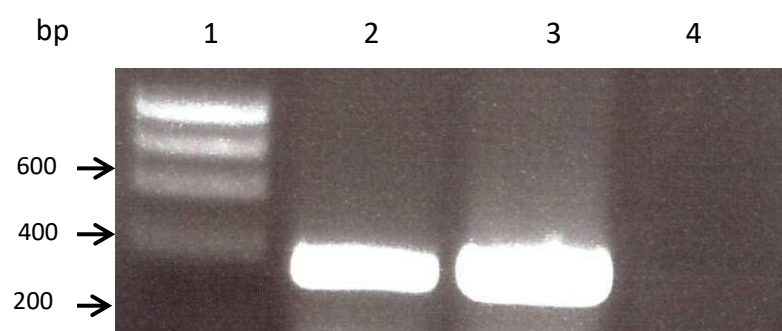


Figure 5.9: The BP reaction identifying the presence of a *SITET-8* RNAi gene fragment inside the PCR8/GW/TOPO entry vector

Lane	ID
1	DNA Hyperladder I
2	SITET-8.RNAi fragment 1
3	SITET-8.RNAi fragment 2
4	Negative Control (Water)

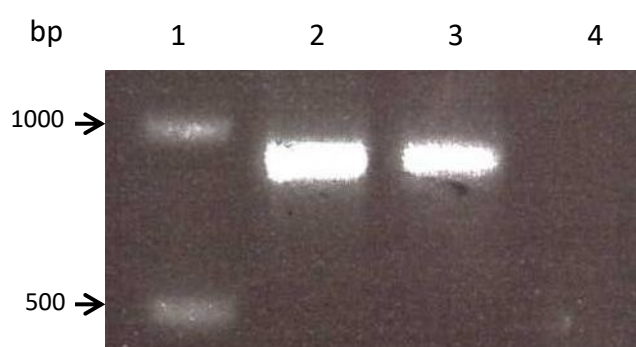


Figure 5.10: The BP reaction. identifying the presence of a *SITET-8* overexpression gene fragment inside the PCR8/GW/TOPO entry vector

Lane	ID
1	DNA Hyperladder I
2	SITET-8.OE fragment 1
3	SITET-8.OE fragment 2
4	Negative Control (Water)

The second step of the cloning procedure involved transfer of the *SITET-8* into plasmids containing the 35S promoter. Plasmids pENTR-L1-SLTET-8/RNAi-L2 and pENTR-L1-SLTET-8/OE-L2 containing the *SITET-8* gene fragments were used for the LR recombination reaction to produce expression clones for use in transformed plant tissues. The gateway binary destination vectors used were pFRN-GW-R1-R2, and PGWB8 for the RNAi and overexpression constructs respectively. Both cassettes confer expression using a constitutive 35S promoter where pFRN is designed to trigger gene silencing through hairpin molecules. This vector, like many other silencing constructs harbours two independent gateway cassettes separated by an intron spacer allowing two copies of the gene fragment to be inserted in opposite orientations. Both *SITET-8* gene fragments were inserted into their corresponding destination vectors using a single LR clonase reaction. The success of the recombination reactions was determined by amplification of the correct size products (802bp for the OE fragment and 302bp for the RNAi fragment) after cloning and plasmid preparation (Figs. 5.11 and 5.12).

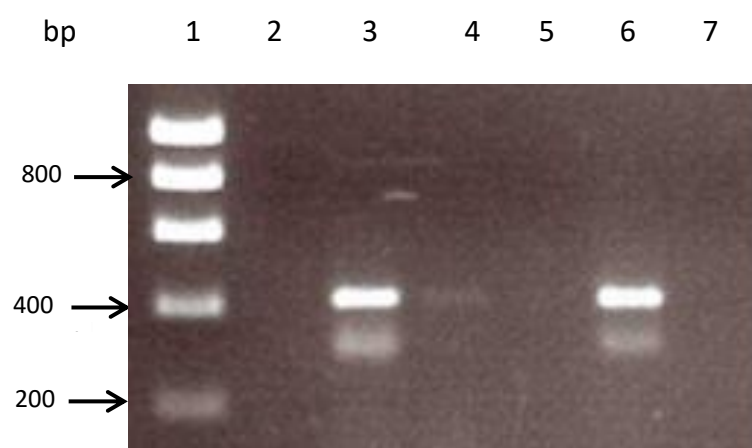


Figure 5.11: The LR reaction identifying the presence of a *SITET-8* RNAi gene fragment inside the pFRN-GW-R1-R2 destination vector

Lane	ID
1	DNA Hyperladder I
2	SITET-8.RNAi fragment 1
3	SITET-8.RNAi fragment 2
4	SITET-8.RNAi fragment 3
5	SITET-8.RNAi fragment 4
6	SITET-8.RNAi fragment 5
7	Negative Control (Water)

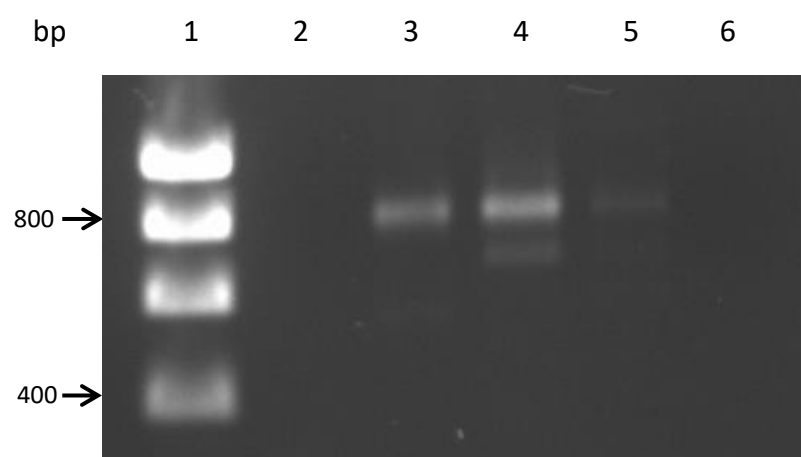


Figure 5.12: The LR reaction identifying the presence of a *SITET-8* overexpression gene fragment inside the PGWB8 destination vector

Lane	ID
1	DNA Hyperladder I
2	SITET-8.OE fragment 1
3	SITET-8.OE fragment 2
4	SITET-8.OE fragment 3
5	SITET-8.OE fragment 4
6	Negative Control (Water)

The final stage of the vector construction was the transformation of pEXPR/35S-SLTET-8/RNAi (302bp) and pEXPR/35S-SLTET-8/OE (802bp) into *Agrobacterium tumefaciens* strain EHA105 using electro-competent cells. Colony PCR to amplify the *SLTET-8* fragments was performed to confirm the presence of the gene fragments in the expression clones (Fig. 5.13 and 5.14).

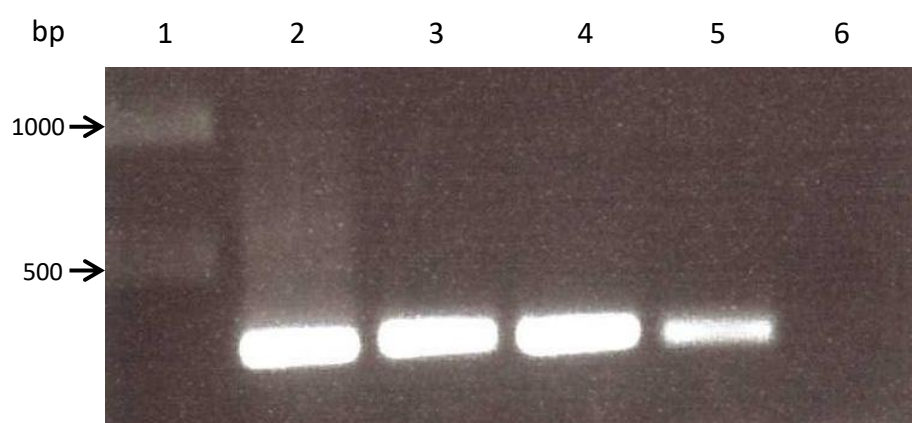


Figure 5.13: *Agrobacterium* transformation. Colony PCR analysis identifying the presence of a *SITET-8* RNAi gene fragment inside *Agrobacterium* strain EHA105

Lane	ID
1	DNA Bioline 1KB Hyperladder
2	SITET-8.RNAi fragment 1
3	SITET-8.RNAi fragment 2
4	SITET-8.RNAi fragment 3
5	SITET-8.RNAi fragment 4
6	Negative Control (Water)

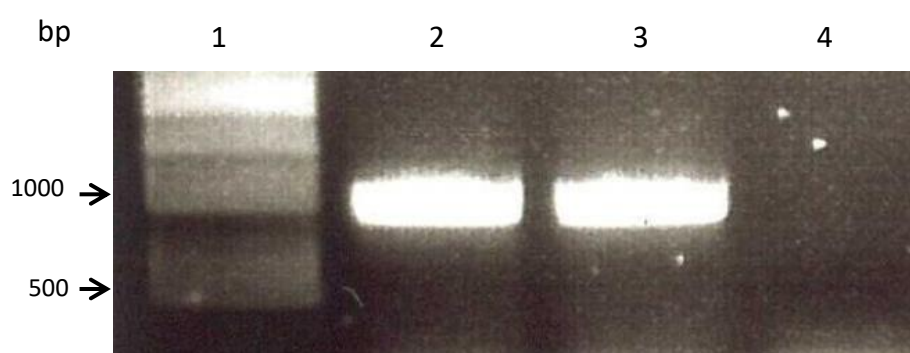


Figure 5.14: *Agrobacterium* transformation. Colony PCR analysis identifying the presence of a *SITET-8* overexpression gene fragment inside *Agrobacterium* strain EHA105

Lane	ID
1	DNA Bioline 1KB Hyperladder
2	SITET-8.OE fragment 1
3	SITET-8.OE fragment 2
4	Negative Control (Water)

Regeneration of transgenic plants from 35S promoter constructs

An estimated 1000 cotyledons were used in total with the *SITET-8* gene but the experiment still failed to produce any successful transformation events. Transformed cotyledons using both constructs did not yield any substantial regeneration in tissue culture after three to four weeks of subculture. The tips of the transformed explants showed some evidence of callus formation after 5-7 days in subculture suggesting the occurrence of cell division. The growth of the explants was very slow compared with untransformed cotyledons under no selection pressure that were being used as a positive control for shoot regeneration. The transformation of tomato cotyledons using the *SITET-8* overexpression and RNAi expression clones was repeated a number of times in an attempt to improve transformation efficiency. However similar results were obtained each time the experiment was run suggesting that changing the levels of *SITET-8* compromised shoot regeneration and was lethal. This experiment was stopped in favour of using construct driven by a fruit-related promoter.

Overexpression and silencing of the *SITET-8* gene under control of a PG promoter.

Vector construction and validation

The *SITET-8* gene fragments for over expression and RNAi were as described in the previous section. Cloning into the initial destination vector was validated by PCR generating amplicons of expected sizes (630, 1200 and 2400) (Fig 5.15) and then sequencing of the insert.

M13 primers were used to validate the correct insertion of the gene fragments into the initial destination vector. M13 primers flank the attP sites of pDONR221 and will therefore amplify the size of the gene fragment that has been inserted. Untransformed pDONR221 acts as both a negative and positive control by amplifying the ccdB and CmR region of the plasmid.

Once the gene fragments were verified to have been successfully inserted into the initial destination vector, they were kept at -20°C until use in the LR reaction.

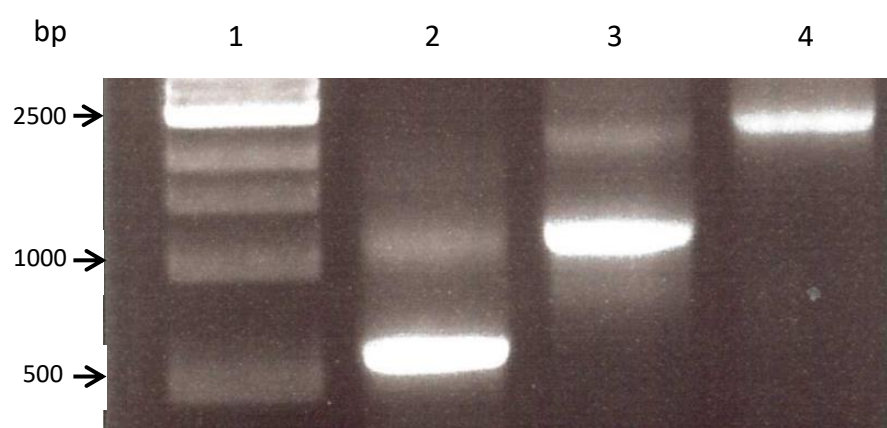


Figure 5.15: The BP reaction identifying the presence of *SITET-8* RNAi and overexpression gene fragments inside the pDONR221 entry vector

Lane	ID
1	DNA Hyperladder I
2	SITET-8.RNAi fragment 1
3	SITET-8.OE fragment 2
4	Negative Control (Untransformed pDONR221)

The entry vector containing the *SITET-8* gene fragment was used in the LR reaction to generate the plant transformation vector. The successful insertion of the *SITET-8* gene fragments was confirmed by the survival of bacterial clones on LB medium containing the appropriate antibiotic selection. PCR was also performed to confirm the presence of the *SITET-8* gene fragments inside the transformation vector containing the insert of 360, and 800 kb (Fig. 5.16 & 5.17).

Once the insertion of the gene fragments was confirmed, the purified plasmid constructs were kept at -20°C until they were transformed into *Agrobacterium* strain EHA105.

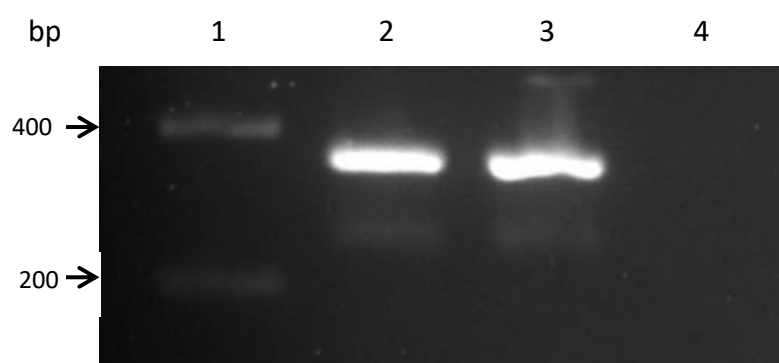


Figure 5.16: The LR reaction identifying the presence of a SITET-8 RNAi gene fragment inside the PK8-GW1WG-PG-B4 destination vector

Lane	ID
1	DNA Hyperladder I
2	SITET-8.RNAi fragment 1
3	SITET-8.RNAi fragment 2
4	Negative Control (Water)

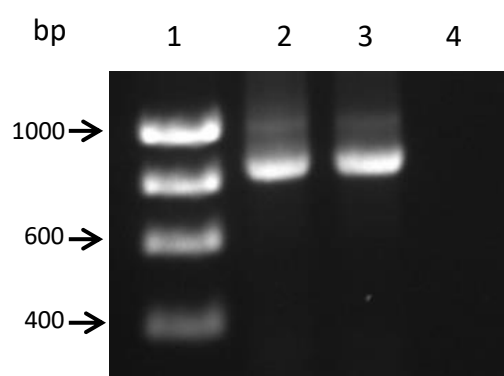


Figure 5.17: The LR reaction identifying the presence of a *SITET-8* overexpression gene fragment into the PK7M24GWi3 destination vector

Lane	ID
1	DNA Hyperladder I
2	SITET-8.OE fragment 1
3	SITET-8.OE fragment 2
4	Negative Control (Water)

The completed expression vectors (pEXPR/PG-TET280/RNAi and pEXPR/PG-TET280/OE) were then transformed into *Agrobacterium tumefaciens* strain EHA105 using electro-competent cells. The right incorporation of the expression clones was assured by the survival of colonies on LB agar under antibiotic selection and colony PCR was used to amplify the *S/TET-8* fragments to confirm the presence of the gene fragments (360 & 800 kb) in the expression clones (Fig 5.18).

Those colonies that had been confirmed to contain the completed expression vectors and were suspended in liquid LB and grown at 28°C for 48 hours ready for use in the transformation of tomato cotyledons.

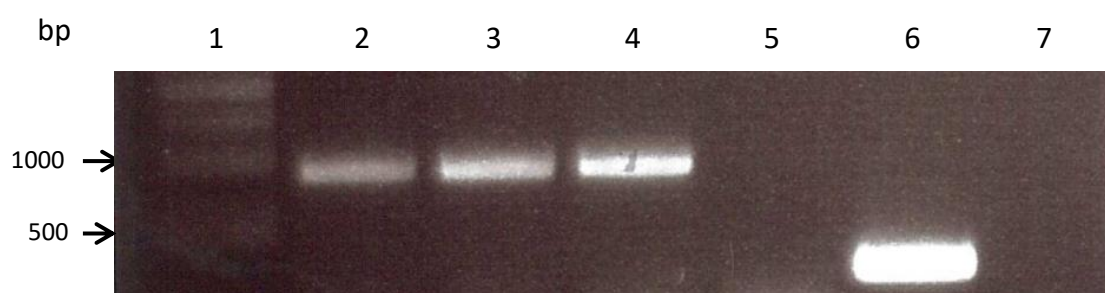


Figure 5.18: Agrobacterium transformation analysis identifying the presence of a SITET-8 RNAi and overexpression gene fragments inside Agrobacterium strain EHA105

Lane	ID
1	DNA Bioline 1KB Hyperladder
2	SITET-8.OE fragment 1
3	SITET-8.OE fragment 2
4	SITET-8.OE fragment 3
5	Negative Control (Water)
6	SITET-8.RNAi fragment 1
7	Negative Control (Water)

Unlike the 35S constructs, the PG vectors resulted in significant callus development and some regeneration of shoots. Transformed cotyledons produced a white fibrous callus after two to three weeks in subculture and a few shoots emerged in weeks four to six. Growth was slower in the RNAi constructs with shoots emerging after six to eight weeks. Cotyledons that produced shoots were very few, estimated to be in the ratio of 1:30. Shoots were excised from the leaf tips using flame sterilised forceps and placed in rooting medium.

Kanamycin was omitted from the rooting medium to help promote healthy growth in developing roots and shoots. By this point, selection of successfully transformed cotyledons was complete and the presence of kanamycin in the agar medium will no longer have any impact in promoting plant growth.

Unfortunately, none of the transformed shoots produced roots when transferred to rooting media and after 14 days all turned brown and died.

The *SITET-8* transformation into tomato was unsuccessful despite several attempts and using both constitutive and fruit-related promoters. The role of tetraspanins in plants is not well understood, but they may be essential for a range of plant developmental processes. It is likely that the use of the 35S promoter directly or indirectly affected the outcome of this transformation probably due to the importance of this gene in plants. In tomato, the RNA-seq data in the genome paper show twelve differentially expressed tetraspanins involved in all plant tissues at all stages of growth with strong conservation across clades (The Tomato Genome Consortium, 2012). Constitutive expression of the tetraspanin may therefore be interfering with the developmental process required in the regeneration of plant material following transformation by *Agrobacterium*.

The tetraspanins are most commonly characterized as cell adhesion proteins and there are a number of studies identifying their importance in developmental processes that rely on strong structural interlocking, although evidence from plants is rather sparse. For example, they have been

characterized in sperm-egg cell fusion in humans (Jégou et al., 2011), and gamete interactions during double fertilization in flowering plants (Sprunck & Dresselhaus, 2009). The regeneration of plant material after transformation with *Agrobacterium* requires cell division and adhesion for complete callus formation which leads to shoot and root regeneration. Absence of these proteins may prevent complete cell division and differentiation, ultimately causing death in those explants whose expression of the protein is silenced. In addition to cell-to-cell adhesion, tetraspanins are known to facilitate signalling and trafficking between the cell in response to external biotic and abiotic stimuli. This has been corroborated by the *trn2-1* mutant in *Arabidopsis* causing displacement of auxin foci leading to asymmetric distribution of auxin and subsequently, leaf patterning (Cnops et al., 2006). Auxin is fundamental in driving cell proliferation and expansion and has been characterised in dividing mesophyll tissues in concentrations ten times higher than tissues growing by elongation (Ljung, Bhalerao, & Sandberg, 2001). This is a strong indicator that complex control of IAA is needed for normal leaf and plant development. Previous studies have categorised the importance of maintaining an equilibrium between cell division, cell expansion and cell differentiation and as such, altering auxin distribution can severely impact plant establishment and development (Pien, Wyrzykowska, McQueen-Mason, Smart, & Fleming, 2001; Wyrzykowska, Pien, Shen, & Fleming, 2002). The tetraspanins have been seen to have a significant impact on auxin redistribution in developing leaf tissue by facilitating the canalization of auxin into the formation of procambium, the effects of which prevent cell proliferation and differentiation (Cnops et al., 2006) and may offer an explanation to the transformation efficiency and viability of the cotyledons.

Agrobacterium tumefaciens is a bacterium that causes crown gall disease in plants. The bacterium attaches itself to damaged plant cells and leaks the T_i plasmid region into the host cells allowing the transferred DNA (T-DNA) to be incorporated into the plant genome (Gelvin, 2003). This process has been used for the purposes of plant genetic engineering by using specific gene sequences

inside the T_i plasmid to be introduced into a host for study. The tetraspanins are a family of highly conserved proteins linked to cell adhesion in plants, animals, and bacteria. There have been numerous studies characterising the importance of the tetraspanins in bacterial invasion of host species facilitating HIV, listeria, and meningitis (Green et al., 2011; Tham et al., 2010; van Spriel & Figdor, 2010b) where in many of these studies, suppression of the selected tetraspanin yielded lower instances of infection from exposure.

Given the challenges of investigating the role of tetraspanins in tomato we decided to focus on two alternative novel target genes that have been associated with ripening. A heat shock transcription factor and a zinc finger protein that have both been previously identified in the Seymour lab to be linked to the master ripening-regulatory gene *RIN* based on microarray data and correlation analysis. These experiments are described in the next two chapters.

Chapter 6

Characterizing the role of a heat shock transcription factor
and a zinc finger protein in tomato ripening

6.1 Introduction

Based on microarray data (R. Liu et al., 2015) and K-means clustering performed by Bradley et al., (unpublished data). A heat-shock transcription factor-like gene (Solyc06g053960) and a gene encoding a zinc-finger protein (Solyc08g063040) were shown to be closely correlated with the expression of the *RIN* gene; a master regulator of ripening (Fig. 6.1). The expression analysis for both these targets is closely linked to the onset of ripening and suggests they play a key role in this process. In this chapter, we have named these genes *SIHST-14* and *SIZFP* respectively.

The role of heat shock transcription factors and zinc finger proteins in the ripening process has not been investigated. Heat shock proteins are a class of molecular chaperones that are necessary for developmental processes including seed germination and embryogenesis but are typically known for their role in response to abiotic stress within the plant kingdom (W. Wang, Vinocur, Shoseyov, & Altman, 2004). Their role in plant development is linked to folding, aggregation, and transformation of chloroplasts to chromoplasts (Frydman, 2001; Neta-Sharir, Isaacson, Lurie, & Weiss, 2005; Richter & Buchner, 2001) and heat shock transcription factors are responsible for regulating their expression.

A small heat-shock protein has previously been linked to cell-wall depolymerisation in tomato and was proposed to act by regulating thermal denaturation of depolymerizing enzymes during elevated periods of high temperature. The investigation found that pectin depolymerisation was heavily dependent on the activity of a small heat-shock protein VIS1 to maintain enzymatic functions throughout daytime temperature increases (Ramakrishna, Deng, Ding, Handa, & Ozminkowski, 2003).

The amino acid sequence of the *SIHST-14* (Solyc06g053960) gene exhibits a high level of conservation with *SIHSF-8* (72%) and the *SIHSF-24* transcription factors (60%,) as well as a number of *SIHSF* isoforms (99%; Fig. 6.2, and Table

8.1 found in the appendices) supporting its identification as a putative tomato transcription factor.

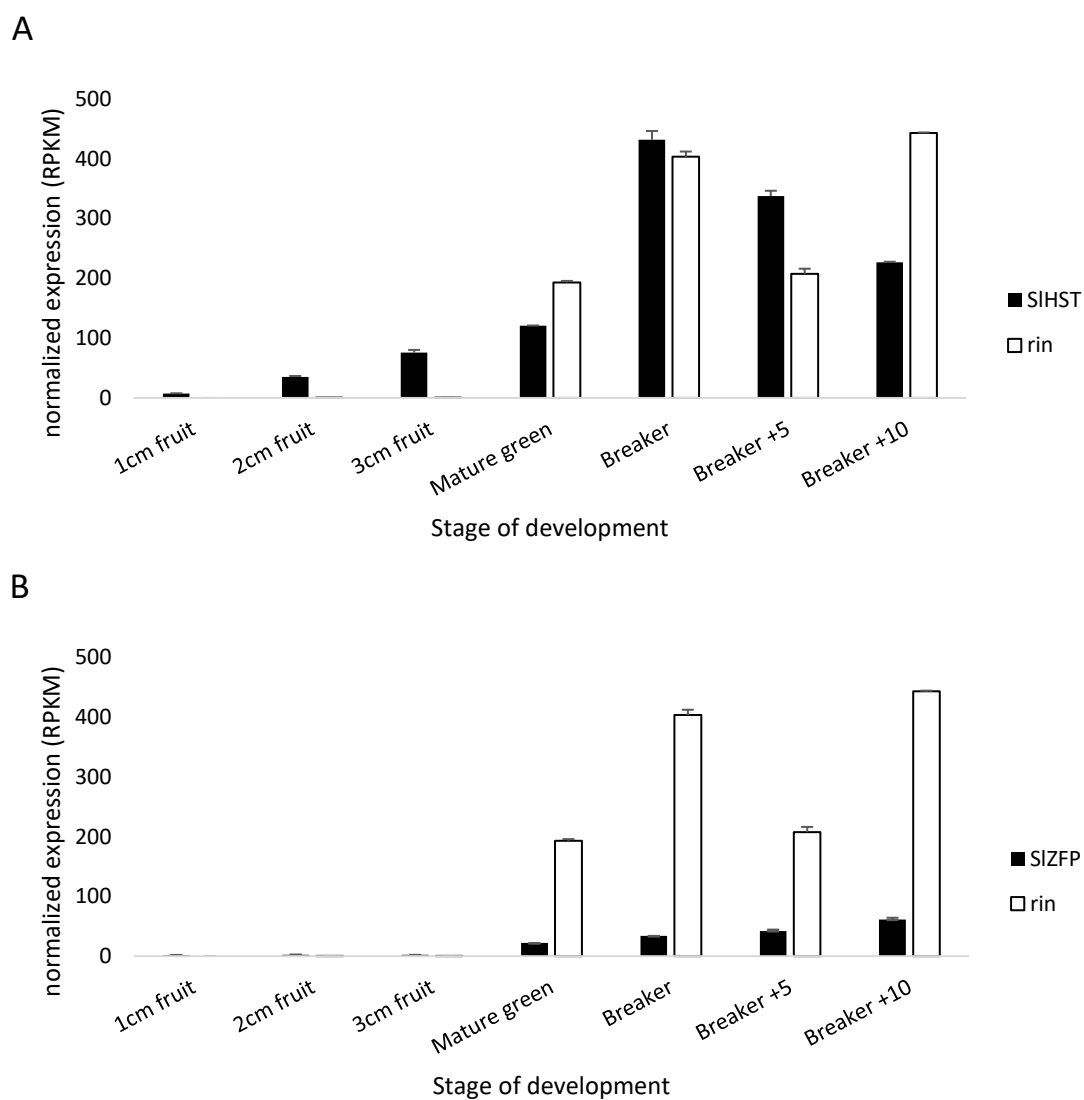


Figure 6.1: Expression of target genes linked to LeMADS-RIN. Expression data of two target genes compared with LeMADS-RIN. **(A)** *SIHST-14* (Solyc06g053960) and *rin* expression. **(B)** *SIZFP* (Solyc08g063040) and *rin* expression. This data presents the relationship between the target genes and LeMADS-RIN, highlighting their potential role in fruit ripening.

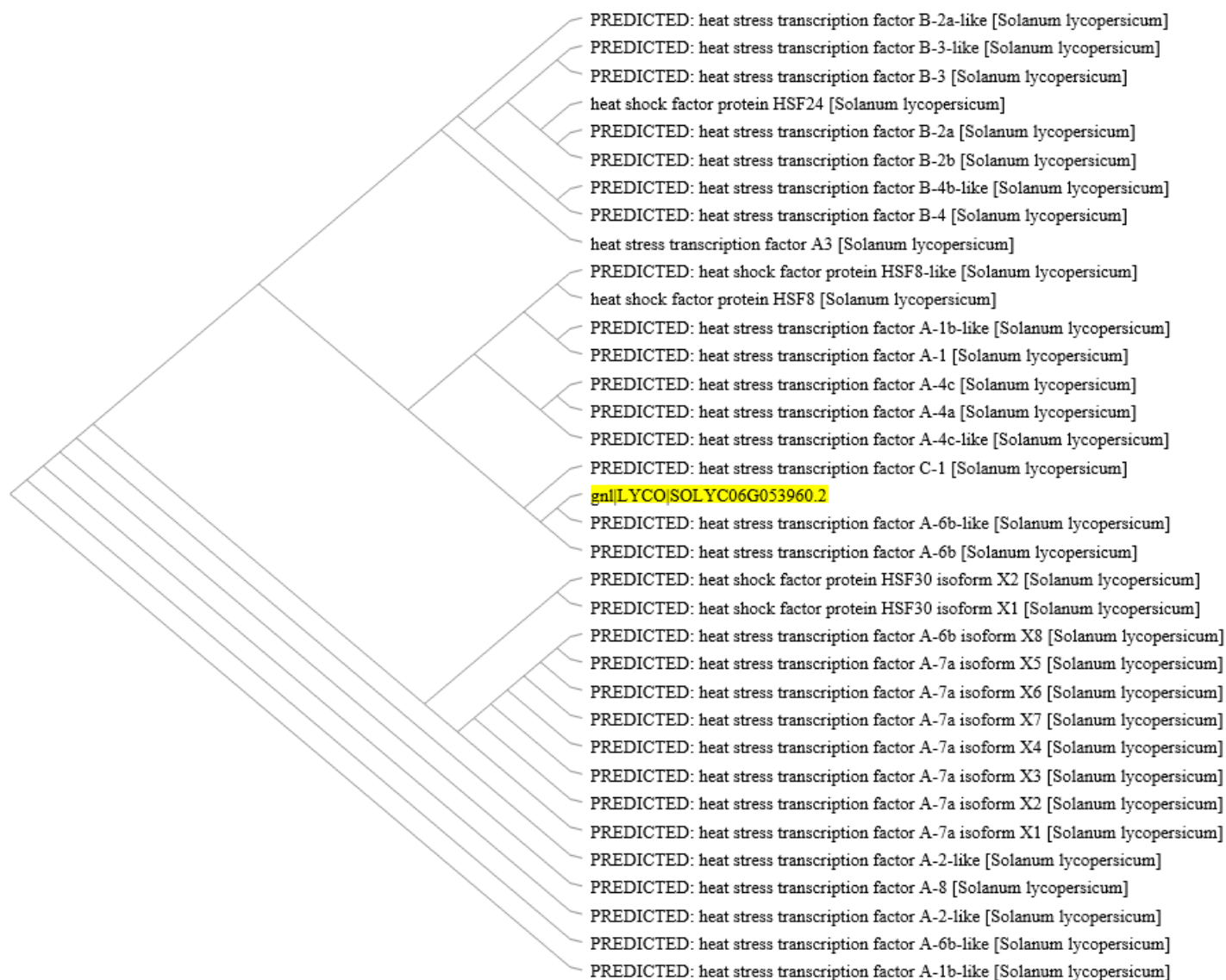


Figure 6.2: ClustalW analysis of *SIHST-14*. Phylogeny tree illustrating the related amino acid sequences in *S. lycopersicum*, the majority of related proteins are transcription factors which is indicative of the role of *SIHST-14* as a transcriptional regulator of ripening.

In addition to the heat-shock transcription factor, a zinc-finger protein was selected as a target for investigation. Zinc-finger proteins are among the most abundant molecules in eukaryotic organisms including a significant proportion of transcription factors. In plants, they have been linked to the regulation of flowering, organ development, and salt tolerance (Sakamoto, Maruyama, Sakuma, Meshi, & Iwabuchi, 2004; Weingartner, Subert, & Sauer, 2011; Zhou et al., 2013). In tomato, at least 116 C₂H₂ zinc-finger transcription factors have been described (The Tomato Genome Consortium, 2012) suggesting they play a key role in plant and fruit development but few have been studied in more detail.

One such zinc-finger protein (Soly07g006880) has previously been linked to tomato floral development (Xiao et al., 2009), and more recently in fruit development and ripening (Weng et al., 2015). The *SIZFP-2* gene is expressed mainly in developing fruits and has been shown to inhibit ABA production and seed germination. It is known, that an ABA-deficient mutant will promote carotenoid accumulation (Galpaz, Wang, Menda, Zamir, & Hirschberg, 2008). The same phenotype was observed from knock-down mutants in the *SIZFP-2* line cementing the role of *SIZFP-2* in the ABA biosynthetic pathway. Our target, the *SIZFP* gene has been linked to LeMADS-RIN suggesting it elucidates further downstream expression of ripening related genes. Phylogenetic analysis of *SIZFP* suggests that its closest similarity is a MAGPIE-zinc finger protein in Arabidopsis which have been shown to regulate cell division and tissue boundaries (Fig. 6.3, Welch et al. 2007).

Fruit ripening requires the activity of thousands of genes linked concurrently to a number of biochemical and physiological pathways. It is likely that direct targets of LeMADS-RIN will promote expression of key proteins associated with ripening related pathways. In this chapter we have investigated the role of two targets, *SIHST-14* and *SIZFP* within fruit ripening.

<i>SIZFP</i>	MIKGM LGDDSMSNLTSASNEASISSTNNRIEIGSHVLPQLQNIQTQPPNKKKRNLPGN	60
AT1G03840	M+KG++ D+S+SNLTS S E S S+ Q P +KKKR LPGN	40
<i>SIZFP</i>	PDPEAEVVALSPRSLLATNRFVCEICNKGFRDQNLQLHRRGHNLPWKLKQRSNKEV-KK	119
AT1G03840	PDPEAEV+ALSP++LLATNRF+CEICNKGFRDQNLQLHRRGHNLPWKLKQR+NKEV +K	100
<i>SIZFP</i>	KVYVCPEASCVHHHPSRALGDLTGIIKKHFCRKHGEKKWKCEKCSKRYAVQSDWKAHSKIC	179
AT1G03840	KVYVCPE +CVHHHPSRALGDLTGIIKKHFCRKHGEKKWKCEKCSKRYAVQSDWKAHSKIC	160
<i>SIZFP</i>	GTREYRCDCGTLFSRRDSFITHRAFCDALTEESSRTIIPP--PNSSTSH-----	226
AT1G03840	GTREYRCDCG LFSRRDSFITHRAFCDAL EE++R I P SS SH	220
<i>SIZFP</i>	----HLNLHTLqnfqmkqeqqqqnn-----DLSSQLFI-----QNPNG	260
AT1G03840	LN +L Q + + +LSS F+ QNP+	280
<i>SIZFP</i>	NSSNMFGAPP--PHMSATALLQKAAQIGVTSSSHTAN---NMsattffspttstttgiam	315
AT1G03840	+ F APP PH SATALLQKAAQ+GVT S + +M ++	340
<i>SIZFP</i>	sgsgsgagVARQYHPFEnnnnnntntDFVTGNTSFPDFGASVTPGFMEQV-----	366
AT1G03840	+ S + AR+ ++F +SF + A VTPGF+EQV	388
<i>SIZFP</i>	-----HDMQNMMATTAPSLPCTSFDEGFG-----RGA-----HLMRQ	398
AT1G03840	HDM ++ T+ +SF+ F R + H +	448
<i>SIZFP</i>	GKEN-----NEGLTRDFLGLRAFPH	418
AT1G03840	KE+ N+GLTRDFLGL+AFPH	491

Figure 6.3: *SIZFP* protein sequence alignment. The closest characterized protein to Solyc08g063040 is a MAGPIE-zinc finger protein in Arabidopsis.

6.2 Materials and Methods

Plant Materials

Tomato (*Solanum lycopersicum*), cv Ailsa Craig was grown under standard cultural practices with regular supplementary nitrogen, phosphorus and potassium fertilizers and fruits were harvested at mature green and various times after the breaker stage (Chapter 2). After harvest, fruits were weighed with colour, soluble solids, and texture also being made. The fruits were then quartered and the seeds removed before the pericarp was frozen in liquid nitrogen and stored at -80°C.

Vector Construction

The vectors for silencing the *SLHST-14* and *SIZFP* genes using RNAi constructs driven by the 35S promoter were generated by Dr Natalie Chapman of the Plant and Crop Sciences Division, University of Nottingham prior to the start of this project and sent to the University of California, Davis. Here transformation of Ailsa Craig tomato was performed and plantlets returned to the UK and RHUL for characterisation and analysis. UoN generated the homozygous lines for the *SLHST-14* while RHUL undertook the same protocols for *SIZFP*.

Single copy analysis of T1 progeny from T0 transgenic lines

DNA was extracted from juvenile plants a few weeks after germination from young plant leaves growing close to apical tip and samples were stored at -20°C until use. Gene specific primers and Taqman probes for *SLHST-14* and phytoene desaturase (PDS) were used and are listed in the appendices. The serial dilutions, qPCR conditions followed the Taqman universal Master-mix protocol. The QPCR experiment was designed to detect the presence of the transgene and allow determination of copy number. Azygous individuals will have no detectable signal with heterozygous and homozygous individuals having different signal intensities.

Transgene expression in homozygous lines

To confirm the expression of the transgene in tomato fruit tissue RNA was obtained from fruits 7 days after the breaker using a column based extraction method (Ambion® RiboPure™). The quality of RNA was assessed by running a 2% agarose gel. The presence of sharp and clear 28s and 18s bands in a 2:1 ratio indicated intact RNA. A cDNA template was generated and samples were then stored at -20°C until needed. Gene specific primers and Taqman probes for *SIHST-14* and elongation factor-1 α (*EF-1 α*) were used and are listed in the appendices. The serial dilutions, qPCR reactions and qPCR conditions followed the Taqman universal Master-mix protocol described in section 2.8. Gene expression was calculated from the crossing point (Cq) values of *SIHST-14* relative to the *EF-1 α* reference gene.

Fruit phenotyping

Fruit weight, colour, and texture were analysed using protocols previously described in Chapter 2.

6.3 Results and Discussion

Identification of homozygous lines

To assess the copy number of the T₁ progeny, 12 T₁ seeds were sown. QPCR of genomic DNA using fluorescent hybridisation probes was then performed. The presence of azygous and transgenic lines was apparent in plant lines A and B (Fig. 6.4). Elevated levels of signal in lines A3, 4, 5, 11, and B6 were taken to indicate transgenes incorporated into one (heterozygous) or both (homozygous) parental genomes. Absence of a signal is indicative of a wild-type azygous line which will be kept for use as a control (A9, B3, and B7).

qPCR was used to quantify expression of the *SIHST-14* gene in transgenic and azygous controls (Fig. 6.5). Expression in the selected transgenic lines was silenced indicating that the expression construct was successfully inhibiting expression of the *SIHST-14* gene. Plant line 1 (Fig 6.4: A9) was initially thought to be azygous but was shown to have no expression of *SIHST-14* in qPCR and was discarded from use in further investigations.

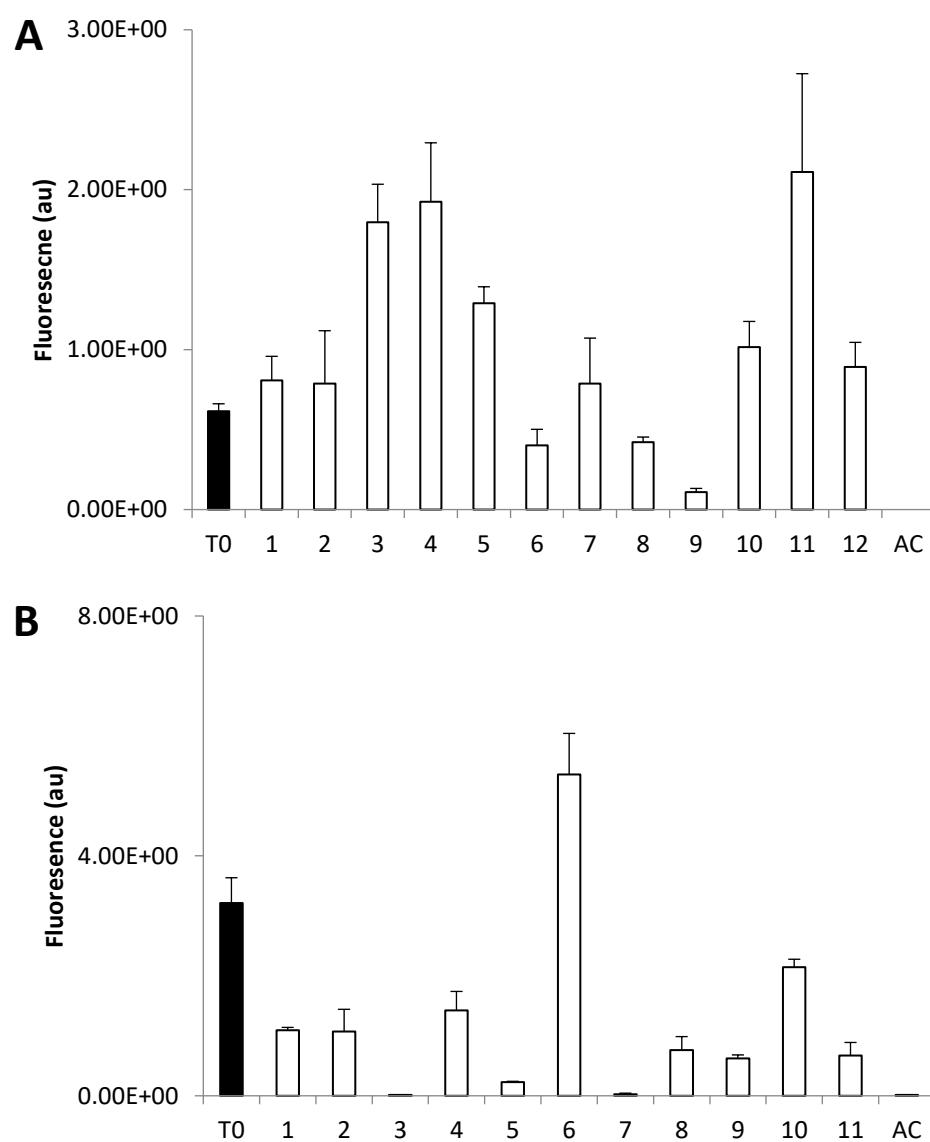


Figure 6.4: Assessment of copy number in *SIHST-14* transformed tomato plants. **A)** Plant line A **B)** Plant line B. Values represent the mean \pm SE of three technical replicates.

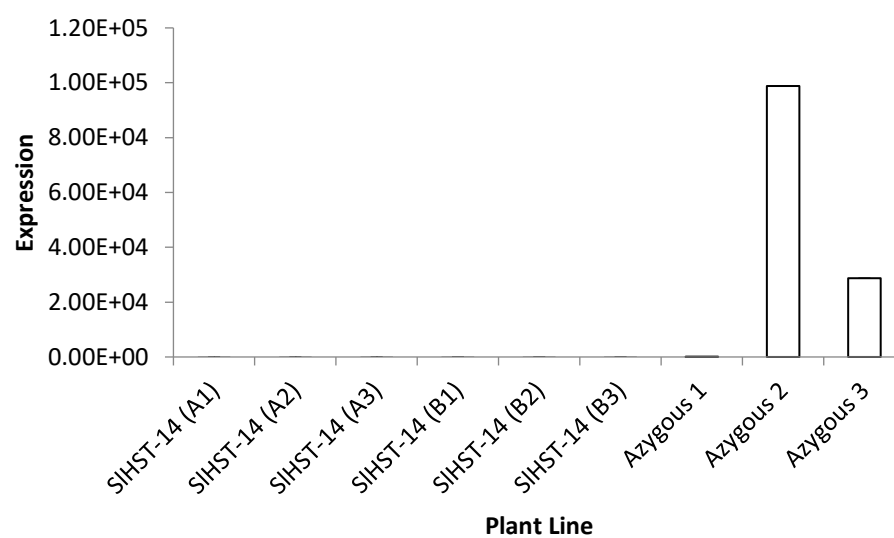


Figure 6.5: RNA expression of *SIHST-14* in transgenic and azygous lines. qPCR was used to confirm silencing of the *SIHST-14* gene in transgenic lines. One azygous line was shown to also be silencing *SIHST-14* gene, this line was removed from further study.

Assessment of fruit weight and colour in selected homozygous *SIHST-14* lines

Fruits were assessed at the red-ripe stage (BR+7) unless otherwise stated. Assessment of fruit weight showed no significant ($P>0.05$) difference between the transgenic lines and the azygous controls, suggesting that suppression of *SIHST-14* has no effect on fruit weight (Fig. 6.6).

Fruit colour was also assessed using a Minolta colorimeter CR400 and no significant ($P>0.05$) differences were found in the tomatoes along the black-white and blue-yellow axis of the colorimeter. However, a significant difference was observed along the red-green axis. Transgenic lines are shown to have a higher intensity value for the red-green wavelengths, with a higher intensity being attributed to increased red pigment accumulation suggesting an effect of *SIHST-14* silencing on carotenoid accumulation during ripening (Fig. 6.7).

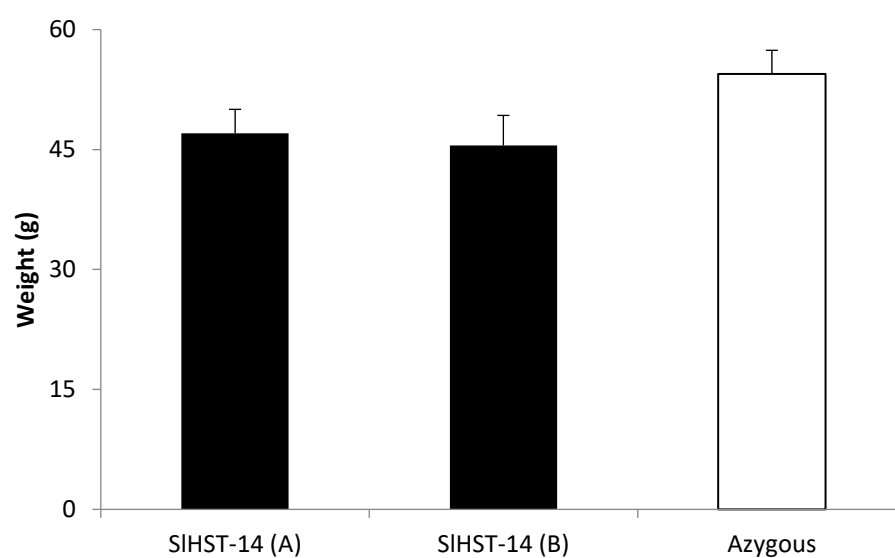


Figure 6.6: Assessment of fruit weight in homozygous plants from line A and Line B. Values represent the mean \pm SE of three biological replicates.

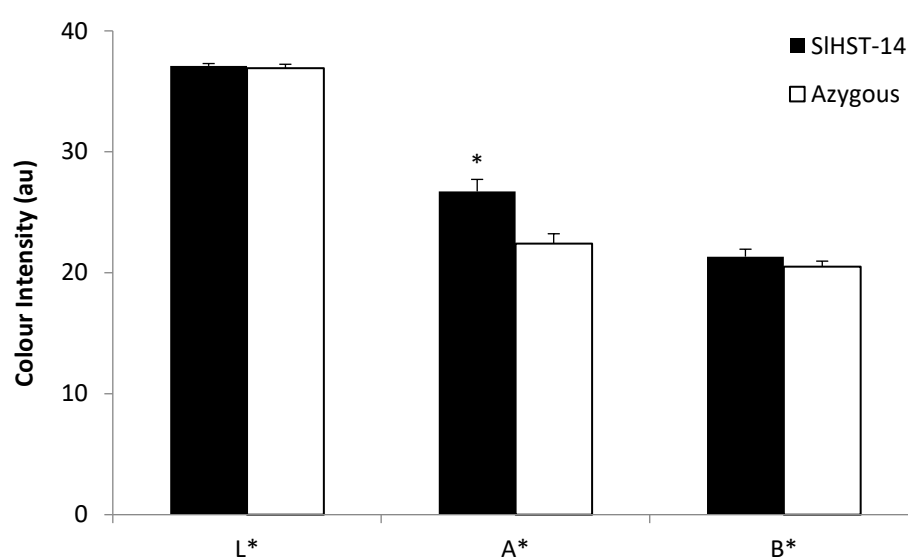


Figure 6.7: Assessment of homozygous tomato colour index. Values represent the mean \pm SE of three biological and technical replicates. Asterisks in all graphs mark significant differences: P 0.05 = *, P0.01 = **, and P 0.001 = ***.

Assessment of fruit texture in T₁ lines and subsequent generations

Fruits were harvested at a number of stages from mature green, to BR+14. Fruit texture in the inner pericarp of transgenic lines was observed to be significantly ($P < 0.05$) different in the MG, B4, and B+7 stages of ripening (Fig. 6.8: A). In mature green fruits the maximum load measurements for the transgenic *SHST-14* lines were significantly ($P < 0.05$) lower than in the azygous controls. This difference was no longer seen by the BR stage and by BR+4 it was the transgenic lines that were seen to have significantly ($P < 0.05$) firmer texture than the control fruit. Fruit texture in the outer pericarp of transgenic lines followed much the same pattern as the inner pericarp (Fig 6.8: B). The differences in fruit texture indicate that silencing *SHST-14* gene expression reduces the rate of fruit softening especially at the orange-ripe stage.

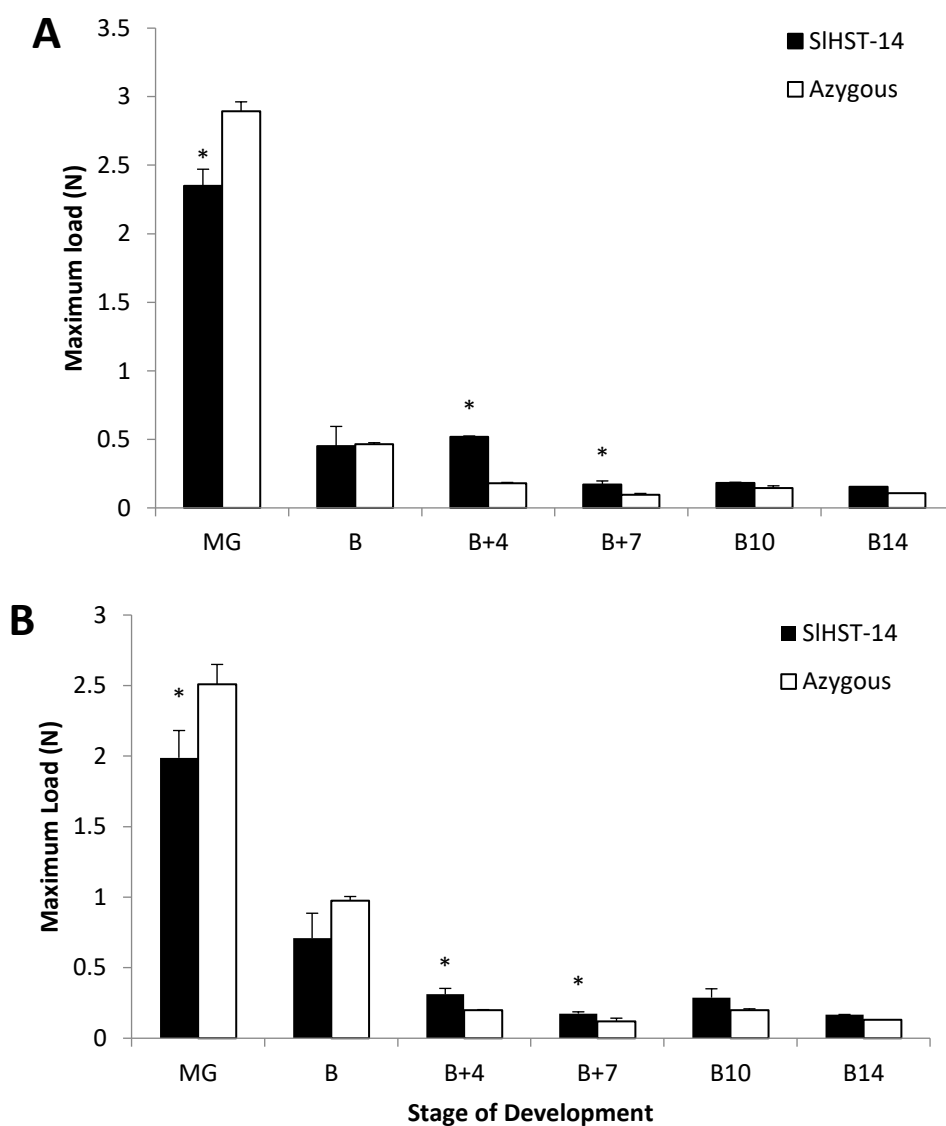


Figure 6.8: Effects of silencing *SIHST-14* on fruit texture. **A)** Inner pericarp and **B)** Outer pericarp maximum load of homozygous T1 *SIHST-14* line. Values represent the mean \pm SE of three biological replicates where $n=25$ and 15 for transgenic and controls respectively. Asterisks in all graphs mark significant differences: $P \leq 0.05 = *$, $P \leq 0.01 = **$, and $P \leq 0.001 = ***$.

Transgenic lines were found to accumulate more red pigment seven days after the onset of softening. In the transgenic lines the *SLHST-14* gene is silenced and the increased rate of carotenoid biosynthesis as determined by colour index at the orange-ripe stage may be because the *SLHST-14* gene is no longer promoting expression of heat-shock proteins leading to a reduced rate of chaperone activity provided in the absence of abiotic stress. There are a number of enzymes involved in the carotenoid biosynthetic pathway, and downregulation of those involved in re-cycling of enzymes such as β -cyclase has been shown to promote β -carotene and lycopene accumulation (Pecker, Gabbay, Cunningham, & Hirschberg, 1996), it is likely that a similar mechanism is being seen in the *SLHST-14* line by the absence of HSPs downstream of *SLHST-14* being unable to facilitate protein folding and aggregation.

It is possible that the rate of enzyme biosynthesis including for cell wall degrading enzymes may be down regulated indirectly due to silencing of *SLHST-14* which promotes expression of other heat-shock proteins (Boston, Viitanen, & Vierling, 1996) and therefore delays enzymatic degradation of the cell wall for a period of time. It is likely then, that by the breaker + 10 stage of fruit softening, the cell wall degrading enzymes have had enough time to fully depolymerize the cell wall and would explain why we see a return to a texture measurement similar to that of the azygous line.

To better understand the molecular mechanisms by which fruit softening is being affected, we investigated the transcriptome of the *SLHST-14* transgenic lines using RNA-seq (Chapter 7).

The role of a Zinc-finger protein on fruit softening

The *SIZFP* RNAi line was grown under glasshouse conditions. Fruits were tagged at anthesis and again at the BR stage. Fruits were collected when they were red-ripe (BR+7) and texture measurements were carried out on the inner and outer pericarp tissue to assess the effects of *SIZFP* on fruit softening (Fig. 6.9). There were no significant ($P>0.05$) differences in the inner pericarp tissue from the *SIZFP* line. However, the outer pericarp tissue showed significant ($P<0.05$) effects on tissue firmness with the *SIZFP* RNAi lines having twice to four times the maximum load to that of the control at the red-ripe stage.

Zinc-finger proteins have previously been shown to elucidate fruit ripening related phenotypes linked to the ABA biosynthetic pathway (Weng et al., 2015). In this chapter, we build on this foundation and present the role of a zinc-finger protein on cell-wall depolymerisation by means of a single 35S:RNAi mutant line. Fruits from the *SIZFP* line were found to have significantly ($P<0.05$) firmer texture in red-ripe fruit than the wild-type azygous line. Given the nature of zinc-finger proteins, their abundance in eukaryotic organisms, and their prevalence as transcriptional regulators it is likely that a zinc-finger deficient mutant line is negatively regulating ripening related genes downstream of LeMADS-RIN such as polygalacturonase, pectin-methylesterase, or pectate lyase.

RNA-seq was then used to understand the mechanism of action of the Heat shock transcription factor.

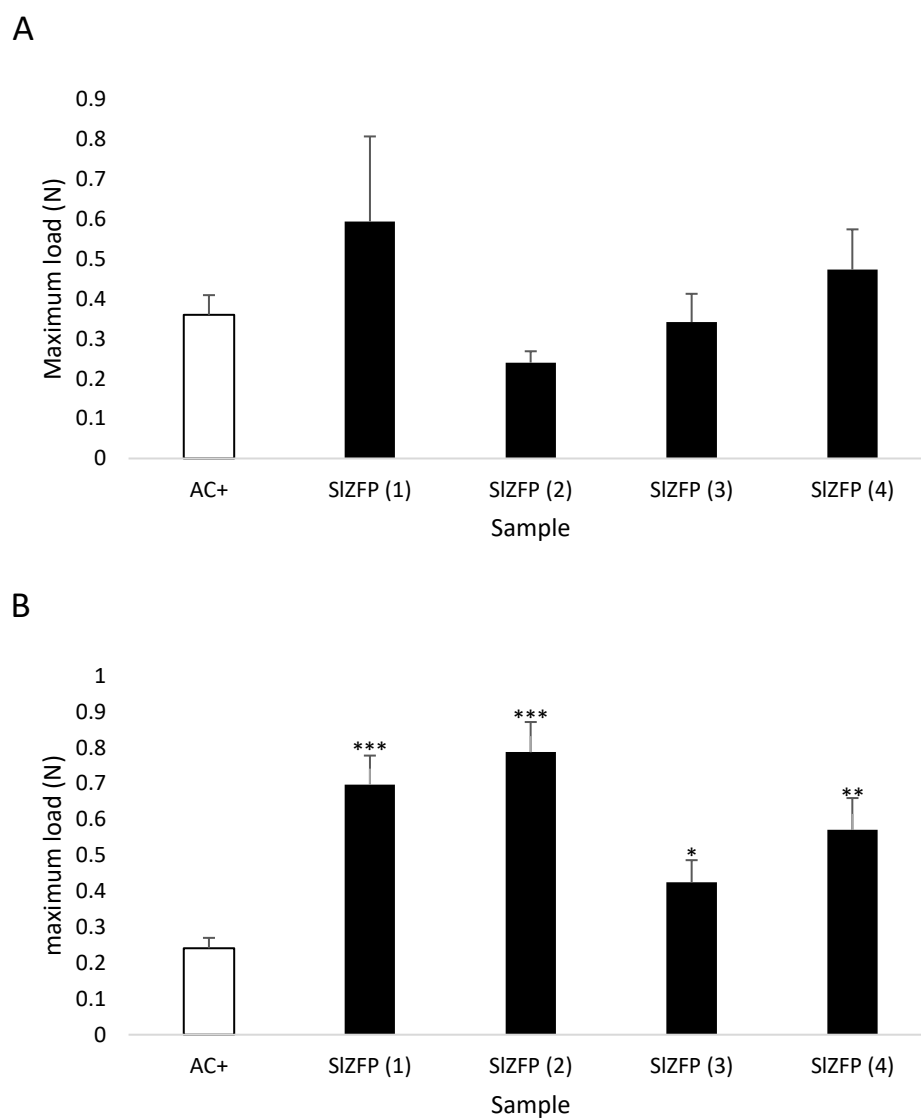


Figure 6.9: Assessment of *SIZFP* homozygous fruit texture at the red-ripe stage. **A)** Inner pericarp and **B)** Outer pericarp. Values represent the mean \pm SE of three biological replicates. Asterisks in all graphs mark significant differences: P 0.05 = *, P 0.01 = **, and P 0.001 = ***.

Chapter 7

The effects of silencing of a heat-shock transcription factor-like gene on the tomato ripening transcriptome

7.1 Introduction

In Chapter six, we characterized the phenotypic effects of silencing a tomato heat-shock transcription factor-like gene using RNAi. The fruit produced from this line exhibited a firmer texture four and seven days after the breaker stage and were also seen to exhibit colour differences compared with the non-transgenic controls. These results suggest that *SHST-14* has a role in cell-wall depolymerisation and the carotenoid biosynthetic pathways.

The advent of next-generation DNA sequencing (NGS) has provided a shift in the way the transcriptome can be analysed. RNA-seq allows for a higher range of detection and throughput over conventional microarray analysis and targeted RNA-seq is fast becoming an instrumental tool in molecular biology to fully understand the role of genes in the wider context of developmental processes at the transcriptional level (Ozsolak & Milos, 2011). Targeted RNA-seq has been used in a number of applications which have included the identification of RNA-editing sites, translocations of cancers, and tissue/allele-specific gene expression in humans (Levin et al., 2009; Li et al., 2009; Morris et al., 2014; Zhang et al., 2009). This technique provides an opportunity for us to investigate and understand the role of ripening-related genes and their downstream effects on biochemical and physiological pathways in fruit development.

The *SHST-14* gene was chosen as a target for investigation because it is a likely direct target of LeMADS-RIN (Martel et al., 2011). Here the transcriptome of fruit from a homozygous 35S: *SHST-14* RNAi line are investigated in comparison to those from an azygous control to explore the mechanistic basis of the altered colour and texture in these RNAi lines reported in Chapter 6.

7.2 Materials and methods

Plant materials and fruit collection

Transgenic and azygous lines were grown under glasshouse conditions described in Chapter 2. Flowers were tagged at anthesis and fruits upon reaching the breaker stage, the fruits were collected on days 4, 7, 10, and 14 and stored at -80°C until needed for use.

RNA extraction, storage, and sequencing

RNA was extracted from fruit pericarp tissue the protocol from the Ambion® RiboPure™ Kit, Ambion (UK). The procedure is described in detail in section 2.6. Once the concentration and integrity of the RNA samples was confirmed, the samples were vacuum dried and stored in 'RNA-stable' coated tubes for long-term storage at room temperature. Samples were then shipped to Syngenta Biotechnology Inc. for library preparation and next generation sequencing.

Examination of RNA integrity

3µl of RNA was loaded onto a 2% agarose gel in TBE (89 mM Tris-HCl pH 7.8, 89 mM borate, 2 mM EDTA) with 0.5µg/ml ethidium bromide added to the gel. A loading buffer was added to the RNA samples to a final concentration of 1X and the gel was run at 50V for 25 minutes.

Software

The core analysis of the data obtained from the RNA-seq was completed using Hisat2, HTSeq-count, and EdgeR for the read mapping, counting, and differential expression respectively. A number of preparatory and intermediate steps were used with routine bioinformatics methods using R-Bioconductor packages: Pathview and Gage. This work was undertaken in collaboration with Andrew Warry in the Advanced Data Analysis Centre at Nottingham University.

7.3 Results and Discussion

RNA sequence quality and fragment mapping

RNA was extracted using a column based extraction method described in section 2.6 and RNA quality was assessed using an agarose gel electrophoresis system (Fig 7.1) and indicated intact RNA of high quality.

The total read counts for fragments obtained from the RNA samples were compared with the total fragments mapped (Fig 7.2: A), this allowed the relative efficiency of mapping to be quantified (Fig 7.2: B). At B+7, two transgenic replicates and three azygous replicates were mapped. At B+10, three transgenic and two azygous replicates were mapped. The average percentage of fragments mapped was 95.71% with a range of all samples being within 2.62% of the median. These were high values which emphasises the quality of the RNA and provides a high degree of accuracy and confidence for the mapping of reads.

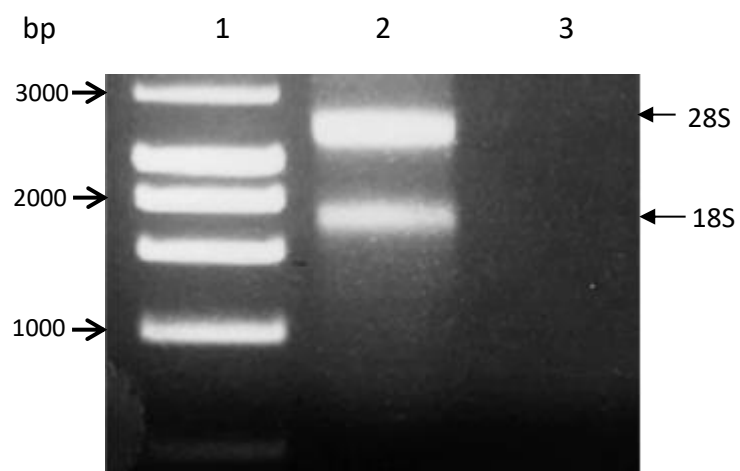


Figure 7.1: Gel electrophoresis of RNA sample. Gel showed distinct 18S and 28S RNA bands with no smearing to highlight quality of RNA samples extracted from fruit pericarp tissue.

Lane	ID
1	DNA Hyperladder I
2	RNA sample <i>SIHST-14 B7(ii)</i>
3	Negative control (Water)

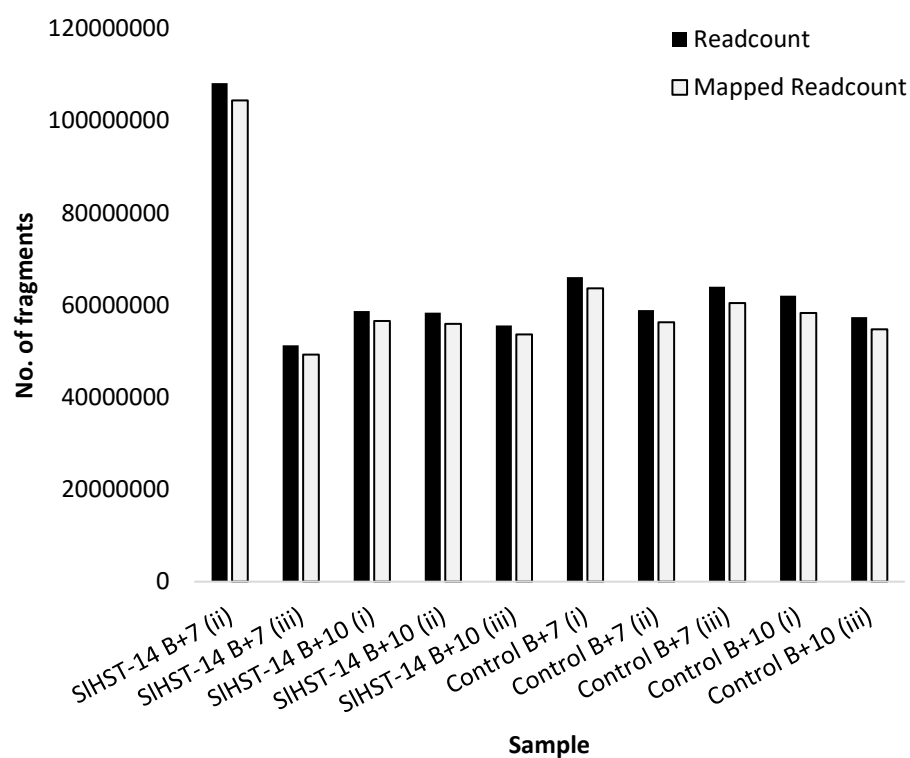
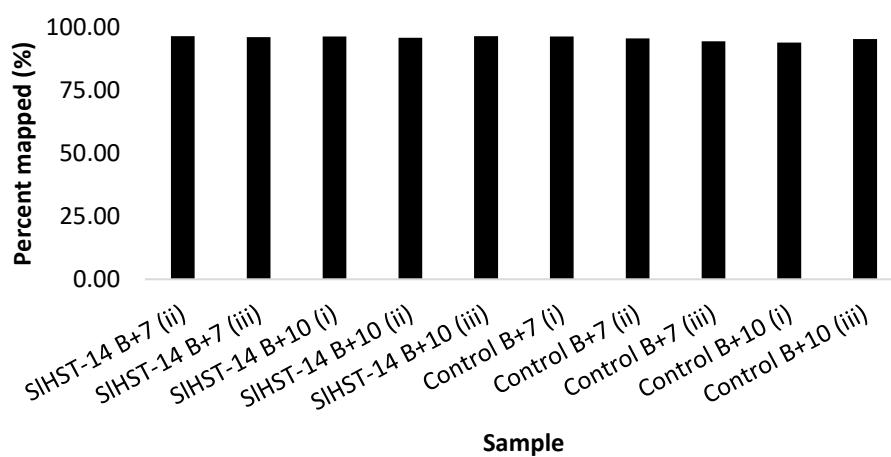
A**B**

Figure 7.2: RNA-seq read-count and percentage mapped. Analysis of RNA quality showing **(A)** Number of fragments read and mapped **(B)** percentage of fragments mapped. B+7 and B+10 = stage of ripening, (i) = replicate count.

Differential gene expression in fruit ripening

The transcriptomes of fruits from the *SIHST-14* RNAi and control azygous lines were compared at two stages of fruit ripening, B+7, and B+10.

Multidimensional scaling plots (MDS) were used to identify larger trends or biases in the data set (Fig 7.3). MDS analysis assigns a dissimilarity score according to the sequence alignment of each gene sequence and maps these scores in a three dimensional space to provide a visual representation of the differences in RNA expression. A clear distinction can be seen between the expression of the *SIHST-14* line (Fig 7.3: Salmon) and the control line (Fig 7.3: Blue) suggesting that there is significant differential gene expression between *SIHST-14* RNAi and azygous control lines at both the B+7 (Fig. 7.3: A) and B+10 (Fig. 7.3: B) stages of fruit ripening. We will then look to assess differential expression between individual and clusters of genes.

Analysing the expression data using a volcano plot indicates the expression of a large number of genes were affected by the silencing of *SIHST-14* both at B+7 and B+10 (Fig. 7.4). In the plots, each node represents a gene and whether it is up-regulated or down-regulated in the azygous control line based on the colour of the node.

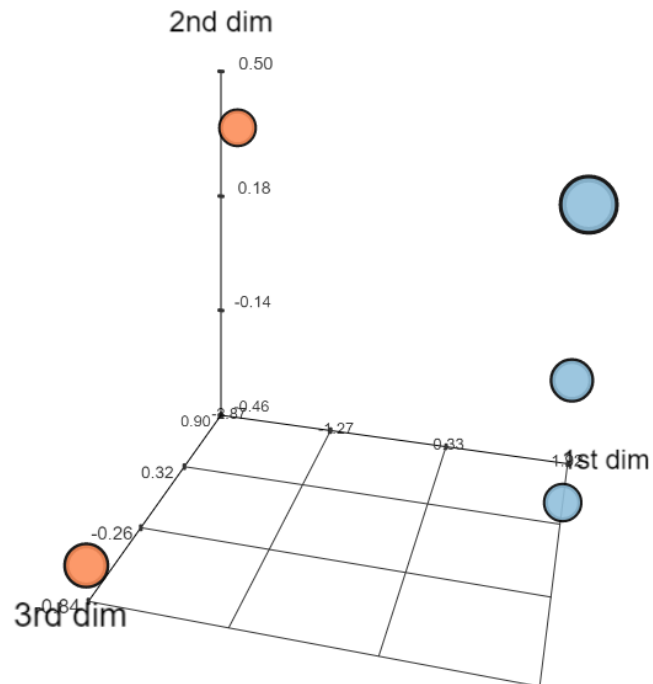
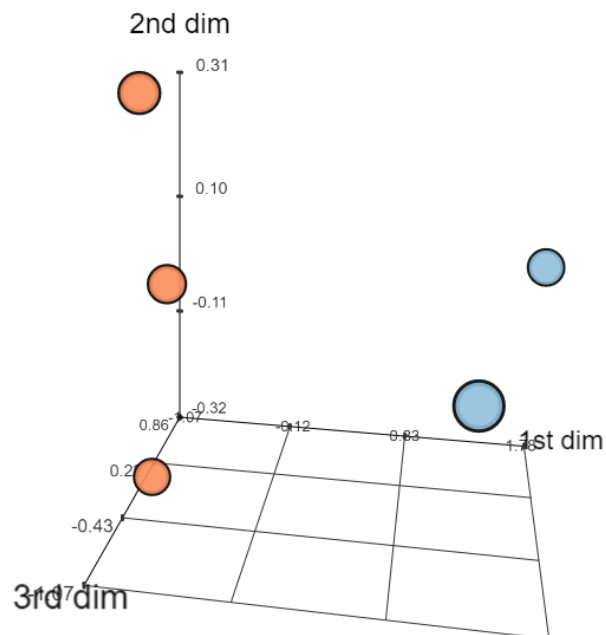
A**B**

Figure 7.3: MDS plot showing differentially expressed gene clusters. The two plots describe the *SIHST-14* (Salmon), and Control lines (Blue) at the **A)** B+7 and **B)** B+10 stages of fruit ripening. The plot represents the dissimilarity scores of gene sequences between the two lines highlighting the level of differential expression in the *SIHST-14* line.

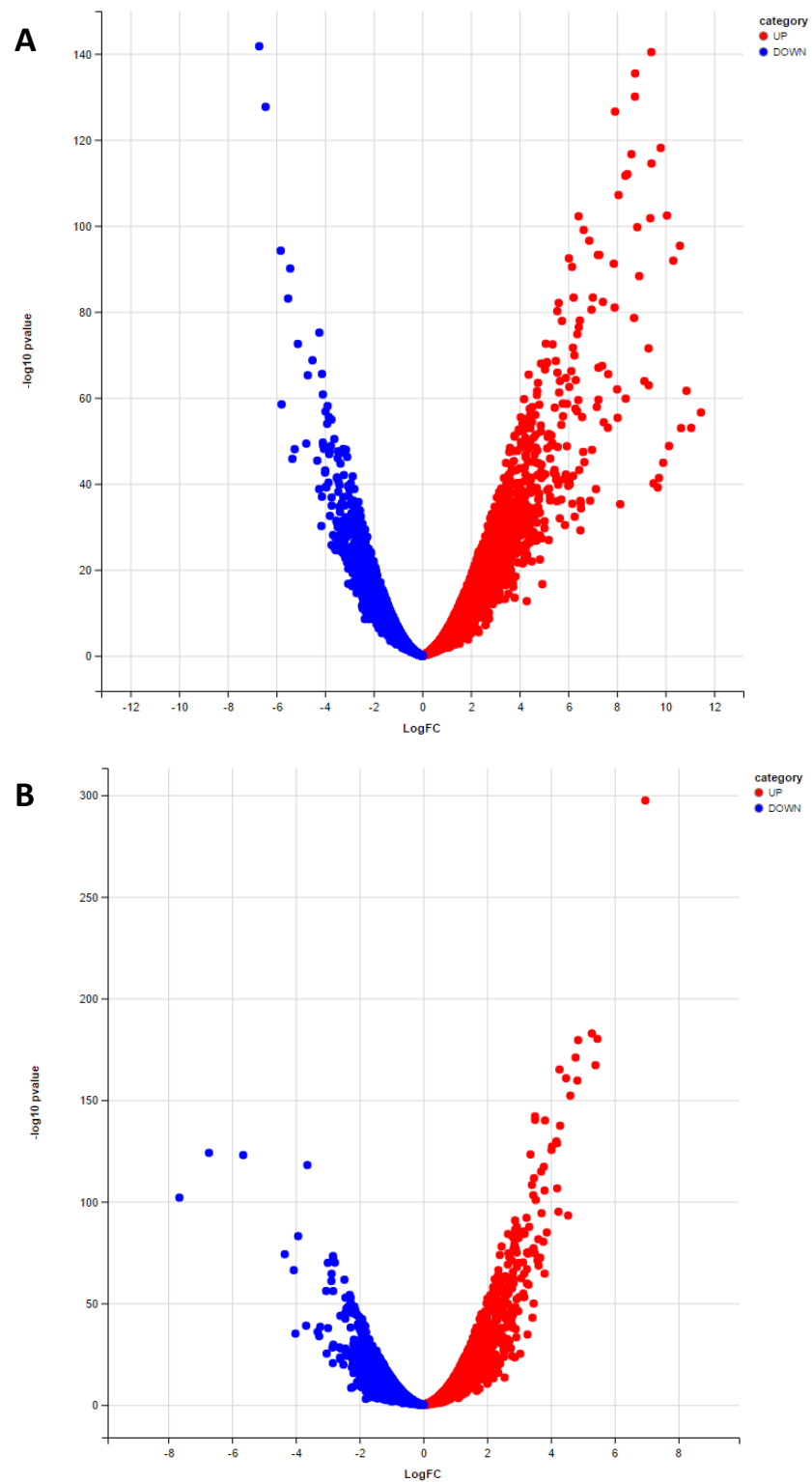


Figure 7.4: Volcano plot of differentially expressed genes. **A)** B+7 and **B)** B+10. The plot illustrates the most differentially expressed genes by fold change on the x-axis and significance of change on the y-axis. The red dots represent genes up-regulated in the control line.

There were 4793 differentially expressed genes with more than a 2-fold change in expression between the control and the *SIHST-14* lines at B+7 and B+10. Heat maps were made to visualise gene clusters according to their GO annotations, we chose firstly to investigate those genes linked to the onset of ripening (Fig. 7.5), each row represents a gene linked to ripening and the columns represent the replicates obtained from the RNA samples (2 for the *SIHST-14* and 3 for the azygous control). A large number of genes were seen to be linked to ripening and show down-regulation in the *SIHST-14* line. Of note, Silencing the *SIHST-14* gene disrupted a number of transcriptional regulators throughout ripening which may have a significant effect on downstream transcription of key ripening related genes, these genes included an ethylene response factor (Solyc03g026270), a bHLH transcription factor (Solyc07g043580), BZIP domain class transcription factor (Solyc02g092620.2), and a GATA transcription factor (Solyc05g056120.2) (Fig. 7.5: Arrowheads).

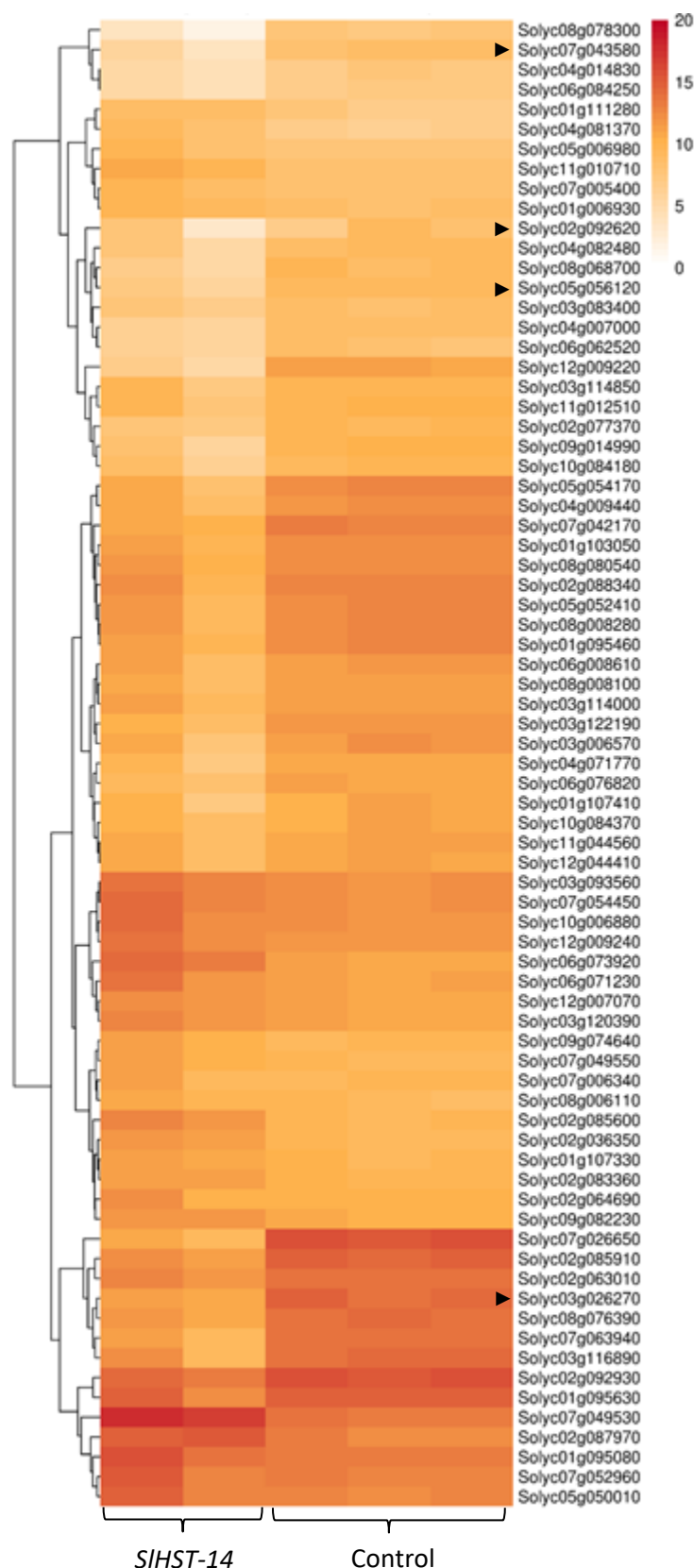


Figure 7.5: Heat map of differential gene expression of ripening related genes at B+7. Genes were clustered according to their GO: ontologies. There are a number of differentially expressed genes linked to the cell wall with both up and down-regulation occurring in the *SIHST-14* line. The arrowheads highlight the down-regulation of a number of transcription factors linked to ripening including an ethylene response factor (Solyc03g026270), a bHLH transcription factor (Solyc07g043580), BZIP domain class transcription factor (Solyc02g092620.2), and a GATA transcription factor (Solyc05g056120.2).

Differential expression continued between ripening related genes in the *SIHST-14* and control lines at the B+10 stage (Fig. 7.6). A number of transcription factors which include two ethylene response transcription factors (Solyc12g008350.1, Solyc06g082590.1), a MYB (Solyc10g084370.1), WRKY (Solyc05g015850.2), and BHLH (Solyc07g043580.2) transcription factor, and an auxin response protein (Solyc08g021820.2) were found to be down-regulated in the *SIHST-14* line (Fig. 7.6: Arrowheads), this is consistent with the role of *SIHST-14* as a transcriptional activator.

Moreover, three highly important cell-wall degrading enzymes were shown to be down-regulated in the *SIHST-14* line. The genes encoding PG, PME, and PL enzymes which are crucial to depolymerisation of pectins in the tomato cell wall (JJ Giovannoni & DellaPenna, 1989; Jolie et al., 2010; Uluisik et al., 2016) and silencing of the *SIHST-14* line thus provides a transcriptional explanation to the delay in fruit softening reported in Chapter 6.

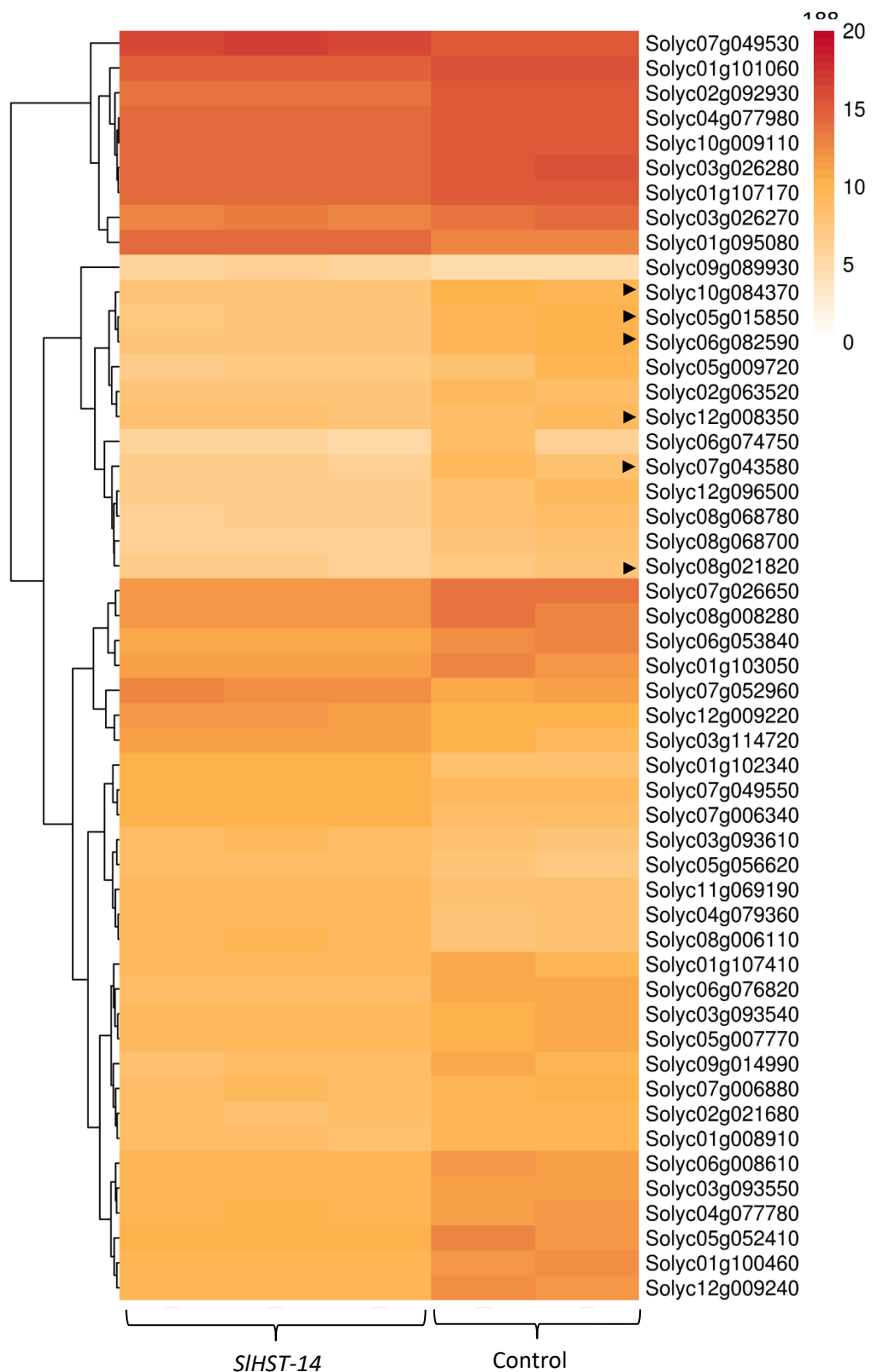


Figure 7.6: Heat map of differential gene expression of ripening related genes at B+10. Genes were clustered according to their GO: ontology. There are a number of differentially expressed genes linked to the cell wall with both up and down-regulation occurring in the *SIHST-14* line. The arrowhead highlights the down-regulation of a number of transcription factors in the *SIHST-14* line including two ethylene response transcription factors (Solyc12g008350.1, Solyc06g082590.1), a MYB (Solyc10g084370.1), WRKY (Solyc05g015850.2), and BHLH (Solyc07g043580.2) transcription factor, and an auxin response protein (Solyc08g021820.2).

Differential expression of genes in the transgenic line were sorted according to the top twenty up- and down-regulated genes at B7 and B10 (Table. 7.1, 7.2, 7.3, & 7.4). At B7, there are a number of ripening related genes that are down-regulated which include Polygalacturonases (Soly10g080210.1, Soly07g065090.1), Pectinesterases (Soly07g064180.2, Soly12g009270.1, Soly03g112170.1), Chitinases (Soly07g005100.2, Soly10g017970.1), and Heat shock proteins (Soly03g082420.2, Soly06g076540.1). This provides additional information impacting the phenotype seen in Chapter 6.

Table 7.1: The 20 most down-regulated genes in B+7 fruit. A number of cell-wall and ripening related genes are seen to be significantly ($P<0.05$) affected by silencing of the SIHST-14 gene.

GENE	Human Readable Description	logFC	logCPM	PValue	FDR
Solyc01g008710.2	Mannan endo-1 4-beta-mannosidase (AHRD V1 ***- D2S259_HALTV); contains Interpro domain(s) IPR018087 Glycoside hydrolase, family 5, conserved site	-6.70	6.03	2.75E-62	4.24E-58
Solyc10g080210.1	Polygalacturonase A (AHRD V1 **** Q9M6S2_ACTCH); contains Interpro domain(s)	-6.44	12.34	3.61E-56	1.11E-52
Solyc12g055730.1	Lipase (AHRD V1 ***- Q5S8F1_RICCO); contains Interpro domain(s)	-5.82	4.24	1.22E-41	9.36E-39
Solyc09g090970.2	Major allergen Mal d 1 (AHRD V1 ***- Q84LA7_MALDO); contains Interpro domain(s)	-5.78	6.09	4.07E-26	7.65E-24
Solyc09g082340.2	Vicilin-like protein (Fragment) (AHRD V1 **-- Q9SEW4_9ROSI); contains Interpro domain(s)	-5.52	6.35	8.29E-37	4.12E-34
Solyc07g064180.2	Pectinesterase (AHRD V1 ***- B9RXQ4_RICCO); contains Interpro domain(s) IPR018040 Pectinesterase, active site	-5.43	6.44	7.66E-40	4.37E-37
Solyc03g112440.1	Oleolin (AHRD V1 ***- O04925_SESIN); contains Interpro domain(s)	-5.34	4.14	1.29E-20	1.19E-18
Solyc09g010430.1	Unknown Protein (AHRD V1)	-5.25	3.79	1.36E-21	1.40E-19
Solyc05g011890.1	Sulfotransferase family protein (AHRD V1 **** D7LQL2_ARALY); contains Interpro domain(s)	-5.11	6.45	3.17E-32	1.11E-29
Solyc07g056510.2	Glutathione S-transferase (AHRD V1 **** D3Y4H6_9ROSI); contains Interpro domain(s) I	-4.77	10.62	3.72E-22	4.24E-20
Solyc04g071580.2	Unknown Protein (AHRD V1); contains Interpro domain(s)	-4.71	5.59	4.64E-29	1.15E-26
Solyc02g065280.2	Methyl jasmonate esterase (AHRD V1 **-* Q56SE1_SOLTU); contains Interpro domain(s)	-4.51	5.83	1.43E-30	4.51E-28
Solyc09g082110.2	Seed maturation protein (AHRD V1 **-- Q2Q4X9_MEDTR); contains Interpro domain(s)	-4.32	4.09	1.96E-20	1.79E-18
Solyc08g081790.1	Dirigent protein (AHRD V1 ***- Q9SDR7_FORIN); contains Interpro domain(s)	-4.24	5.91	1.46E-17	9.13E-16
Solyc10g080840.1	Cytochrome P450	-4.23	5.03	2.31E-33	8.68E-31
Solyc04g051470.1	Unknown Protein (AHRD V1)	-4.15	3.43	7.85E-14	2.87E-12
Solyc03g112170.1	Pectinesterase inhibitor (AHRD V1 **** A2Q674_MEDTR); contains Interpro domain(s)	-4.12	5.10	8.52E-17	4.86E-15
Solyc08g007850.1	Unknown Protein (AHRD V1)	-4.12	4.02	3.44E-29	8.98E-27
Solyc04g079960.1	Geranylgeranyl pyrophosphate synthase 2 (AHRD V1 ***- Q1A7S9_SOLLC); contains Interpro domain(s)	-4.09	6.18	2.90E-22	3.36E-20
Solyc09g015010.2	Unknown Protein (AHRD V1)	-4.09	3.65	4.08E-27	8.50E-25

Table 7.2: The 20 most up-regulated genes in B+7 fruit. A number of cell-wall and ripening related genes are seen to be significantly ($P < 0.05$) affected by silencing of the SIHST-14 gene.

Gene	Human Description	Readable	logFC	logCPM	PValue	FDR
Solyc03g045140.2	Cyclopropane-fatty-acyl-phospholipid synthase (AHRD V1 *- C7LRK7_DESBD);		11.460	1.798	2.67E-25	4.47E-23
Solyc08g036620.2	Protein TIFY 5A (AHRD V1 ***- TIF5A_ARATH);		11.058	1.400	9.68E-24	1.34E-21
Solyc03g111280.1	Cytochrome P450		10.863	1.209	1.73E-27	3.74E-25
Solyc10g076400.1	Os03g0291800 protein (Fragment) (AHRD V1 ***- Q0DSS4_ORYSJ);		10.640	0.991	1.02E-23	1.40E-21
Solyc07g008110.2	Blue copper protein (Fragment) (AHRD V1 *- O82576_MAIZE);		10.592	3.166	3.90E-42	3.16E-39
Solyc01g079960.2	Xylanase inhibitor (Fragment) (AHRD V1 *- Q53IQ3_WHEAT);		10.322	2.952	1.24E-40	7.95E-38
Solyc08g074890.2	Unknown Protein (AHRD V1)		10.146	0.509	6.52E-22	7.22E-20
Solyc06g084070.2	Auxin responsive protein (AHRD V1 ***- D9IQE6_CATRO);		10.061	3.514	3.44E-45	4.07E-42
Solyc12g088130.1	BHLH transcription factor (AHRD V1 *- A9YWR2_MEDTR		9.906	0.275	3.22E-20	2.83E-18
Solyc03g031630.2	Calcium-binding EF-hand family protein-like (AHRD V1 ***- Q6ZFI7_ORYSJ);		9.802	8.237	5.07E-52	1.11E-48
Solyc01g105650.2	1-aminocyclopropane-1-carboxylate oxidase (AHRD V1 *- ACCO_MUSAC);		9.732	0.107	1.11E-18	8.23E-17
Solyc01g110590.2	Auxin-induced SAUR-like protein (AHRD V1 ***- Q8S349_CAPAN);		9.680	0.056	9.90E-18	6.40E-16
Solyc05g052420.1	Absciscic acid receptor PYL6 (AHRD V1 *- PYL6_ARATH)		9.508	-0.109	3.88E-18	2.69E-16
Solyc05g009200.1	Unknown Protein (AHRD V1)		9.425	3.809	1.89E-50	3.24E-47
Solyc04g025530.2	Glutamate decarboxylase (AHRD V1 **** Q111D8_CITSI);		9.419	7.563	1.06E-61	8.16E-58
Solyc03g119540.2	CONSTANS-like zinc finger protein (AHRD V1 *- D0EP06_SOYBN);		9.376	3.392	6.41E-45	6.58E-42
Solyc12g005000.1	Unknown Protein (AHRD V1)		9.312	1.960	4.85E-28	1.10E-25
Solyc10g005120.1	Flavanone 3-hydroxylase (AHRD V1 *- Q5XPX2_GINBI);		9.305	1.890	8.94E-32	2.93E-29
Solyc03g116820.2	Phox domain-containing protein (AHRD V1 ***- D7L4Y9_ARALY)		9.133	1.719	1.81E-28	4.23E-26
Solyc02g076830.1	S-locus-specific glycoprotein (Fragment) (AHRD V1 *- Q84V84_CICIN);		8.921	4.063	4.53E-39	2.49E-36
Solyc08g077900.2	Expansin-like protein (AHRD V1 ***- Q0WRS3_ARATH		8.840	5.162	5.13E-44	4.94E-41

Table 7.3: The 20 most down-regulated genes in B+10 fruit. A number of cell-wall and ripening related genes are seen to be significantly ($P < 0.05$) affected by silencing of the SIHST-14 gene.

Gene	Human Description	Readable	logFC	logCPM	PValue	FDR
Solyc03g083920.1	Protein FAR1-RELATED SEQUENCE 5 (AHRD V1 **--FRS5_ARATH);		-7.65	2.35	5.11E-45	2.56E-42
Solyc03g097580.2	MtN3-like protein (AHRD V1 **--Q9LUE3_ARATH); contains Interpro domain(s)		-6.72	2.40	1.38E-54	1.09E-51
Solyc05g018410.1	Enoyl-CoA hydratase (AHRD V1 **** A3WX21_9BRAD)		-5.65	2.83	4.12E-54	2.94E-51
Solyc07g022920.2	BSD domain containing protein expressed (AHRD V1 ***-Q851F1_ORYSJ);		-4.35	1.92	6.28E-33	1.47E-30
Solyc10g005360.2	Gibberellin 2-beta-dioxygenase 7 (AHRD V1 **-*B6SZM8_MAIZE);		-4.06	1.70	1.62E-29	2.97E-27
Solyc02g070180.1	FAD-binding domain-containing protein (AHRD V1 **--D7MF10_ARALY);		-4.01	-0.24	5.86E-16	3.15E-14
Solyc07g053640.1	Arabinogalactan-protein (AHRD V1 *-* Q41256_NICAL)		-3.93	2.88	8.63E-37	2.75E-34
Solyc01g100880.2	MtN21 nodulin protein-like (AHRD V1 ***- B6TBZ6_MAIZE);		-3.68	0.32	1.16E-17	7.81E-16
Solyc03g083910.2	Acid beta-fructofuranosidase (AHRD V1 **--Q575T1_WHEAT);		-3.64	11.96	5.62E-52	3.83E-49
Solyc08g077060.2	Zinc finger protein LSD1 (AHRD V1 **-- Q6QUK7_ORYSJ);		3.36	6.00	2.99E-54	2.24E-51
Solyc04g025530.2	Glutamate decarboxylase (AHRD V1 **** Q111D8_CITSJ);		3.40	5.80	9.75E-48	5.63E-45
Solyc03g025670.2	PAR-1c protein (AHRD V1 ***-Q43589_TOBAC);		3.42	2.88	2.31E-19	1.82E-17
Solyc04g071890.2	Peroxidase 4 (AHRD V1 ****B7UCP4_LITCN);		3.45	5.89	1.55E-45	8.00E-43
Solyc07g054750.1	Wound induced protein (AHRD V1 ***- B6U0P9_MAIZE)		3.46	4.30	3.30E-34	9.17E-32
Solyc07g009230.2	Unknown Protein (AHRD V1)		3.46	3.80	2.13E-22	2.28E-20
Solyc10g011910.2	WRKY transcription factor 23 (AHRD V1 ***- C9DI12_9ROSI);		3.47	4.91	3.51E-49	2.11E-46
Solyc12g096890.1	F-box protein PP2-B1 (AHRD V1 **-- PP2B1_ARATH)		3.50	2.18	4.25E-33	1.03E-30
Solyc11g071740.1	Calmodulin-like protein (AHRD V1 ***- Q0VJ70_DATME);		3.50	9.55	2.19E-62	2.99E-59
Solyc03g117590.2	Chaperone protein dnaJ (AHRD V1 *-* C5UZI2_CLOBO);		3.50	7.72	1.24E-61	1.55E-58
Solyc06g050500.2	Absciscic acid receptor PYL4 (AHRD V1 ***- PYL4_ARATH);		3.52	6.95	1.60E-44	7.76E-42
Solyc02g014030.1	Pto-like, Serine/threonine kinase protein, resistance protein		3.58	2.28	1.31E-31	2.78E-29

Table 7.4: The 20 most up-regulated genes in B+10 fruit. A number of cell-wall and ripening related genes are seen to be significantly ($P<0.05$) affected by silencing of the SIHST-14 gene.

GENE	human_readable_description	logFC	logCPM	PValue	FDR
Solyc06g033850.2	Dehydration-responsive element-binding protein 2D (AHRD V1 *-.- DRE2D_ARATH)	6.96	6.11	6.85E-130	1.03E-125
Solyc10g050980.1	Unknown Protein (AHRD V1)	5.46	8.47	6.00E-79	3.00E-75
Solyc06g008620.1	Protein tolB (AHRD V1 *-.- D3SF14_THISK);	5.40	4.29	2.56E-73	6.39E-70
Solyc02g078380.2	Aluminum-induced protein-like protein (AHRD V1 ***- Q8S2R9_THEHA)	5.29	4.83	4.26E-80	3.19E-76
Solyc07g055690.1	S-locus-specific glycoprotein S6 (AHRD V1 ***- SLSG6_BRAOL);	4.86	3.99	1.11E-78	4.16E-75
Solyc12g009300.1	Sucrose synthase (AHRD V1 **** O82693_SOLLC);	4.83	6.51	4.90E-70	8.17E-67
Solyc07g062490.1	S-locus-specific glycoprotein (AHRD V1 ***- SLSG0_BRAOA); contains	4.77	6.38	5.88E-75	1.76E-71
Solyc02g089140.2	B12D-like protein (AHRD V1 ***- Q69F92_PHAVU);	4.61	4.81	8.27E-67	1.24E-63
Solyc08g061490.2	MTD1 (AHRD V1 ***- Q9LLM3_MEDTR)	4.54	3.29	3.32E-41	1.47E-38
Solyc11g011880.1	RLK, Receptor like protein, putative resistance protein with an antifungal domain	4.48	4.13	1.53E-70	2.87E-67
Solyc08g008120.2	Unknown Protein (AHRD V1); contains Interpro domain(s) IPR018276 Ubiquitin ligase, Det1/DDB1-complexing	4.29	3.38	2.19E-60	2.35E-57
Solyc10g055810.1	Endochitinase (Chitinase) (AHRD V1 **** Q43184_SOLTU);	4.27	7.77	2.14E-72	4.59E-69
Solyc06g066420.2	Cold induced protein-like (AHRD V1 *-.- Q94JH8_ORYSJ)	4.24	2.99	5.26E-42	2.47E-39
Solyc07g054800.1	Wound induced protein (AHRD V1 ***- B6T327_MAIZE)	4.20	7.32	5.34E-47	2.97E-44
Solyc02g092580.2	Peroxidase (AHRD V1 **** A0S5Z4_SESIN);	4.20	3.03	1.16E-56	1.09E-53
Solyc01g079940.2	Xylanase inhibitor (Fragment) (AHRD V1 ***- Q53IQ4_WHEAT);	4.17	3.17	4.71E-57	4.71E-54
Solyc01g107090.2	Beta-1 4-xylosidase (AHRD V1 *-.- D7LA14_ARALY)	4.03	6.89	6.09E-56	5.37E-53
Solyc12g057040.1	Cryptochrome 1b	4.02	3.60	3.20E-55	2.67E-52
Solyc01g107100.2	Beta-1 4-xylosidase (AHRD V1 ***- D7LA14_ARALY)	3.87	6.17	1.39E-37	5.08E-35
Solyc11g071760.1	Calmodulin-like protein (AHRD V1 ***- Q0VJ70_DATME);	3.8150 78173	5.039678 076	1.61E-61	1.86E-58

For such a large amount of differentially expressed genes, we clustered the genes according to their GO: ontology and related them to their corresponding KEGG pathways to isolate the most affected cellular mechanisms in the *SIHST-14* line. The data was localized within the cell (Fig 7.7) and by far the largest clustering of genes whose enrichment value in the control was more than ten times that of the transgenic line are involved in translation. This is not surprising as the *HST* genes primarily promote expression of HSPs whose primary role within the cell is to facilitate protein aggregation, binding, and folding. This lends weight to the hypothesis that *SIHST-14* is disrupting translation of key proteins required in ripening at the transcriptional level and thus, delaying depolymerisation of the cell-wall during ripening.

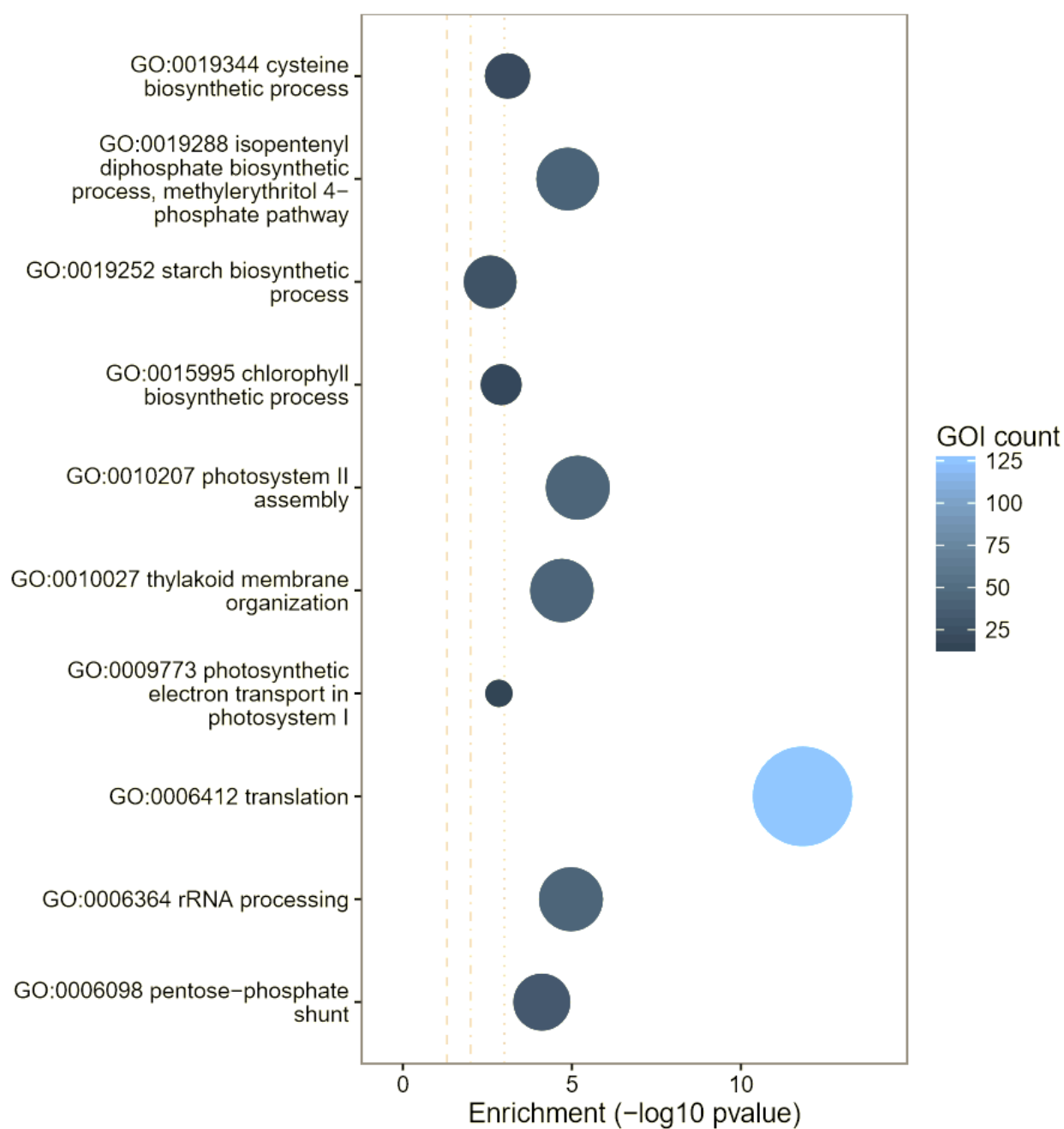


Figure 7.7: Cellular localization of differential expression of genes affected by silencing *SIHST-14* in tomato. The diagram shows the localization of differentially expressed genes to be affecting translation the most.

Ripening-related pathways affected by silencing *SIHST-14*

Superimposing the identities of the differentially expressed genes on the KEGG pathways (Kanehisa, 1996) indicated that a number of ripening-related pathways were impacted by silencing of the *SIHST-14* transcription factor. The *SIHST-14* RNAi line resulted in down-regulation of the pyrabactin synthetic growth inhibitor (PYR/PYL) and the 2C protein phosphatases (PP2Cs; Fig 7.8). The PYR/PYL gene encodes an ABA-binding protein that maintains a negative regulatory signalling pathway that controls abscisic acid signalling through the PP2C family (Park et al., 2014). Absciscic acid (ABA) is essential in fruit development and a number of ABA-deficient mutants have been characterized which result in an elevation in plastid number and lycopene content (Galpaz et al., 2008).

It is likely, that the *SIHST-14* transgenic line is inhibiting ABA signalling by modulation of the PYR/PYL growth inhibitor which in turn leads to an increase in plastid content and lycopene production and therefore a change in colour of the fruit (seen in Chapter 6). Carotenoid biosynthesis is a key contributor to the development of a ripe tomato conferring a distinctive colour change and acts as a precursor to flavour compounds which have significant commercial value.

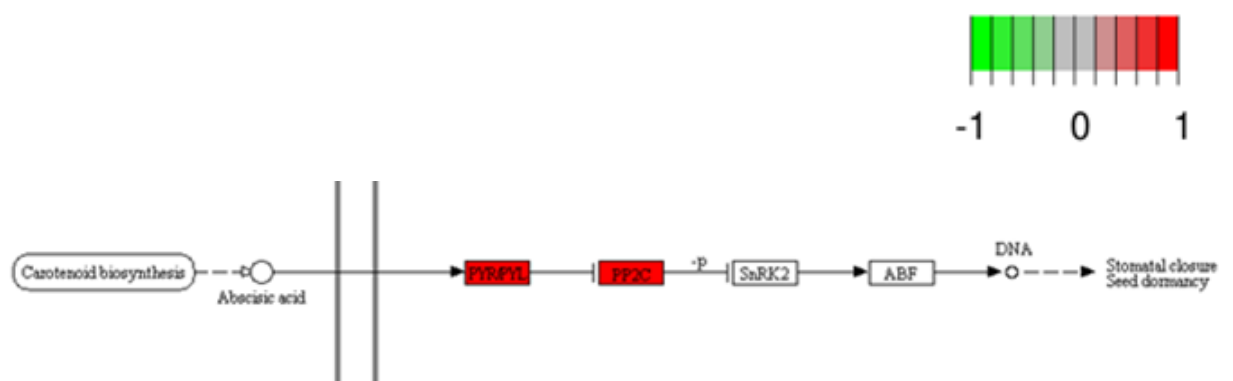


Figure 7.8: Differential expression of *SIHST-14* in carotenoid biosynthesis. **Red:** Up-regulated in the control line. The diagram shows the effect of the *SIHST-14* silenced line the carotenoid biosynthetic pathway. It is shown to down-regulate an ABA-binding protein that negatively regulates abscisic acid signalling through the PP2C family which promote lycopene accumulation.

The *SlHST-14* silenced fruit also resulted in changes in the expression of genes involved in the action of ethylene. Expression of the EIN3-binding F-box protein (EBF) was down regulated in the *SlHST-14* RNAi line suggesting a role in the ethylene signalling pathway (Fig 7.9). The EIN3 proteins promote the transcription of ethylene response factors (ERFs) which are involved in the downstream transcription of ethylene-related genes in climacteric fruit (Potuschak et al., 2003). The EBF proteins negatively regulate ethylene signalling by marking EIN3 for degradation which is then stabilized by the presence of ethylene to promote the plant response which has been shown to be instrumental in the timing of the switch to fruit ripening (Kevany, Tieman, Taylor, Cin, & Klee, 2007; Potuschak et al., 2003).

Independent silencing of the *Sl-EBF1* and *Sl-EBF-2* lines in tomato are indistinguishable from the control plant. Double mutants however, exhibit a much stronger phenotype including dwarfism and accelerated fruit ripening (Y. Yang et al., 2010). These results were not seen in the *SlHST-14* line suggesting that ripening is not being effected despite down-regulation of the EBF1/2 genes in tomato pericarp tissue. EBF1 was found to be down-regulated in the *SlHST-14* mutant but expression of EBF2 was unaltered and explains why we didn't observe accelerated ripening in the *SlHST-14* line.

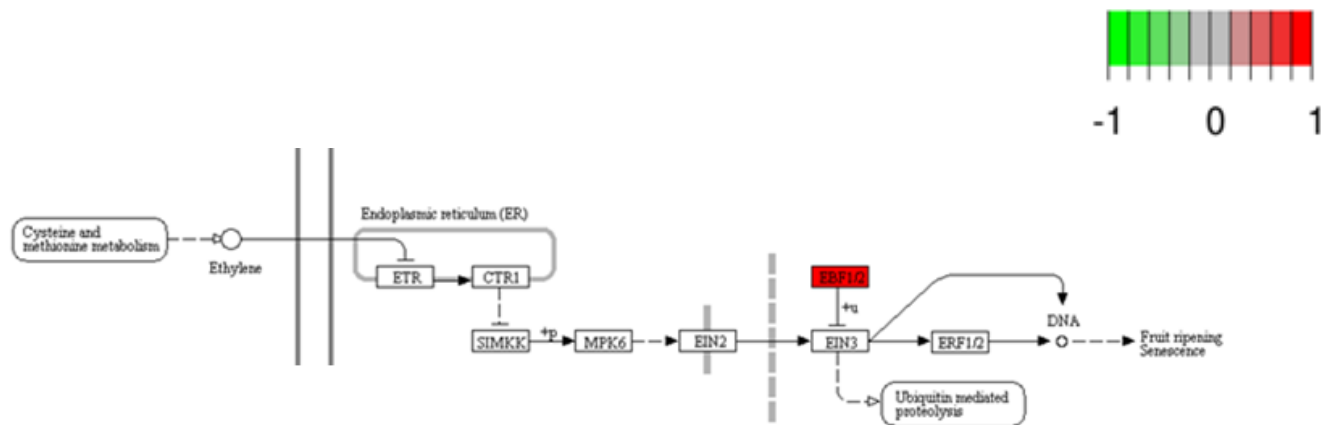


Figure 7.9: Differential expression of *SIHST-14* in the tomato ethylene response pathway. **Red:** Up-regulated in the control line. The diagram shows effect of the *SIHST-14* silenced line has on ethylene perception in tomato, the silencing plant line was found to down-regulate EBF1 whereby EBF2 was unaltered which promotes normal fruit ripening.

Cell wall genes and fruit softening

At both B7 and B10, the expression of cell wall degrading enzymes is impacted by *SIHST-14* silencing at B7 and B10 (Fig. 7.10). PME (Solyc07g064170) has been shown to remove methyl groups which allows PG (Solyc10g080210.1) to hydrolyse the pectic polysaccharides, and silencing of these genes throughout fruit ripening has been observed to have small but significant effects on shelf life (Sheehy et al., 1988; Tieman, Harriman, Ramamohan, & Handa, 1992). Moreover, a recent report has characterised the effect of silencing a pectate lyase gene (Solyc03g111690) in tomato fruit. Transgenic PL lines exhibited firmer inner and outer pericarp tissues at B4 and B7 and marks the first instance that specific control over fruit ripening can be achieved without altering flavour and colour (Uluışik et al., 2016). PL was also found to be down-regulated (LogFC: -1.30, P-value: 7.91E-10) in the *SIHST-14* line highlighting the impact on cell wall remodelling. The expression of these cell-wall degrading enzymes along with chitinase, and EBF1 was found to be significantly (Fig 7.10: A, $P < 0.05$) lower in the *SIHST-14* plant line where reduced expression of cell wall hydrolases is likely to result in delayed cell wall remodelling and fruit softening which helps to explain the slower softening phenotype at the B+7 and B+10 stages that were observed in the transgenic lines (Chapter 6).

Moreover, three HSPs were found to be significantly ($P < 0.05$) up-regulated in the *SIHST-14* RNAi line (Solyc09g065660.2, Solyc12g098520.1, Solyc07g055710.2). Previously, a heat shock protein has previously been linked to pectin depolymerisation by reduction of thermal denaturation of the enzymes, producing fruit with thicker juice viscosity (Ramakrishna et al., 2003). This suggests that there may be some functional redundancy within the HSP superfamily and that these genes (Solyc09g065660.2, Solyc12g098520.1, Solyc07g055710.2) may also have roles as transcriptional regulators and are being utilized in the absence of *SIHST-14*.

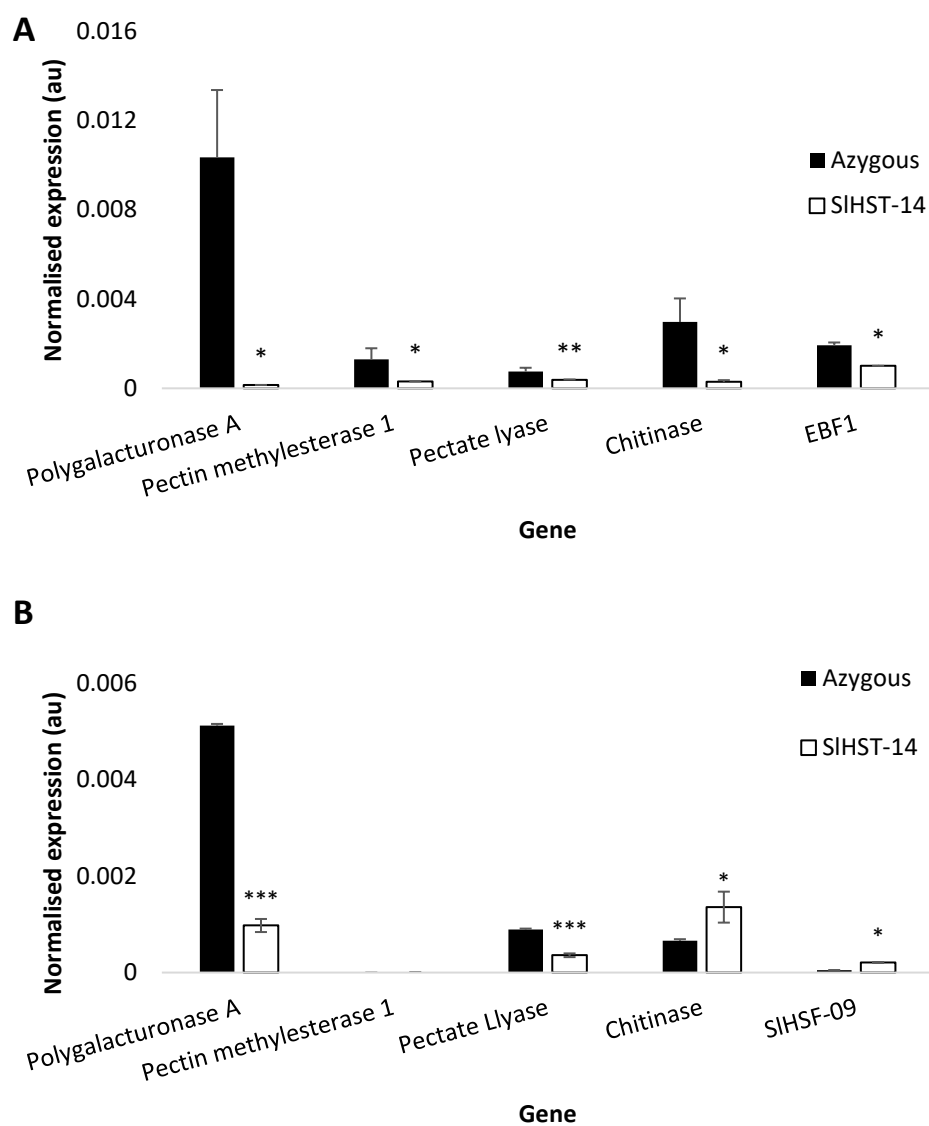


Figure 7.10: Differential expression of ripening related genes at B7 and B10. Differential expression showing **A)** differential expression at B7 and **B)** differential expression at B10.

The identification differential expression in key cell-wall degrading enzymes highlights the role of *SHST-14* in regulating fruit ripening at the transcriptional level. RNA-seq has shown that cell wall remodelling has been altered by the down-regulation of ripening related genes by a heat-shock transcription factor that is a direct target of LeMADS-RIN. This suggests that *SHST-14* works to enhance the expression of genes linked to LeMADS-RIN and offers a downstream target for control in fruit softening.

Chapter 8

General discussion and future work

The aim of the project was to identify novel genes associated with texture and shelf-life in tomato. Initially, an endogenously expressed root-related tetraspanin (*SITET-6*) was over-expressed in tomato based on data associating an orthologue of this gene with long shelf-life in melon. However, the gene showed no obvious phenotype and had no effect on fruit softening. An orthologous gene in *Arabidopsis* conferred a gravitropic phenotype in roots, but no clear root phenotype was observed in the *SITET-6* over expression line. A second tetraspanin was selected because it is endogenously expressed in fruit tissue and is likely involved in ripening. Unfortunately, transformations of this construct in Ailsa Craig tomatoes were unsuccessful and this may have been due to a critical role for this gene in plant regeneration from tissue culture.

The project then focused on two transcription factors whose expression profile was highly correlated with the *RIPENING INHIBITOR* or *RIN* gene; a master regulator of ripening. These genes were a zinc finger protein (Soly08g063040) and a heat-shock transcription factor (Soly06g053960). Silencing these genes was found to confer firmer inner and outer pericarp texture during the ripening process. RNA-seq analysis of the heat-shock transcription factor transgenic lines revealed differential expression of genes associated with cell-wall remodelling and lycopene biosynthesis indicating a role for this transcription factor in these developmental processes.

Although substantial efforts were made to investigate the role of tetraspanins in tomato ripening the experiments were extremely challenging and the role of these genes still remains to be elucidated. Also, the work on the novel *SIHST-14* and *SIZFP* proteins provides the start point for experiments to place them within the regulatory network controlling ripening. I will now speculate on the role of tetraspanins based on the literature and suggest further work based on the findings in the thesis.

Tetraspanins

The tetraspanins were first characterised in plants by mutagenesis of an *Arabidopsis* population resulting in a single T-DNA mutant in *AtTET-1*. Silencing of the *ekoko* mutant conveyed strong root and leaf phenotypes but it is important to note that over-expression of the gene failed to produce any effect on the morphology of the plant (Olmos, Reiss, & Dekker, 2003). Tetraspanins have since been described in every plant tissue and are involved from the very early stages of development (F. Wang et al., 2015) and are essential for cell signalling pathways, auxin distribution (Cnops et al., 2006), and reproduction (Boavida, Qin, Broz, Becker, & McCormick, 2013). There is however, no current understanding into their role in fruit ripening and maturation.

Twelve tetraspanins have been described in *Solanum lycopersicum*, of which *SITET-8* expression is closely linked to fruit ripening. A similar expression pattern is also seen for *RIN* (Martel et al., 2011) and *CNR* (Eriksson et al., 2004), both significant transcriptional regulators of fruit ripening which suggests that *SITET-8* is likely to also have a significant role in fruit development and ripening.

There are several possible mechanisms in which *SITET-8* could potentially influence fruit ripening. In bacteria, and fungi the tetraspanins form enriched micro-domains encompassing other tetraspanins and other membrane bound proteins which are heavily involved in cell adhesion, morphology and motility within plasma membranes which facilitate pathogenic entry into host cells (Stipp et al., 2003). This provides the organisms with a structural mechanism by which it can invade. Moreover, Silencing of these genes has been shown to lower instances of invasion by pathogens (Gourgues, Brunet-Simon, Lebrun, & Levis, 2003; Tham et al., 2010). Therefore, it is possible that *SITET-8* has a structural role in fruit ripening providing cell-adhesion and structural integrity to the fruit whilst the cell wall is being broken down by enzymes. Moreover,

over-expression of the gene may reinforce intercellular micro-domains and decrease the rate of cell wall degradation and prolong shelf-life.

Conversely, tetraspanins have been shown to be instrumental in a number of immune response pathways which regulate signal transduction, cytokine production and leukocyte proliferation in HIV (Grigorov et al., 2009), Feline immunodeficiency virus (FIV) (Willett, Hosie, Shaw, & Neil, 1997), Human T-cell leukaemia virus (HTLV) (Pique et al., 2000), Porcine reproductive and respiratory syndrome virus (PRRSV) (Shanmukhappa, Kim, & Kapil, 2007), and human papillomavirus (HPV) (Spoden et al., 2008). Their role in the WUSCHEL–CLAVATA3 feedback loop signalling cascade in plants is also well documented (Clark, 2001) and suggests that they also play a multi-functional role in plant development. Therefore, there is potential for *SITET-8* to facilitate ligand binding and subsequent signalling cascades in fruit from the onset of ripening that may influence auxin distribution, cell-wall enzyme activity, or carotenoid biosynthesis. The effects of over-expression or silencing could therefore promote either an increase or decrease in cellular activity depending on the role of *SITET-8* and the signalling cascade being effected which will in turn, significantly affect the ripening process.

Over-expression of the *SITET-6* in fruit tissue had no observable effect on fruit ripening. Moreover, in a previous report where over-expression of a tetraspanin was seen to have no effect, the knock-down mutant produced strong leaf and root phenotypes in *Arabidopsis* (Olmos et al., 2003). It is therefore, more likely in future investigations that silencing of the *SITET-6* and *SITET-8* genes will provide a clearer indication into the role of the tetraspanins on fruit development and ripening. However, this will depend on finding a suitable transgenic system where silencing of the gene still allows regeneration of viable plants; which was not the case during this project.

The transgenic plants

A significant part of this project was undertaken to generate transgenic plants to determine the role of the tetraspanin family in fruit softening. Two approaches were taken in this investigation. (1) to knock-down and over-express the *SITET-8* gene using a constitutive 35S promoter, and (2) to knock-down and over-express the *SITET-8* gene using a fruit specific polygalacturonase promoter.

In this investigation, the transformants from both constructs failed to establish roots and shoots suggesting that the constructs were lethal to the plant highlighting the importance of tetraspanins in early plant development. Recent studies have shown significant functional redundancy in the tetraspanin family (Boavida et al., 2013; F. Wang et al., 2012) suggesting that the decision to use a 35S promoter may provide an explanation to the viability of the cotyledons. It is likely, given the high level of conservation between tetraspanins, that the construct was targeting additional genes to the chosen target which have been shown to be of significance in the early stages of plant growth (F. Wang et al., 2015, 2012). The tetraspanin proteins have been characterised in every plant tissue and every stage of development (The Tomato Genome Consortium, 2012; F. Wang et al., 2015) and disruption of one or many of these proteins in the early stages of growth can interfere with vital cell signalling pathways leading to death of the plant (Cnops et al., 2006).

Transformation efficiency may also explain why we were unable to obtain a viable transgenic line. Between 400 and 500 cotyledons for each construct were transformed. The number of transformants exhibiting shoot regeneration for the tetraspanin constructs was <10. Using *Agrobacterium* strain EHA105, optimal efficiency has been empirically determined to be in the region of 40% (Chetty et al., 2013), but has also been reported to be as low as 19% or 4% (Cruz-Mendívil et al., 2011; H. J. Sun, Uchii, Watanabe, & Ezura, 2006). Moreover, in all strains of *Agrobacterium*, 7-11% of non-transgenic plants will regenerate on selective media (McCormick et al., 1986).

Due to time constraints, we were unable to complete our investigation using the transgenic lines described. The significance of tetraspanins to plant growth and development have been previously characterised in *Arabidopsis* and this report emphasizes their importance in other plants. Future work on these genes in tomato will need to address the choice of promoter for driving the transgene. Furthermore, given the nature of the tetraspanins in early plant growth and development as structural cell-wall proteins and with an emerging understanding of their role in cell signalling pathways, it is very likely that *SITET-8* will have a significant impact on fruit maturation and softening.

Novel genes linked to fruit softening and the potential for discovery of new ripening related genes

Plant heat shock proteins were first characterised in tomato (Scharf, Rose, Zott, Schöff, & Nover, 1990) and have since been characterised in *Arabidopsis*, rice and more recently, grasses (Guo et al., 2008; Z. Yang et al., 2014). Their primary role is to maintain protein homeostasis by facilitating synthesis, folding, and restoration of denatured proteins often due to environmental stresses (Boston et al., 1996). It is not surprising then, to find that plants comprise a larger array of heat-shock proteins than their eukaryotic counterparts (Guo et al., 2008).

There are 24 heat-shock transcription factors identified in tomato that encode for the 26 HSPs among other proteins, eight of these HSPs are very highly expressed in fruit ripening and four which exhibit a significant increase in expression after heat stress treatment (X. Yang et al., 2016). *SlHST-14* was found to be a direct target of LeMADS-RIN (Martel et al., 2011) suggesting it has a key role in fruit ripening (The Tomato Genome Consortium, 2012). An RNAi line was used to characterize the role of *SlHST-14* in fruit ripening and was found to convey firmer fruit texture 4 and 7 days after the breaker stage. This highlights the significance of the heat-shock transcription factor in fruit softening and provides a foundation on which further transcriptional regulators can be characterised.

Fruit ripening is a complex developmental process encompassing thousands of genes and signalling pathways to promote the breakdown of plant cell-walls and facilitate carotenoid biosynthesis, it is likely that the heat shock transcription factors are involved in controlling the expression of heat-shock proteins which are responsible for the aggregation and folding of cell-wall degrading enzymes such as PG, PME, and PL whose absence would lead to fewer enzyme complexes and may explain why silencing of *SlHST-14* produced fruit with firmer texture. It is clear that the heat-shock transcription factor plays a significant role in fruit ripening with half of all identified heat-shock

proteins being expressed at some level during fruit ripening (X. Yang et al., 2016). This report provides a starting point by which further investigations can build upon to give a better understanding of the transcriptional regulation in fruit development.

Future work in this area could include (1) Further analysis into the expression profiles of all genes linked to fruit ripening to assess the downstream effect of silencing target genes to identify the genes the target most likely interacts with. This will provide invaluable information as the precise role of the heat-shock transcription factors and associated heat shock proteins during fruit softening which is not currently understood. (2) further investigation of single gene knock-down lines which would help to isolate and characterize the role of transcription factors and may provide, like as seen in this report small but significant differences in fruit texture or carotenoid biosynthesis. (3) a double or triple mutant combination of fruit specific heat-shock TFs which may provide a more comprehensive phenotype to target long shelf-life in tomato. Selection of potential targets would have to consider the endogenous expression of each candidate. In this report, we looked to assess the downstream effects of silencing a targeted heat-shock transcription factor and characterized those genes shown to interact with it during fruit ripening.

A zinc finger protein RNAi line was also found to promote firmer outer pericarp tissues highlighting the importance in the down-stream transcriptional regulation of genes linked to *LeMADS-RIN*. It is likely that *SIZFP* works as a transcriptional regulator during ripening as it is expressed from the BR stage through to BR+10. These data establish a precedent by which further genes can be identified and be linked to fruit softening by their expression profiles. Phylogenetic analysis of *SIZFP* has shown that its most closely related characterized protein is a MAGPIE-zinc finger protein in Arabidopsis. MAGPIE expression has been shown to regulate the expression of genes by interacting with other transcription factors (Welch et al., 2007). This provides a potential mechanism by which *SIZFP* can influence fruit softening. Further work will look to assess the downstream effects of *SIZFP* on ripening related TFs using RNA-

seq but in this report we chose to investigate the heat-shock transcription factor in more detail as it is more highly associated with *LeMADS-RIN*.

To conclude, this report has shown that targeting genes linked to known regulators of ripening like *rin* by their expression profiles is a reliable method to further investigate the transcriptional regulation of fruit development. Characterizing downstream regulators of fruit ripening will eventually pave the way to developing an understanding of the function of most of the regulatory genes controlling fruit development. This will allow modulation of specific ripening processes to achieve fine control of all aspects of ripening and novel insights into the mechanistic basis of this unique developmental process.

References

- Bemer, M., Karlova, R., Ballester, A. R., Tikunov, Y. M., Bovy, A. G., Wolters-Arts, M., ... de Maagd, R. a. (2012). The tomato FRUITFULL homologs TDR4/FUL1 and MBP7/FUL2 regulate ethylene-independent aspects of fruit ripening. *The Plant Cell*, 24(11), 4437–51. <https://doi.org/10.1105/tpc.112.103283>
- Bharti, S., Kumar, P., Tintschl-ko, A., Bharti, K., Treuter, E., & Nover, L. (2004). Tomato Heat Stress Transcription Factor HsfB1 Represents a Novel Type of General Transcription Coactivator with a Histone-Like Motif Interacting with the Plant CREB Binding Protein Ortholog HAC1, 16(June), 1521–1535. <https://doi.org/10.1105/tpc.019927.1>
- Boavida, L. C., Qin, P., Broz, M., Becker, J. D., & McCormick, S. (2013). Arabidopsis tetraspanins are confined to discrete expression domains and cell types in reproductive tissues and form homo- and heterodimers when expressed in yeast. *Plant Physiology*, 163(2), 696–712. <https://doi.org/10.1104/pp.113.216598>
- Boston, R. S., Viitanen, P. V, & Vierling, E. (1996). Molecular chaperones and protein folding in plants. In W. Filipowicz & T. Hohn (Eds.), *Post-Transcriptional Control of Gene Expression in Plants* (pp. 191–222). inbook, Dordrecht: Springer Netherlands. https://doi.org/10.1007/978-94-009-0353-1_9
- Bremer, B., Bremer, K., & Chase, M. (2009). An update of the Angiosperm Phylogeny Group classification for the orders and families of flowering plants: APG III. *Botanical Journal of ...*, 161, 105–121.
- Brewer, M. T., Moyseenko, J. B., Monforte, A. J., & Van Der Knaap, E. (2007). Morphological variation in tomato: A comprehensive study of quantitative trait loci controlling fruit shape and development. *Journal of Experimental Botany*, 58(6), 1339–1349. <https://doi.org/10.1093/jxb/erl301>
- Butelli, E., Titta, L., Giorgio, M., Mock, H.-P., Matros, A., Peterek, S., ... Martin, C. (2008). Enrichment of tomato fruit with health-promoting anthocyanins by expression of select transcription factors. *Nature Biotechnology*, 26(11), 1301–8. <https://doi.org/10.1038/nbt.1506>
- Caffall, K. H., & Mohnen, D. (2009). The structure, function, and biosynthesis of plant cell wall pectic polysaccharides. *Carbohydrate Research*, 344(14), 1879–1900. Journal Article, Research Support, U.S. Gov't, Non-P.H.S., Review. <https://doi.org/10.1016/j.carres.2009.05.021>
- Cara, B., & Giovannoni, J. J. (2008). Molecular biology of ethylene during tomato fruit development and maturation. *Plant Science*, 175(1–2), 106–113. <https://doi.org/10.1016/j.plantsci.2008.03.021>
- Chan-Schaminet, K. Y., Baniwal, S. K., Bublak, D., Nover, L., & Scharf, K.-D. (2009). Specific interaction between tomato HsfA1 and HsfA2 creates hetero-oligomeric superactivator complexes for synergistic activation of

heat stress gene expression. *The Journal of Biological Chemistry*, 284(31), 20848–20857. Journal Article, Research Support, Non-U.S. Gov't.
<https://doi.org/10.1074/jbc.M109.007336>

- Chao, Q., Rothenberg, M., & Solano, R. (1997). Activation of the ethylene gas response pathway in Arabidopsis by the nuclear protein ETHYLENE-INSENSITIVE3 and related proteins. *Cell*, 89(1), 1133–1144.
- Charrin, S., le Naour, F., Silvie, O., Milhiet, P.-E., Boucheix, C., & Rubinstein, E. (2009). Lateral organization of membrane proteins: tetraspanins spin their web. *The Biochemical Journal*, 420(2), 133–54.
<https://doi.org/10.1042/BJ20082422>
- Charrin, S., Manié, S., Oualid, M., Billard, M., Boucheix, C., & Rubinstein, E. (2002). Differential stability of tetraspanin/tetraspanin interactions: role of palmitoylation. *Federation of the Societies of Biochemistry and Molecular Biology*, 516(1–3), 139–44.
- Cheniclet, C., Rong, W. Y., Causse, M., Frangne, N., Bolling, L., Bordeaux, V. S., & Ornon, V. (2005). Cell Expansion and Endoreduplication Show a Large Genetic Variability in Pericarp and Contribute Strongly to Tomato Fruit Growth 1, 139(December), 1984–1994.
<https://doi.org/10.1104/pp.105.068767.1984>
- Chetty, V. J., Ceballos, N., Garcia, D., Narvez-Vsquez, J., Lopez, W., & Orozco-Cardenas, M. L. (2013). Evaluation of four *Agrobacterium tumefaciens* strains for the genetic transformation of tomato (*Solanum lycopersicum* L.) cultivar Micro-Tom. *Plant Cell Reports*, 32(2), 239–247.
<https://doi.org/10.1007/s00299-012-1358-1>
- Clark, S. E. (2001). Meristems: start your signaling. *Current Opinion in Plant Biology*, 4(1), 28–32.
- Cnops, G., Neyt, P., & Raes, J. (2006). The TORNADO1 and TORNADO2 genes function in several patterning processes during early leaf development in *Arabidopsis thaliana*. *The Plant Cell* ..., 18(April), 852–866.
<https://doi.org/10.1105/tpc.105.040568.1>
- Cong, B., & Tanksley, S. D. (2006). FW2.2 and cell cycle control in developing tomato fruit: a possible example of gene co-option in the evolution of a novel organ. *Plant Molecular Biology*, 62(6), 867–880. article.
<https://doi.org/10.1007/s11103-006-9062-6>
- Cordain, L., Miller, J. B., Eaton, S. B., Mann, N., Holt, S. H., & Speth, J. D. (2000). Plant-animal subsistence ratios and macronutrient energy estimations in worldwide hunter-gatherer diets. *The American Journal of Clinical Nutrition*, 71(3), 682–92.
- Cosgrove, D. J. (2005). Growth of the plant cell wall. *Nature Reviews. Molecular Cell Biology*, 6(11), 850–61. <https://doi.org/10.1038/nrm1746>

- Cruz-Mendívil, A., Rivera-López, J., Germán-Báez, L. J., López-Meyer, M., Hernández-Verdugo, S., López-Valenzuela, J. A., ... Valdez-Ortiz, A. (2011). A simple and efficient protocol for plant regeneration and genetic transformation of tomato cv. micro-tom from leaf explants. *HortScience*, 46(12), 1655–1660.
- Damberger, F. F., Pelton, J. G., Harrison, C. J., Nelson, H. C., & Wemmer, D. E. (1994). Solution structure of the DNA-binding domain of the heat shock transcription factor determined by multidimensional heteronuclear magnetic resonance spectroscopy. *Protein Science : A Publication of the Protein Society*, 3(10), 1806–1821. Journal Article, Research Support, Non-U.S. Gov't, Research Support, U.S. Gov't, Non-P.H.S., Research Support, U.S. Gov't, P.H.S. <https://doi.org/10.1002/pro.5560031020>
- Dawson, D. M., Melton, L. D., & Watkins, C. B. (1992). Cell Wall Changes in Nectarines (*Prunus persica*) 1. *Plant Physiology*, 100(3), 1203–1210.
- DeSalle, R., Mares, R., & Garcia-España, A. (2010). Evolution of cysteine patterns in the large extracellular loop of tetraspanins from animals, fungi, plants and single-celled eukaryotes. *Molecular Phylogenetics and Evolution*, 56(1), 486–91. <https://doi.org/10.1016/j.ympev.2010.02.015>
- Dorcey, E., Urbez, C., Blázquez, M. a, Carbonell, J., & Perez-Amador, M. a. (2009). Fertilization-dependent auxin response in ovules triggers fruit development through the modulation of gibberellin metabolism in Arabidopsis. *The Plant Journal : For Cell and Molecular Biology*, 58(2), 318–32. <https://doi.org/10.1111/j.1365-313X.2008.03781.x>
- Edrington, T. C., Yeagle, P. L., Gretzula, C. L., & Boesze-Battaglia, K. (2007). Calcium-dependent association of calmodulin with the C-terminal domain of the tetraspanin protein peripherin/rds. *Biochemistry*, 46(12), 3862–71. <https://doi.org/10.1021/bi061999r>
- Eriksson, E. M., Bovy, A., Manning, K., Harrison, L., Andrews, J., De Silva, J., ... Seymour, G. B. (2004). Effect of the Colorless non-ripening mutation on cell wall biochemistry and gene expression during tomato fruit development and ripening. *Plant Physiology*, 136(4), 4184–97. <https://doi.org/10.1104/pp.104.045765>
- Fernandez, A. I., Viron, N., Alhagdow, M., Karimi, M., Jones, M., Amsellem, Z., ... Hilson, P. (2009). Flexible tools for gene expression and silencing in tomato. *Plant Physiology*, 151(4), 1729–40. <https://doi.org/10.1104/pp.109.147546>
- Fischer, R., & Bennett, A. (1991). Role of cell wall hydrolases in fruit ripening. *Annual Review of Plant Biology*, 42, 675–703.
- Frary, A., Nesbitt, T. C., Frary, A., Grandillo, S., Knaap, E. van der, Cong, B., ... Tanksley, S. D. (2000). fw2.2: A Quantitative Trait Locus Key to the Evolution of Tomato Fruit Size. *Science*, 289(5476), 85–88. JOUR.

- French, A., Ubeda-Tomas, S., Holman, T. J., Bennett, M. J., Pridmore, T., & Centre. (2009). High-Throughput Quantification of Root Growth Using a Novel Image-Analysis Tool. *Society*, 150(August), 1784–1795. <https://doi.org/10.1104/pp.109.140558>
- Fry, S. C. (2004). Primary cell wall metabolism : tracking the careers of wall polymers in living plant cells. *New Phytologist*, 641–675. <https://doi.org/10.1111/j.1469-8137.2003.00980.x>
- Frydman, J. (2001). Folding of newly translated proteins in vivo: the role of molecular chaperones. *Annual Review of Biochemistry*, 70, 603–47. <https://doi.org/10.1146/annurev.biochem.70.1.603>
- Galpaz, N., Wang, Q., Menda, N., Zamir, D., & Hirschberg, J. (2008). Absciscic acid deficiency in the tomato mutant high-pigment 3 leading to increased plastid number and higher fruit lycopene content. *Plant Journal*, 53(5), 717–730. <https://doi.org/10.1111/j.1365-313X.2007.03362.x>
- Garcia-España, A., Chung, P.-J., Sarkar, I. N., Stiner, E., Sun, T.-T., & Desalle, R. (2008). Appearance of new tetraspanin genes during vertebrate evolution. *Genomics*, 91(4), 326–34. <https://doi.org/10.1016/j.ygeno.2007.12.005>
- Gelvin, S. B. (2003). Agrobacterium-Mediated Plant Transformation: the Biology behind the “Gene-Jockeying” Tool. *Microbiology and Molecular Biology Reviews*, 67(1), 16–37. <https://doi.org/10.1128/MMBR.67.1.16>
- Giersen, D., & Kader, A. A. (1986). Fruit ripening and quality. In J. G. Atherton & J. Rudich (Eds.), *The Tomato Crop: A scientific basis for improvement* (pp. 241–280). inbook, Dordrecht: Springer Netherlands. https://doi.org/10.1007/978-94-009-3137-4_6
- Giovannoni, j j, Noensie, e n, Ruezinsky, d m, Lu, x h, Tracy, s l, Ganai, m w, ... Tanksley, s d. (1995). Molecular-genetic analysis of the ripening-inhibitor and non-ripening loci of tomato - a first step in genetic map-based cloning of fruit ripening genes. *Molecular and General Genetics*, 248(2), 195–206. article. <https://doi.org/10.1007/BF02190801>
- Giovannoni, J. (2001). Molecular biology of fruit maturation and ripening. *Annual Review of Plant Biology*, 52(1), 725–749.
- Giovannoni, J., & DellaPenna, D. (1989). Expression of a chimeric polygalacturonase gene in transgenic rin (ripening inhibitor) tomato fruit results in polyuronide degradation but not fruit softening. *The Plant Cell*, 1(January 1989), 53–63.
- Giovannoni, J. J. (2004). Genetic regulation of fruit development and ripening. *The Plant Cell*, 16 Suppl, S170–S180. <https://doi.org/10.1105/tpc.019158>
- Giovannoni, J. J. (2007). Fruit ripening mutants yield insights into ripening control. *Current Opinion in Plant Biology*, 10(3), 283–9.

<https://doi.org/10.1016/j.pbi.2007.04.008>

- Goulao, L., & Oliveira, C. (2008). Cell wall modifications during fruit ripening: when a fruit is not the fruit. *Trends in Food Science & Technology*, 19(1), 4–25. <https://doi.org/10.1016/j.tifs.2007.07.002>
- Gourgues, M., Brunet-Simon, a., Lebrun, M.-H., & Levis, C. (2003). The tetraspanin BcPls1 is required for appressorium-mediated penetration of *Botrytis cinerea* into host plant leaves. *Molecular Microbiology*, 51(3), 619–629. <https://doi.org/10.1046/j.1365-2958.2003.03866.x>
- Grandillo, S., Ku, M. H., & Tanksley, D. S. (1999). Identifying the loci responsible for natural variation in fruit size and shape in tomato. *Theoretical and Applied Genetics*, 99(6), 978–987. article. <https://doi.org/10.1007/s001220051405>
- Green, L. R., Monk, P. N., Partridge, L. J., Morris, P., Gorringer, A. R., & Read, R. C. (2011). Cooperative role for tetraspanins in adhesin-mediated attachment of bacterial species to human epithelial cells. *Infection and Immunity*, 79(6), 2241–2249. <https://doi.org/10.1128/IAI.01354-10>
- Grigorov, B., Attuil-Audenis, V., Perugi, F., Nedelec, M., Watson, S., Pique, C., ... Muriaux, D. (2009). A role for CD81 on the late steps of HIV-1 replication in a chronically infected T cell line. *Retrovirology*, 6(1), 1–16. article. <https://doi.org/10.1186/1742-4690-6-28>
- Guo, J., Wu, J., Ji, Q., Wang, C., Luo, L., Yuan, Y., ... Wang, J. (2008). Genome-wide analysis of heat shock transcription factor families in rice and Arabidopsis. *Journal of Genetics and Genomics*, 35(2), 105–118. article. [https://doi.org/http://dx.doi.org/10.1016/S1673-8527\(08\)60016-8](https://doi.org/http://dx.doi.org/10.1016/S1673-8527(08)60016-8)
- Gustafson-Brown, C., Savidge, B., & Yanofsky, M. F. (2016). Regulation of the arabidopsis floral homeotic gene *APETALA1*. *Cell*, 76(1), 131–143. JOUR. [https://doi.org/10.1016/0092-8674\(94\)90178-3](https://doi.org/10.1016/0092-8674(94)90178-3)
- Hahn, A., Bublak, D., Schleiff, E., & Scharf, K.-D. (2011). Crosstalk between Hsp90 and Hsp70 chaperones and heat stress transcription factors in tomato. *The Plant Cell*, 23(2), 741–55. <https://doi.org/10.1105/tpc.110.076018>
- Heerklotz, D., Döring, P., Bonzelius, F., Winkelhaus, S., & Do, P. (2001). The Balance of Nuclear Import and Export Determines the Intracellular Distribution and Function of Tomato Heat Stress Transcription Factor HsfA2 The Balance of Nuclear Import and Export Determines the Intracellular Distribution and Function of Tomato Heat. *Molecular and Cellular Biology*, 21(5), 1759–1768. <https://doi.org/10.1128/MCB.21.5.1759>
- Henrissat, B., Coutinho, P. M., & Davies, G. J. (2001). A census of carbohydrate-active enzymes in the genome of *Arabidopsis thaliana*. *Plant Molecular*

Biology, 47(1–2), 55–72.

- Hobson, G. E. (1968). Cellulase Activity during the Maturation and Ripening of Tomato Fruit.
- Hua, J., & Meyerowitz, E. M. (1998). Ethylene responses are negatively regulated by a receptor gene family in *Arabidopsis thaliana*. *Cell*, 94(2), 261–271. [https://doi.org/10.1016/S0092-8674\(00\)81425-7](https://doi.org/10.1016/S0092-8674(00)81425-7)
- Jégou, A., Ziyyat, A., Barraud-Lange, V., Perez, E., Wolf, J. P., Pincet, F., & Gourier, C. (2011). CD9 tetraspanin generates fusion competent sites on the egg membrane for mammalian fertilization. *Proceedings of the National Academy of Sciences of the United States of America*, 108(27), 10946–51. <https://doi.org/10.1073/pnas.1017400108>
- Jiménez-Bermúdez, S., Redondo-Nevado, J., Muñoz-Blanco, J., Caballero, J. L., López-Aranda, J. M., Valpuesta, V., ... Mercado, J. A. (2002). Manipulation of strawberry fruit softening by antisense expression of a pectate lyase gene. *Plant Physiology*, 128(2), 751–759. <https://doi.org/10.1104/pp.010671>
- Jolie, R. P., Duvetter, T., Van Loey, A. M., & Hendrickx, M. E. (2010). Pectin methylesterase and its proteinaceous inhibitor: a review. *Carbohydrate Research*, 345(18), 2583–95. <https://doi.org/10.1016/j.carres.2010.10.002>
- Kanehisa, M. (1996). (KEGG) Toward pathway engineering: A new database of genetic and molecular pathways. *Science & Technology Japan*, 59, 34–38.
- Kevany, B. M., Tieman, D. M., Taylor, M. G., Cin, V. D., & Klee, H. J. (2007). Ethylene receptor degradation controls the timing of ripening in tomato fruit. *Plant Journal*, 51(3), 458–467. <https://doi.org/10.1111/j.1365-3113X.2007.03170.x>
- Khaw, K., & Barrett-Connor, E. (1987). DIETARY FIBER AND REDUCED ISCREMIC HEART DISEASE MORTALITY RATES IT MEN AND WOMEN: A 12-YEAR PROSPECTIVE STUDY. *American Journal of Epidemiology*, 92093, 1093–1102.
- Klee, H. J., & Giovannoni, J. J. (2011). Genetics and control of tomato fruit ripening and quality attributes. *Annual Review of Genetics*, 45, 41–59. <https://doi.org/10.1146/annurev-genet-110410-132507>
- Kramer, M., Sanders, R., Bolkan, H., Waters, C., Sheeny, R. E., & Hiatt, W. R. (1992). Postharvest evaluation of transgenic tomatoes with reduced levels of polygalacturonase: processing, firmness and disease resistance. *Postharvest Biology and Technology*, 1(3), 241–255. article. [https://doi.org/http://dx.doi.org/10.1016/0925-5214\(92\)90007-C](https://doi.org/http://dx.doi.org/10.1016/0925-5214(92)90007-C)
- Larsson, S. C., Bergkvist, L., & Wolk, A. (2009). Glycemic load, glycemic index and breast cancer risk in a prospective cohort of Swedish women.

International Journal of Cancer. Journal International Du Cancer, 125(1), 153–7. <https://doi.org/10.1002/ijc.24310>

- Lelièvre, J.-M., Latchè, A., Jones, B., Bouzayen, M., & Pech, J.-C. (1997). Ethylene and fruit ripening. *Physiologia Plantarum*, 101(4), 727–739. article. <https://doi.org/10.1111/j.1399-3054.1997.tb01057.x>
- Levin, J. Z., Berger, M. F., Adiconis, X., Rogov, P., Melnikov, A., Fennell, T., ... Gnirke, A. (2009). Targeted next-generation sequencing of a cancer transcriptome enhances detection of sequence variants and novel fusion transcripts. *Genome Biol*, 10(10), R115. <https://doi.org/10.1186/gb-2009-10-10-r115>
- Li, J. B., Levanon, E. Y., Yoon, J.-K., Aach, J., Xie, B., LeProust, E., ... Church, G. M. (2009). Genome-Wide Identification of Human RNA Editing Sites by Parallel DNA Capturing and Sequencing. *Science*, 324(5931), 1210–1213. article. <https://doi.org/10.1126/science.1170995>
- Lin, Z., Arciga-Reyes, L., Zhong, S., Alexander, L., Hackett, R., Wilson, I., & Grierson, D. (2008). SITPR1, a tomato tetratricopeptide repeat protein, interacts with the ethylene receptors NR and LeETR1, modulating ethylene and auxin responses and development. *Journal of Experimental Botany*, 59(15), 4271–87. <https://doi.org/10.1093/jxb/ern276>
- Lippman, Z., & Tanksley, S. D. (2001). Dissecting the genetic pathway to extreme fruit size in tomato using a cross between the small-fruited wild species *Lycopersicon pimpinellifolium* and *L. esculentum* var. Giant Heirloom. *Genetics*, 158(1), 413–422.
- Liu, H., & Charny, Y. (2013). Common and distinct functions of Arabidopsis class A1 and A2 heat shock factors in diverse abiotic stress responses and development. *Plant Physiology*, 163(1), 276–290. Journal Article, Research Support, Non-U.S. Gov't. <https://doi.org/10.1104/pp.113.221168>
- Liu, R., How-Kit, A., Stammitti, L., Teyssier, E., Rolin, D., Mortain-Bertrand, A., ... Gallusci, P. (2015). A DEMETER-like DNA demethylase governs tomato fruit ripening. *Proceedings of the National Academy of Sciences of the United States of America*, 112(34), 10804–9. <https://doi.org/10.1073/pnas.1503362112>
- Ljung, K., Bhalerao, R. P., & Sandberg, G. (2001). Sites and homeostatic control of auxin biosynthesis in Arabidopsis during vegetative growth. *Plant Journal*, 28(4), 465–474. <https://doi.org/10.1046/j.1365-313X.2001.01173.x>
- Lord, E. M., & Russell, S. D. (2002). The mechanisms of pollination and fertilization in plants. *Annual Review of Cell and Developmental Biology*, 18, 81–105. <https://doi.org/10.1146/annurev.cellbio.18.012502.083438>

- Manning, K., Tör, M., Poole, M., Hong, Y., Thompson, A. J., King, G. J., ... Seymour, G. B. (2006). A naturally occurring epigenetic mutation in a gene encoding an SBP-box transcription factor inhibits tomato fruit ripening. *Nature Genetics*, 38(8), 948–52. <https://doi.org/10.1038/ng1841>
- Martel, C., Vrebalov, J., Tafelmeyer, P., & Giovannoni, J. J. (2011). The tomato MADS-box transcription factor RIPENING INHIBITOR interacts with promoters involved in numerous ripening processes in a COLORLESS NONRIPENING-dependent manner. *Plant Physiology*, 157(3), 1568–79. <https://doi.org/10.1104/pp.111.181107>
- Masciopinto, F., Campagnoli, S., Abrignani, S., Uematsu, Y., & Pileri, P. (2001). The small extracellular loop of CD81 is necessary for optimal surface expression of the large loop, a putative HCV receptor. *Virus Research*, 80(1–2), 1–10.
- Matas, A. J., Yeats, T. H., Buda, G. J., Zheng, Y., Chatterjee, S., Tohge, T., ... Rose, J. K. C. (2011). Tissue- and cell-type specific transcriptome profiling of expanding tomato fruit provides insights into metabolic and regulatory specialization and cuticle formation. *The Plant Cell*, 23(11), 3893–910. <https://doi.org/10.1105/tpc.111.091173>
- McCormick, S. (1997). Transformation of tomato with *Agrobacterium tumefaciens*. In K. Lindsey (Ed.), *Plant Tissue Culture Manual: Supplement 7* (pp. 311–319). inbook, Dordrecht: Springer Netherlands. https://doi.org/10.1007/978-94-009-0103-2_17
- McCormick, S., Niedermeyer, J., Fry, J., Barnason, A., Horsch, R., & Fraley, R. (1986). Leaf disc transformation of cultivated tomato (*L. esculentum*) using *Agrobacterium tumefaciens*. *Plant Cell Reports*, 5(2), 81–84. article. <https://doi.org/10.1007/BF00269239>
- Meyer, K. a, Kushi, L. H., Jacobs, D. R., Slavin, J., Sellers, T. a, & Folsom, a R. (2000). Carbohydrates, dietary fiber, and incident type 2 diabetes in older women. *The American Journal of Clinical Nutrition*, 71(4), 921–30.
- Minic, Z., & Jouanin, L. (2006). Plant glycoside hydrolases involved in cell wall polysaccharide degradation. *Plant Physiology and Biochemistry : PPB / Société Française de Physiologie Végétale*, 44(7–9), 435–49. <https://doi.org/10.1016/j.plaphy.2006.08.001>
- Mishra, S. K., Tripp, J., Winkelhaus, S., Tschiersch, B., Theres, K., Nover, L., & Scharf, K. D. (2002). In the complex family of heat stress transcription factors, HsfA1 has a unique role as master regulator of thermotolerance in tomato. *Genes and Development*, 16(12), 1555–1567. <https://doi.org/10.1101/gad.228802>
- Morris, C. a, Owen, J. R., Thomas, M. C., El-Hiti, G. a, Harwood, J. L., & Kille, P. (2014). Intracellular localization and induction of a dynamic RNA-editing event of macro-algal V-ATPase subunit A (VHA-A) in response to copper.

Plant, Cell & Environment, 37(1), 189–203.
<https://doi.org/10.1111/pce.12145>

- Muñoz-Bertomeu, J., Miedes, E., & Lorences, E. P. (2013). Expression of xyloglucan endotransglucosylase/hydrolase (XTH) genes and XET activity in ethylene treated apple and tomato fruits. *Journal of Plant Physiology*, 170(13), 1194–1201. <https://doi.org/10.1016/j.jplph.2013.03.015>
- Neta-Sharir, I., Isaacson, T., Lurie, S., & Weiss, D. (2005). Dual role for tomato heat shock protein 21: protecting photosystem II from oxidative stress and promoting color changes during fruit maturation. *The Plant Cell*, 17(6), 1829–38. <https://doi.org/10.1105/tpc.105.031914>
- Olmos, E., Reiss, B., & Dekker, K. (2003). The ekeko mutant demonstrates a role for tetraspanin-like protein in plant development. *Biochemical and Biophysical Research Communications*, 310(4), 1054–1061. <https://doi.org/10.1016/j.bbrc.2003.09.122>
- Ozsolak, F., & Milos, P. M. (2011). RNA sequencing: advances, challenges and opportunities. *Nature Reviews. Genetics*, 12(2), 87–98. <https://doi.org/10.1038/nrg2934>
- Paran, I., & Van Der Knaap, E. (2007). Genetic and molecular regulation of fruit and plant domestication traits in tomato and pepper. *Journal of Experimental Botany*, 58(14), 3841–3852. <https://doi.org/10.1093/jxb/erm257>
- Park, S., Fung, P., Nishimura, N., Jensen, D. R., Fujii, H., Zhao, Y., ... Cutler, S. R. (2014). Absciscic Acid Inhibits Type 2C. *Science*, 324(May), 1068–1069. <https://doi.org/10.1126/science.1173041>
- Pecker, I., Gabbay, R., Cunningham, F. X., & Hirschberg, J. (1996). Cloning and characterization of the cDNA for lycopene β -cyclase from tomato reveals decrease in its expression during fruit ripening. *Plant Molecular Biology*, 30(4), 807–819. article. <https://doi.org/10.1007/BF00019013>
- Péret, B., Li, G., Zhao, J., Band, L. R., Voß, U., Postaire, O., ... Bennett, M. J. (2012). Auxin regulates aquaporin function to facilitate lateral root emergence. *Nature Cell Biology*, 14(10), 991–8. <https://doi.org/10.1038/ncb2573>
- Pien, S., Wyrzykowska, J., McQueen-Mason, S., Smart, C., & Fleming, a. (2001). Local expression of expansin induces the entire process of leaf development and modifies leaf shape. *Proceedings of the National Academy of Sciences of the United States of America*, 98(20), 11812–7. <https://doi.org/10.1073/pnas.191380498>
- Pique, C., Lagaudrière-Gesbert, C., Delamarre, L., Rosenberg, A. R., Conjeaud, H., & Dokh  lar, M.-C. (2000). Interaction of CD82 Tetraspanin Proteins with HTLV-1 Envelope Glycoproteins Inhibits Cell-to-Cell Fusion and Virus

Transmission. *Virology*, 276(2), 455–465. article.
<https://doi.org/http://dx.doi.org/10.1006/viro.2000.0538>

- Potuschak, T., Lechner, E., Parmentier, Y., Yanagisawa, S., Grava, S., Koncz, C., & Genschik, P. (2003). EIN3-dependent regulation of plant ethylene hormone signaling by two arabidopsis F box proteins: EBF1 and EBF2. *Cell*, 115(6), 679–689. Journal Article, Research Support, Non-U.S. Gov't.
- Proseus, T. E., & Boyer, J. S. (2005). Turgor pressure moves polysaccharides into growing cell walls of *Chara corallina*. *Annals of Botany*, 95(6), 967–79. <https://doi.org/10.1093/aob/mci113>
- Ramakrishna, W., Deng, Z., Ding, C., Handa, A. K., & Ozminkowski, R. H. J. (2003). A Novel Small Heat Shock Protein Gene, vis1, Contributes to Pectin Depolymerization and Juice Viscosity in Tomato Fruit. *Plant Physiology*, 131(February), 725–735. <https://doi.org/10.1104/pp.012401.depolymerization>
- Richardson, C., & Hobson, G. E. (1987). Compositional changes in normal and mutant tomato fruit during ripening and storage. *Journal of the Science of Food and Agriculture*, 40(3), 245–252. <https://doi.org/10.1002/jsfa.2740400307>
- Richter, K., & Buchner, J. (2001). Hsp90: chaperoning signal transduction. *Journal of Cellular Physiology*, 188(3), 281–90. <https://doi.org/10.1002/jcp.1131>
- Rose, J. K. C., Labavitch, J. M., & Vicente, A. R. (2007). The linkage between cell wall metabolism and fruit softening : looking to the future. *Journal of the Science of Food and Agriculture*, 87(August 2006), 1435–1448. <https://doi.org/10.1002/jsfa>
- Rose, J. K., Lee, H. H., & Bennett, a B. (1997). Expression of a divergent expansin gene is fruit-specific and ripening-regulated. *Proceedings of the National Academy of Sciences of the United States of America*, 94(11), 5955–60.
- Rubinstein, E. (2011). The complexity of tetraspanins. *Biochemical Society Transactions*, 39(2), 501–5. <https://doi.org/10.1042/BST0390501>
- Sakamoto, H., Maruyama, K., Sakuma, Y., Meshi, T., & Iwabuchi, M. (2004). Arabidopsis Cys2 / His2-Type Zinc-Finger Proteins Function as Transcription Repressors under Drought. *Society*, 136(September), 2734–2746. <https://doi.org/10.1104/pp.104.046599.2734>
- Scharf, K. D., Berberich, T., Ebersberger, I., & Nover, L. (2012). The plant heat stress transcription factor (Hsf) family: structure, function and evolution. *Biochim Biophys Acta*, 1819(2), 104–119. <https://doi.org/10.1016/j.bbagr.2011.10.002>
- Scharf, K. D., Rose, S., Zott, W., Schöff, F., & Nover, L. (1990). Three tomato

genes code for heat stress transcription factors with a region of remarkable homology to the DNA-binding domain of the yeast HSF. *The EMBO Journal*, 9(13), 4495–4501.

- Scutt, C. (2006). An evolutionary perspective on the regulation of carpel development. *Journal of Experimental Botany*, 57(2000), 2143–2152. <https://doi.org/10.1093/jxb/erj188>
- Seigneuret, M. (2006). Complete predicted three-dimensional structure of the facilitator transmembrane protein and hepatitis C virus receptor CD81: conserved and variable structural domains in the tetraspanin superfamily. *Biophysical Journal*, 90(1), 212–27. <https://doi.org/10.1529/biophysj.105.069666>
- Serrani, J. C., Ruiz-Rivero, O., Fos, M., & García-Martínez, J. L. (2008). Auxin-induced fruit-set in tomato is mediated in part by gibberellins. *The Plant Journal : For Cell and Molecular Biology*, 56(6), 922–34. <https://doi.org/10.1111/j.1365-313X.2008.03654.x>
- Seymour, G. B., Chapman, N. H., Chew, B. L., & Rose, J. K. C. (2013). Regulation of ripening and opportunities for control in tomato and other fruits. *Plant Biotechnology Journal*, 11(3), 269–78. <https://doi.org/10.1111/j.1467-7652.2012.00738.x>
- Seymour, G. B., Ostergaard, L., Chapman, N. H., Knapp, S., & Martin, C. (2013). Fruit development and ripening. *Annual Review of Plant Biology*, 64, 219–41. <https://doi.org/10.1146/annurev-arplant-050312-120057>
- Shanmukhappa, K., Kim, J. K., & Kapil, S. (2007). Role of CD151, A tetraspanin, in porcine reproductive and respiratory syndrome virus infection. *Virology Journal*, 4, 62. <https://doi.org/10.1186/1743-422X-4-62>
- Sheehy, R. E., Kramer, M., & Hiatt, W. R. (1988). Reduction of polygalacturonase activity in tomato fruit by antisense RNA. *Proceedings of the National Academy of Sciences of the United States of America*, 85(23), 8805–9.
- Shin, W.-H., Park, S.-J., & Kim, E.-J. (2006). Protective effect of anthocyanins in middle cerebral artery occlusion and reperfusion model of cerebral ischemia in rats. *Life Sciences*, 79(2), 130–7. <https://doi.org/10.1016/j.lfs.2005.12.033>
- Shulaev, V., Schlauch, K., & Mittler, R. (2005). Cytosolic Ascorbate Peroxidase 1 Is a Central Component of the Reactive Oxygen Gene Network of Arabidopsis, 17(January), 268–281. <https://doi.org/10.1105/tpc.104.026971.1>
- Sinesio, F., Cammareri, M., Moneta, E., Navez, B., Peparaio, M., Causse, M., & Grandillo, S. (2010). Sensory quality of fresh French and Dutch market

tomatoes: a preference mapping study with Italian consumers. *Journal of Food Science*, 75(1), S55-67. <https://doi.org/10.1111/j.1750-3841.2009.01424.x>

- Smith, C. J., Watson, C. F., Ray, J., Bird, C. R., Morris, P. C., Schuch, W., & Grierson, D. (1988). Antisense RNA inhibition of polygalacturonase gene expression in transgenic tomatoes. *Nature*, 334, 724–726.
- Solano, R., & Stepanova, A. (1998). Nuclear events in ethylene signaling: a transcriptional cascade mediated by ETHYLENE-INSENSITIVE3 and ETHYLENE-RESPONSE-FACTOR1. *Genes & Development*, 12(1), 3703–3714.
- Somerville, C., Bauer, S., Brininstool, G., Facette, M., Hamann, T., Milne, J., ... Youngs, H. (2004). Toward a systems approach to understanding plant cell walls. *Science (New York, N.Y.)*, 306(5705), 2206–11. <https://doi.org/10.1126/science.1102765>
- Spoden, G., Freitag, K., Husmann, M., Boller, K., Sapp, M., Lambert, C., & Florin, L. (2008). Clathrin- and caveolin-independent entry of human papillomavirus type 16 - Involvement of tetraspanin-enriched microdomains (TEMs). *PLoS ONE*, 3(10). <https://doi.org/10.1371/journal.pone.0003313>
- Sprunck, S., & Dresselhaus, T. (2009). Gamete interactions during double fertilization in flowering plants. *Zellbiologie Aktuell*, (3), 22–27.
- Stipp, C. S., Kolesnikova, T. V., & Hemler, M. E. (2003). Functional domains in tetraspanin proteins. *Trends in Biochemical Sciences*, 28(2), 106–12. [https://doi.org/10.1016/S0968-0004\(02\)00014-2](https://doi.org/10.1016/S0968-0004(02)00014-2)
- Sugio, A., Dreos, R., Aparicio, F., & Maule, A. J. (2009). The cytosolic protein response as a subcomponent of the wider heat shock response in Arabidopsis. *The Plant Cell*, 21(2), 642–654. Journal Article, Research Support, Non-U.S. Gov't. <https://doi.org/10.1105/tpc.108.062596>
- Sun, H. J., Uchii, S., Watanabe, S., & Ezura, H. (2006). A highly efficient transformation protocol for Micro-Tom, a model cultivar for tomato functional genomics. *Plant and Cell Physiology*, 47(3), 426–431. <https://doi.org/10.1093/pcp/pci251>
- Sun, W., Bernard, C., van de Cotte, B., Van Montagu, M., & Verbruggen, N. (2001). At-HSP17.6A, encoding a small heat-shock protein in Arabidopsis, can enhance osmotolerance upon overexpression. *The Plant Journal : For Cell and Molecular Biology*, 27(5), 407–15.
- Szymkowiak, E. J., & Irish, E. E. (1999). Interactions between jointless and wild-type tomato tissues during development of the pedicel abscission zone and the inflorescence meristem. *The Plant Cell*, 11(2), 159–75. <https://doi.org/10.1105/tpc.11.2.159>

- Tanksley, S. D. (2009). The Genetic , Developmental , and Molecular Bases of Fruit Size in Tomato and Shape Variation. *The Plant Cell*, 16(Supplement 2004), 181–190. <https://doi.org/10.1105/tpc.018119.S182>
- Tham, T. N., Gouin, E., Rubinstein, E., Boucheix, C., Cossart, P., & Pizarro-Cerda, J. (2010). Tetraspanin CD81 is required for *Listeria monocytogenes* invasion. *Infection and Immunity*, 78(1), 204–209. <https://doi.org/10.1128/IAI.00661-09>
- The Tomato Genome Consortium. (2012). The tomato genome sequence provides insights into fleshy fruit evolution. *Nature*, 485(7400), 635–41. <https://doi.org/10.1038/nature11119>
- Thom, E. (2007). The Effect of Chlorogenic Acid Enriched Coffee on Glucose Absorption in Healthy Volunteers and Its Effect on Body Mass When Used Long-term in Overweight and Obese People. *Journal of International Medical Research*, 35(6), 900–908. <https://doi.org/10.1177/147323000703500620>
- Tieman, D. M., Harriman, R. W., Ramamohan, G., & Handa, A. K. (1992). An Antisense Pectin Methylesterase Gene Alters Pectin Chemistry and Soluble Solids in Tomato Fruit. *The Plant Cell*, 4(6), 667–679. <https://doi.org/10.1105/tpc.4.6.667>
- Tieman, D. M., Taylor, M. G., Ciardi, J. a, & Klee, H. J. (2000). The tomato ethylene receptors NR and LeETR4 are negative regulators of ethylene response and exhibit functional compensation within a multigene family. *Proceedings of the National Academy of Sciences of the United States of America*, 97(10), 5663–8. <https://doi.org/10.1073/pnas.090550597>
- Todd, C., & Maecker, T. (1997). The tetraspanin facilitators. *The Journal of the Federation of American Societies for Experimental Biology*, 11, 428–22.
- Toufighi, K., Brady, S. M., Austin, R., Ly, E., & Provart, N. J. (2005). The Botany Array Resource: e-Northern, Expression Angling, and promoter analyses. *The Plant Journal : For Cell and Molecular Biology*, 43(1), 153–163. Journal Article, Research Support, Non-U.S. Gov't. <https://doi.org/10.1111/j.1365-313X.2005.02437.x>
- Tsuda, T., Horio, F., Uchida, K., Aoki, H., & Osawa, T. (2003). Nutrient-Gene Interactions Dietary Cyanidin 3- O - α - D -Glucoside-Rich Purple Corn Color Prevents Obesity and Ameliorates Hyperglycemia in Mice. *Nutrient-Gene Interactions*, 133(May), 2125–2130.
- U.S. Dept. of Agriculture, National Agricultural Statistics Service, V. S. (2009). *U.S. Tomato Statistics*.
- Ulusik, S., Chapman, N. H., Smith, R., Poole, M., Adams, G., Gillis, R. B., ... Seymour, G. B. (2016). Genetic improvement of tomato by targeted control of fruit softening. *Nature Biotechnology*, (November).

<https://doi.org/10.1038/nbt.3602>

- van der Knaap, E., & Tanksley, D. S. (2001). Identification and characterization of a novel locus controlling early fruit development in tomato. *Theoretical and Applied Genetics*, 103(2), 353–358. article.
<https://doi.org/10.1007/s001220100623>
- van der Knaap, E., & Tanksley, S. D. (2003). The making of a bell pepper-shaped tomato fruit: identification of loci controlling fruit morphology in Yellow Stuffer tomato. *TAG. Theoretical and Applied Genetics. Theoretische Und Angewandte Genetik*, 107, 139–147. <https://doi.org/10.1007/s00122-003-1224-1>
- van Spriel, A. B., & Figdor, C. G. (2010a). The role of tetraspanins in the pathogenesis of infectious diseases. *Microbes and Infection*, 12(2), 106–112. <https://doi.org/10.1016/j.micinf.2009.11.001>
- van Spriel, A. B., & Figdor, C. G. (2010b). The role of tetraspanins in the pathogenesis of infectious diseases. *Microbes and Infection / Institut Pasteur*, 12(2), 106–12. <https://doi.org/10.1016/j.micinf.2009.11.001>
- Vincent, H., Wiersema, J., Kell, S., Fielder, H., Dobbie, S., Castañeda-Álvarez, N. P., ... Maxted, N. (2013). A prioritized crop wild relative inventory to help underpin global food security. *Biological Conservation*, 167, 265–275. <https://doi.org/10.1016/j.biocon.2013.08.011>
- Vincken, J.-P., Schols, H. a, Oomen, R. J. F. J., McCann, M. C., Ulvskov, P., Voragen, A. G. J., & Visser, R. G. F. (2003). If homogalacturonan were a side chain of rhamnogalacturonan I. Implications for cell wall architecture. *Plant Physiology*, 132(4), 1781–9. <https://doi.org/10.1104/pp.103.022350.in>
- Voß, U., Wilson, M. H., Kenobi, K., Gould, P. D., Robertson, F. C., Peer, W. a., ... Bennett, M. J. (2015). The circadian clock rephases during lateral root organ initiation in *Arabidopsis thaliana*. *Nature Communications*, 6(May), 7641. <https://doi.org/10.1038/ncomms8641>
- Vrebalov, J. (2002). A MADS-Box Gene Necessary for Fruit Ripening at the Tomato Ripening-Inhibitor (Rin) Locus. *Science*, 296(5566), 343–346. <https://doi.org/10.1126/science.1068181>
- Wang, F., Muto, A., Van de Velde, J., Neyt, P., Himanen, K., Vandepoele, K., & Van Lijsebettens, M. (2015). Functional Analysis of Arabidopsis TETRASPANIN Gene Family in Plant Growth and Development. *Plant Physiology*, 169(November), pp.01310.2015. <https://doi.org/10.1104/pp.15.01310>
- Wang, F., Vandepoele, K., & Van Lijsebettens, M. (2012). Tetraspanin genes in plants. *Plant Science : An International Journal of Experimental Plant Biology*, 190, 9–15. <https://doi.org/10.1016/j.plantsci.2012.03.005>

- Wang, H.-X., Kolesnikova, T. V., Denison, C., Gygi, S. P., & Hemler, M. E. (2011). The C-terminal tail of tetraspanin protein CD9 contributes to its function and molecular organization. *Journal of Cell Science*, 124(Pt 16), 2702–10. <https://doi.org/10.1242/jcs.085449>
- Wang, W., Vinocur, B., & Altman, A. (2003). Plant responses to drought, salinity and extreme temperatures: towards genetic engineering for stress tolerance. *Planta*, 218(1), 1–14. <https://doi.org/10.1007/s00425-003-1105-5>
- Wang, W., Vinocur, B., Shoseyov, O., & Altman, A. (2004). Role of plant heat-shock proteins and molecular chaperones in the abiotic stress response. *Trends in Plant Science*, 9(5), 244–52. <https://doi.org/10.1016/j.tplants.2004.03.006>
- Weingartner, M., Subert, C., & Sauer, N. (2011). LATE, a C²H₂ zinc-finger protein that acts as floral repressor. *Plant Journal*, 68(4), 681–692. <https://doi.org/10.1111/j.1365-313X.2011.04717.x>
- Welch, D., Hassan, H., Blilou, I., Immink, R., Heidstra, R., & Scheres, B. (2007). Arabidopsis JACKDAW and MAGPIE zinc finger proteins delimit asymmetric cell division and stabilize tissue boundaries by restricting SHORT-ROOT action. *Genes and Development*, 21(17), 2196–2204. <https://doi.org/10.1101/gad.440307>
- Weng, L., Zhao, F., Li, R., Xu, C., Chen, K., & Xiao, H. (2015). The zinc finger transcription factor SlZFP2 negatively regulates abscisic acid biosynthesis and fruit ripening in tomato. *Plant Physiology*, 167(3), 931–49. <https://doi.org/10.1104/pp.114.255174>
- Wilkinson, J. Q., Lanahan, M. B., Clark, D. G., Bleecker, a B., Chang, C., Meyerowitz, E. M., & Klee, H. J. (1997). A dominant mutant receptor from Arabidopsis confers ethylene insensitivity in heterologous plants. *Nature Biotechnology*, 15, 444–447. <https://doi.org/10.1038/nbt0597-444>
- Willats, W. G., McCartney, L., Mackie, W., & Knox, J. P. (2001). Pectin: cell biology and prospects for functional analysis. *Plant Molecular Biology*, 47(1–2), 9–27.
- Willett, B., Hosie, M., Shaw, A., & Neil, J. (1997). Inhibition of feline immunodeficiency virus infection by CD9 antibody operates after virus entry and is independent of virus tropism. *Journal of General Virology*, 78(3), 611–618.
- Winter, D., Vinegar, B., Nahal, H., Ammar, R., Wilson, G. V., & Provart, N. J. (2007). An “Electronic Fluorescent Pictograph” browser for exploring and analyzing large-scale biological data sets. *PloS One*, 2(8), e718. <https://doi.org/10.1371/journal.pone.0000718>
- World Cancer Res. Fund (WCRF), A. I. C. R. (AICR). (2007). Food, Nutrition,

Physical Activity, and the Prevention of Cancer: a Global Perspective.
WCRF/AICR, Washington, DC.

- Wyrzykowska, J., Pien, S., Shen, W. H., & Fleming, A. J. (2002). Manipulation of leaf shape by modulation of cell division. *Development*, 129(4), 957–964.
- Xiao, H., Radovich, C., Welty, N., Hsu, J., Li, D., Meulia, T., & van der Knaap, E. (2009). Integration of tomato reproductive developmental landmarks and expression profiles, and the effect of SUN on fruit shape. *BMC Plant Biology*, 9, 49. <https://doi.org/10.1186/1471-2229-9-49>
- Yang, S., & Hoffman, N. (1984). Ethylene biosynthesis and its regulation in higher plants. *Annual Review of Plant Physiology*, 35(132), 155–189.
- Yang, X., Zhu, W., Zhang, H., Liu, N., & Tian, S. (2016). Heat shock factors in tomatoes: genome-wide identification, phylogenetic analysis and expression profiling under development and heat stress. *PeerJ*, 4, e1961. <https://doi.org/10.7717/peerj.1961>
- Yang, Y., Wu, Y., Pirrello, J., Regad, F., Bouzayen, M., Deng, W., & Li, Z. (2010). Silencing Sl-EBF1 and Sl-EBF2 expression causes constitutive ethylene response phenotype, accelerated plant senescence, and fruit ripening in tomato. *Journal of Experimental Botany*, 61(3), 697–708. <https://doi.org/10.1093/jxb/erp332>
- Yang, Z., Wang, Y., Gao, Y., Zhou, Y., Zhang, E., Hu, Y., ... Xu, C. (2014). Adaptive evolution and divergent expression of heat stress transcription factors in grasses. *BMC Evolutionary Biology*, 14(1), 147. <https://doi.org/10.1186/1471-2148-14-147>
- Zhang, K., Li, J. B., Gao, Y., Egli, D., Xie, B., Deng, J., ... Church, G. M. (2009). Digital RNA allelotyping reveals tissue-specific and allele-specific gene expression in human. *Nature Methods*, 6(8), 613–618. Journal Article, Research Support, N.I.H., Extramural, Research Support, Non-U.S. Gov't. <https://doi.org/10.1038/nmeth.1357>
- Zhou, Z., Sun, L., Zhao, Y., An, L., Yan, A., Meng, X., & Gan, Y. (2013). Zinc Finger Protein 6 (ZFP6) regulates trichome initiation by integrating gibberellin and cytokinin signaling in *Arabidopsis thaliana*. *New Phytologist*, 198(3), 699–708. <https://doi.org/10.1111/nph.12211>
- Zhu, H., Zhu, B., & Shao, Y. (2006). Tomato fruit development and ripening are altered by the silencing of LeEIN2 gene. *Journal of Integrative Plant Biology*, 48(12), 1478–1485. <https://doi.org/10.1111/j.1672-9072.2006.00366.x>

Appendices

8.1 Gene Sequences

SITET-6 (Solyc04g049080) cDNA

ATGTATAGATTTAGCAACACAGTAATAGGTTTCTTGAATCTATTCACACTTTTAGCATC
 CATTCCGATCATAGGTGCTGGATTATGGATGGCAAGGAGTAGTACAACATGTGGTG
 GACTTGATGTGCCTGGTAAAGTATATAAAGAGTATCATCTTCAAAATTACTCACCATG
 GTTGAGAAAGAGGATTAAGGATCCTCAATATTGGCTCACTGTTAGAGCTTGTATTTT
 GGGTTCCAAGACTTGTGCTAATGTTATTACTTGGACTCCCTATGATTATCTTACGAAA
 GATTTGACTCCTATTCAGTCAGGATGTTGCAAGCCACCAACAGCATGCAACTATGGA
 TTGACAACAATGACACAAGAGGCAGATTGTTACCAATGGAACAATGATCCAAATTTG
 CTATGCTATGAGTGTGATTTCATGCAAAGCTGGAGTTCTTGAAGATGTGAGAAGGGAT
 TGGCAAAAGATATCAGTTCTTAACATTGTCATGCTTGTCTTACTCATTGGAATTTACTC
 CATTGGTTGTTGTGCTTTTCAAAACACCAAAAGGGCTGTATCTGATTATCCACATGGT
 GAAAACCGTATGTATAAAGTCAGACCGAGATGGGATTTCTACTGGTGGAGATGGTG
 GCATGACAGGAGACATCAGCTTTATTAG

SITET-8 (Solyc07g006280) over-expression cDNA

ATGGTGCGGTGTAGTAACAATTTAGTGGGGATTCTGAATATAGTGACACTTTTGCTG
 TCGATCCCAATTATAGGAGGAGGGATATGGTTGTCAAAACAAGCAAATACAGAGTG
 TGAGAGGTTTCTTGAAAAGCCAGTAATAGCAATAGGTGTTTTATATTGCTTGTTTCA
 TTGGCTGGTATAATTGGATCTTGCTGTAGAGTTACTTGGTTACTTTGGGTTTATCTAC
 TTGTTATGTTTTGTTGATTTTGTTGCTTTTCTGTTTCACAATCTTTGCTTTTGTTGGA
 CTAATAAGGGTGCTGGTGAAACAATTTCTGTAGAGGGTATAAGGAGTATAGATTTG
 GGGATTACTCTAATTGGTTGCAGAAAAGAGTTGATAAGCATTGGAATAGAATTCATA
 GTTGTTTGCAGGATAGTAAGATTTGTGATACTTTGATTCAGGAATCAAATACTAAAGC
 TGATGATTTCTTCAAGAAACATCTATCTGCTCTTCAGTCTGGTTGCTGCAAGCCATCA
 AATGACTGTAACCTCCAGTACGTGAGCCCAACAACTGGACAAGATCATCGACCTCA
 TCCACTACCAATCCAGACTGTGCTACATGGAGCAACGAGTCAAATTTATTGTGCTATG
 GCTGCCAATCCTGCAAAGCTGGGCTGCTAGACAACATCAAAAGTGACTGGAAGAGG
 GTAGCTGTGCTCAACATCATTTTCTCATCTTCTCATCATCGTCTACTCTATCGGATG
 TTGTGCTTTCAGGAACAACCGAGAGGACAATGCTTGGAAGCGTTATCCTTAA

SITET-8 (Solyc07g006280) RNAi cDNA

ACACTCTCTGTTGAGTCTCGACTGCTTTATGTTGCGTATCGTATTAGACTATAGATCA
 CTTAGTATGAGTTTATGCTCTTTCTTGACAGAGTGATTTCTTCTGCTAGACAATTTA
 CTTGTGGCTTTTGGATATATGTGAATTCCTATTATTGAATTCCTTGTTTAGAATTGTCT
 TCTTGATTAGATGGAGTCTTTCATCTACATTTTTTCTGTTGAACAAATTTGTGTTAGA
 TTTGTATGGTGGAGAATTTTGCATTTCTTGATATTTTGTGGGATACACTCGTGTTTGG

TATCTGTATTGAGGTTTGATTAAGTTTAGAAAAATTCATATCTGAGAGTAAAGATGTG
CACTTGTTTGATTGGATAGAGCCTTTCATGGTGGGGACTTTTGCATTCTTGATAAT
TTCTTTTGGTTT

SIHST-14 (Solyc06g053960) cDNA

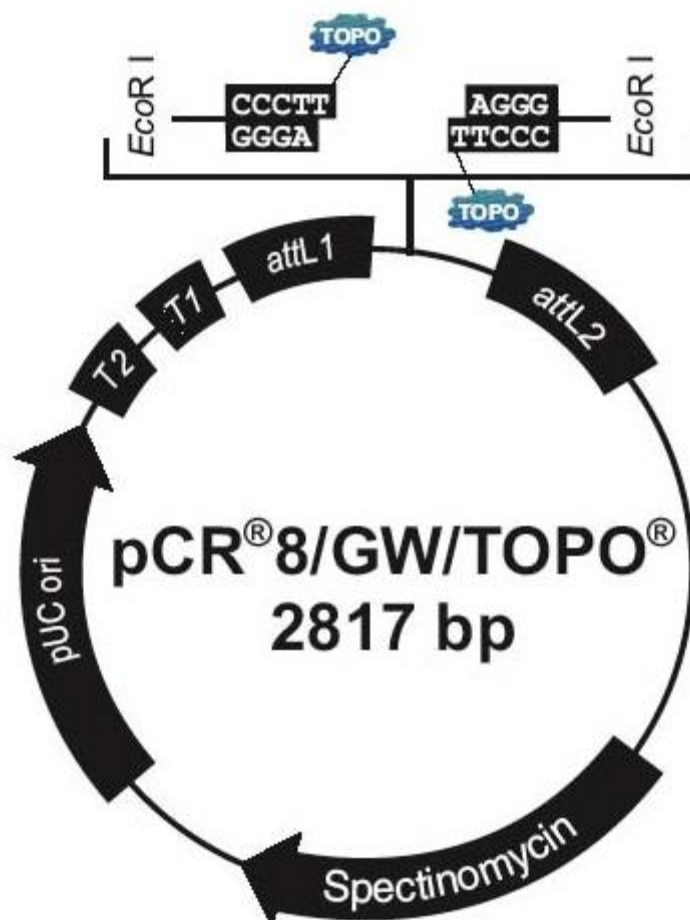
AGTTCTCATTACTCTCTTGCTAATATACCTCCAATATTGCAAACATATTAATTTGTCCTA
ATTCTTTCTCCCTCTTACCCATACTCCAAATTAATTAACCCTATCTTTTCTCATATATC
CACAACTCCTTTATTACCTTTGCCAAGATCCTCTATCTTCTTAACCTTTGACATTGACTC
AAAAATATTGTTATACTCATCTTTGTTGAAGAATCAAAGCATGGATCATTTTGGTAAT
TTAATAAAAGAAGAGTTTGATGGATCATTTTTGACGCCTCAACCGAAGGAGTGTCTT
CATGAGAATGGACCTCCACCATTCTTACAAAAACATATGAACCTTGTGGATGATCCAA
GTAACAACGACGTCGTTTCTTGGAGTAGAGGTTACAATAGTTTCATAGTATGGGATC
CCCAGAATTTGGCCATTAATTTTCTACCAAGGTATTTCAAGCATAACAATTTCTCAAGC
TTTGTGAGGCAGCTCAATACTTATGGATTTAGGAAAGTAAATCCAGACCATTGGGAA
TTTGCTAATGAAGGTTTTCTGAGAGGGGAAAAAGCATCTCTTGAGAACAATAAGGAGA
AGAAAACCAAGTAATTTTCATCAAGTCTTCGTCATCAATTAATAATCAAGCATCAAAAG
GCTACTAAATCACAACTTCAAGCTATGGAGCAAAAGCTTCAAGGGACAGAAATCAAA
CAAGAGCAAATAATGAGTTTTTTGGCTAAAGCATTACATAATCCAAATTTTGTGGAGC
AAATAATGCAACAAAATGATAAAAGGAAACAACCTGAAGAAGCAATGAAGAAGAAG
AGGAGGAGGCCAATTGATTATTATGAAGCTGGTCCTAGTAATATAATTAAGTTAGAA
CCTCAAGATCATGATATTATTA

NPTII cDNA

CCTGAATGAACTGCAGGACGAGGCAGCGCGGCTATCGTGGCTGGCCACGACGGGC
GTTCTTTGCGCAGCTGTGCTCGACGTTGTCACTGAAGCGGGAAGGGACTGGCTGCT
ATTGGGCGAAGTGCCGGGGCAGGATCTCCTGTCATCTCGCCTTGCTCCTGCCGAGAA
AGTATCCATCATGGCTGATGCAATGCGGCGGCTGCATACGCTTGATCCGGCTACCTG
CCCATTCGACCACCAAGCGAAAC

8.2 Plasmid Maps

8.2.1 PCR8/GW/TOPO



Comments for pCR[®]8/GW/TOPO[®] 2817 nucleotides

rrnB T2 transcription termination sequence: bases 268-295

rrnB T1 transcription termination sequence: bases 427-470

M13 forward (-20) priming site: bases 537-552

attL1: bases 569-668

GW1 priming site: bases 607-631

TOPO[®] recognition site 1: bases 678-682

TOPO[®] recognition site 2: bases 683-687

attL2: bases 696-795

GW2 priming site: bases 733-757

T7 Promoter/priming site: 812-831 (c)

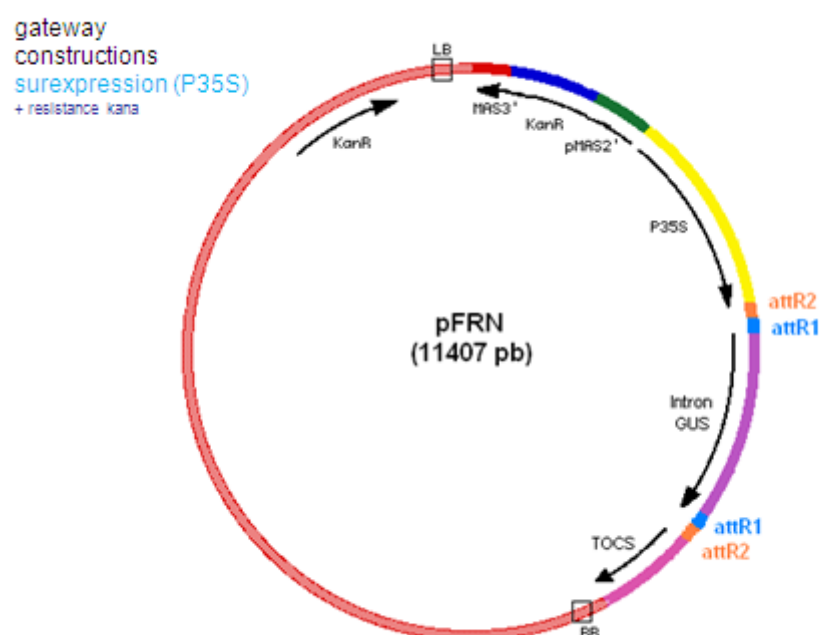
M13 reverse priming site: bases 836-852

Spectinomycin promoter: bases 930-1063

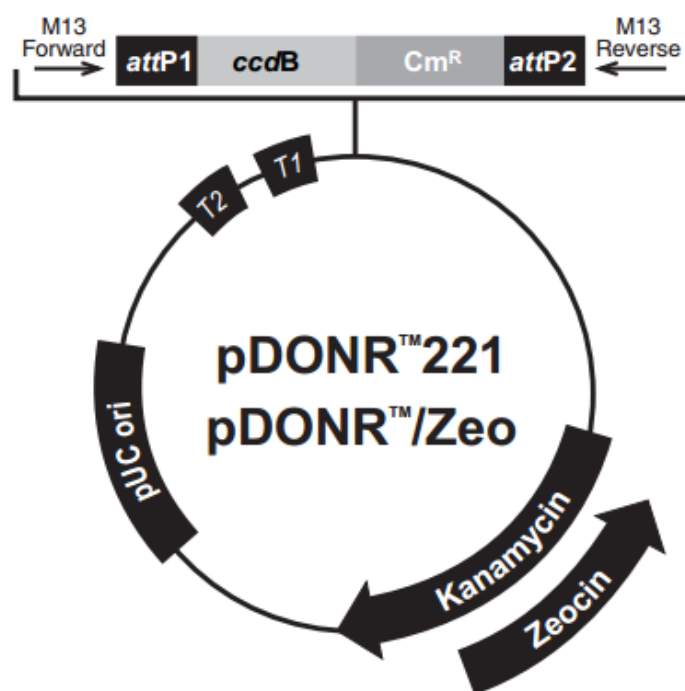
Spectinomycin resistance gene (*Spn^R*): 1064-2074

pUC origin: bases 2141-2814

8.2.2 PFRN Binary Vector



8.2.3 pDONR™221



Comments for:

	pDONR™221 4762 nucleotides	pDONR™/Zeo 4291 nucleotides
<i>rrnB</i> T2 transcription termination sequence (c):	268-295	268-295
<i>rrnB</i> T1 transcription termination sequence (c):	427-470	427-470
M13 Forward (-20) priming site:	537-552	537-552
<i>attP1</i> :	570-801	570-801
<i>ccdB</i> gene (c):	1197-1502	1197-1502
Chloramphenicol resistance gene (c):	1847-2506	1847-2506
<i>attP2</i> (c):	2754-2985	2754-2985
T7 Promoter/priming site (c):	3000-3019	3003-3022
M13 Reverse priming site:	3027-3043	3027-3043
Kanamycin resistance gene:	3156-3965	---
EM7 promoter (c):	---	3486-3552
Zeocin resistance gene (c):	---	3111-3485
pUC origin:	4086-4759	3615-4288

8.3 Media

Contents were dissolved in 1 litre of distilled ionised water. For LB agar*, agar was added to a final concentration of 1.5%. The mixture was then heated to boiling and sterilised by autoclaving at 15 psi, from 121-124°C for 15 minutes.

Table 8.1: Media recipes

Luria Broth Media (LB)		ACB media	
Tryptone	10 g	MS salts	4.4 g/L
Yeast Extract	5 g	Sucrose	30 g/L
NaCl	10 g	B5 Vitamins	
		Kinetin	0.1 mg/L
		NAA	2 mg/L
		pH	5.7
MSR3 media		3C5ZR media	
MS salts	4.4 g/ L	Zeatin	1.75mg/ L
Sucrose	30 g/ L	IAA	0.87 mg/ L
R3 Vitamins	1 ml/ L		
pH	5.9		
Bacto-agar	8 g/ L		
APM media		MS 2-4D media	
Yeast extract	0.5% w/v	MS-salts	4.4 g/ L
Casamino acids	0.05% w/v	Sucrose	30 g/ L
Mannitol	0.8% w/v	KH ₂ PO ₄	0.2 g/ L
(NH ₄) ₂ SO ₄	0.2% w/v	R3 vitamins	1 ml/ L
NaCl	0.5% w/v	Kinetin stock	0.1 mg/ L
		2-4D stock	0.2 mg/ L
		pH	5.7
MS – media		R3 Vitamins	
MS salts	4.4 g/ L	Thiamine	1 g/ L
Sucrose	30 g/ L	Nicotinic acid	0.5 g/ L
pH	5.9	Pyridoxine	0.5 g/ L

8.4 Primer and probe Sequences

Table 8.2: Primer Sequences for PCR Amplification

Primer ID	Sequence 5'-3'
ST_4S_F	GGCGAATTCGACCCAAGTTT
ST_4S_R	GCACCTATGATCGGAATGGA
NPT2_F	TTGGGTGGAGAGGCTATTTCG
NPT2_R	CTTCCCGCTTCAGTGACAAC
RNAi_F4	TGCTTTATGTTGCGTATCGTATT
RNAi_R4	GCTCTATCCAATCAAACAAGTGC
TSP8-F	GGTCTGTGTCGTTTTGCTCA
TSP8-R	AGGATAACGCTTCCAAGCATTGTCCTATCCATACGATGTACCTGATTACGCTTAA
GW1	GTTGCAACAAATTGATGAGCAATGC
GW2	GTTGCAACAAATTGATGAGCAATTA
ST_4S_F	GGCGAATTCGACCCAAGTTT
ST_4S_R	GCACCTATGATCGGAATGGA
NPTIIF	CCTGAATGAACTGCAGGACG
NPTIIR	GTTTCGCTTGGTGGTCGAAT
ELF-1 α F	ACCTTTGCTGAATACCCTCCATTG
ELF-1 α R	CACAGTTCACCTCCCTTCTTCTG
PG-1F	AAGACTTGGCAGGGAGGATC
PG-1R	TATGGCCACCTTTGTTGCAC
PME-1F	CGCAAAGTTGGCTAAGTGGT
PME-1R	TACCCGAACCTCCATCAGC
SlyHSP-09F	ATTCCTTGCCACAAAGCCTG
SlyHSP-09R	GCATCATGTGAAGGTGGCAA

Table 8.3: Probe Sequences for QPCR

Probe ID	Sequence 5'-3'
NPTII061001	GGCTGATGCAATGCGGCGGC
NPTII061002	AGCTGTGCTCGACGTTGTCAC
ELF-1 α P	TCGTTTTGCTGTGAGGGACATGAGGCA
PG-1	TGGACAAGCTAGCAACATCA
PME-1	CATTAGCGATGCTTGCCTCT
SlyHSP-09	ATACTCAGCGAGGATGCCTC

8.5 Phylogenetic protein analysis of *SIHST*Table 8.4: Phylogenetic protein analysis of *SIHST*

Name	Identities	E-Value	Score
Heat stress transcription factor A-6b-like	99.275	1.24E-101	294
Heat stress transcription factor A-6b	70.629	3.88E-65	202
Heat stress transcription factor A-7a isoform X5	68.807	1.57E-53	172
Heat stress transcription factor A-7a isoform X6	68.807	1.64E-53	172
Heat stress transcription factor A-7a isoform X7	68.807	1.67E-53	172
Heat stress transcription factor A-7a isoform X4	68.807	1.79E-53	172
Heat stress transcription factor A-7a isoform X3	68.807	2.54E-53	172
Heat stress transcription factor A-7a isoform X2	68.807	7.18E-53	172
Heat stress transcription factor A-7a isoform X1	68.807	7.33E-53	172
Heat shock factor protein HSF30 isoform X2	58.333	2.15E-50	163
Heat shock factor protein HSF30 isoform X1	58.333	2.67E-50	163
Heat stress transcription factor A-2-like	62.264	4.21E-47	155
Heat shock factor protein HSF8	72.34	3.72E-46	156
Heat stress transcription factor A-1	71.134	7.63E-46	155
Heat stress transcription factor A-1b-like	64.815	1.13E-44	152
Heat stress transcription factor A3	60.36	3.33E-44	151
Heat shock factor protein HSF8-like	54.472	4.03E-43	148
Heat stress transcription factor A-4c-like	69.474	7.99E-43	145
Heat stress transcription factor A-4c	57.377	1.18E-42	145
Heat stress transcription factor B-4	62.617	4.17E-42	142
Heat stress transcription factor A-4a	56.557	6.20E-42	143
Heat shock factor protein HSF24	60.194	1.67E-41	139

8.6 Tomato expression data

Table 8.5: Tomato expression data

Sol. ID	GO: Ontology	Normalized expression (RPKM)						
		1cm fruit	2cm fruit	3cm fruit	MG	BR	BR+5	BR+10
Solyc05g012020	MADS-box TF							
Solyc05g012020	MADS-RIN	0	0.05	0.08	193.195	403.36	207.51	442.955
Solyc06g053960	Heat stress TF A3	7.215	35.32	75.845	120.805	432.195	337.83	227.105
	Zinc finger							
Solyc08g063040	protein	1.96	2.425	2.095	21.93	33.735	42.18	61.325

8.7 RNA-seq

Table 8.6: Differential expression of mutant SIHST and non-mutant line BR+7

Gene	Sol. ID	Control 1	Control 2	Control 3	<i>SIHST-14</i>	<i>SIHST-14</i>	Regulation
Polygalacturonase A	Solyc10g080210.1	285368	289084	275837	48997	60848	DOWN
Pectin methylesterase 1	Solyc07g064170.2						
Chitinase	Solyc10g017970.1	33656	39305	36518	60376	91856	UP
SIHSF-06	Solyc09g065660.2	81	79	63	192	108	UP
SIHSF-09	Solyc12g098520.1	3130	2671	2539	11854	11806	UP
SIHSF-21	Solyc07g055710.2	164	194	131	1766	1206	UP

Table 8.7: Differential expression of mutant *SIHST* and non-mutant line BR+10

Gene	Sol. ID	Control 1	Control 2	<i>SIHST-14 1</i>	<i>SIHST-14 2</i>	<i>SIHST-14 3</i>	Regulation
Polygalacturonase A	Solyc10g080210.1	1396773	361136	8644	8177	9360	DOWN
Pectin methylesterase 1	Solyc07g064170.2	170264	39171	18649	16573	19390	DOWN
Chitinase	Solyc10g017970.1	181246	198576	27915	13843	11518	DOWN
SIHSF-06	Solyc09g065660.2	134	16	789	965	957	UP
SIHSF-09	Solyc12g098520.1	7948	1920	17834	18970	23971	UP
SIHSF-21	Solyc07g055710.2	197	43	1860	2179	2473	UP

Conference Poster

FruitNet

A Novel Gene Correlation Network For Tomato Ripening

Mike Thomas*, Pawel Widars, James Gilbert, Natalie Chapman, Simon Pearce, Neil Graham, Charles Baxter, Graham Seymour, Charlie Hodgman, and Natalio Krasnogor
CPB, School of Biosciences, University of Nottingham, Sutton Bonington, Leics LE12 5RD (MT, N.C., S.P., G.B.S. and C.H.); KDS, School of Computer Science, University of Nottingham, Nottingham, NG8 1BB (PW, J.G. and N.K.); Syngenta, Jealott's Hill International Research Centre, UK (C.B.)

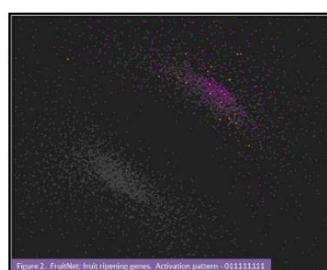
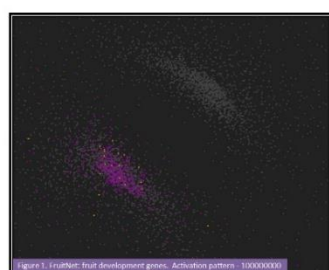


The University of
Nottingham

UNITED KINGDOM · CHINA · MALAYSIA

Introduction

- Fruit ripening is a complex developmental process [2,4] involving the transformation of a seed containing organ into a palatable fruit found to be attractive to seed dispersers and agricultural consumers.
- FruitNet is a novel gene correlation network utilizing an intuitive point-and-click interface comprising the expression profiles of over 1000 genes associated with different stages of the ripening tomato.
- Ethylene is central to the control of ripening together with the MADS-box transcription factor RIPENING INHIBITOR (MADS-RIN) associated with the development of colour, taste, and texture [1].
- Here, we introduce the utilization of FruitNet in the characterization of MADS-RIN and COLOURLESS NON-RIPENING (SPL-CNR) as ripening regulators.



Method

Expression profile

- A Tomato Affymetrix GeneChip over 13 time points during ripening was generated. Positive correlations between genes above 0.925 are represented as edges.

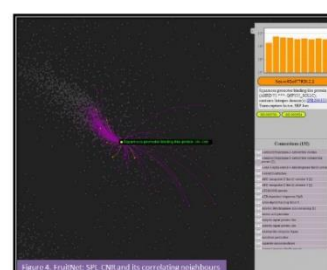
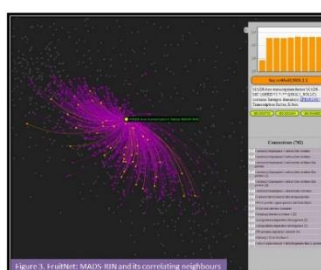
- Selected nodes are green with connected TFs and other genes in orange and purple, with the expression data for the selected gene displayed (Fig3: A).

Gene Ontology

- Nodes are identified by their unique Sol Genomics ID (Fig3: B), and are described using their corresponding Gene Ontology (Fig3: C).

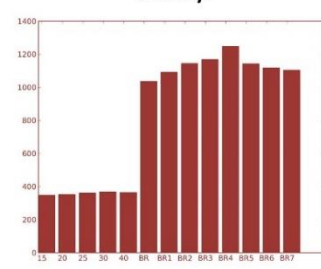
Connections

- Directly connected genes are listed (Fig3: D).



MADS-RIPENING INHIBITOR (RIN)

- Encodes a genetic regulatory component necessary to trigger climacteric respiration and ripening-related ethylene biosynthesis.
- Functions as sequence-specific DNA binding transcription factor activity.



A Selection of Genes Highly Associated with RIN in the Network

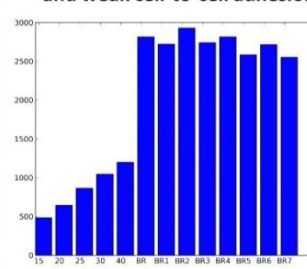
Correlation	Name
0.986	Phytoene synthase 1
0.985	Exostosin
0.985	NAC-NOR domain protein
0.981	Pectinacetylase
0.981	Cytochrome P450
0.981	Zinc finger A20 /AN1 domain
0.977	Phosphofructokinase
0.974	Polygalacturonase 2A
0.970	Lipoxygenase
0.968	Ethylene receptor

SPL- COLOURLESS NON-RIPENING (CNR)

A Selection of Genes Highly Associated with CNR in the Network

Correlation	Name
0.962	Serine-threonine kinase
0.960	Glutamate decarboxylase
0.948	Ascorbate peroxidase
0.943	Xyloglucan endotransglucosylase
0.934	Multiprotein bridging factor 1
0.931	Purine permease protein
0.929	Actin-depolymerizing factor
0.929	Transcription factor HY5
0.928	NAC-NOR domain protein
0.927	Zinc finger A20 /AN1 domain

- Dominant pleiotropic tomato-ripening mutation.
- Mature fruits have colourless pericarp, yellow skin and remain firm.
- Reduced ethylene biosynthesis and weak cell-to-cell adhesion.



FruitNet: Highest Interacting Transcription Factors

Name	Connections	Name	Connections
TDR4/FUL	738	Homeobox Protein	582
MADS-RIN	702	NAC-NOR domain protein	555
GRAS Family Protein	688	SCARECROW	540
Zinc finger A20 /AN1 domain	625	ERF	495
BZIP	600	AP2	477

The recently published tomato genome⁽³⁾ has provided a vast reservoir of information allowing the accuracy of FruitNet to be confirmed.

Community analysis of MADS-RIN, and SPL-CNR have characterized novel genes highly associated with fruit ripening including significant regulators of carotenoid biosynthesis (Phytoene synthase 1), ripening (NAC-NOR), and cell proliferation/apoptosis (serine-threonine kinase).

FruitNet provides a novel tool for the identification of new and important ripening-related genes and a foundation for the analysis of the 'molecular circuits' that control this complex biological process.

[1] Klee, H.J. & Giovannoni, J.J., 2011. Genetics and control of tomato fruit ripening and quality attributes. *Annual review of genetics*, 45, 41–59. [2] Seymour, G.B. et al., 2013. Fruit development and ripening. *Annual review of plant biology*, 64, 219–41. [3] Seymour, G. et al., 2008. Genetics and epigenetics of fruit development and ripening. *Current opinion in plant biology*, 11(1), 58–63. [4] Tomato, T. & Consortium, G., 2012. The tomato genome sequence provides insights into fleshy fruit evolution. *Nature*, 485(7400), 635–41.